A Small Dose of Toxicology: Role of Mitochondrial Dysfunction in Hepatic and Skeletal Muscle Toxicity

Inauguraldissertation

Zur
Erlangung der Würde eines Doktors der Philosophie
vorgelegt der Philosophisch-Naturwissenschaftlichen Fakultät
der Universität Basel

von
Priska M. Kaufmann
aus Wikon (LU)

Basel, 2005

Genehmigt von der Philosophisch-Naturwissenschaftlichen Fakultät auf Antrag der Herren:

Prof. Dr. Dr. Stephan Krähenbühl

Prof. Dr. Jürgen Drewe

Basel, den 11.01.2005

Prof. H.-J. Wirz
Dekan

Für meine Eltern

To know that we know what we know,
and to know that we do not know what we do not know,
that is true knowledge.

Nikolaus Kopernikus (1473-1543)

Table of contents

1. Acknowledgments/Danksagung

What can I possibly say in acknowledgment of the people to whom I owe so much. Even a most gifted author is telling you that it is a very hard job to put thoughts in words, you might can imagine how difficult it is for me to express how much I am indebted to so many of you and how much I am thanking you.

Molière, this famous French author who already kept my mind busy during the Matura once said: People don't die from a disease they die from the medicine. Ok, it is a quote of the 17th century and fortunately not quite true nowadays, unfortunately it is not entirely wrong either. I would like to thank Stephan for giving me the opportunity, the challenge, the impetus, the chance and the confidence to carry out studies in this field in his lab. In his lab where he is head, guiding and leading the group, providing ideas and pulling the team together… Not to mention all the fundraising work and more which has been constantly done in the background to keep the way clear for us. A special thank to Jürgen, for being part of my committee and for the support and joy having given me. On this occasion I also would like to express my appreciation to Hans Leuenberger for being chairman.

Im Grunde und erster Linie sind es immer die Verbindungen mit Menschen, die dem Leben und der Arbeit ihren Wert geben. Und so ist es mir ein Verlangen, ein Bedürfnis und ein Vergnügen, mich bei den Menschen an und auf meinem Weg zu bedanken. Ich möchte mich bei allen ehemaligen und gegenwärtigen 410-ern, 411-ern, Ex-Rosettis, Neo-MGH-lern und ZLF-lern bedanken, die in den letzten 4 Jahren Freude, Überraschung, Nervenkitzel, Frustration, Erstaunen, Ärger, Spass, Euphorie, Melancholie, Entdeckungen, Misserfolg und Erfolg geteilt sowie Hilfe und Unterstützung geschenkt haben. Speziellen Dank gebührt Liliane für ihre unglaubliche Gabe zu wissen was wo ist und wer was braucht um mit einem Lächeln durchs Labor zu gehen…. Michi für seine schier unerschöpfliche Geduld, Hilfe, Beratung, Rückhalt, Beruhigung, Unterstützung, Beistand, Trost und Unterhaltung…. Markus für seinen Humor…. Der Coffeegang für die Pausen...

Natürlich und glücklicherweise gab und gibt es ein Leben ausserhalb des Labors. Ich möchte die Chance ergreifen, mich bei Sara & Simon, Tanja & Lukas, Corinna, Cordula, Brigitte, Dominique & Sascha, Barbara, Andrea und Sabrina zu bedanken für ihre Freundschaft, die fröhlichen Momente, die wir teilten und die Zeit, welche wir verbrachten. Obwohl nicht direkt beteiligt tragt ihr unwissentlich einen grossen Anteil am Zustandekommen dieser Diss. Ein grosses Cheers auch an Centurion und seine Truppe in der Hard-Apotheke dafür dass ihr mich in Eurem Kreise behalten habt.

Змейчо, твояа съм и ти си мой.... I am not a machine but i still live my dream; when I look at you I.... schön und einzigartig, dass Du Träume und Leben mit mir teilst!! Obwohl es nicht die Naturwissenschaft ist welche uns verbindet, so ist es doch die Naturwissenschaft die uns indirekt verbunden hat. Ganz einfach: Мерси, благодаря и много целувки!!! Auf die Zukunft Змейчо!

Zwei Dinge sollten Kinder von ihren Eltern bekommen: Wurzeln und Flügel. Ich bin in der glücklichsten aller Lagen. Meine Eltern haben mir beides mit auf den Weg gegeben. Mit meinen Eltern möchte ich auch meine beiden Brüder Markus und Stephan hier nennen.... Es ist ganz einfach: Ohne Euch wär ich nicht hierher gelangt und was ich Euch verdanke passt in keine Danksagung und auf kein Papier!!

2. Summary

Research over the last decade has extended the prevailing view of mitochondrial function well beyond its critical bioenergetic role in supplying ATP. Recently, it has been recognized that mitochondria play a critical role in cell regulatory and signaling events, in the responses of cells to drug effects, genetic stresses and cell death. Based on this, four studies were conducted in order to gain more insight into several aspects of mitochondrial toxicity of drugs, consequences of mitochondrial dysfunction and role of mitochondria in cell death induction.

Project 1 (Chapter 7) aimed to investigate the mechanisms leading to liver steatosis in rats treated with trimethylhydraziniumpropionate, an inhibitor of butyrobetaine hydroxylase. Rats were treated with trimethylhydraziniumpropionate for three or six weeks and were studied after 24h of starvation. Beside the mechanisms leading to liver steatosis, we also investigated adaptive changes secondary to a decrease in the hepatic carnitine pool and to impaired in vivo mitochondrial β-oxidation. Our studies demonstrate that hepatic carnitine deficiency is the most important cause for liver steatosis in trimethylhydraziniumpropionate-treated rats and suggest that reduced mitochondrial fatty acid oxidation may be partially compensated by increased peroxisomal fatty acid metabolism due to proliferation of peroxisomes.

Project 2 (Chapter 8) describes a study about hepatic toxicity of benzarone and benzbromarone having its source in clinical findings. Both drugs have similar structural features like amiodarone, a well-known mitochondrial toxin. Liver toxicity of benzarone and benzbromarone and of the two analogues benzofuran and 2-butylbenzofuran was therefore investigated using freshly isolated rat hepatocytes or freshly isolated rat liver mitochondria. In particular, we were interested in mitochondrial mechanisms leading to cell damage or even death. We also investigated the structure-toxicity relationship by including the molecular analogues benzofuran and 2-butylbenzofuran along with amiodarone, benzarone and benzbromarone in our studies. We could show that benzarone, benzbromarone as well as amiodarone are toxic to liver cells and liver mitochondria. The side chain at position 2 enhances the toxic potential to some extent but does not fully explain it. Bromide atoms in the p-hydroxybenzene moiety are not essential for the toxicity of these compounds but clearly enhance the toxic potential. The benzofuran structure alone was not responsible for the toxic effects. Hepatic injury associated with the ingestion of these drugs can be explained by mitochondrial damage with subsequent induction of cell death.

Myotoxicity, rhabdomyolysis in particular, is a rare but severe adverse drug reaction of statins. The aim of project 3 (Chapter 9) was to evaluate the mitochondrial toxicity of five different statins and to assess their role in cell death induction in skeletal muscle cells. Lipophilic statins reduced cell viability and impaired mitochondrial functions, such as β-oxidation and respiratory chain, which are essential for cell survival. As a consequence, the mitochondrial membrane potential dissipated, the mitochondrial permeability transition pore opened and apoptosis inducing factors were released. Mitochondrial dysfunction and the subsequent release of mitochondrial proteins are tightly linked to the process of programmed cell death, also called apoptosis. Consistently, induction of apoptosis could be convincingly demonstrated, since lipophilic statins did cause DNA fragmentation and an increase in annexin V stained cells. Myotoxicity, a known side effect after treatment with statins, in particular rhabdomyolysis in response to lipophilic statin treatment can be explained at least in part by mitochondrial toxicity and the subsequent induction of apoptosis of myocytes.

Project 4 (Chapter 10) was dealing with a putative drug-drug interaction. The aim of the study was to investigate the mechanisms by which venoocclusive disease was provoked in a patient, who was treated with immunodepressive doses of cyclophosphamide and roxithromycin. We therefore determined first the effect of roxithromycin on the metabolism of cyclophosphamide in vitro. Furthermore, by the use of cultured human umbilical endothelial cells, we could confirm the toxicity of the cyclophosphamide/roxithromycin combination and were able to investigate the underlying mechanisms of cell death induction. Roxithromycin causes an overall inhibition of hepatocyte cyclophosphamide metabolism and inhibition of P-glycoprotein, leading to an accumulation of cyclophosphamide in hepatocytes and possibly also endothelial cells. Apoptosis is the principle mechanism of toxicity of cyclophosphamide in endothelial cells, most probably associated with activation of the mitochondrial pathway of initiation of apoptosis.

3. Zusammenfassung

Die Forschung des letzten Jahrzehntes zeigte, dass Mitochondrien weit mehr sind als die Kraftwerke der Zelle. Ihnen kommt eine entscheidende und ausschlaggebende Rolle bei der Zellregulation und Signalauslösung respektive -weiterleitung im Zusammenhang mit Arzneimittelnoxen, genetischen Stressfaktoren oder Zelltod zu. Basierend auf den Erkenntnissen dieses neueren Forschungsgebiets wurden vier Studien durchgeführt, mit dem gemeinsamen Ziel mehr über unterschiedliche Aspekte der mitochondrialen Toxizität von Arzneistoffen, Folgeerscheinungen der mitochondrialen Dysfunktion und die Rolle der Mitochondrien in der Zelltodinduktion zu erfahren.

Das erste Projekt (Kapitel 7) war darauf gerichtet herauszufinden, welche Mechanismen der Auslösung einer Lebersteatose in Ratten nach Behandlung mit Trimethylhydraziniumpropionat zu Grunde liegen. Es handelt sich dabei um einen Inhibitor der Butyrobetainhydroylase. Abgesehen vom Mechanismus der zur Lebersteatose führt, wurden ausserdem sekundär induzierte, adaptive Veränderungen untersucht, welche als Folge des reduzierten Carnitinpools und der verringerten in vivo β-Oxidation auftraten. Es konnte gezeigt werden, dass die hepatische Carnitindefizienz die Hauptursache für die Lebersteatose in mit Trimethylhydraziniumpropionat behandelten Ratten ist. Die Einschränkung der mitochondrialen Fettsäureoxidation wird möglicherweise teilweise durch verstärkten peroxisomalen Fettsäuremetabolismus in Folge peroxisomaler Proliferation kompensiert.

Das zweite Projekt (Kapitel 8) handelt von der hepatischen Toxizität von Benzaron und Benzbromaron. Die Arbeit ging aus klinischen Fallberichten über Leberschädigung nach Behandlung mit Benzaron oder Benzbromaron hervor. Beide Arzneimittel weisen auffällige strukturelle Ähnlichkeiten mit Amiodaron auf, welches seit längerem als mitochondriales Toxin bekannt ist. Deshalb wurde die Lebertoxizität der zwei Arzneistoffe Benzaron und Benzbromaron, sowie der beiden Strukturanaloga Benzofuran und 2-Butylbenzofuran untersucht. Als Modell dienten frisch isolierte Hepatozyten sowie frisch isolierte Lebermitochondrien. Insbesondere fokussierten wir auf die mitochondrialen Mechanismen welche zur Zellschädigung oder sogar Zelltod führen. Des Weiteren wollten wir einen Beitrag zur Aufklärung der Beziehung zwischen Struktur und Toxizität leisten. Es konnte gezeigt werden, dass Benzaron, Benzbromaron und Amiodaron toxisch sind für ganze Leberzellen wie auch für isolierte Mitochondrien. Die Seitenkette an Position 2 erhöht das toxische Potential in bestimmten Ausmassen, vermag es jedoch nicht vollständig zu erklären. Die Bromatome wiederum sind nicht essentiell für die Toxizität verstärken diese aber deutlich. Das Benzofurangerüst alleine ist nicht verantwortlich für die toxischen Wirkungen. Die Leberschädigung im Zusammenhang mit der Einnahme von Benzaron oder Benzbromaron kann durch die Auslösung eines mitochondrialen Schadens mit nachfolgender Induktion des Zelltodes erklärt werden.

Muskuläre Toxizität, insbesondere Rhabdomyolyse, sind seltene aber schwerwiegende unerwünschte Wirkungen von Statinen. Das Ziel des dritten Projektes (Kapitel 9) war es, die mitochondriale Toxizität fünf verschiedener Statine auf die Skelettmuskulatur zu bestimmen und deren Rolle in der Zelltodinduktion zu untersuchen. Lipophile Statine reduzierten die Überlebensrate von Rattenmyoblasten und verschlechterten die mitochondrialen Funktionen wie jene der β-Oxidation und der Atmungskette, welche essentiell sind für das Überleben einer Zelle. In Folge davon verschwand das mitochondriale Membranpotential, eine Pore in der mitochondrialen Membran öffnete sich und Apoptose induzierende Faktoren wurden ins Zytoplasma freigesetzt. Die mitochondriale Dysfunktion mit der anschliessenden Freisetzung mitochondrialer Proteine sind eng mit dem so genannten

programmierten Zelltod (Apoptose) gekoppelt. Folgerichtig konnte überzeugend gezeigt werden, dass die lipophilen Statine zu Fragmentierung der DNA und zur Zunahme Annexin V-gefärbter Zellen führte. Muskuläre Toxizität und insbesondere Rhabdomyolyse ist ein bekanntes Problem unter Statintherapien, welche mindestens teilweise durch mitochondriale Toxizität und darauf folgende Apoptoseauslösung erklärt werden kann.

Das vierte Projekt (Kapitel 10) beschäftigt sich mit einer vermuteten Arzneimittelinteraktion. Bei einer Patientin trat unter Therapie mit immunosuppressiven Cyclophosphamiddosen und Roxithromycin das Krankheitsbild „veno-occlusive disease“ auf. Das Ziel der Arbeit war es der dieser Komplikation zu Grunde liegende Mechanismus zu erforschen. In einem ersten Schritt wurde der Effekt von Roxithromycin auf den Cyclophosphamidmetabolismus in vitro bestimmt. Ausserdem konnte mittels einer kultivierter humaner umbilikalen Endothelzelllinie die Toxizität der Cyclophosphamid/Roxithromycin-Kombination bestätigt werden und ermöglichte uns dadurch den Toxizitätsmechanismus zu erforschen. Roxithromycin bewirkt eine umfassende Hemmung des hepatischen Cylcophosphamidmetabolismus wie auch des P-Glykoproteins. Vermutlich kommt es zu einer Akkumulation von Cyclophosphamid in Hepatozyten und in Endothelzellen. Apoptose ist der Haupttoxizitätsmechanismus in Endothelzellen, vermutlich via Aktivierung des mitochondrialen Wegs der Apoptoseauslösung.

4. Abbreviations

AC	Acrolein
ADP	Adenosine diphosphate
ADR	Adverse drug reaction
Ami	Amiodarone
AOX	Acyl-CoA oxidase
Ato	Atorvastatin
ATP	Adenosine triphosphate
B	Benzarone
BB	Benzbromarone
BF	Benzofuran
BBF	2-Butlybenzofuran
CA	Chloroacetaldehyde
Cer	Cerivastatin
Cn	Carnitine
Conj	Conjugation
CoA	Coenzyme A
CPA	Cyclophosphamide
CPT	Carnitine palmitoyltransferase
Cy A	Cyclosporin A
CYP	Cytochrome P450
DAB	Diaminobenzidine
DMEM	Dublecco’s Modified Eagle Medium
DMSO	Dimethylsulfoxide
ECV 304	Human umbilical vein endothelial cell
EDTA	Ethylenediaminetetraacetic acid
ER	Endoplasm(at)ic reticulum
Ery	Erythromycin
FACS	Fluorescence activated cell sorting
Fas	Fas ligand
Flu	Fluvastatin
FSC	Forward scatter
FU	Fluorescence unit
HEPES	N-(2-Hydroxyethyl)piperazine-N’-(2-ethanesulfonic acid)
HDL	High densitiy lipoprotein
HMG-CoA	Hydroxymethylglutaryl coenzyme A
HPLC	High performance liquid chromatography
Imm	Inner mitochondrial membrane
Ip	intraperitoneal
Lca	Long-chain acylcarnitine
JC-1	5,5’,6,6’-Tetrachloro-1,1’,3,3’.tetraethylbenzimidazolylcarbocyanide iodide
LDH	Lactate dehydrogenase

LDL	Low density lipoprotein
L6	Rat skeletal muscle myoblasts
MPT	Mitochondrial permeability transition
MOPS	3-[N-morpholino]propanesulfonic acid
MPP^+	1-Methyl-4-phenylpyridinium
MPTP	1-Methyl-4-phenyl-1,2,3,6-tetrahydropyridine
MSM	Mannitol sucrose mops
MTX	Methotrexate
NADH	β-Nicotinamide adenine dinucleotide
NADPH	β-Nicotinamide adenine dinucleotide phosphate
n.d.	Not determined
Neo	Neomycin plasmid; negative control to Fas ligand plasmid
Omm	Outer mitochondrial membrane
P338/MDR	murine monocytic leukaemia cell line
PBS	Phosphate buffered saline pH 7.4
P-gp	P-glycoprotein
PPAR	peroxisome proliferator-activated receptor
PPI	Propidium iodide
Prav	Pravastatin
ψ_m	Mitochondrial membrane potential
R 123	Rhodamine 123
RCR	Respiratory control ratio
ROS	Reactive oxygen species
ROX	Roxithromycin
Sca	Short-chain acylcarinitine
SD	Standard deviation
SDS	Sodium dodecyl sulfate
SEM	Standard error of the mean
Sim	Simvastatin
Tris	Tris(hydroxymethyl)-aminomethan
TPP^+	Tetraphenylphosphonium bromide
VLDL	Very low density lipoprotein
VOD	Veno-occlusive disease

5. Introduction

5.1. Toxicology

5.1.1. Background

Toxicology! What an exciting word with interesting connotations. It initially evoked thoughts of poisons, poisoners, intrigue, cloak-and-dagger, villains, victims and perpetrator as well as plants and chemicals as instruments of ill. But what does to word conjure up today? Polluted water, air laden with noxious gases, foods contaminated with pesticides or antibiotics, soil loaded with heavy metals and people suffering from undesired effects of modern therapeutic agents (1)

Toxicology is a young science. However, its origins are very old. The earliest cultures having developed knowledge of drugs and poisons were the Egyptians (The Ebers Papyrus), the Chinese (Pen Ts'ao) and the Hindus (Rig-Veda). Knowledge on poisonous substances was recognized in essentially all over recorded history and was passed down. In Roman and Greek times, poisons, generally of plant origin, were used for murder and suicide, considered to be the „easier alternative". Of Cleopatra it is bequeathed that in 30 B.C. she chose „to fall on her asp rather than to fall on her sword", many years after she poisoned her younger brother in order to claim the throne. Poisoning for nefarious purposes has remained a problem ever since, and much of the earlier impetus to the development of toxicology was primarily forensic.

Philippus Theophrastus Aureolus Bombastus von Hohenheim (Paracelsus 1492? – 1541) determined that specific chemicals were actually responsible for the toxicity of a plant or animal poison, as opposed to the Greek concept of a mixture or blend. He also documented that the body's response to those chemicals depended on the dose received. His studies revealed that small doses of a substance might be harmless or beneficial whereas larger doses could be toxic. This is now known as the dose-response relationship, a major concept of toxicology. Paracelsus is often quoted for his statement: *"All substances are poisons; there is none which is not a poison. The right dose differentiates a poison and a remedy."*

Another motive for the development of toxicology has been the careful description of adverse reactions to medicinal products that began to appear in the eighteenth century. Thus, William Withering described digitalis toxicity in 1785, and in 1790, Hahnemann carried out toxicological studies on himself and his healthy friends with therapeutic agents of his time.

In World War I a variety of poisonous chemicals were used in the battlefields of Northern France. This was the stimulus for much work on mechanisms of toxicity as well as medical countermeasures to poisoning. In fact, war played as great a part in the development of toxicology as of many other sciences. Major extensive and rapid developments in the scientific basis and practice of toxicology have been obvious since the 1950s (2).

The essence of toxicology in our today's understanding is that it is an integrative discipline that combines the elements of biology, chemistry, mathematics, physics and medicine. Toxicological research is driven by the need to understand and assess the human and ecological risks of exposure to chemicals and other toxicants as well as by interest in using toxic agents to elucidate basic biological and pathobiological processes. The level of research activity in this field nowadays is high and the rate of change of knowledge very rapid.

5.1.2. Toxicology today

5.1.2.1. Categories of toxicology

As a consequence of the markedly expanded scope of toxicology, the number of differing subdisciplines, which have emerged have increased considerably. Classifications are necessary and useful to organize information and concepts. They are neither rigid nor discrete but overlapping and broad instead.

Roughly, the main activities in toxicology fall into three main categories: *descriptive, mechanistic and regulatory*. Although each has distinctive characteristics, each contributes to the other, and all are vitally important to chemical risk assessment. A mechanistic toxicologist is concerned with identifying and understanding the cellular, biochemical and molecular mechanisms by which chemicals exert toxic effects. A descriptive toxicologist is concerned directly with toxicity testing, which provides information for safety evaluation and regulatory requirements. A regulatory toxicologist has the responsibility for deciding on the basis of data provided by descriptive and mechanistic toxicology, whether a drug or another chemical poses a sufficiently low risk to be marketed for a stated purpose. In addition to the above categories, there are other specialized areas of toxicology, such as *forensic, clinical, environmental,* and *occupational* toxicology (3)

5.1.2.2. Aims of toxicology: Risk Assessment

Due to the large scope of toxicology nowadays, one finds more than one definition on toxicology in the literature. While a clinician would focus on the clinical safety of drugs, an environmental toxicologist emphasizes the toxicity of compounds on flora and fauna, whereas a regulatory toxicologist aims at estimation of risk and of the contribution to the risk/benefit ratio for its intended use. A term that has become very important for toxicologist independent of the individual field is the so-called “risk assessment”. Risk assessment or safety assessment, respectively, consists of four components: (I) identify hazard, (II) characterize hazard, (III) describe exposure, and (IV) present risk. In this context it is important to point out, that hazard describes the potential for a damaging effect whereas the risk includes the likelihood that a hazard would occur. In case of drug development these data are contributing to the go or no-go decision in drug development. However, in the interpretation of safety data, risk-benefit considerations need to be applied. The therapeutic benefit has to be analyzed in view of the indication. The degree of adverse drug reaction, which is acceptable, is different for an anti-cancer therapy compared to treatment of hypertension.

5.1.3. Principles of toxicology

As Paracelsus proposed centuries ago, the dose differentiates whether a substance will be a remedy or a poison. A xenobiotic in small amounts may be non-toxic and even beneficial but when the dose is increased, toxic and lethal effects may result.

With the exception of adverse drug reaction on the basis of immunological or idiosyncratic processes, the dose-response relationship is a fundamental and essential concept in toxicology. It correlates exposures and the spectrum of induced effects. Generally: the higher the dose, the more severe the response. The dose-response relationship is based on observed data from experimental animal, human clinical, or cell studies.

Knowledge of the dose-response relationship:

- establishes causality that the chemical has in fact induced the observed effects
- establishes the lowest dose where an induced effect occurs - the threshold effect
- determines the rate at which injury builds up - the slope for the dose response.

Within a population, the majority of responses to a toxicant are similar; however, a wide variance of responses may be encountered, some individuals are susceptible and others resistant. The dose-response curve normally takes the form of a sigmoid curve (see Figure 1, Panel A). Small doses are not toxic. The point at which toxicity first appears is known as the threshold dose level. From that point, the curve increases with higher dose levels. Knowledge of the shape and slope of the dose-response curve is extremely important in predicting the toxicity of a substance at specific dose level (see Figure 1, Panel B).

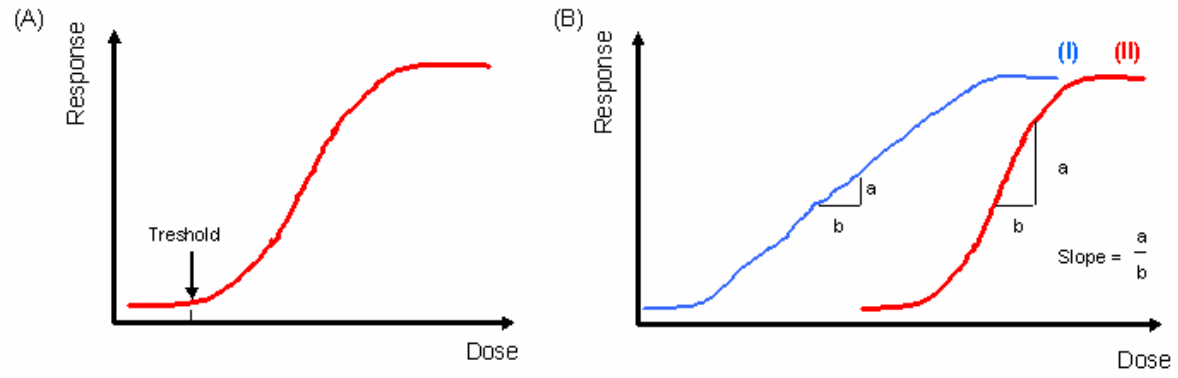

Figure 1: dose-response curve:
Panel A: The dose-response relationship normally describes a sigmoid curve with the threshold level indicating the dose at which first signs of toxicity appear.
Panel B: The shape and the slope of the curve are essential parameters in order to predict the toxic potential of a xenobiotic. Compound I has a lower threshold level whereas compound II has a higher slope value indicating a small dose range from first signs to maximal manifestation of toxicity.

5.2. Mitochondria

5.2.1. Origin

About 2 billion years ago, cell destined to be the ancestors of all eukaryontic cells entered into a partnership with an ancestor of today's purple bacteria. This collaboration promised benefits to both parties: it allowed them to exploit the energy opportunities inherent in the emerging oxygen atmosphere, which was toxic to most forms of life. The result was a protoeukariontic cell, and the endosymbiotic bacteria were to become mitochondria. For very many years, the mitochondria were considered to be the powerhouse of the cell and appreciated for their essential role in energy supply. But in the 1990s a flurry of publications highlightened a new task, that of an organellar cerebus, the gatekeeper of cell death. It was natural to wonder whether the life-supporting functions of mitochondria were somehow linked to a death-promoting activity.

5.2.2. Introduction

Mitochondria derive from bacterial origin and have two membranes: a circular outer membrane limiting the intermembrane space, and an inner membrane with inner folds (the mitochondrial cristae), which limits the mitochondrial matrix. Enzymes involved in β-oxidation of fatty acids or TCA cycle are in the matrix, together with the mitochondrial DNA (mtDNA), whereas the enzymes of the respiratory chain are sitting in the inner mitochondrial membrane. Cytochrome c, engaged in the electron transport of the respiratory chain, is located in the mitochondrial intermembrane space (Figure 2).

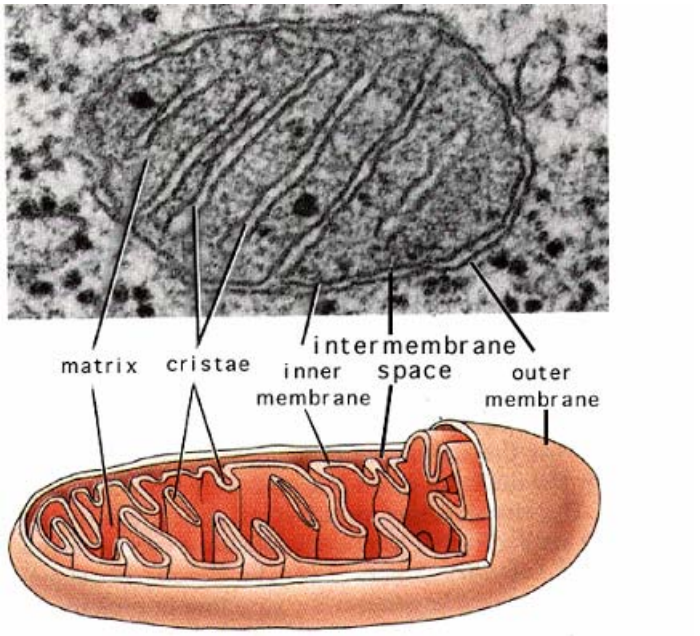

Figure 2: Structure of mitochondria:
Mitochondria are organelles with two well-defined compartments: the matrix, surrounded by the inner mitochondrial membrane, and the intermembrane space, surrounded by the outer mitochondrial membrane. The inner membrane is folded into numerous cristae, which greatly increases the surface. It contains the complexes of the electron transport chain, the ATP synthase and the adenine nucleotide transporter. To function properly, the inner membrane is almost impermeable in physiological conditions.

At the contact sites between inner and outer mitochondria a large conductance channel is located, known as the mitochondrial permeability transition (mpt) pore. The structure and composition remain only partially defined, but its constituents include both inner membrane proteins (such as adenine nucleotide translocator) and outer membrane proteins, such as porin (voltage-dependent anion channel), which operate most likely in concert, creating a channel through which molecules < 1500 Da pass.

Mitochondria produce most of the cell energy by the oxidation of various fuels and the oxidative phosphorylation. The β-oxidation of fatty acyl-coenzyme A derivatives and oxidation of acetyl-CoA by the TCA cycle are associated with the conversion of NAD^+ and FAD into NADH and $FADH_2$. These reduced cofactors are then reoxidized by the respiratory chain. Most electrons migrate along the respiratory chain up to cytochrome c oxidase, where they safely combine with protons and oxygen to form water. This transport of electrons along the respiratory chain is associated with the extrusions of protons from the matrix into the intermembrane space. This creates a high

electrochemical potential across the inner mitochondrial membrane, whose potential energy is used to synthesize ATP.

MtDNA is extremely sensitive to oxidative damage owing to its proximity to the inner membrane with the electron transport chain, the absence of protective histones and incomplete repair mechanisms (4).

5.2.3. Mitochondrial Dysfunction & Mitochondrial Cytopathies

Mitochondrial dysfunction describes the conditions in which the proper function of mitochondria is impaired resulting in inadequate energy production, independent of its actual trigger. These dysfunctions can be drug induced, due to pathogenic conditions such as cholestasis (5) as well as of acquired or inherited origin. The latter are also termed mitochondrial cytopathies. Mitochondrial dysfunctions include inhibition of the respiratory chain, uncoupling of oxidative phosphorylation or inhibition of fatty acid oxidation.

The association between mitochondrial abnormalities and disease has been known for about forty years, with the description of a patient with hypermetabolism and a skeletal muscle biopsy demonstration large numbers of abnormal mitochondria (6-8)

Mitochondrial cytopathies are inherited or acquired disorders. They can be caused by inheritable genetic mutations, acquired somatic mutations, or the aging process itself. The two most common inheritance patterns are Mendelian and Maternal. Mitochondrial cytopathies actually include more than 40 different identified diseases that have different genetic features. The disorders range in severity from minimal symptoms to death. The result is often muscle weakness, fatigue and problems with the heart, eyes and various other systems. Some mitochondrial cytopathies include Leber hereditary optic neuropathy (LHON), myoclonus epilepsy with ragged-red fibers (MERRF), mitochondrial encephalomyopathy, lactic acidosis and stroke-like syndrome (MELAS), Leigh syndrome and Kearn-Sayre syndrome (KSS) (9).

That mitochondria represent a target for drug toxicity is not surprising, bearing in mind their central role in energy generation and metabolic function. Principle mechanisms of drug induced mitochondrial toxicities are: (a) inhibition of the electron transport chain, (b) uncoupling of oxidative phosphorylation, (c) inhibition of fatty acid metabolism, (d) oxidation of mtDNA or (e) inhibition of mitochondrial DNA synthesis. The list of toxins known to cause mitochondrial injury nowadays is increasingly long, including drugs like valproate, salicylate (10-13), diclofenac (14), naproxen (15) benzbromarone (see chapter 8), bupivacaine (16), buprenorphine (17), amiodarone (18), zidovudine (19), extracts from kava kava, bacterial toxins like cereulide (20) or aflatoxin (21). Mitochondrial dysfunction with subsequent possible induction of organ failure is well described for many drugs. However, the question arises, why only a certain population taking a specific toxic compound develops side effects and what in particular makes them vulnerable. Further investigations are needed to cast more light on this matter. With regards to mitochondria, some factors are known to increase the risk of developing unwanted effects. Reduced mitochondrial metabolism represents a risk factor for induction of toxicity. This reduction might be due to inborn deficiencies in mitochondrial metabolism or due to co-administration of drugs known to inhibit mitochondrial functions.

5.3. Drug Toxicity

5.3.1. From the Status Quo to the "Magic Bullet"

In the early 1900s, the German scientist Paul Ehrlich described an ideal drug as a „magic bullet"; such a drug would be targeted precisely at a disease site and would not harm healthy tissues. Although many new drugs are targeted more accurately than their predecessors, none of them, as of yet, hit the target precisely. Most drugs produce several effects, but usually only one effect, namely the therapeutic effect, is desired for the treatment of a disorder. The other actions of a drug may be regarded as adverse effects, whether they are intrinsically harmful or not.

Not surprisingly, adverse drug reactions (ADR) are common. Most ADRs are relatively mild, and many disappear when the drug is stopped or the dose is reduced. Some gradually subside as the body adjusts to the drug. Other ADRs are more serious and last longer. Up to 5% of hospital admissions in the United States are estimated to be for treatment of adverse drug reactions (22-24). Each time a person is hospitalized, the risk of having at least one adverse drug reaction is 10 to 30% (25-27). The risk is directly correlated to the amount of different drugs a person is treated with and to the age of the patient (23, 28).

Many ADRs represent an exaggeration of the drug's effects (type A or augmented reaction). This type is usually predictable and in many cases avoidable. It may occur if the dosage of a drug is too high, if another drug reduces the metabolism of the first drug (see next paragraph) or if the elimination of a drug is impaired. The reaction is related to the exposure. Around 70 to 80% of total adverse drug reactions account for type A reactions. Some adverse drug reactions result from mechanisms that may not be fully understood (type B or bizarre reactions). This type of reaction is largely unpredictable, normally dose-independent and tends to be potentially severe or even life threatening. Type B reaction, also called idiosyncratic drug reactions, can be due to intolerance, allergy or pseudoallergy (24).

ADRs can be caused if an organism is exposed to one xenobiotic at one time. Medical treatment, however, consist often of multiple exposures. Xenobiotics administered or received simultaneously may act independently of each other. However, in many cases, the presence of one chemical may drastically affect the response to another chemical. The toxicity of a combination of chemicals may be less or it may be more than would be predicted from the known effects of each individual chemical. The effect that one chemical has on the toxic effect of another chemical is known as an interaction.

As mentioned before, some ADRs are unpredictable. Related to this, the issue of idiosyncratic drug reactions should be raised. There are host-related factors that will contribute to determining whether a xenobiotic will induce an ADR or not. These host factors are only partially known but may include both genetic and acquired factors. Such a host (patient)-specific mixture of characteristics is called "idiosyncrasy". The term implies that the reactions are based on specific combinations of factors, that is characteristic for an individual and which predisposes the individual to succumb to overt manifestation of toxicity. Idiosyncratic drug reactions involve many different mechanisms. Immune-mediated toxicity is one of them. Abnormalities in biochemical pathways leading to metabolic idiosyncrasy have also been defined, which refers back, at least in part, to the topic of mitochondrial dysfunction and cytopathies (29)

5.3.2. Development of drug toxicity

Chemicals may adversely affect the function and/or structure of living organisms. The characterization of these harmful or toxic effects is essential. It is also valuable to understand the mechanisms responsible for the manifestation of toxicity – that is, how a toxicant enters an organism, how it interacts with target molecules, and how the organism deals with this insult. Elucidation of the mechanisms of toxicity has led to a better understanding of fundamental physiologic and biochemical processes. Consequently there are various pathways that may lead to toxicity (see figure 3). A common course is when a toxicant delivered to its target reacts with it, and the resultant cellular dysfunction manifests itself in toxicity. An example of this route of toxicity is that taken by the puffer fish poison tetrodotoxin. After ingestion (step 1) it reacts with its target (step 2b), resulting in blockade of Na^+ channels, inhibition of the activity of motoneurons (step 3) and ultimatively skeletal muscle paralysis. No repair mechanisms can prevent the onset of such toxicity.

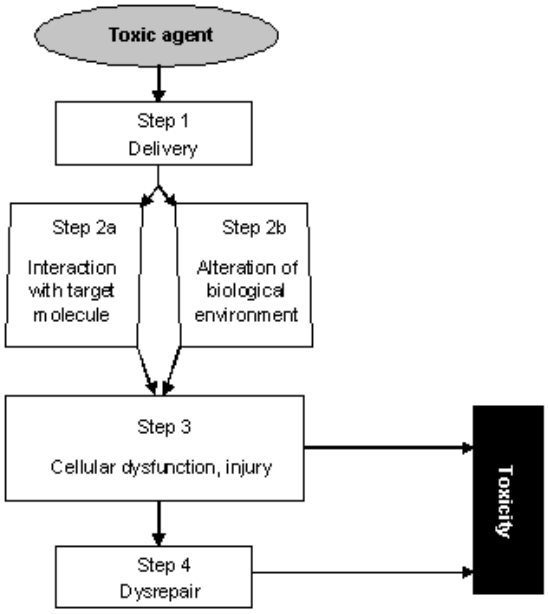

Figure 3: Potential stages in the development of toxicity after chemical exposure (30)

Sometimes a xenobiotic does not react with a specific target molecule but rather adversely influences the biological environment, causing molecular, organellar, cellular or organ dysfunction leading to deleterious effects. For example, 2.4-dinitrophenol, after entering the mitochondrial matrix (step 1), collapses the proton gradient across the inner mitochondrial membrane by its mere presence (step 2b), causing mitochondrial dysfunction (step 3), which is manifested in toxic effects such as seizures or hyperthermia.

The most complex path of toxicity involves more steps. First the toxicant is delivered to its target(s) (step 1), after which the ultimate toxicant interacts with endogenous target molecules (step 2a), triggering perturbations in cell function and/or structure (step 3), which initiate repair mechanisms at the molecular, cellular, and/or tissue levels (step 4). When the perturbations induced exceed repair capacity or when repair becomes malfunctional, toxicity occurs (30).

As a result of the huge number of potential toxicants and the multitude of biological structures and processes that can be impaired, there is a tremendous number of possible toxic effects.

Considering the focus of the succeeding chapters, emphasis was put on basic toxic mechanisms of particular importance for this thesis.

5.3.3. Mechanisms of drug toxicity

Toxic damage to cells can cause individual cell death and if sufficient cells are lost, the result can be tissue or organ failure, ultimately leading to death of the organism. Apparent adverse drug reactions, cell damage or tissue damage have an underlying mechanism on the molecular, biochemical or cellular level. Toxicity occurs due to specific changes within the cell. These events lead to impairment of internal cellular maintenance, which can be considered as a comprehensive basic concept of drug toxicity. It is interesting to note, that in all disorders, mitochondria play a key role.

There are three critical biochemical mechanisms how chemicals may initiate cell damage , namely ATP depletion, sustained rise in intracellular Ca^{2+} and overproduction of reactive oxygen species (ROS).

5.3.3.1. Biochemical changes

5.3.3.1.1. ATP depletion

ATP plays a central role in cellular maintenance. Chemical energy is released by hydrolysis of ATP to ADP or AMP. The ADP is rephosphorylated in the mitochondria by ATP synthase. Coupled to oxidation of hydrogen to water, this process is termed oxidative phosphorylation.

Oxidative phosphorylation requires (a) the delivery of hydrogen in the form of NADH to the initial electron transport complex: (b) delivery of oxygen to the terminal electron complex,: (c) delivery of ADP and inorganic phosphate to ATP synthase; (d) flux of electrons along the electron transport chain; and (e) return of protons across the inner mitochondrial membrane into the matrix down the electrochemical gradient to drive ATP synthase. Chemicals can impede these processes, interfering with mitochondrial ATP synthesis. Impairing agents can interfere at different stages, like inhibitors of hydrogen delivery to the electron transport chain (i.e. inhibition of β-oxidation), inhibitors of the electron transport chain (i.e. rotenone, cyanide, amiodarone, antimycin), inhibitors of oxygen delivery to the electron transport chain, inhibitors of ADP phosphorylation (i.e. oligomycin, uncouplers), or chemicals causing mitochondrial DNA damage and impaired transcription of key mitochondrial proteins. Impairment of oxidative phosphorylation is detrimental to cells because failure of ADP rephosphorlylation results in accumulation of ADP and its breakdown products as well as depletion of ATP. These changes cause a cascade of aftereffects, which may be devastating and disastrous in such a tightly and subtly regulated system like a cell.

5.3.3.1.2. Sustained rise of intracellular Ca^{2+}

Intracellular Ca^{2+} levels are highly regulated. The 10’000-fold difference between extracellular and cytosolic Ca^{2+} concentration is maintained by the impermeability of the plasma membrane to Ca^{2+} and by transport mechanisms that remove Ca^{2+} from the cytoplasm. Ca^{2+} is actively pumped from the cytosol across the plasma membrane and is sequestered in the endoplasmatic reticulum and mitochondria. Because they are equipped with a low-affinity transporter, the mitochondria play a significant and essential role in Ca^{2+} sequestration when the cytoplasmatic Ca^{2+} levels rise into the

micromolecular range. Toxicants induce elevation of cytoplasmatic Ca^{2+} by promoting Ca^{2+} influx or inhibiting Ca^{2+} efflux from the cytoplasm. Toxicants also increase cytosolic Ca^{2+} inducing its leakage from mitochondria. Sustained elevation of intracellular Ca^{2+} is harmful because it can result in (a) depletion of energy reserves, (b) dysfunction of microfilaments, (c) activation of hydrolytic enzymes, and (d) generation of ROS.

5.3.3.1.3. Overproduction of reactive oxygen species (ROS)

There are a number of xenobiotics that can directly generate ROS, such as transition metals. However, mitochondria are the major source of ROS in a cell. Overproduction can be secondary to inhibition of the mitochondrial electron transport chain, due to leakage of reduced molecular oxygen from complex III. Similarly complex I also provides superoxide anions (31). For example, mitochondria form O_2^--anions, which in turn are converted into H_2O_2 and the potent reactive species hydroxyl radical (OH). As already mentioned in the chapter before, oxidative stress causes a sustained elevation of cellular Ca^{2+} with all its consequences. The alteration of mitochondrial Ca^{2+} concentration has been suggested to be an important event in the induction of oxidative stress. ROS have been shown to mediate cell death in a number of systems (32).

5.3.4. Mitochondrial permeability transition (MPT)

The before mentioned biochemical changes such as mitochondrial Ca^{2+} uptake, generation of ROS, depletion of ATP as well as decreased mitochondrial membrane potential (ψ_m) are all considered as causative factors for an abrupt increase in the mitochondrial inner membrane permeability, believed to be caused by opening of a proteinaceous pore („megachannel“) that spans both mitochondrial membranes (33, 34). As this pore is permeable to solutes of size < 1500 Da, its opening permits free influx of protons into the mitochondrial matrix, causing a rapid dissipation of the ψ_m and impairment of ATP generation, osmotic driven influx of water, resulting in mitochondrial swelling as well as release of molecules located in the mitochondrial intermembrane space (i.e. cytochrome c) (35). The principle is shown in Figure 4. It has to be emphasized that up to now, the precise composition and function of this pore is controversial and the model presented here is broadly accepted but still hypothetical.

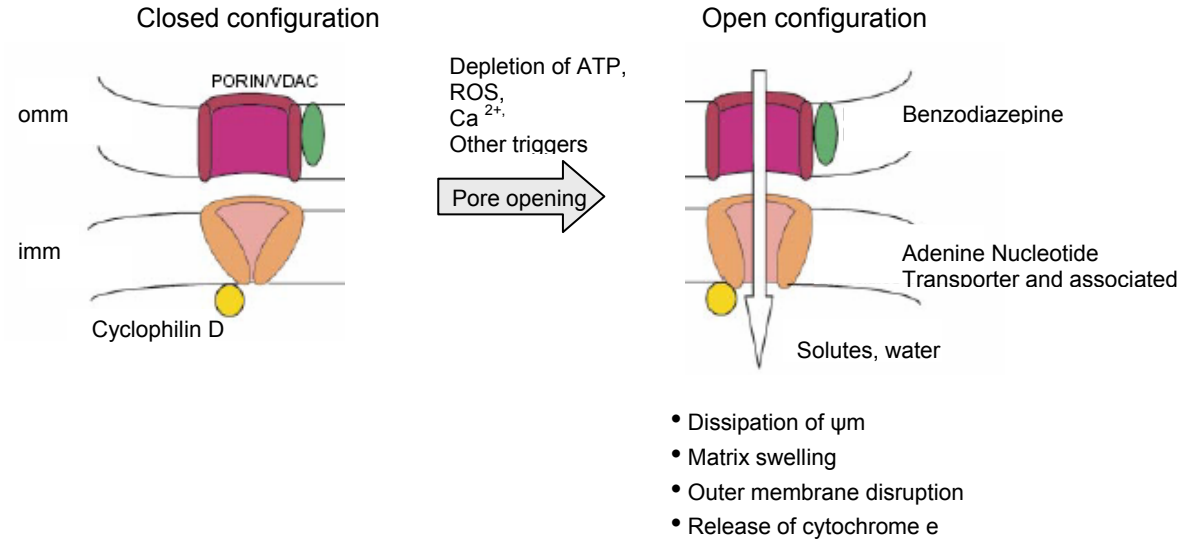

Figure 4: The mitochondrial permeability transition: A speculative model showing some of the components of the permeability transition pore (36). In the open configuration, water and solutes enter the matrix, causing matrix swelling and outer membrane disruption, leading to release of cytochrome c and other proteins (imm = inner mitochondrial membrane, omm = outer mitochondrial membrane).

The significance of cytochrome c release is twofold. (a) As cytochrome c is the penultimate link in the electron transport chain, its loss will impair ATP generation and increase formation of ROS, and thus potentially drive the cell toward cell death. (b) Simultaneously, the released cytochrome c (and other proteins set free from the intermembrane space) represents a signal or an initial link in the chain of events directing the cell to the apoptotic pathway. Upon binding, together with ATP, to an adapter protein (Apaf-1), cytochrome c can induce proteolytic cleavage of the Apaf-1-bound latent procaspace-9 to active caspase-9 and thereby execute apoptosis.

Such mitochondria might be incapable of synthesizing ATP. If so, then even glycolysis may become compromised by the insufficient ATP supply. A complete bioenergetic catastrophe ensues in the cell if the metabolic disorder evoked by the toxic agent is so extensive that most or all mitochondria in a cell undergo MPT, causing depletion of ATP on the cellular level, which in the end causes a complete failure of maintenance of cellular structure and function possibly culminating in cell death.

5.3.5. Cell Death

5.3.5.1. Mechanisms of Cell Death

Toxic cell death can occur via two processes, which are fundamentally different in their nature and biological significance (37). These are termed necrosis and apoptosis. “Apoptosis” comes from the ancient Greek meaning “falling off petals from a flower” or “falling off leaves from a tree”. The name refers to the morphological feature of formation of apoptotic bodies from a cell (38).

Necrosis or „accidental“ cell death was the classic model and was thought to be the universal mode of cell death until apoptosis was identified in 1972 as a separate mode of cell death. Necrotic cell death is the typical consequence of severe acute cellular injury, such as occurs in strokes or heart

attacks. The cellular events leading up to necrotic cell death are somewhat variable from one cell type to another, but certain events occur regularly. One of the earliest changes is the formation of protrusions of the plasma membrane, called blebs. Cellular swelling accompanies this formation. Irreversible injury occurs when one of these blebs ruptures, leading to failure of the plasma membrane permeability barrier, release of intracellular enzymes and metabolites, and collapse of electrical and ionic gradients across the plasma membrane.

Apoptosis, unlike necrosis, is a form of physiological cell death that causes cell deletion without inflammation and describes a process of controlled cell deletion and that has an opposite role to mitosis in the regulation of cell population. In apoptosis, cells begin a characteristic sequence of structural and biochemical changes. These changes include cell shrinkage, alteration of plasma membrane lipids, condensation of chromatin, DNA degradation, and shedding of membrane-bound cytoplasmatic fragments containing organelles and chromatin. These apoptotic bodies are taken up by macrophages. One major pathway for the induction of apoptosis is the receptor-mediated or extrinsic pathway. The receptors triggering this pathway are located in the plasma membrane and are activated by extracellular ligands. Typical death receptors are Fas (also called CD-95) and tumor-necrosis factor receptor (TNF-R). The receptor-induced pathway leads to recruitment of capsase-8 or -10 to the death signaling complex without involving mitochondria at this stage. However, mitochondria are engaged through the formation of tBid (Bcl-2 protein family) at a later stage, leading to amplification of the signal (38). The mitochondrial pathway is activated by a variety of extra- and intracellular stresses, including oxidative stress and treatment with cytotoxic drugs. Members of the protein family Bcl-2 modify and regulate apoptotic pathways by a variety of either pro (Bax, Bak, Bid) and antiapoptotic proteins (Bcl-2, Bcl-X_L). They up or down-regulate the caspase cascade or act on mitochondria directly. The apoptotic signal leads to the release of cytochrome c from the mitochondrial intermembrane space into the cytosol, where it binds to the Apoptotic Protease Activation Factor (Apaf-1). This triggers the activation of caspases (38).

5.3.5.2. Role of Mitochondria in Cell Death

It appears that most if not all chemical-induced cell death will involve mitochondria, the resulting mitochondrial dysfunction may ultimately trigger either necrosis or apoptosis and that MPT is a crucial event in both (see Figure 5). Given the importance of mitochondria for cell life, it comes as no surprise that mitochondrial dysfunction and failure leads to cell death (35). The decisive mitochondrial events in cell death are MPT and release of cytochrome c, thus caspase activation.

As already pointed out, there are several common features in the process of apoptosis and necrosis. It is of interest to know that toxic agents can cause both apoptosis and necrosis (39, 40). Many substances induce apoptosis at low but necrosis at higher doses (40, 41) .In addition, induction of cell death by cytotoxic agents may involve similar metabolic disturbances and most importantly MPT (33-35). So, regulatory mechanisms underlying apoptosis and necrosis partially on the mitochondrial level (42, 43). What determines, then, whether an injured cell undergoes apoptosis or necrosis – which may have a significant impact on the surrounding tissue? Recent findings suggest that the availability of ATP is critical determining the form of cell death. Lack of ATP depletion favors the execution of the apoptotic program, which involves ATP-requiring steps, one of which is formation of the complex between Apaf-1, cytochrome c and the procaspase-9 (44). For instance, cells triggered

to undergo apoptosis are instead forced to die by necrosis when energy levels are rapidly compromised. Thus, the initial death signal is propagated without leading to apoptosis.

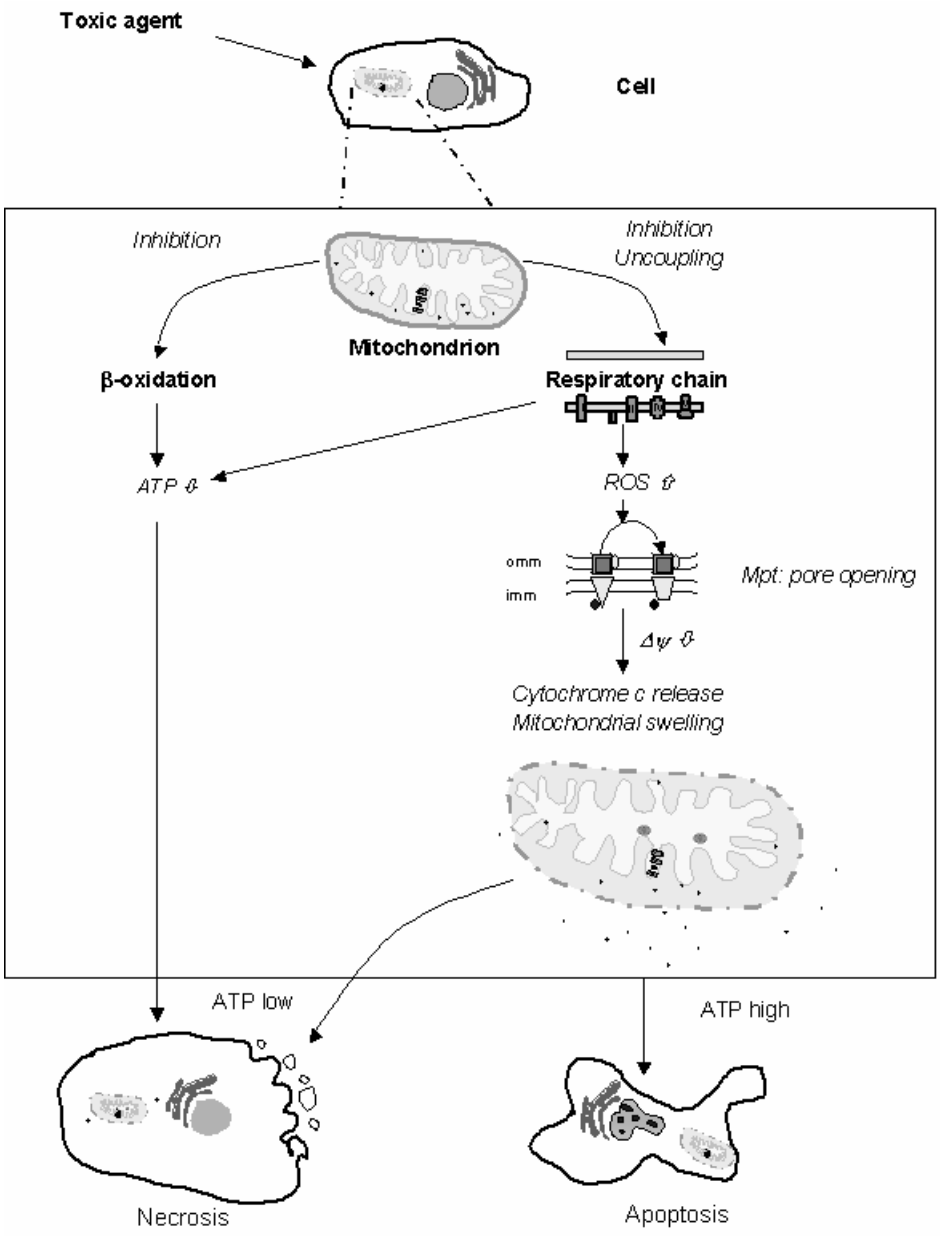

Figure 5: putative role of mitochondria in cell death induction
Mitochondrial toxins can inhibit β-oxidation and the respiratory chain, leading to a decrease in mitochondrial and cellular ATP levels. Additionally, they can uncouple oxidative phosphorylation, which, in particular in combination with the inhibition of the electron transport, increases the generation of reactive oxygen species (ROS) leading to permeabilization of the mitochondrial membranes by opening of the mitochondrial permeability transition pore. This pore is located in the inner and outer mitochondrial membrane (imm and omm, respectively). The osmotically driven influx of water results in an increase in mitochondrial volume. Since the inner mitochondrial membrane is highly invaginated and thus expandable, an increase in volume can cause a rupture of the outer mitochondrial membrane. Proteins from the intermembrane space (i.e. cytochrome c) can be released into the cytoplasm and activate apoptotic pathways. If ATP stocks were highly depleted, the same triggers would lead to necrosis instead of apoptosis.

5.4. References

1. Gallo MA. History and Scope of Toxicology. In: Klaasen Cd, ed. Toxicology, The Basic Science of Poisons. 6th. New York: McGraw-Hill, 2001: 3-10.
2. Ballantyne B, Marrs TC, Turner P. Fundamentals of Toxicology. In: Ballantyne B, Marrs Tc,Turner P, ed. General & Applied Toxicology. Abridged Edition. London: The Macmillan Press, 1995: 3-38.
3. Eaton DL, C. KD. Principles of Toxicology. In: C Kd, ed. Toxicology, The Basic Science of Poisons. 6th. New York: McGraw-Hill, 2001: 11-34.
4. Pessayre D, Mansouri A, Haouzi D, Fromenty B. Hepatotoxicity due to mitochondrial dysfunction. Cell Biol Toxicol 1999; 15: 367-373.
5. Lang C, Berardi S, Schafer M, Serra D, Hegardt FG, Krahenbuhl L, Krahenbuhl S. Impaired ketogenesis is a major mechanism for disturbed hepatic fatty acid metabolism in rats with long-term cholestasis and after relief of biliary obstruction. J Hepatol 2002; 37: 564-571.
6. Castellani R, Hirai K, Aliev G, Drew KL, Nunomura A, Takeda A, Cash AD, et al. Role of mitochondrial dysfunction in Alzheimer's disease. J Neurosci Res 2002; 70: 357-360.
7. Holt IJ, Harding AE, Morgan-Hughes JA. Deletions of muscle mitochondrial DNA in patients with mitochondrial myopathies. Nature 1988; 331: 717-719.
8. Wallace DC, Singh G, Lott MT, Hodge JA, Schurr TG, Lezza AM, Elsas LJ, 2nd, et al. Mitochondrial DNA mutation associated with Leber's hereditary optic neuropathy. Science 1988; 242: 1427-1430.
9. Cohen BH, Gold DR. Mitochondrial cytopathy in adults: what we know so far. Cleve Clin J Med 2001; 68: 625-642.
10. Nulton-Persson AC, Szweda LI, Sadek HA. Inhibition of cardiac mitochondrial respiration by salicylic acid and acetylsalicylate. J Cardiovasc Pharmacol 2004; 44: 591-595.
11. Oh KW, Qian T, Brenner DA, Lemasters JJ. Salicylate enhances necrosis and apoptosis mediated by the mitochondrial permeability transition. Toxicol Sci 2003; 73: 44-52.
12. Trost LC, Lemasters JJ. Role of the mitochondrial permeability transition in salicylate toxicity to cultured rat hepatocytes: implications for the pathogenesis of Reye's syndrome. Toxicol Appl Pharmacol 1997; 147: 431-441.
13. Al-Nasser IA. Salicylate-induced kidney mitochondrial permeability transition is prevented by cyclosporin A. Toxicol Lett 1999; 105: 1-8.
14. Boelsterli UA. Diclofenac-induced liver injury: a paradigm of idiosyncratic drug toxicity. Toxicol Appl Pharmacol 2003;1 92: 307-322.
15. Salgueiro-Pagadigorria CL, Kelmer-Bracht AM, Bracht A, Ishii-Iwamoto EL. Naproxen affects Ca(2+) fluxes in mitochondria, microsomes and plasma membrane vesicles. Chem Biol Interact 2004; 147 :49-63.
16. Irwin W, Fontaine E, Agnolucci L, Penzo D, Betto R, Bortolotto S, Reggiani C, et al. Bupivacaine myotoxicity is mediated by mitochondria. J Biol Chem 2002; 277: 12221-12227.
17. Berson A, Fau D, Fornacciari R, Degove-Goddard P, Sutton A, Descatoire V, Haouzi D, et al. Mechanisms for experimental buprenorphine hepatotoxicity: major role of mitochondrial dysfunction versus metabolic activation. J Hepatol 2001; 34: 261-269.
18. Spaniol M, Bracher R, Ha HR, Follath F, Krahenbuhl S. Toxicity of amiodarone and amiodarone analogues on isolated rat liver mitochondria. J Hepatol 2001; 35: 628-636.

19. Sales SD, Hoggard PG, Sunderland D, Khoo S, Hart CA, Back DJ. Zidovudine phosphorylation and mitochondrial toxicity in vitro. Toxicol Appl Pharmacol 2001; 177: 54-58.
20. Mahler H, Pasi A, Kramer JM, Schulte P, Scoging AC, Bar W, Krahenbuhl S. Fulminant liver failure in association with the emetic toxin of Bacillus cereus. N Engl J Med 1997; 336: 1142-1148.
21. Schafer DF, Sorrell MF. Power failure, liver failure. N Engl J Med 1997; 336: 1173-1174.
22. Einarson TR. Drug-related hospital admissions. Ann Pharmacother 1993; 27: 832-840.
23. Beard K. Adverse reactions as a cause of hospital admission in the aged. Drugs Aging 1992; 2: 356-367.
24. Lazarou J, Pomeranz BH, Corey PN. Incidence of adverse drug reactions in hospitalized patients: a meta-analysis of prospective studies. Jama 1998; 279: 1200-1205.
25. Gonzalez-Martin G, Caroca CM, Paris E. Adverse drug reactions (ADRs) in hospitalized pediatric patients. A prospective study. Int J Clin Pharmacol Ther 1998; 36: 530-533.
26. Vargas E, Terleira A, Hernando F, Perez E, Cordon C, Moreno A, Portoles A. Effect of adverse drug reactions on length of stay in surgical intensive care units. Crit Care Med 2003; 31 :694-698.
27. Peyriere H, Cassan S, Floutard E, Riviere S, Blayac JP, Hillaire-Buys D, Le Quellec A, et al. Adverse drug events associated with hospital admission. Ann Pharmacother 2003; 37: 5-11.
28. Routledge PA, O'Mahony MS, Woodhouse KW. Adverse drug reactions in elderly patients. Br J Clin Pharmacol 2004; 57: 121-126.
29. Boelsterli UA. Mechanistic Toxicology. London & New York: Taylor & Francis Group, 2003: 231-233.
30. Gregus Z, Klaasen CD. Mechanisms of Toxicology. In: Klaasen Cd, ed. Toxicology, The Basic Science of Poisons. 6th. New York: McGraw-Hill, 2001: 35-82.
31. Young TA, Cunningham CC, Bailey SM. Reactive oxygen species production by the mitochondrial respiratory chain in isolated rat hepatocytes and liver mitochondria: studies using myxothiazol. Arch Biochem Biophys 2002; 405: 65-72.
32. Hildeman DA, Mitchell T, Teague TK, Henson P, Day BJ, Kappler J, Marrack PC. Reactive oxygen species regulate activation-induced T cell apoptosis. Immunity 1999; 10: 735-744.
33. Lemasters JJ, Nieminen AL, Qian T, Trost LC, Elmore SP, Nishimura Y, Crowe RA, et al. The mitochondrial permeability transition in cell death: a common mechanism in necrosis, apoptosis and autophagy. Biochim Biophys Acta 1998; 1366: 177-196.
34. Kroemer G, Dallaporta B, Resche-Rigon M. The mitochondrial death/life regulator in apoptosis and necrosis. Annu Rev Physiol 1998; 60: 619-642.
35. Lemasters JJ, Qian T, Bradham CA, Brenner DA, Cascio WE, Trost LC, Nishimura Y, et al. Mitochondrial dysfunction in the pathogenesis of necrotic and apoptotic cell death. J Bioenerg Biomembr 1999; 31: 305-319.
36. Green DR, Reed JC. Mitochondria and apoptosis. Science 1998;281:1309-1312.
37. Kerr JF, Wyllie AH, Currie AR. Apoptosis: a basic biological phenomenon with wide-ranging implications in tissue kinetics. Br J Cancer 1972; 26: 239-257.
38. Lawen A. Apoptosis-an introduction. Bioessays 2003; 25: 888-896.
39. Corcoran GB, Fix L, Jones DP, Moslen MT, Nicotera P, Oberhammer FA, Buttyan R. Apoptosis: molecular control point in toxicity. Toxicol Appl Pharmacol 1994; 128: 169-181.
40. Kroemer G. The pharmacology of T cell apoptosis. Adv Immunol 1995; 58: 211-296.

41. Hirsch T, Susin SA, Marzo I, Marchetti P, Zamzami N, Kroemer G. Mitochondrial permeability transition in apoptosis and necrosis. Cell Biol Toxicol 1998; 14: 141-145.
42. Kroemer G, Reed JC. Mitochondrial control of cell death. Nat Med 2000; 6: 513-519.
43. Reed JC, Kroemer G. Mechanisms of mitochondrial membrane permeabilization. Cell Death Differ 2000; 7: 1145.
44. Nicotera P, Leist M, Ferrando-May E. Intracellular ATP, a switch in the decision between apoptosis and necrosis. Toxicol Lett 1998; 102-103: 139-142.

6. Aims of the thesis

This thesis contains four publications on toxicity, covering several aspects of this field. All of them have a mutual underlying interest in learning more about mechanisms of toxicity. It needs thorough and profound knowledge on what is going wrong, before countermeasures can be tackled in order to prevent complications after drug treatment. Even though the aim of the “magic bullet” might never be reached it should be approached stepwise towards a more “tailor made” medicine. In order to do this, in a first step, several analytical methods and assays need to be established and set up.

The aim of the first project was to study basic principles of toxicity. The interest in the study of an animal model for carnitine deficiency due to treatment with trimethylhydraziniumpropionate (THP) was twofold. First, knowledge on the pathogenesis of carnitine deficiency was generated, and secondly, general principles of mitochondrial toxicity and its consequences like liver steatosis were analyzed and elucidated.

The second project was looking into induction of hepatic toxicity due therapy with benzarone and benzbromarone. The idea to conduct this study derived from case reports about hepatic failure after treatment with benzbromarone/benzarone with knowledge on the structural similarity to the well-known hepatic toxin amiodarone in the back of the head. Besides amiodarone, also benzofuran and 2-butylbenzofuran were included in the study, in order to gain more insight into chemical structures responsible for toxicity.

The focus of the third project was on mitochondrial toxicity on the muscular level. Statins are known to cause rhabdomyolysis dose-dependently in rare cases. The mechanism responsible has not been clear yet but mitochondria have been claimed to be responsible, at least in part. The question raised by this project was whether mitochondrial toxicity can indeed be blamed for muscular side effects of statin therapy. Basic concepts of mitochondrial liver toxicity established in the preceding projects were expanded into and adapted for skeletal muscle tissue.

Last but not least, the fourth project again found its origin in the clinics but dealing with another aspect of drug toxicity, namely drug-drug interactions. A patient happened to suffer from veno-occlusive disease under a low dose, thus immunosuppressive treatment of an anticancer drug shortly after having added a macrolide antibiotic to the therapy (see appendix). The aim of the study was to clarify whether a drug-drug interaction was responsible for the complication emerged from this therapy and if so what the underlying mechanism was.

7. Mechanisms of liver steatosis in rats with systemic carnitine deficiency due to treatment with trimethylhydraziniumpropionate

Markus Spaniol[1], Priska Kaufmann[1], Konstantin Beier[2], Jenny Wüthrich[1], Hubert Scharnagl[3], Winfried März[3], Stephan Krähenbühl[1]

[1]Division of Clinical Pharmacology and Toxicology, University Hospital, Basel, Switzerland, [1]Institute of Anatomy, University of Basel, Switzerland and [3]Division of Clinical Chemistry, Department of Medicine, Albert Ludwigs-University, Freiburg, Germany

Journal of Lipid Research 2003;44:144-53

7.1. Summary

Rats with systemic carnitine deficiency induced by treatment with trimethylhydraziniumpropionate (THP) develop liver steatosis. This study aims to investigate the mechanisms leading to steatosis in THP-induced carnitine deficiency. Rats were treated with THP (20 mg/100 g) for 3 or 6 weeks and were studied after starvation for 24 h. Rats treated with THP had reduced in vivo palmitate metabolism and developed mixed liver steatosis at both time points. The hepatic carnitine pool was reduced in THP-treated rats by 65% to 75% at both time points. Liver mitochondria from THP-treated rats had increased oxidative metabolism of various substrates and of β-oxidation at 3 weeks, but reduced activities at 6 weeks of THP treatment. Ketogenesis was not affected. The hepatic content of CoA was increased by 23% at 3 weeks and by 40% at 6 weeks in THP treated rats. The cytosolic content of long-chain acyl-CoAs was increased and the mitochondrial content decreased in hepatocytes of THP treated rats, compatible with decreased activity of carnitine palmitoyltransferase I in vivo. THP-treated rats showed hepatic peroxisomal proliferation and increased plasma VLDL triglyceride and phospholipid concentrations at both time points. A reduction in the hepatic carnitine pool is the principle mechanism leading to impaired hepatic fatty acid metabolism and liver steatosis in THP-treated rats. Cytosolic accumulation of long-chain acyl-CoAs is associated with increased plasma VLDL triglyceride, phospholipid concentrations, and peroxisomal proliferation.

7.2. Introduction

Liver steatosis is a frequent finding in liver biopsies and a frequent cause of asymptomatic elevation of transaminases (1). Several risk factors have been identified, among them ingestion of certain drugs (2-5), alcohol abuse (6), viral hepatitis (7), diabetes (8), increased body weight (8, 9), and intoxications (10). While impaired mitochondrial β-oxidation is considered to be the principle cause for microvesicular steatosis (11), the mechanisms leading to macrovesicular steatosis have so far not been identified in detail. As shown in Fig. 1**,** important possibilities leading to this finding include a decrease in VLDL export and/or an increase in VLDL formation, which may result from impaired mitochondrial fatty acid metabolism or from other causes.

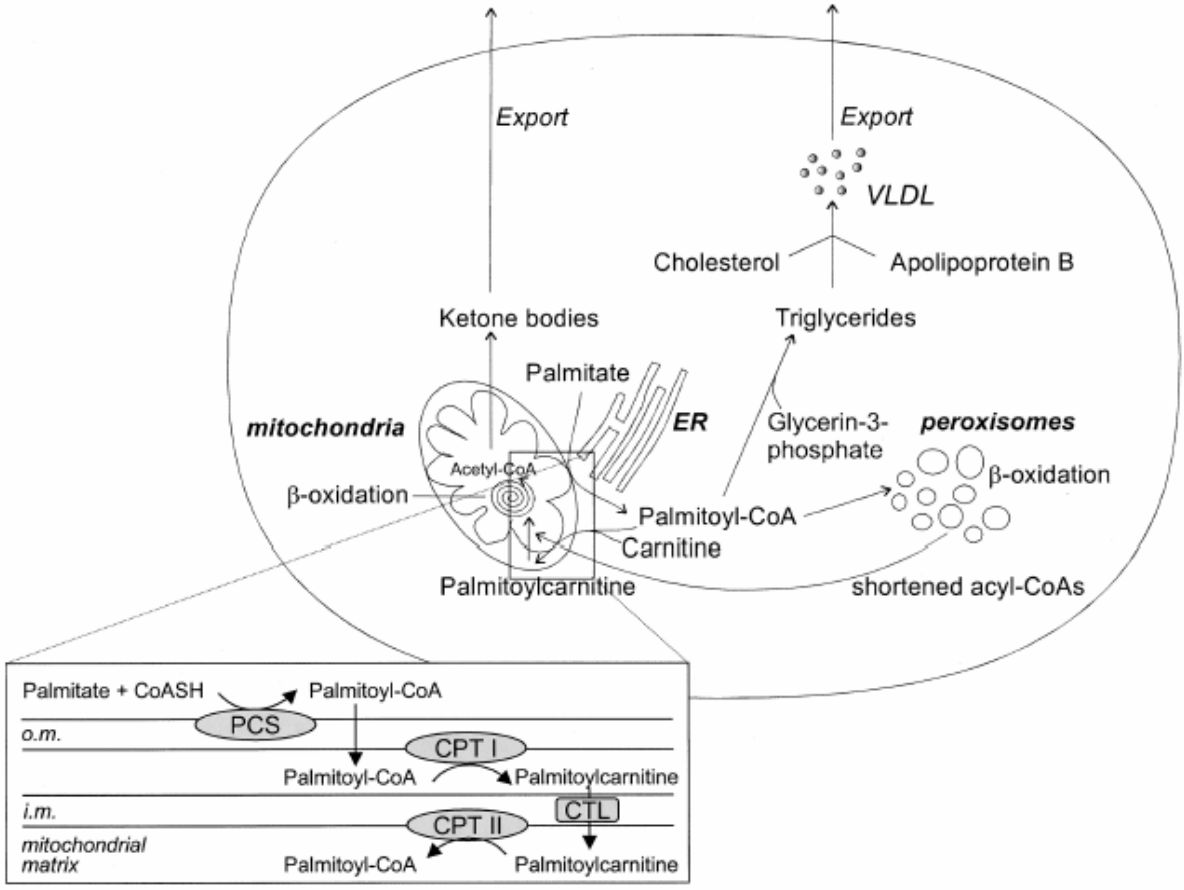

Figure 1: Hepatic metabolism of long-chain fatty acids. Palmitate and other long-chain fatty acids are activated by palmitoyl-CoA (PCS) on the outer mitochondrial membrane, converted to palmitoylcarnitine by carnitine palmitoyltransferase I (CPT I), transported into the mitochondrial matrix and reconverted to palmitoyl-CoA by CPT II (see magnification). Palmitoyl-CoA is degraded to acetyl-CoA by the β-oxidation cycle. Acetyl-CoA can be converted to ketone bodies (major pathway) or be degraded in the Krebs cycle. Palmitoyl-CoA can also be β-oxidized by peroxisomes, which produce medium-chain acyl-CoAs that are converted to the corresponding acyl-carnitines and can be metabolized to acetyl-CoA by mitochondria. In addition, cytosolic palmitoyl-CoA can also be used for the formation of triglycerides and phospholipids, which are both substrates for the formation of VLDL particles. See text for additional explanations. CTL, carnitine-acylcarnitine translocase, i.m., inner mitochondrial membrane, o.m., outer mitochondrial membrane.

We have recently developed and characterized a rat model with systemic carnitine deficiency (12). In this model, carnitine deficiency is induced within 3 weeks by feeding trimethylhydraziniumpropionate (THP), which inhibits carnitine biosynthesis and increases renal excretion of carnitine. Interestingly, rats treated with THP develop combined micro- and macrovesicular liver steatosis within 3 weeks but have no macro- or microscopic accumulation of lipids in skeletal muscle or heart (12, 13). Since carnitine is essential for transport of long-chain fatty acids into the mitochondrial matrix (14), it can be speculated that at least the microvesicular part of liver steatosis in THP-treated rats could be caused by hepatic carnitine deficiency. In support of this assumption, both in children with primary systemic carnitine deficiency and in mice with systemic carnitine deficiency (JVS mice), microvesicular liver steatosis has been reported (15, 16). However, at least the macrovesicular part of liver steatosis in rats treated with THP cannot be explained by an

isolated defect in mitochondrial β-oxidation of fatty acids, suggesting additional mechanisms. Since the morphology of liver steatosis in THP-treated rats resembles that found in certain types of steatotic livers in humans, e.g., certain types of alcohol-induced liver steatosis (17) or steatosis observed during administration of amiodarone (18), knowledge about the mechanisms leading to liver steatosis in THP-treated rats may also be relevant for understanding this disease in humans. We therefore decided to study the mechanisms leading to liver steatosis in rats treated with THP for 3 or 6 weeks. Beside the mechanisms leading to liver steatosis, we also investigated adaptive changes secondary to a decrease in the hepatic carnitine pool and to impaired in vivo mitochondrial β-oxidation. Our studies demonstrate that hepatic carnitine deficiency is the most important cause for liver steatosis in THP-treated rats and suggest that reduced mitochondrial fatty acid oxidation may be partially compensated by increased peroxisomal fatty acid metabolism due to proliferation of peroxisomes.

7.3. Materials and Methods

7.3.1. Induction of carnitine deficiency in vivo palmitate metabolism

The experiments have been reviewed and accepted by the State Ethics Committee of animal research. Carnitine deficiency was induced in male Sprague-Dawley rats by feeding vegetarian food poor in carnitine (Kliba Futter 2435, Basel, Switzerland) and THP (20 mg/100 g/day) for 3 or 6 weeks (n = 6 rats for each time point) (12). Control rats were kept for the same periods of time with the same rat chow ad libitum (n = 12). In order to investigate a potential toxic effect on mitochondrial metabolism by THP itself in vivo, rats (n = 3 in each group) were treated with THP (20 mg/100 g/day), with l-carnitine (50mg/100 g/day), or with the combination of THP and l-carnitine (same dosages) for 3 weeks. Metabolism of palmitate was determined in vivo after 3 weeks of treatment with THP by intraperitoneal injection of [^{14}C]palmitate and determination of exhaled $^{14}CO_2$ as described previously (19).

7.3.2. Isolation of rat liver mitochondria

Rats were killed by decapitation and mitochondria were isolated from the liver by differential centrifugation according to a previously described method (20). This method yields mitochondria of high purity with only minor contamination by peroxisomes or lysosomes (21). The mitochondrial protein content was determined using the biuret method with bovine serum albumin as a standard (22). The content of mitochondrial protein per g liver was determined by correcting for the recovery of the mitochondria isolated using the activities of citrate synthase and succinate dehydrogenase as described previously (21).

7.3.3. Oxidative metabolism of intact mitochondria

Oxygen consumption by freshly isolated liver mitochondria was measured in a chamber equipped with a Clark-type oxygen electrode (Yellow Springs Instruments, Yellow Springs, OH) at 30°C as described previously (23). The concentrations of the substrates used were 20 mmol/L for L-glutamate and succinate, 40 μmol/L for palmitoyl-L-carnitine, 20 μmol/L for palmitoyl-CoA and 80 μmol/L for palmitate. All incubations with fatty acids contained 5 mmol/L L-malate, incubations with

palmitoyl-CoA and palmitate contained in addition 2 mmol/L L-carnitine and incubations with palmitate contained in addition 250 μmol/L ATP and 250 μmol/L CoASH.

7.3.4. In vitro mitochondrial β-oxidation and formation of ketone bodies

The β-oxidation of [1-^{14}C] palmitic acid by liver mitochondria was assessed as described by Fréneaux et al. (24) with some modifications described previously (25). This assay measures the formation of acid-soluble products from mitochondrial palmitate metabolism, which equals production of ketone bodies and citric acid cycle intermediates (24). Ketone body formation was measured using freeze-thawed mitochondria according to Chapman et al. (26) with some modifications as described previously (25). The reactions were stopped by adding 100 µl of 30% perchloric acid (w/v). After having removed the precipitate by centrifugation, the supernatants were analyzed for acetoacetate according to Olsen (27).

7.3.5. Activities of the enzyme complexes of the respiratory chain

Complex I (NADH:decylubiquinone-1 oxidoreductase) was determined spectrophotometrically as described by Veitch et al. (28) with some modifications. Briefly, 0.1 mg mitochondria were preincubated in 35 mmol/L potassium phosphate buffer pH 7.4, 5 mmol/L magnesium chloride, 2 mmol/L potassium cyanide, and 60 µmol/l decylubiquinone at 30°C. The reaction was started by the addition of 0.13 mmol/L NADH and the decrease of absorption was recorded spectrophotometrically at 340 nm using rotenone as inhibitor. Complex II (succinate:dichloroindophenol oxidoreductase) was determined according to a previously described method (23). This method is based on the reduction of dichloroindophenol by complex II using succinate as a substrate. The reaction is followed spectrophotometrically at 600 nm in the presence and absence of the inhibitor thenoyltrifluoroacetone. Complex III ubiquinol:ferricytochrome c oxidoreductase) was determined spectrophotometrically at 550 nm by the conversion of ferricytochrome c to ferrocytochrome c using decylubiquinol as substrate (29). The reaction velocity was assessed as the difference in absorption with and without antimycin as inhibitor. Complex IV (cytochrome c oxidase) activity was measured by following the oxidation of ferrocytochrome c at 550 nm as described by Wharton and Tzagaloff (30).

7.3.6. Determination of CoA and carnitine

Liver samples (about 50 mg/1 mL, prepared without thawing) were homogenized in 3% perchloric acid and centrifuged for 5min at 10,000*g* . Mitochondria (100µL corresponding to about 10 mg protein) were mixed with 20µL 0.2 mol/L dithiothreitol and precipitated with 1.88 mL3.2% perchloric acid. The suspension was vortexed, kept on ice for 5 min, and then centrifuged for 10 min at 10,000*g*. This perchloric acid treatment yields an acid soluble (supernatant) and an acid insoluble fraction (pellet). The acid soluble fraction is used to measure free and acetyl-CoA and, after alkaline hydrolysis, total acid soluble CoA. The difference between these values represents short chain acyl-CoA. Long chain CoA is determined in the pellet after alkaline hydrolysis. Total CoA refers to the sum of total acid soluble CoA and longchain acyl-CoA. In these fractions, CoASH and acetyl-CoA, total acid soluble CoA (supernatant), and long-chain acyl-CoA (pellet) were determined using the CoA recycling assay of Allred and Guy (31), with some modifications in the work-up as described before (32). Since the CoA recycling assay does not differentiate CoASH and acetyl-CoA, acetyl-CoA was

determined specifically using a radioenzymatic assay as described previously (33). For the determination of carnitine, liver tissue was worked up as described above for CoA. Plasma was also treated with perchloric acid (final concentration 3%) to obtain a supernatant and a pellet. The determination of carnitine in these fractions was performed using the radioenzymatic assay described by Brass and Hoppel (34). Direct analysis of the supernatant yields free carnitine, and, after alkaline hydrolysis, total acid soluble carnitine. The difference between free and total acid soluble carnitine is the short-chain acylcarnitine fraction (up to a chain-length of the acyl-group of about 10). Long-chain acylcarnitines were determined in the pellet after alkaline hydrolysis. Addition of total acid soluble and long-chain acylcarnitine yields total carnitine.

7.3.7. Lipid determinations in liver

Lipids from rat livers were extracted according to the method described by Bligh and Dyer (35). Briefly, about 100 mg of liver tissue were homogenized in 2 ml 20 mmol/L potassium phosphate buffer, pH 7.4, and the lipids were extracted by the addition of 5.0 ml chloroform-methanol (1:1, v/v). The samples were vortexed and incubated for 60 min under periodical stirring. Then, 2.5 mL chloroform and 0.8 mL 0.74% potassium chloride were added and the mixture centrifuged for 5 min at 500 *g* . The lower phase was separated and washed with 1.5 mL of a mixture containing 0.74% potassium chloride-chloroform-methanol (94:96:6, v/v/v). The organic phase was then evaporated to dryness and the lipid extract stored at –20° C until analysis. For lipid determination, liver extracts were resuspended in 250µL isopropanol. Total cholesterol, triacylglycerides, and free fatty acids were measured using enzymatic methods and reagents from Wako (Neuss, Germany). The measurements were calibrated using standards from Roche Diagnostics (Mannheim, Germany).

7.3.8. Determination of plasma lipids

Total cholesterol (TC), free cholesterol (FC), triacylglycerides (TG), phospholipids (PL), HDL cholesterol (HDL-C), and free fatty acids (FFA) were measured using enzymatic methods and reagents from Wako (Neuss, Germany). The measurements were performed on a Wako 30R automatic analyzer (Wako) and were calibrated using standards from Roche Diagnostics (Mannheim, Germany). Esterified cholesterol was calculated as the difference between TC and FC. The determination of the lipoprotein fractions was performed by a combined ultracentrifugation-precipitation method (36, 37). VLDL were removed quantitatively by ultracentrifugation using a TFT 56.6 rotor (Kontron, Germany) with adapters for 0.8 mL polycarbonate tubes. Five hundred microliters of plasma was pipetted into tubes and 0.1 mL of 0.9% sodium chloride solution was layered on top of the plasma. After centrifugation (18 h at 30,000 rpm, 10°C), the floating VLDL fraction was aspired with a 2 mL syringe until the supernatant was completely clear. The volume was reconstituted to the original weight with 0.9% saline. LDL were precipitated in the infranatant using phosphotungstic acid/magnesium chloride (PTA, Roche, Mannheim, Germany), and HDL lipids were measured in the supernatant after LDL precipitation. Lipids in the LDL fraction were calculated as the difference between the concentrations in the density fraction d > 1.006 kg/L and the HDL fraction.

7.3.9. Cytochemical localization of catalase in liver sections

Livers from control rats and rats treated with THP for 3 weeks were fixed by perfusion through the portal vein with a fixative containing 0.25% glutaraldehyde and 2% sucrose in 0.1 mol/L PIPES buffer, pH 7.4. The tissue was cut into 70 μm sections with a DSK-Microslicer (Dosaka EM Co., Kyoto, Japan). The sections were incubated in alkaline diaminobenzidine (DAB) medium for cytochemical visualization of catalase (38), followed by osmication and embedding in Epon 812.

7.3.10. SDS-PAGE and immunoblotting

For Western blotting, tissues were homogenized in a buffer containing 250 mmol/L sucrose, 5 mmol/L MOPS, 1 mmol/L EDTA, 0.1 % ethanol, pH 7.4, using an Ultra-Turrax (IKA Labortechnik, Staufen, Germany). Equal amounts of protein (20 μg per sample) were subjected to SDS-PAGE. After electrotransfer of the polypeptides onto nitrocellulose the sheets were incubated overnight with the primary antibody at a concentration of 1 μg protein/mL. The polyclonal antibody against acyl-CoA oxidase (AOX) was a generous gift of Prof. Dr. A. Völkl, Institute of Anatomy and Cell Biology, University of Heidelberg. Its specificity was assessed as described previously (39). After repeated washing, a peroxidase conjugated goat anti-rabbit antibody (Sigma, München, Germany) was added for 1 h at room temperature. The immunoreactive bands were visualized by enhanced chemoluminescence (ECL, Amersham International, Little Chalfont, England) according to the manufacturer's protocol.

The blots for subunit IV of cytochrome c oxidase and apolipoprotein B were performed according to the method described above. The polyclonal antibody against subunit IV of cytochrome c oxidase was obtained from molecular probes (Juro Supply, Lucerne, Switzerland) and used at a dilution of 0.5μg/mL. The polyclonal antibody against apolipoprotein B was obtained from LabForce AG (4208 Nunningen, Switzerland) and used at a dilution of 0.5μg/mL.

7.3.11. Determination of acyl-CoA oxidase activity

Acyl-CoA oxidase activity was determined according to a previously described method (40). This method is based on the production of hydrogen peroxide by the action of acyl-CoA oxidase which is measured spectrophotometrically at 502 nm using dichlorofluorescein diacetate as a chromophore. Briefly, 50 mg of frozen liver tissue were homogenized in 20 mmol/L potassium phosphate buffer, pH 7.4, and the volume made up to 2.0 mL. 100 μL of this homogenate were preincubated in 1.9 mL of 10 mmol/L potassium phosphate buffer pH 7.4 containing 0.05 mg 2',7' dichlorfluorescein diacetate, 5.2 mg sodium azide, 74 mU horse radish peroxidase and 0.01% Triton-X at 37° C for 5 minutes. The reaction was started by the addition of 15 μmol/L palmitoyl-CoA and the increase in absorbance was recorded spectrophotometrically over 3 minutes at 502 nm. Activities were calculated using an extinction coefficient of 91'000 l x mol^{-1} x cm^{-1}.

7.3.12. Statistics

Data are presented as mean SD. Groups were compared using the Student's *t*-test (comparison of two groups) or ANOVA followed by Tukey's protected Student's *t*-test (> 2 groups).

Since the values of control animals were generally not different between 3 and 6 weeks, they were pooled unless indicated otherwise.

7.4. Results

The studies were carried out to find out the principle mechanisms leading to liver steatosis in rats with systemic carnitine deficiency due to treatment with THP. Rats were treated with THP for 3 or 6 weeks and studied after starvation for 24 hours. As shown in Figure 2, and in agreement with previous studies (12, 13), rats treated with THP for 3 weeks developed micro- and macrovesicular liver steatosis predominantly in zone I and II of the liver lobules. Similar findings were obtained after 6 weeks of treatment with THP (results not shown).

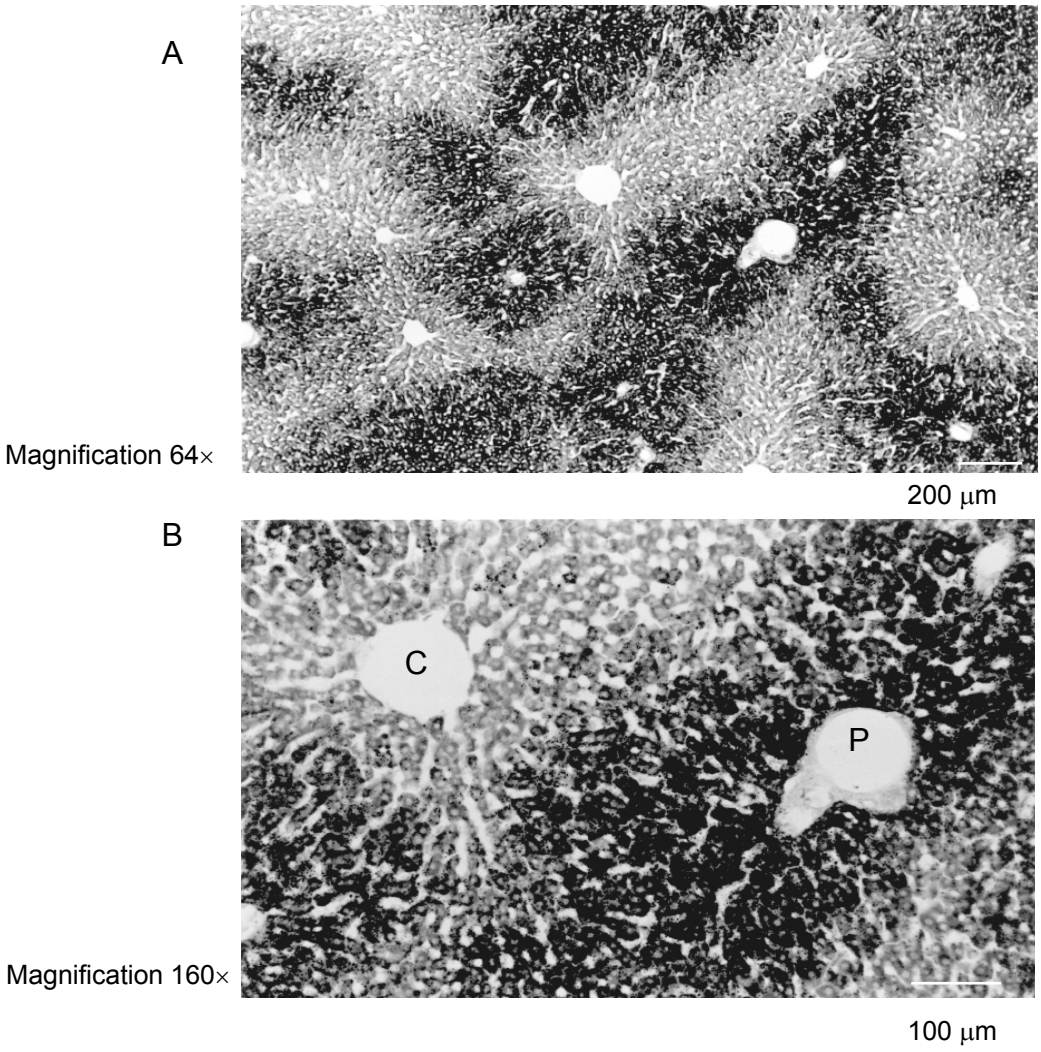

Figure 2: Liver steatosis in rats treated with THP for 3 weeks. Cryosections stained with Sudan Black for specific labeling of lipids. As shown in A (enlargement 64x), lipids accumulate predominantly in zones 1 and 2 of the liver lobules, while zone 3 is spared. A higher enlargement (Fig. 2B, enlargement 160x) shows that the size of the lipid droplets varies, small and larger droplets can be detected in most hepatocytes, in particular in the periportal regions. Similar findings were present after 6 weeks of treatment with THP. In comparison, livers from control animals contained no fat (not shown). P, portal vein; C, central vein.

Palmitate metabolism was assessed in vivo in rats treated with THP for 3 weeks and corresponding control rats by injecting l-[^{14}C]palmitate ip and measuring the amount of $^{14}CO_2$ exhaled over the next 2 h. The percentage of radioactivity exhaled was decreased in THP treated rats (28.2 ± 6.3% vs. 54.8 ± 8.2% of the dose injected, $P < 0.05$), compatible with reduced hepatic metabolism of long-chain fatty acids. Accordingly, the hepatic lipid content was increased significantly ($P < 0.05$) in rats treated with THP for 6 weeks for all lipid classes investigated [cholesterol 0.77 ± 0.09 vs. 0.58 ± 0.09 mg/g liver (THP-treated vs. control), triglycerides 4.63 ± 2.78 vs. 1.54 ± 0.46 mg/g liver, and free fatty acids 0.80 ±0.09 vs. 0.58 ± 0.02 µmol/g liver]. As can be seen in Fig. 1, reduced metabolism of longchain fatty acids can be due to impaired activation of fatty acids, impaired transport of fatty acids into the mitochondrial matrix, impaired β-oxidation and/or an impaired function of the respiratory chain. As expected from the mechanism by which THP reduces the body carnitine content, namely inhibition of carnitine biosynthesis and increased renal excretion of carnitine (12), the liver carnitine pool was reduced in THP-treated rats, showing a drop by ~ 70% in comparison to control rats (Table 1). Since carnitine is essential for the function of CPT I (Fig. 1), this finding may explain liver steatosis in THP-treated rats. Interestingly, both the short-chain acylcarnitine to free carnitine and the longchain acylcarnitine to free carnitine ratios were increased in livers of rats treated for 6 weeks, compatible with accumulation of β-oxidation intermediates due to impaired β-oxidation of fatty acids (23).

Table 1: Liver and plasma carnitine pool

	Control (n=12)	THP 3 weeks (n=6)	THP 6 weeks (n=6)
Liver (nmol/g liver wet weight)			
Free Cn	266 ± 73	74 ± 31[a]	75 ± 16[a]
SCA Cn	127 ± 52	38 ± 20[a]	51 ± 17[a]
LCA Cn	50 ± 21	14 ± 12[a]	26 ± 8[a]
Total Cn	442 ± 75	125 ± 3[a]	153 ± 27[a]
SCA Cn/Free Cn	0.48±0.13	0.51±0.15	0.68±0.15[a]
LCA Cn/Free Cn	0.19±0.07	0.19±0.12	0.35±0.09[ab]
Plasma (µmol/L)			
Free Cn	29.8 ± 9.3	5.6 ± 0.8[a]	4.6 ± 1.6[a]
SCA Cn	33.4 ± 12.9	5.4 ± 0.8[a]	4.9 ± 1.3[a]
LCA Cn	9.3 ± 1.5	1.6 ± 0.7[a]	1.6 ± 2.7[a]
Total Cn	72.6 ± 24.9	12.6 ± 0.7[a]	11.0 ± 4.2[a]

Cn, carnitine; LCA Cn, long-chain acylcarnitine; SCA Cn, short-chain acylcarnitine. Control and THP-treated rats (20 mg/100 g body weight) were studied after 3 or 6 weeks of treatment in the fasted state. The carnitine pools were determined by a radioenzymatic assay as described in Materials and Methods. Data are presented as mean ± SD.

a $P < 0.05$ versus control.

b $P < 0.05$ THP 6 weeks versus THP 3 weeks.

Since β-oxidation is primarily a mitochondrial function, these findings prompted us to study the function of the respiratory chain and oxidative metabolism of fatty acids in isolated mitochondria (Table

2). Surprisingly, state-3 oxidation rates tended to be higher in rats treated with THP for 3 weeks but were generally decreased in rats treated for 6 weeks. This decrease was observed particularly for succinate, palmitic acid, palmitoyl-CoA, and palmitoylcarnitine, suggesting a defect in the activity of complex II of the electron transport chain and of β-oxidation. It is noteworthy that the experiments with palmitate and palmitoyl-CoA were performed in the presence of exogenous carnitine. When no exogenous carnitine was added to these substrates, state-3 oxidation rates were not different between mitochondria of control and THP-treated rats, and were approximately only 10% of the rates obtained with control mitochondria in the presence of exogenous carnitine.

Table 2: State 3 oxidation rates by isolated rat liver mitochondria

	Control (n=12)	THP 3 weeks (n=6)	THP 6 weeks (n=6)
L-Glutamate (20mM)	82 ± 24	101 ± 17	80 ± 23
Succcinate (20mM)	150 ± 40	207 ± 31[a]	123 ± 31[b]
Palmitoyl-L-carnitine (40μM)	82 ± 26	116 ± 18[a]	62 ± 13[b]
Palmitoyl-CoA (20μM)	83 ± 17	97 ± 28	68 ± 14[b]
Palmitate (80μM)	46 ± 10	63 ± 14[a]	29 ± 10[ab]

Control and THP-treated rats (20 mg/100 g body weight) were studied after 3 or after 6 weeks of treatment in the fasted state. Mitochondria were isolated by differential centrifugation and state 3 oxidation rates were determined in the presence of the substrates indicated using a Clark-type oxygen electrode as described in Materials and Methods. Units are natoms oxygen x minute x 1 x milligram of mitochondrial protein^{-1}. Results are presented as mean ± SD.

a $P < 0.05$ versus control rats.

b $P < 0.05$ THP 6 weeks versus THP 3 weeks.

In order to exclude a major effect of carnitine deficiency on the mitochondrial electron transport chain, the activity of the enzyme complexes of the electron transport chain was determined. As shown in Table 3, the activities of complexes I to IV were unchanged or increased after 3 weeks of treatment with THP, when compared with control values. After 6 weeks of treatment, the activity of complex II was significantly decreased, whereas the activities of complex I, III, and IV were not altered in comparison to control rats. These findings agree well with the data obtained by the oxygen electrode.

Table 3: Activities of enzyme complexes of the electron transport chain in isolated rat liver mitochondria

	Control (n=12)	THP 3 weeks (n=6)	THP 6 weeks (n=6)
Complex I	17.5 ± 6.8	22.3 ± 12.6	15.5 ± 5.6
Complex II	12.0 ± 3.0	15.1 ± 5.9[a]	10.5 ± 4.1[b]
Complex III	1780 ± 440	1560 ± 340	1560 ± 420
Complex IV	419 ± 149	381 ± 195	367 ± 129

Control and THP treated rats (20 mg/100 g body weight) were studied after 3 or 6 weeks of treatment in the fasted state. Enzyme activities were determined using spectrophotometric methods as described in Materials and Methods. Units are mU x mg mitochondrial protein^{-1}. Data are presented as mean ± SD.
a $P < 0.05$ versus control rats.
b $P < 0.05$ THP 6 weeks versus THP 3 weeks.

Since reduced fatty acid oxidation could not be explained entirely by a reduced activity of the electron transport chain, we investigated the function of CPT I and of mitochondrial β-oxidation (Table 4). A direct toxic effect of THP on mitochondrial fatty acid metabolism was excluded, since THP did not impair CPT I activity or mitochondrial β-oxidation up to a concentration of 500 µmol/l and the addition of L-carnitine to THP prevented the development of liver steatosis in vivo (Fig. 3). CPT I activity, which can be rate-limiting for mitochondrial β-oxidation (41), was not different between mitochondria from THPtreated or control animals at 3 weeks, but showed a significant reduction in THP-treated rats at 6 weeks. Considering mitochondrial β-oxidation, no differences between THP-treated and control rats were observed after 3 weeks of treatment, whereas β-oxidation was reduced in rats treated with THP for 6 weeks. In contrast, ketogenesis was not affected at both time points. In agreement with ketogenesis, the β-hydroxybutyrate concentrations in liver and plasma were not different between control and THPtreated rats.

Table 4: In vitro β-oxidation and ketogenesis

	Control (n=12)	THP 3 weeks (n=6)	THP 6 weeks (n=6)
CPT I			
β-oxidation	0.86 ± 0.22	0.84 ± 0.2	0.45 ± 0.14[ab]
ketogenesis	15.0 ± 4.0	16.7 ± 6.3	16.4 ± 5.7
ketone bodies			
liver	1.96 ± 0.4	2.11 ± 0.5	1.94 ± 0.1
plasma	903 ± 189	829 ± 172	805 ± 165

Control rats and THP treated rats (20 mg/100 g body weight) were studied after 3 or 6 weeks of treatment in the fasted state. Activities were determined using radioactive substrates as described in Materials and Methods. Units are mU x mg mitochondrial protein^{-1} for CPT I activity, β-oxidation and ketogenesis and nmol x mg liver wet weight^{-1} and µmol x l^{-1} for ketone bodies in liver and plasma, respectively. Data are presented as mean ± SD.

a $P < 0.05$ versus control rats.

b $P < 0.05$ THP 6 weeks versus THP 3 weeks.

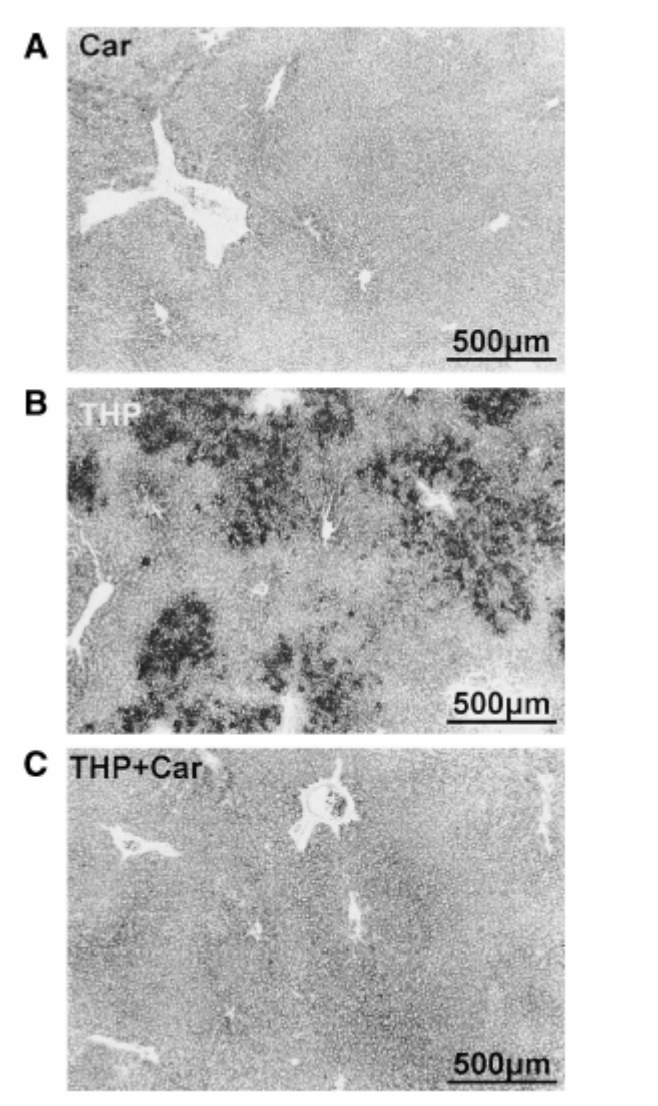

Figure 3: Effect of l-carnitine on liver steatosis in rats treated with THP for 3 weeks. Cryosections stained with Sudan Black for specific labeling of lipids (enlargement 44x). Treatment of l-carnitine (50 mg/100 g/day for 3 weeks) is not associated with accumulation of fat (A). Similar to Fig. 2, treatment with THP (20 mg/100 g/day for 3 weeks) is associated with fat accumulation in the periportal region (B). The addition of L-carnitine (50 mg/100 g/day for 3 weeks) to THP (20 mg/100 g/day for 3 weeks) prevents the accumulation of fat almost completely (C).

The results obtained so far show a decrease in the hepatic carnitine pool, impaired metabolism of palmitic acid, accumulation of hepatic fat at 3 weeks and 6 weeks of treatment with THP, and impaired hepatic mitochondrial β-oxidation and activity of CPT I at 6 weeks. These results therefore suggest that carnitine deficiency, which is present at both time points, is the major cause for liver steatosis in THP-treated rats, whereas decreased mitochondrial β-oxidation/CPT I activity may contribute at 6 weeks of treatment with THP. In order to investigate the consequences of carnitine deficiency in more detail, we determined the cytosolic and the mitochondrial CoA pools (Table 5). Expressed per gram of liver, the CoA pool was increased in THP treated rats at both time points. This increase could be explained by a rise in free and acetyl-CoA, whereas the short- and long-chain acyl-CoA contents were not different from control rats. In contrast to total liver, the mitochondrial CoA content was decreased in THPtreated rats both when expressed per mitochondrial protein content or

per mitochondria contained in 1 g of liver. This decrease could be explained by a reduced mitochondrial content in short- and long-chain CoAs. Consequently, the cytosolic CoA content (calculated as the difference between the total content and the content in the mitochondria per g liver) was increased in THP-treated rats and this increase was found for all CoA fractions determined.

Table 5: Liver CoA pool

	Control (n=12)	THP 3 weeks (n=6)	THP 6 weeks (n=6)
Total liver			
CoASH + acetyl-CoA	223 ± 73	301 ± 89 [a]	365 ± 64 [a]
Short-chain acyl-CoA	68 ± 57	63 ± 27	68 ± 47
Long-chain acyl-CoA	90 ± 31	102 ± 32	97 ± 13
Total CoA	380 ± 84	466 ± 61 [a]	528 ± 90 [a]
Liver cytosol			
CoASH + acetyl-CoA	172 ± 63	n.d.	323 ± 62 [a]
Short-chain acyl-CoA	26 ± 15	n.d.	52 ± 23 [a]
Long-chain acyl-CoA	55 ± 16	n.d.	75 ± 10 [a]
Total CoA	251 ± 46	n.d.	446 ± 43 [a]
Liver mitochondria			
CoASH	381 ± 156	n.d.	365 ± 64
Acetyl-CoA	76 ± 15	n.d.	51 ± 22 [a]
Short-chain acyl-CoA	379 ± 129	n.d.	159 ± 91 [a]
Long-chain acyl-CoA	315 ± 92	n.d.	212 ± 55 [a]
Total CoA	1160 ± 160	n.d.	793 ± 108 [a]

Control and THP treated rats (20 mg/100 g body weight) were studied after 3 or 6 weeks of treatment in the fasted state. CoASH and acyl-CoAs (except acetyl-CoA) were determined fluorimetrically, and acetyl-CoA by a radioenzymatic method as described in Materials and Methods. Units are nmol x g liver wet weigh^{-1} (total liver and liver cytosol) or nmol xg mitochondrial protein^{-1}. The cytosolic CoA content was calculated by subtracting the mitochondrial from the total liver content as described in Materials and Methods. Data are presented as mean ± SD. *a* $P < 0.05$ versus control rats.

Mitochondrial dysfunction can be associated with secondary hepatic changes such as mitochondrial proliferation (21, 23). Mitochondrial proliferation was assessed by determining the mitochondrial protein content per gram of liver and by performing Western blots of subunit IV of cytochrome c oxidase. Mitochondrial protein content was not significantly different between control and THP treated rats (111 ± 25 mg /g in control rats, and 89 ±16 and 103 ± 23 mg/g in rats treated with THP for 3 and 6 weeks, respectively). In addition, the protein content of COX subunit IV, as assessed by Western blotting, was not different between THP and control rats (results not shown), excluding mitochondrial proliferation. When mitochondrial fatty acid metabolism is impaired, peroxisomal proliferation could be a consequence due to hepatic accumulation of long-chain fatty acids and fatty acid metabolites that may stimulate peroxisome proliferator-activated receptor (PPAR)α (42). Indeed, a significant panlobular peroxisomal proliferation occurred in livers of THP-

treated rats (Fig. 4). In agreement with these results, peroxisomal fatty acyl-CoA oxidase activity and protein content were both increased in THP-treated rats (Fig. 5). In comparison to lipid accumulation (Fig. 2), the increase in the number of peroxisomes shows no significant lobular gradient (enlargement 640x).

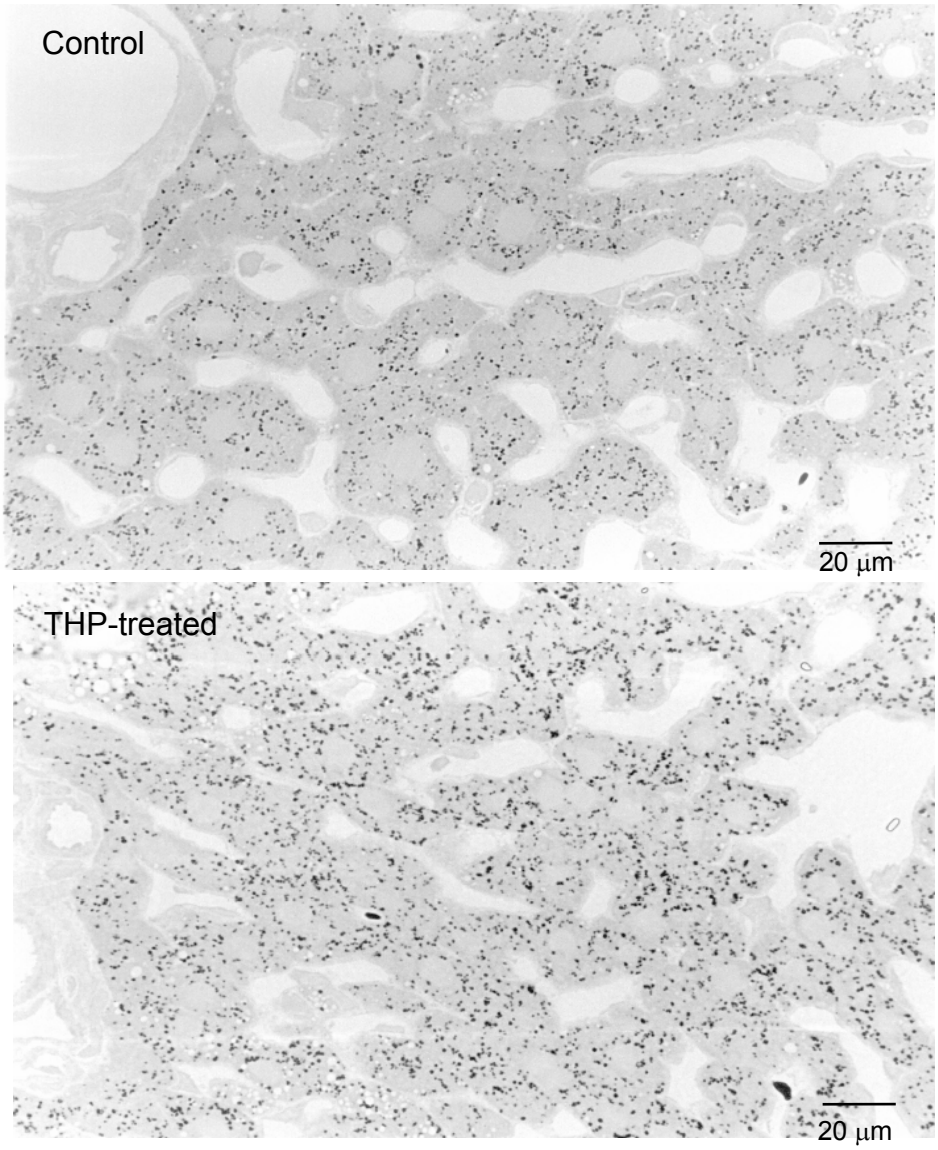

Magnification 640 ×

Figure 4: Hepatic peroxisomal proliferation in rats treated with THP for 3 weeks. Peroxisomes were stained with the alkaline DAB method for cytochemical localization of catalase. Hepatocytes of rats treated with THP contain an increased number of peroxisomes. In comparison to lipid accumulation (Fig. 2), the increase in the number of peroxisomes shows no significant lobular gradient (enlargement 640x). *a* $P < 0.05$ versus control rats.

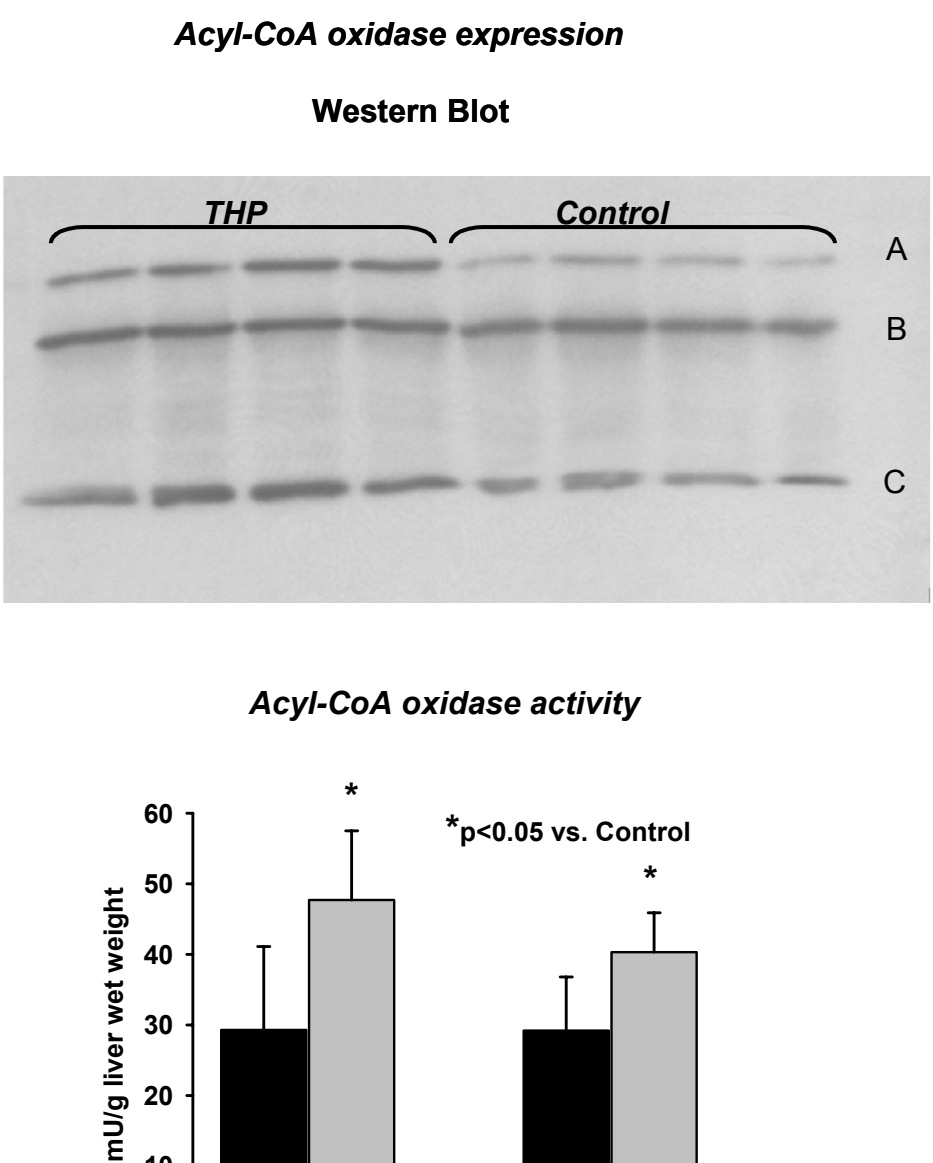

Figure 5: Protein expression and activity of acyl-CoA oxidase. Similar to earlier observations, the Western blot of liver homogenate with polyclonal antibodies against acyl-CoA oxidase (AOX) reveals three bands (58, 59). These three bands correspond to AOX subunits A (71.9 kDa), B (51.7 kDa), and C (20.5 kDa). All three bands exhibited a significant (*P* _ 0.05) augmentation in livers from THP-treated rats. The densitometric analysis yielded 3.52 ± 1.29 versus 1.00 ± 0.43 for band A (THP-treated vs. control), 1.55 ± 0.12 versus 1.00 ± 0.27 for band B, and 1.70 ± 0.39 versus 1.00 ± 0.17 for band C. The activity for AOX was increased ~ 1.5-fold, corresponding well with the densitometric results for bands B and C.

A third consequence of decreased mitochondrial fatty acid oxidation could be an increase in the hepatic VLDL production. This was assessed indirectly by measuring the plasma lipid composition. As shown in Table 6, VLDL triglycerides and phospholipids were all increased in THPtreated versus control rats, which may reflect increased hepatic availability of activated fatty acids (as shown above)

with increased hepatic VLDL synthesis. On the other hand, Western blot analysis revealed that the hepatic content of apoB was not different between THPtreated and control rats (results not shown).

Table 6: Plasma lipid and lipoprotein analysis

	CON (n=6)	THP (n=6)
Lipids and glycerol		
Triglycerides	0.47 ± 0.12	0.58 ± 0.12
Phospholipids	1.17 ± 0.17	1.51 ± 0.35[a]
Cholesterol	0.12 ± 0.0.03	0.13 ± 0.0.02
Free fatty acids	0.72±0.10	0.71±0.20
Glycerol	0.023±0.004	0.023±0.005
Very low density lipoproteins (VLDL)		
Triglycerides	0.49 ± 0.15	0.72 ± 0.15[a]
Phospholipids	0.10 ± 0.03	0.16 ± 0.03[a]
Cholesterol	0.11 ± 0.02	0.08 ± 0.03
Low density lipoproteins (LDL)		
Phospholipids	0.23 ± 0.03	0.31 ± 0.14
Cholesterol	0.25 ± 0.05	0.28 ± 0.12
High density lipoproteins (HDL)		
Triglycerides	0.15 ± 0.01	0.15 ± 0.02
Phospholipids	0.90 ± 0.09	1.09 ± 0.31
Cholesterol	0.52 ± 0.07	0.55 ± 0.18

Control and THP treated rats (20 mg/100 g body weight) were studied after weeks of treatment in the fasted state. Plasma lipoproteins were isolated using a combined centrifugation/precipitation technique and lipids were analyzed enzymatically as described in Materials and Methods. Data are presented as mean ± SD. Units are mmol/l for free fatty acids and g x l^{-1} for all other lipids or metabolites.

a $P < 0.05$ THP versus CON.

7.5. Discussion

Our study demonstrates that THP-treated rats have an ~70% reduction in the hepatic carnitine content, reduced in vivo metabolism of palmitate, liver steatosis, accumulation of long-chain acyl-CoAs in the cytosol of the hepatocytes, hepatic proliferation of peroxisomes, and increased plasma VLDL.

The study was designed to find out the mechanisms leading to micro- and macrovesicular steatosis THPtreated rats. Liver steatosis was present already at 3 weeks of treatment, a time point when THP-treated rats had developed systemic carnitine deficiency, and had reduced in vivo metabolism of palmitate, whereas oxidative metabolism and β-oxidation of isolated liver mitochondria was normal or even higher in mitochondria from THP-treated as compared with control rats. Since

THP has no apparent toxicity on liver mitochondria, liver steatosis is explained, at least at this early time point, entirely by a reduction in the hepatic carnitine pool.

After 6 weeks of treatment with THP, oxidative metabolism of different substrates (including fatty acids) as well as β-oxidation and activity of CPT I were reduced in THPtreated rats, suggesting that impaired mitochondrial function could contribute to the development of liver steatosis. Although the study was not designed to find out the mechanisms leading to mitochondrial dysfunction at this time point, it can be speculated that it may reflect changes in the lipid composition of mitochondrial membranes and/or oxidative damage to mitochondria, as observed in other animal models with alterations in hepatic fatty acid metabolism (43) or liver steatosis (44, 45).

In THP-treated rats, the hepatic content of long-chain acyl-CoAs was increased at 3 and 6 weeks, compatible with a decreased cytosolic conversion of long-chain acyl-CoAs to the respective carnitine derivatives due to carnitine deficiency and/or reduced activity of CPT I (see Fig. 1 for explanation). Peroxisomal proliferation may result from stimulation of PPARα by accumulated fatty acids and fatty acid derivatives in THP-treated rats (42), and may represent a mechanism to compensate for decreased mitochondrial metabolism of fatty acids. In support of this interpretation, a significant increase in the surface density of peroxisomes has been described in humans with liver steatosis (46). Since peroxisomes produce also medium chain acyl-CoAs during β-oxidation, the observed increase in the cytosolic content of short-chain acyl-CoAs and of the short-chain acylcarnitine to carnitine ratio may result from increased peroxisomal metabolism of long-chain fatty acids. Mediumchain acylcarnitines may serve as additional substrates for mitochondrial β-oxidation in THP-treated rats since they can enter the mitochondria without the action of CPT I.

In THP-treated rats, carnitine deficiency was associated with a significant increase in the cytosolic CoA content of the hepatocytes, whereas the mitochondrial content decreased. CoA is synthesized from pantothenate, cysteine, and ATP, with the rate-limiting step being phosphorylation of pantothenate located in the cytosol (47). Mitochondria obtain CoA either by endogenous biosynthesis [the final steps in CoA synthesis are also found in mitochondria (48) or by transport across the inner mitochondrial membrane by a specific transport system (49). In comparison, degradation of CoA appears to be a cytosolic process (50). Interestingly, rats treated with clofibrate, a ligand for PPARα leading to peroxisomal proliferation (51), also reveal an increase in the hepatic CoA pool (52-54), suggesting that an increase in the hepatic CoA pool and peroxisomal proliferation may somehow be connected. The rise in the hepatic CoA pool by clofibrate has clearly been shown to result from increased biosynthesis (54) and the distribution of CoA between the mitochondria and the cytosol was not affected in clofibrate-treated rats (53). In contrast, in THP treated rats, the total hepatic CoA pool is increased due to a rise in the cytosolic content of CoA, whereas the mitochondrial content is decreased. Since the changes in the hepatic CoA pool could already be observed at 3 weeks of treatment with THP, a time point when β-oxidation was not impaired, these alterations in the CoA pool did probably not affect significantly hepatic fatty acid metabolism in THP-treated rats.

In THP-treated rats, the phospholipid and triglyceride contents were increased in the VLDL fraction in plasma and also per gram of liver, whereas the hepatic apoB content was unchanged. These findings are compatible with increased loading of VLDL with triglycerides and phospholipids in the liver, which is most probably a consequence of increased cytosolic availability of fatty acids and acyl-CoAs due to impaired mitochondrial fatty acid metabolism. Hepatic accumulation of triglycerides has been associated with the development of macrovesicular steatosis of the liver (9, 11). Since isolated inhibition of mitochondrial fatty acid metabolism is considered to result in microvesicular

steatosis (11), secondary accumulation of cytosolic triglycerides and phospholipids in the presence of initial mitochondrial damage may explain the development of a mixed type of liver steatosis over time.

Despite reduced in vivo metabolism of palmitate and decreased activity of CPT I, as well as mitochondrial β-oxidation in THP-treated rats, the plasma and liver β-hydroxybutyrate concentrations were not different from control rats. Hepatic long-chain fatty acid metabolism is controlled at two sites, namely at CPT I and mitochondrial HMG-CoA synthase (55, 56), both of them regulated enzymes. Since ketogenesis was assessed specifically and was not different between mitochondria from THP-treated and control rats, the activity of the HMG-CoA synthase can be assumed to be identical in THP-treated and control rats. The observed decrease of palmitate metabolism in THP rats in vivo, which is explained primarily by hepatic carnitine deficiency and, at 6 weeks, also reduced activity of CPTI/mitochondrial β-oxidation, could therefore be expected to result in decreased hepatic production of ketone bodies, e.g., β-hydroxybutyrate. Indeed, in agreement with reduced CPT I activity/mitochondrial β-oxidation, liver mitochondria from THP-treated rats contained less acetyl-CoA than control mitochondria. On the other hand, the plasma and liver β-hydroxybutyrate concentrations were not different between THP-treated and control rats. Among the possibilities to explain this discrepancy are decreased consumption of ketone bodies by peripheral tissues such as skeletal muscle, or increased production of ketone bodies by extrahepatic tissues such as kidneys in THP-treated rats. These two possibilities are unlikely, however, since not only plasma, but also the hepatic β-hydroxybutyrate concentration was unaffected by treatment with THP. The most likely possibility is therefore that during starvation, the HMG-CoA cycle becomes rate-limiting for ketogenesis. During starvation, the activity of CPT I increased due to a decrease in the hepatic concentration of malonyl-CoA, an endogenous inhibitor of CPT I (55). This increase in CPT I activity during starvation may be sufficient so that ketogenesis is controlled solely by the HMG-CoA cycle, as suggested by our findings. In support of this interpretation, starved rats with acute cholestasis have reduced production of ketone bodies and a reduced activity of HMG-CoA synthase, the ratelimiting enzyme of the HMG-CoA cycle, while the function of CPT I is normal (25). On the other hand, ketogenesis is reduced in JVS mice, an animal model with severe systemic carnitine deficiency (57). The hepatic carnitine content in JVS mice is less than 5% of normal, limiting the activity of CPT I to a higher extent than in THP-treated rats. In JVS mice, ketogenesis was maximal at carnitine concentrations above 100 nmol/g liver wet weight (57), a value which is just reached in THP-treated rats.

We conclude that a reduction in the hepatic carnitine pool is the principle mechanism leading to impaired hepatic fatty acid metabolism and liver steatosis after 3 weeks of treatment with THP. After 6 weeks of treatment, impaired activity of CPT I and mitochondrial β-oxidation may contribute. Cytosolic accumulation of fatty acids and long-chain acyl-CoAs is associated with increased plasma VLDL triglyceride and phospholipid concentrations and peroxisomal proliferation.

Acknowledgements

We would like to thank Dr. André Miserez and Ulrich Keller for helpful comments about the protocol. The studies were supported by a grant of the Swiss National Science Foundation to S.K. (31-59812.99).

7.6. References

1. Skelly MM, James PD, Ryder SD. Findings on liver biopsy to investigate abnormal liver function tests in the absence of diagnostic serology. J Hepatol 2001; 35: 195-199.
2. Lewis JH, Ranard RC, Caruso A, Jackson LK, Mullick F, Ishak KG, et al. Amiodarone hepatotoxicity: prevalence and clinicopathologic correlations among 104 patients. Hepatology 1989; 9: 679-685.
3. Krahenbuhl S, Mang G, Kupferschmidt H, Meier PJ, Krause M. Plasma and hepatic carnitine and coenzyme A pools in a patient with fatal, valproate induced hepatotoxicity. Gut 1995; 37: 140-143.
4. Oien KA, Moffat D, Curry GW, Dickson J, Habeshaw T, Mills PR, et al. Cirrhosis with steatohepatitis after adjuvant tamoxifen. Lancet 1999; 353: 36-37.
5. Fortgang IS, Belitsos PC, Chaisson RE, Moore RD. Hepatomegaly and steatosis in HIV-infected patients receiving nucleoside analog antiretroviral therapy. Am J Gastroenterol 1995; 90: 1433-1436.
6. Lieber CS. Alcohol and the liver: 1994 update. Gastroenterology 1994; 106: 1085-1105.
7. Goodman ZD, Ishak KG. Histopathology of hepatitis C virus infection. Semin Liver Dis 1995; 15: 70-81.
8. Reid AE. Nonalcoholic steatohepatitis. Gastroenterology 2001; 121: 710-723.
9. Wanless IR, Lentz JS. Fatty liver hepatitis (steatohepatitis) and obesity: an autopsy study with analysis of risk factors. Hepatology 1990; 12: 1106-1110.
10. Mahler H, Pasi A, Kramer JM, Schulte P, Scoging AC, Bar W, et al. Fulminant liver failure in association with the emetic toxin of Bacillus cereus. N Engl J Med 1997; 336: 1142-1148.
11. Fromenty B, Pessayre D. Inhibition of mitochondrial beta-oxidation as a mechanism of hepatotoxicity. Pharmacol Ther 1995; 67: 101-154.
12. Spaniol M, Brooks H, Auer L, Zimmermann A, Solioz M, Stieger B, et al. Development and characterization of an animal model of carnitine deficiency. Eur J Biochem 2001; 268: 1876-1887.
13. Hayashi Y, Muranaka Y, Kirimoto T, Asaka N, Miyake H, Matsuura N. Effects of MET-88, a gamma-butyrobetaine hydroxylase inhibitor, on tissue carnitine and lipid levels in rats. Biol Pharm Bull 2000; 23: 770-773.
14. Bremer J. Carnitine--metabolism and functions. Physiol Rev 1983; 63: 1420-1480.
15. Treem WR, Stanley CA, Finegold DN, Hale DE, Coates PM. Primary carnitine deficiency due to a failure of carnitine transport in kidney, muscle, and fibroblasts. N Engl J Med 1988; 319: 1331-1336.
16. Kuwajima M, Kono N, Horiuchi M, Imamura Y, Ono A, Inui Y, et al. Animal model of systemic carnitine deficiency: analysis in C3H-H-2 degrees strain of mouse associated with juvenile visceral steatosis. Biochem Biophys Res Commun 1991; 174: 1090-1094.
17. Fromenty B, Grimbert S, Mansouri A, Beaugrand M, Erlinger S, Rotig A, et al. Hepatic mitochondrial DNA deletion in alcoholics: association with microvesicular steatosis. Gastroenterology 1995; 108: 193-200.
18. Lewis JH, Mullick F, Ishak KG, Ranard RC, Ragsdale B, Perse RM, Rusnock EJ, Wolke A, Benjamin SB, Seeff LB, Zimmerman HJ. Histopathologic analysis of suspected amiodarone hepatotoxicity. Hum Pathol 1990; 21: 59–67.

19. Visarius TM, Stucki JW, Lauterburg BH. Inhibition and stimulation of long-chain fatty acid oxidation by chloroacetaldehyde and methylene blue in rats. J Pharmacol Exp Ther 1999; 289: 820-824
20. Hoppel C, DiMarco JP, Tandler B. Riboflavin and rat hepatic cell structure and function. Mitochondrial oxidative metabolism in deficiency states. J Biol Chem 1979; 254: 4164-4170.
21. Krahenbuhl S, Talos C, Reichen J. Mechanisms of impaired hepatic fatty acid metabolism in rats with long-term bile duct ligation. Hepatology 1994; 19: 1272-1281.
22. Gornall AG, Bardawill GJ, David M. Determination of serum proteins by means of the biuret reaction. Journal of Biological Chemistry 1949; 177: 751-766.
23. Krahenbuhl S, Chang M, Brass EP, Hoppel CL. Decreased activities of ubiquinol:ferricytochrome c oxidoreductase (complex III) and ferrocytochrome c:oxygen oxidoreductase (complex IV) in liver mitochondria from rats with hydroxycobalamin[c-lactam]-induced methylmalonic aciduria. J Biol Chem 1991; 266: 20998-21003.
24. Freneaux E, Labbe G, Letteron P, The Le D, Degott C, Geneve J, et al. Inhibition of the mitochondrial oxidation of fatty acids by tetracycline in mice and in man: possible role in microvesicular steatosis induced by this antibiotic. Hepatology 1988; 8: 1056-1062.
25. Lang C, Schafer M, Serra D, Hegardt F, Krahenbuhl L, Krahenbuhl S. Impaired hepatic fatty acid oxidation in rats with short-term cholestasis: characterization and mechanism. J Lipid Res 2001; 42: 22-30.
26. Chapman MJ, Miller LR, Ontko JA. Localization of the enzymes of ketogenesis in rat liver mitochondria. J Cell Biol 1973; 58: 284-306.
27. Olsen C. An enzymatic fluorimetric micromethod for the determination of acetoacetate, -hydroxybutyrate, pyruvate and lactate. Clin Chim Acta 1971; 33: 293-300.
28. Veitch K, Hombroeckx A, Caucheteux D, Pouleur H, Hue L. Global ischaemia induces a biphasic response of the mitochondrial respiratory chain. Anoxic pre-perfusion protects against ischaemic damage. Biochem J 1992; 281: 709-715.
29. Krahenbuhl S, Talos C, Wiesmann U, Hoppel CL. Development and evaluation of a spectrophotometric assay for complex III in isolated mitochondria, tissues and fibroblasts from rats and humans. Clin Chim Acta 1994; 230: 177-187.
30. Wharton DC, Tzagoloff A. Cytochrome c oxidase from beef heart mitochondria. Methods Enzymol 1967; 10: 245-250.
31. Allred JB, Guy DG. Determination of coenzyme A and acetyl CoA in tissue extracts. Anal Biochem 1969; 29: 293-299.
32. Krahenbuhl S, Brass EP. Fuel homeostasis and carnitine metabolism in rats with secondary biliary cirrhosis. Hepatology 1991; 14: 927-934.
33. Cederblad G, Carlin JI, Constantin-Teodosiu D, Harper P, Hultman E. Radioisotopic assays of CoASH and carnitine and their acetylated forms in human skeletal muscle. Anal Biochem 1990; 185: 274-278
34. Brass EP, Hoppel CL. Carnitine metabolism in the fasting rat. J Biol Chem 1978; 253: 2688-2693.
35. Bligh EG, Dyer WJ. A rapid method of total lipid extraction and purification. Can J Med Sci 1959; 37: 911-917.
36. Bachorik PS, and Ross JW. National Cholesterol Education Program recommendations for measurement of low-density lipoprotein cholesterol: executive summary. The National

Cholesterol Education Program Working Group on Lipoprotein Measurement. Clin Chem 1995; 41: 1414–1420.

37. Wanner C, Horl WH, Luley CH, Wieland H. Effects of HMG-CoA reductase inhibitors in hypercholesterolemic patients on hemodialysis. Kidney Int 1991; 39: 754-760.
38. Fahimi HD. Cytochemical localization of peroxidatic activity of catalase in rat hepatic microbodies (peroxisomes). J Cell Biol 1969; 43: 275-288.
39. Beier K, Volkl A, Hashimoto T, Fahimi HD. Selective induction of peroxisomal enzymes by the hypolipidemic drug bezafibrate. Detection of modulations by automatic image analysis in conjunction with immunoelectron microscopy and immunoblotting. Eur J Cell Biol 1988; 46: 383-393.
40. Small GM, Burdett K, Connock MJ. A sensitive spectrophotometric assay for peroxisomal acyl-CoA oxidase. Biochem J 1985; 227:205–210.
41. Spurway TD, Sherratt HA, Pogson CI, Agius L. The flux control coefficient of carnitine palmitoyltransferase I on palmitate beta-oxidation in rat hepatocyte cultures. Biochem J 1997; 323: 119-122.
42. Desvergne B, Wahli W. Peroxisome proliferator-activated receptors: nuclear control of metabolism. Endocr Rev 1999; 20: 649-688
43. Krahenbuhl S, Stucki J, Reichen J. Reduced activity of the electron transport chain in liver mitochondria isolated from rats with secondary biliary cirrhosis. Hepatology 1992; 15: 1160-1166.
44. Vendemiale G, Grattagliano I, Caraceni P, Caraccio G, Domenicali M, Dall'Agata M, et al. Mitochondrial oxidative injury and energy metabolism alteration in rat fatty liver: effect of the nutritional status. Hepatology 2001; 33: 808-815.
45. Letteron P, Fromenty B, Terris B, Degott C, Pessayre D. Acute and chronic hepatic steatosis lead to in vivo lipid peroxidation in mice. J Hepatol 1996; 24: 200-208.
46. De Craemer D, Pauwels M, Van den Branden C. Alterations of peroxisomes in steatosis of the human liver: a quantitative study. Hepatology 1995; 22: 744-752.
47. Robishaw JD, Neely JR. Coenzyme A metabolism. Am J Physiol 1985; 248: E1-9.
48. Skrede S, Halvorsen O. Mitochondrial biosynthesis of coenzyme A. Biochem Biophys Res Commun 1979; 91: 1536-1542.
49. Tahiliani AG, Neely JR. A transport system for coenzyme A in isolated rat heart mitochondria. J Biol Chem 1987; 262: 11607-11610.
50. Bremer J, Wojtczak A, Skrede S. The leakage and destruction of CoA in isolated mitochondria. Eur J Biochem 1972; 25: 190-197.
51. Moody DE, Reddy JK. Increase in hepatic carnitine acetyltransferase activity associated with peroxisomal (microbody) proliferation induced by the hypolipidemic drugs clofibrate, nafenopin, and methyl clofenapate. Res Commun Chem Pathol Pharmacol 1974; 9: 501– 510.
52. Horie S, Isobe M, Suga T. Changes in CoA pools in hepatic peroxisomes of the rat under various conditions. J Biochem (Tokyo) 1986; 99: 1345-1352.
53. Brass EP, Ruff LJ. Rat hepatic coenzyme A is redistributed in response to mitochondrial acyl-coenzyme A accumulation. J Nutr 1992; 122: 2094-2100.
54. Skrede S, Halvorsen O. Increased biosynthesis of CoA in the liver of rats treated with clofibrate. Eur J Biochem 1979; 98: 223-229.

55. McGarry JD, Brown NF. The mitochondrial carnitine palmitoyltransferase system. From concept to molecular analysis. Eur J Biochem 1997; 244: 1-14.
56. Nakajima T, Horiuchi M, Yamanaka H, Kizaki Z, Inoue F, Kodo N, et al. The effect of carnitine on ketogenesis in perfused livers from juvenile visceral steatosis mice with systemic carnitine deficiency. Pediatr Res 1997; 42: 108-113.
58. Beier K, Volkl A, Metzger C, Mayer D, Bannasch P, Fahimi HD. Hepatic zonation of the induction of cytochrome P450 IVA, peroxisomal lipid beta-oxidation enzymes and peroxisome proliferation in rats treated with dehydroepiandrosterone (DHEA). Evidence of distinct zonal and sex-specific differences. Carcinogenesis 1997; 18: 1491-1498
59. Reisse S, Rothardt G, Volkl A, Beier K. Peroxisomes and ether lipid biosynthesis in rat testis and epididymis. Biol Reprod 2001; 64: 1689-1694.

8. Mechanisms of benzarone and benzbromarone induced hepatic toxicity

Priska Kaufmann[1], Michael Török[1], Anya Hänni[1], Paul Roberts[1],
Rodolfo Gasser[2], Stephan Krähenbühl[1]

[1]Departments of Clinical Pharmacology & Toxicology and Research, University Hospital Basel, [2]F. Hoffmann-La Roche, Basel, Switzerland

Hepatology 2005;41:925-35

8.1. Abstract

Rationale: Treatment with benzarone or benzbromarone can be associated with hepatic injury. Both drugs share structural similarities with amiodarone, a well known mitochondrial toxin. Hepatotoxicity of benzarone and benzbromarone, and of the analogues benzofuran and 2-butylbenzofuran was therefore investigated.

Main results: In isolated rat hepatocytes, amiodarone, benzarone or benzbromarone (20μmol/L) the mitochondrial membrane potential was 67%, 41% or 18% of the initial value. Benzofuran and 2-butylbenzofuran had no effect up to 100 μmol/L. In isolated rat liver mitochondria, amiodarone, benzarone and benzbromarone, but not benzofuran, decreased state 3 oxidation and respiratory control ratios for L-glutamate (50% decrease of RCR at: amiodarone 9.3μmol/L, benzarone 11.2μmol/L, benzbromarone <1μmol/L). Amiodarone, benzarone and benzbromarone, but not benzofuran, also uncoupled oxidative phosphorylation. Mitochondrial β-oxidation was decreased by 76, 83 or 57% with 100μmol/L amiodarone, benzarone or 50μmol/L benzbromarone, respectively, but was unaffected by benzofuran, whereas ketogenesis was not affected. 2-Butylbenzofuran weakly inhibited state 3 oxidation and β-oxidation only at 100μmol/L. In the presence of 100 μmol/L amiodarone, benzarone or benzbromarone, Generation of reactive oxygen species was increased and mitochondrial leakage of cytochrome c was induced in HepG2 cells, and permeability transition was induced in isolated rat liver mitochondria. At the same concentrations, amiodarone, benzarone and benzbromarone induced apoptosis and necrosis of isolated rat hepatocytes.

In conclusion, hepatotoxicity associated with amiodarone, benzarone and benzbromarone can at least in part be explained by their mitochondrial toxicity and the subsequent induction of apoptosis and necrosis. Side chains attached to the furan moiety are necessary for rendering benzofuran hepatotoxic.

8.2. Introduction

Drug-induced hepatic injury is often regarded as a consequence of the formation and toxicity of reactive metabolites. In recent years, mitochondrial damage has been recognized as an additional important mechanism of drug-induced hepatotoxicity (1). Mitochondrial β-oxidation and oxidative phosphorylation are fundamental physiological processes. Acquired or inherited impairment of these processes can affect the function of many organs, in the liver typically leading to microvesicular steatosis, a potentially fatal disease (2, 3). Microvesicular steatosis has been observed in patients and/or animals being treated with the antiarrhythmic amiodarone (4). Amiodarone is composed of a diiodobenzene ring carrying a diethylaminoethoxy side chain and a benzofuran ring carrying a C_4H_9 side chain (see Figure 1). Amiodarone is a well characterized hepatic mitochondrial toxin. It inhibits enzyme complexes of the electron transport chain, impairs β-oxidation and uncouples oxidative phosphorylation (4-6).

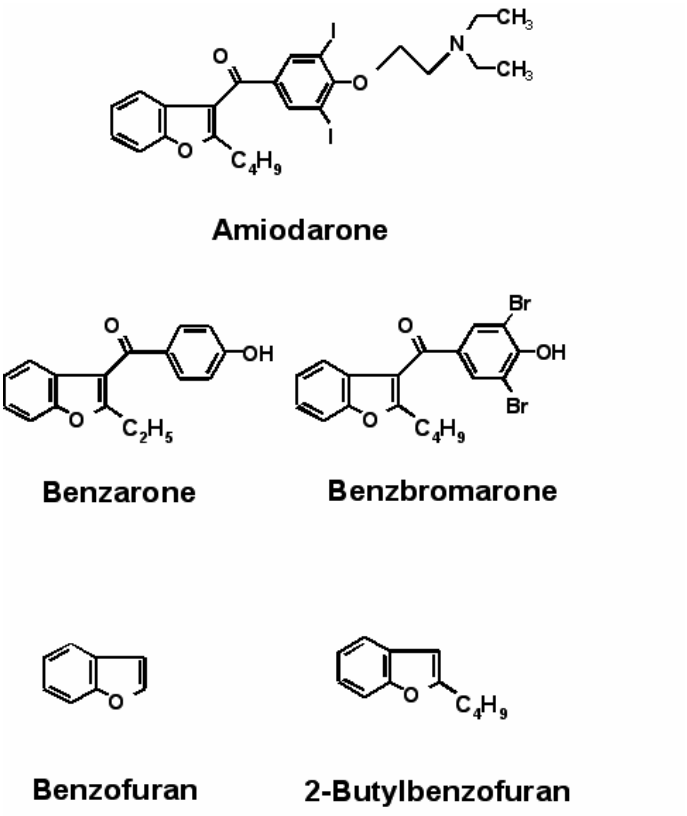

Figure 1: Chemical structures of the substances investigated.

Benzbromarone is another benzofuran derivative acting as an uricosuric agent by reducing the proximal tubular reabsorption of uric acid (7). Benzarone is a non-halogenated benzbromarone derivative used for the treatment of venous vascular disorders (8). As shown in Figure 1, the structures of benzbromarone as well as benzarone are closely related to that of amiodarone. This structural relationship and the fact that these two drugs can also cause hepatic injury (9), in some patients with fatal outcome (8, 10), led us to hypothesize that their mechanism of toxicity may be similar to that of amiodarone. In support of our hypothesis, it has been shown that benzbromarone can inhibit several enzyme complexes of the electron transport chain in isolated mouse liver mitochondria (11).

Many studies during the last couple of years revealed that mitochondria not only provide energy for the cell, but can also “unleash machineries of death” (12). A variety of key events in cell death focus on mitochondria, in particular initiation of apoptosis and necrosis (12-14). Following these considerations, we decided to study the mechanisms of the suspected mitochondrial toxicity of benzarone and benzbromarone and to compare them with those of amiodarone. In particular, we were interested in mitochondrial mechanisms leading to cell damage or even death. We also investigated the structure-toxicity relationship by including the molecular analogues benzofuran and 2-butylbenzofuran along with amiodarone, benzarone and benzbromarone in our studies.

8.3. Materials and Methods

8.3.1. Reagents

Benzarone was obtained from Norchim (Saint Leu d'Esserent, France), benzofuran from Merck (Darmstadt, Germany) and [1-^{14}C]palmitic acid from Amersham Pharmacia Biotech (Dübendorf, Switzerland). 2-Butylbenzofuran was kindly provided by Dr. Huy Riem from the Cardiovascular Therapy Research Unit, University Hospital Zurich (Switzerland). Fetal calf serum and all culture medium supplements were from Gibco (Paisley, UK). Williams E media was from Cambrex (Verviers, Belgium). The 96-well plates were purchased from Becton Dickinson (Franklin Lakes, NJ, USA), the 8-chamber slides from Nalge Nunc (Rochester, NY, USA) and the unifilters as well as the scintillation cocktail from Packard (Meriden, CT, USA). The Vybrant™ Apoptosis Assay Kit #2 was purchased from Molecular probes (Eugene, OR, USA). All other chemicals used were of best quality available and purchased from Sigma–Aldrich (Schnelldorf, Germany).

8.3.2. Cell lines

The hepatocarcinoma cell line HepG2 was kindly provided by Prof. Dietrich von Schweinitz (Department of Pediatric Surgery, University Hospital Basel, Switzerland). The cell line was cultured in Dulbecco's Modified Eagle Media, supplemented with 10% (v/v) inactivated fetal calf serum, 10mmol/L HEPES buffer (pH 7.4), 2mmol/L GlutaMAX®, non-essential amino acids and penicillin/streptomycin (100U/mL). Culture conditions were 5% CO_2 and 95% air atmosphere at 37°C.

8.3.3. Animals

Male Sprague Dawley rats (Iffa Credo /Charles River, Les Onins, France) were used for all experiments. They were fed ad libitum and hold on a 12-hour dark and light cycle. The study protocol had been accepted by the Cantonal Animal Ethics Committee.

8.3.4. Isolation of rat liver mitochondria

At the time of killing, the rats weighed 314 ± 61g. The animals were anesthetized with carbon dioxide and killed by decapitation. The liver (14.2 ± 1.9g) was extirpated, rinsed, weighed, minced and washed with ice-cold MSM buffer (220mmol/L mannitol, 70mmol/L sucrose, 5mmol/L 3-[N-morpholino]propanesulfonic acid (Mops), pH 7.4). All subsequent procedures were carried out on ice. Mitochondria were isolated by differential centrifugation according to the method of Hoppel et al (15). The final mitochondrial pellets were resuspended in MSM buffer and frozen at -70°C if not used freshly. The mitochondrial protein content was determined using the biuret method with bovine serum albumin as standard (16).

8.3.5. Isolation of rat hepatocytes

Hepatocytes were isolated from male rats weighing 200 to 250g by a two step collagenase perfusion of the liver (17) and suspended in Williams E medium (Cambrex, East Rutherforn, NJ, USA) supplemented with 10% heat-inactivated fetal bovine serum, 10mmol/L HEPES buffer, 2mmol/L GlutaMAX®, 1000U/mL penicillin/streptomycin, 0.25µg/mL amphotericin B, 4µg/mL insulin and

0.1µmol/L dexamethasone. Culture conditions were an atmosphere of 5% CO_2 and 95% air at 37°C. In all experiments, initial hepatocyte viability, determined by trypan blue exclusion, was more than 85%.

8.3.6. Mitochondrial membrane potential

The mitochondrial membrane potential was determined as described by Wan et al (18). Briefly, freshly isolated cells were washed twice with incubation buffer containing 137mmol/L sodium chloride, 4.74mmol/L potassium chloride, 2.56mmol/L calcium chloride, 1.18mmol/L potassium phosphate, 1.18mmol/L magnesium chloride, 10mmol/L HEPES and 1g/L glucose, pH 7.4. After labeling the cells with 40nmol/L [^{3}H]- tetraphenylphosphonium bromide ([^{3}H]-TPP^+), the cells were seeded in a 96-well plate and incubated with the test compounds for 1hour at 37°C. The cells were harvested on a unifilter GF/B (Packard, Meriden, CT, USA), which was mixed with 50µL/well scintillation cocktail (Top count, Packard, Meriden, CT, USA), covered with a plate sealer and counted for [^{3}H]-radioactivity.

8.3.7. Oxygen uptake

Oxygen uptake was monitored polarographically using a 1mL chamber equipped with a Clark-type oxygen electrode (Yellow Springs Instruments, Yellow Springs, OH, USA) at 30°C as described previously (15). The oxygen content of respiration buffer equilibrated with air was assumed to be 223nmol O_2/mL at 30°C (19). The final concentrations of the substrates used were 20mmol/L for L-glutamate and succinate. Amiodarone, benzarone, benzbromarone, benzofuran and 2-butylbenzofuran at concentrations given in the tables were dissolved in dimethylsulfoxide (DMSO). Control experiments were carried out in the presence of the solvent containing no inhibitor.

In isolated mitochondria, state 3, state 4 and the respiratory control ratio (RCR) were determined as described previously (20) and as defined by Estabrook (21). The test compounds were added to the mitochondrial incubations before the addition of the respective substrate.

For the determination of oxygen consumption by isolated hepatocytes, 1 x 10^6 cells were treated with oligomycin (final concentration 5µg/mL) in order to inhibit mitochondrial ATPase. After 2 minutes, the test compounds were added to the incubation chamber and the oxygen consumption was determined as a marker for the uncoupling potential of the test compounds. Control experiments were carried out with solvent only.

8.3.8. Mitochondrial β-oxidation and formation of ketone bodies

Beta-oxidation by freshly isolated liver mitochondria was assessed by the formation of ^{14}C-acid-soluble β-oxidation products from [1-^{14}C]palmitic acid in the presence of the test compounds. Experiments were performed as described previously (22) with the modifications described by Spaniol et al (5).

Ketone body formation by liver mitochondria was measured in the presence of an acetyl-CoA-generating system using freeze-thawed mitochondria according to Chapman et al (23) with the modifications described by Spaniol et al (5). The supernatants of the incubations were analyzed for acetoacetate according to Olsen (24), using an enzyme-catalyzed reaction inducing changes in the concentration of β-nicotinamide adenine dinucleotide (NADH).

8.3.9. Activities of mitochondrial β-oxidation enzymes

All enzyme activities were determined using spectrophotometric assays at 37°C. Freeze-thawed mitochondria were treated 1:1 with 5% cholic acid in order to disrupt the mitochondrial membranes. The solution was then diluted one hundred times with 50mmol/L potassium phosphate buffer (pH 7.4). The effects on the enzymes of β-oxidation were only investigated with amiodarone, benzarone, benzbromarone and 2-butylbenzofuran, as they had an inhibitory effect on β-oxidation. The concentrations of the inhibitors were 20 or 100μmol/L. The activities of acyl-CoA dehydrogenase and □-ketothiolase were both determined spectrophotometrically as described by Hoppel et al. (15).

8.3.10. Reactive oxygen species (ROS)

Confluent cultures of HepG2 cells, seeded in 96-well plates, were incubated with Dulbecco's Modified Eagle Media without fetal bovine serum in the presence of 5mmol/L 2,7-dichlorofluorescin diacetate. After incubation, the medium was replaced by phosphate buffered saline (PBS) and cellular fluorescence (λ_{ex} = 485nm, λ_{em} = 520nm) was determined at room temperature using a microtiter plate reader (HTS 7000 Plus Bio Assay Reader, Perkin Elmer, Buckinghamshire, UK).

8.3.11. Mitochondrial swelling

Measurements of mitochondrial swelling were performed using flow cytometry (FACScalibur, Becton Dickinson, NJ, USA) by recording histograms. The mitochondrial suspension containing 1mg of mitochondrial protein was mixed with 200μL of MSM-buffer and subsequently the test compounds added. As Ca^{2+} is a well known inducer of swelling, the effect of 1mmol/L $CaCl_2$ was used as a positive control. Where indicated, 2μL of cyclosporin A (final concentration 2μmol/L) was added as an inhibitor of mitochondrial swelling. For quantification purposes, mean forward scatter was determined.

8.3.12. Hepatocellular ATP content

After having settled down in a 12-well plate (Becton Dickinson, Franklin Lakes, NJ, USA), the freshly isolated hepatocytes (200'000 cells/well) were treated for 8 hours with test compounds. Following treatment, cells were once washed with PBS (pH 7.4), suspended in 1 mL of reagent grade water inside an Eppendorf tube, snap-frozen in liquid nitrogen and stored at –80°C. For the determination of ATP, cells were extracted according to Yang *et al*. (25). In brief, 500μl of the cellular suspension was added to a tube containing 500μl of boiling Millipure water and vortexed. The diluted cellular suspension was then boiled for 10 min to disrupt the cellular membranes and to release their natant ATP into solution. Samples were cooled on ice for 30 s, prior to the removal of cellular debris by centrifugation (12000 rpm, 4°C, 5 min). The concentration of ATP was determined in the supernatant with the well-established luciferin-luciferase method and by use of a commercially prepared reagent kit (FL-AA, Sigma, Deisenhofen, Germany) in accordance with the manufacturers instructions. Values obtained were compared against a linear ATP standard curve, in duplicate at the same time as the unknown samples were analyzed.

8.3.13. Apoptosis and necrosis

Both assays were performed using freshly isolated rat hepatocytes cultured on poly-D-lysine coated (0.1mg/mL, 30min) glass slides. As a positive control for apoptosis, soluble Fas-ligand supernatant was used. Soluble Fas-ligand supernatant was produced by Fas-ligand-transfected N2a cells. The supernatant of mock-transfected of N2a cells was used as a negative control. The soluble Fas-ligand supernatant and the supernatant of mock-transfected N2a cells were both a kind gift of Dr. Felix Bachmann (Aponetics AG, Witterswil, Switzerland). As a positive control for induction of necrosis, the detergent NP 40 was used at a concentration of 0.1%.

Hoechst 33342 nuclear staining: Cells were treated for 8h with different concentrations of test compounds, were then incubated for 30 minutes at room temperature with Hoechst 33342 dye (50μmol/L in PBS) and visualized by fluorescence microscopy (Olympus IX 50, Hamburg, Germany).

Annexin V and propidium iodide (PPI) staining: An *in situ* Apoptosis Detection Kit was used for Annexin V binding and propidium iodide staining (Vybrant™ Apoptosis Assay Kit #2, Molecular probes, Eugene, OR, USA). Cells were treated with the test compounds in a concentration-dependent manner. After an 8h-incubation period, cells were stained with 25μL Annexin V-Alexa Fluor® 488 and 2μL propidium iodide (PPI) (final concentration: 1.5μg/L). After 15 minutes of incubation at room temperature, samples were analyzed by flow cytometry.

8.3.14. Mitochondrial release of cytochrome c

For immunocytochemistry, HepG2 cells were grown in an 8 chamber-slide (coated with poly-D-lysine) for 12 hours at 37°C and then treated with the test compounds for 8 hours. Afterwards, cytochrome c was visualized using an anti-cytochrome c antibody (Sigma, Buchs, Switzerland) and an anti-sheep IgG antibody conjugated with Cy3™ (Jackson Laboratories, West Grove, PA, USA) according to manufacturer's protocol.

8.3.15. Statistical methods

Data are presented as mean ± standard error of the mean±SEM. For statistical comparisons, data of groups were compared by analysis of variances (ANOVA). The level of significance was $p \leq 0.05$. If ANOVA revealed significant differences, comparisons between the control and the other incubations were performed by Dunnett's post test procedure. T-test (unpaired, two-tailed) was performed if only two groups were analyzed.

8.4. Results

8.4.1. Mitochondrial membrane potential

As shown in Figure 2, increasing concentrations of amiodarone, benzbromarone or benzarone resulted in a progressive decrease in the mitochondrial membrane potential. At 20μM, the mitochondrial membrane potential was 18% of the initial value for benzbromarone, 41% for benzarone or 67% for amiodarone. In contrast, benzofuran and 2-butylbenzofuran did not affect the potential up to 100μmol/L. Since these results confirmed that amiodarone, benzarone and benzbromarone are mitochondrial toxins, their effect on mitochondria was characterized further.

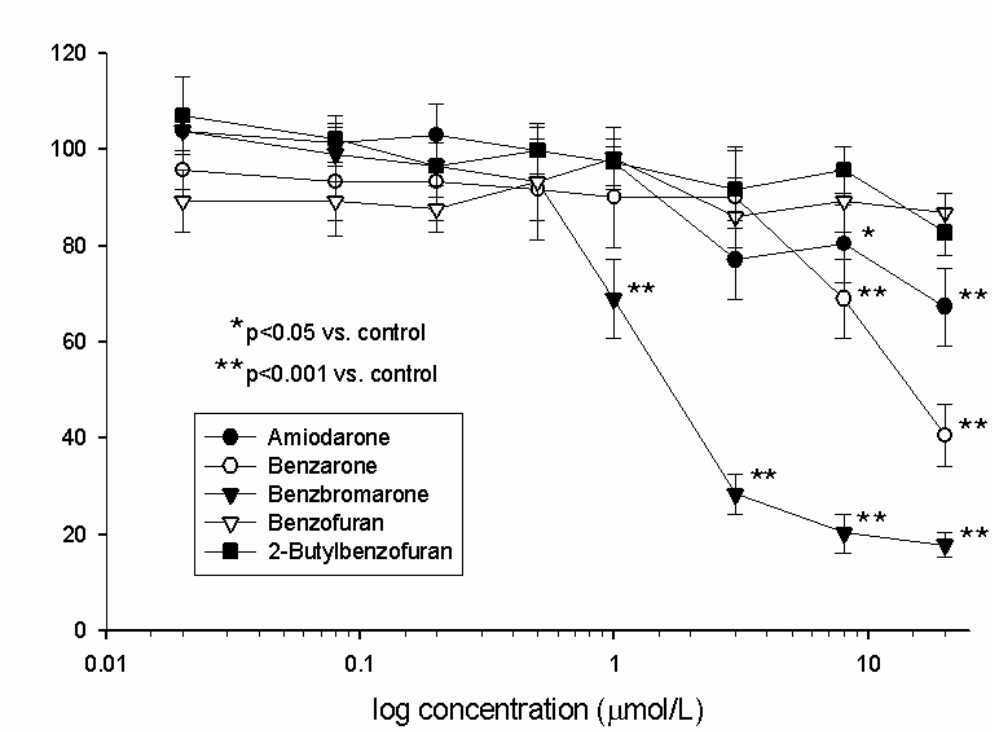

Figure 2: Effect on mitochondrial membrane potential. Rat hepatocytes were labeled with [^{3}H]TPP$^+$ and mitochondrial accumulation of radioactivity was determined. 1% DMSO served as a control and was set at 100%. Means ± SEM of three individual preparations *P < 0.05 vs. control, ** p < 0.01 vs. control.

8.4.2. Oxidative metabolism of mitochondria

The next step was to assess the toxicity of these substances on oxidative metabolism of isolated rat liver mitochondria using L-glutamate or succinate as substrates (Table 1). In the presence of L-glutamate or succinate, amiodarone, benzarone and benzbromarone induced a progressive depression of the RCR. The corresponding concentrations associated with a 50% decrease in the RCR were 9.3 μmol/L for amiodarone and 11.2 μmol/L for benzarone in the presence L-glutamate, and 23.9 μmol/L for amiodarone and 23.3 μmol/L for benzarone in the presence of succinate. For benzbromarone, this concentration was <1μmol/L for both substrates used, whereas 2-butylbenzofuran decreased the RCR less potently (50% decrease at 50 - 100μmol/L) and benzofuran did not affect mitochondrial respiration at all. In contrast to the effects on the RCR, state 3 respiration, reflecting the activity of the respiratory chain, was decreased only at the highest concentration (100μmol/L) of amiodarone, benzarone and benzbromarone, but not by 2-butylbenzofuran or benzofuran. The RCR values were decreased mainly due to an increase in state 4, suggesting uncoupling of oxidative phosphorylation.

Table 1:Effects of the test compounds on oxidative metabolism by isolated rat liver mitochondria. Mean ± SEM of at least 3 experiments using different mitochondrial preparations. *P < 0.05 vs. 1% DMSO; ** p < 0.01 vs. 1% DMSO.

	L-glutamate (20mmol/L) [natoms O_2 x·min^{-1} x·mg^{-1}]		Succinate (20mmol/L) [natoms O_2 x min^{-1} x mg^{-1}]	
	State 3	RCR	State 3	RCR
Control (no inhibitor)	86 ± 3	6.5 ± 1.0	163 ± 28	4.1 ± 0.4
Amiodarone (µmol/L)				
10	95 ± 22	3.0 ± 0.5**	167 ± 44	2.4 ± 0.3**
20	81 ± 10	2.6 ± 0.0**	170 ± 39	2.1 ± 0.3**
50	82 ± 9	1.7 ± 0.2**	157 ± 49	1.6 ± 0.6**
100	34 ± 28**	1.2 ± 0.3**	135 ± 37	1.3 ± 0.5**
Benzarone (µmol/L)				
10	80 ± 34	3.6 ± 0.8	167 ± 16	3.2 ± 0.1
20	65 ± 29	2.0 ± 0.5**	161 ± 27	2.3 ± 0.5**
50	59 ± 28	1.0 ± 0.0**	136 ± 18	1.0 ± 0.0**
100	30 ± 11 **	1.0 ± 0.1**	64 ± 23**	1.0 ± 0.0**
Benzbromarone (µmol/L)				
0.1	114 ± 12	6.3 ± 1.9	190 ± 29	3.0 ± 1.2 **
1	113 ± 19	2.0 ± 0.3**	194 ± 2	1.9 ± 0.1**
10	105 ± 18	1.0 ± 0.0**	121 ± 62	1.2 ± 0.3**
100	34 ± 34**	1.0 ± 0.0**	33 ± 7**	1.0 ± 0.1**
Benzofuran (µmol/L)				
10	76 ± 11	5.9 ± 2.0	161 ± 47	4.1 ± 0.5
20	78 ± 25	5.1 ± 1.0	151 ± 44	3.7 ± 0.4
50	75 ± 15	5.9 ± 1.3	138 ± 38	3.5 ± 0.7
100	72 ± 19	4.9 ± 1.0	172 ± 16	3.5 ± 0.1
2-Butylbenzofuran (µmol/l)				
10	122 ± 53	5.4 ± 0.6	200 ± 51	3.8 ± 0.6
20	114 ± 21	4.9 ± 1.0	211 ± 7	4.4 ± 0.2
50	104 ± 14	4.7 ± 0.8*	192 ± 10	4.4 ± 0.4
100	75 ± 5	3.3 ± 0.5**	183 ± 10	2.2 ± 0.5**

Uncoupling of oxidative phosphorylation was investigated directly using isolated hepatocytes in the presence of oligomycin to block mitochondrial conversion of ATP to ADP (Figure 3).

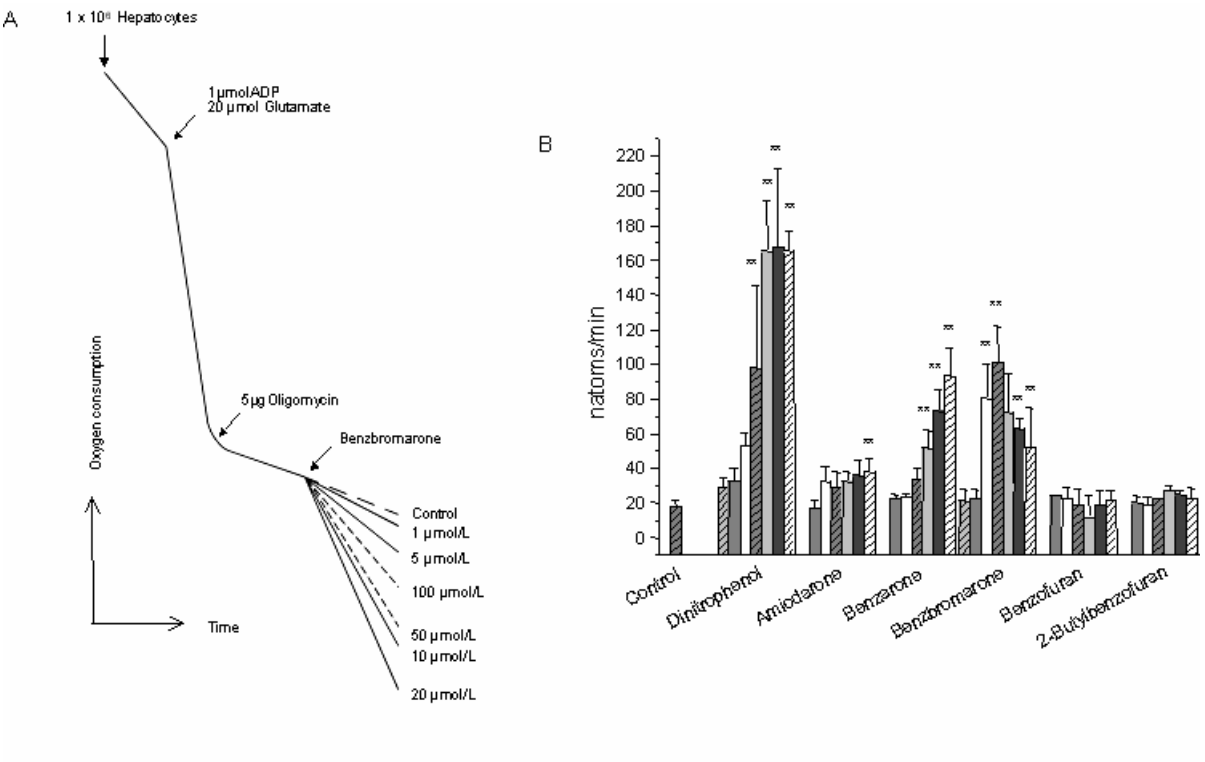

Figure 3: Uncoupling of oxidative phosphorylation using isolated, intact rat hepatocytes. In coupled mitochondria, blocking of the F_0F_1-ATPase by oligomycin results in a restricted electron transport similar to state 4. Uncouplers increase oxygen consumption under these circumstances (panel A). Benzbromarone acts as an uncoupler at concentrations ≤20 □mol/L. At higher concentrations, it also inhibits electron transport. In panel B, respiration rates in the presence of amiodarone (1, 10, 20, 50, 80, 100µmol/L), benzarone (1, 20, 50, 80, 100µmol/L), benzbromarone (0.1, 1, 10, 20, 50, 80, 100µmol/L), benzofuran (1, 10, 20, 50, 80, 100µmol/L) or 2-butylbenzofuran (1, 10, 20, 50, 80, 100µmol/L) are presented. 1% DMSO serves as control. Means ± SEM of four individual mitochondrial preparations. *P < 0.05 vs. 1% DMSO; ** p < 0.01 vs. 1% DMSO.

Benzbromarone increased oxygen consumption by hepatocytes starting at 10µmol/L, showing that it is a potent uncoupler. For concentrations higher than 20µmol/L, the respiration rate was decreasing, reflecting progressive inhibition of the respiratory chain. Amiodarone stimulated respiration only at the highest concentration (100µmol/L) and benzarone from 50µmol/L upwards. Benzofuran and 2-butylbenzofuran did not stimulate state 4 respiration and therefore did not induce uncoupling. These results demonstrate that amiodarone, benzarone and benzbromarone are uncouplers of oxidative phosphorylation and are in agreement with those obtained using isolated mitochondria.

8.4.3. Mitochondrial β-oxidation and formation of ketone bodies

As already known for amiodarone (5), also benzarone and benzbromarone inhibited the formation of acid soluble β-oxidation products in a dose-dependent manner (Table 2). The corresponding IC_{50} values were 34µmol/L for amiodarone, 34µmol/L for benzarone and 2µmol/L for benzbromarone. In comparison, 2-butylbenzofuran was only a weak inhibitor (28% inhibition at 100µmol/L), whereas benzofuran showed no inhibition up to 100µmol/L. Since the formation of acid-

soluble products reflects both, β-oxidation and ketogenesis, ketogenesis was assessed directly. In contrast to the formation of acid soluble products, ketogenesis was not affected by any of the substances investigated (data not shown).

Table 2:Effects of the test compounds on β-oxidation in isolated rat liver mitochondria. Mean ± SEM of at least 3 experiments using different mitochondrial preparations. *P < 0.05 vs. 1% DMSO; ** p < 0.01 vs. 1% DMSO.

Compound	Activity [nmol x·min^{-1} x·mg^{-1}]	Compound	Activity [nmol x·min^{-1} x·mg^{-1}]
Amiodarone (µmol/l)		Benzofuran (µmol/l)	
control	0.64 ± 0.10	control	0.75 ± 0.10
10	0.48 ± 0.10	10	0.73 ± 0.10
20	0.42 ± 0.06 **	20	0.70 ± 0.08
50	0.19 ± 0.04 **	50	0.69 ± 0.09
80	0.12 ± 0.02 **	80	0.73 ± 0.10
100	0.15 ± 0.03 **	100	0.72 ± 0.10
Benzarone (µmol/l)		2-Butylbenzofuran (µmol/l)	
control	0.60 ± 0.10	control	0.62 ± 0.10
5	0.70 ± 0.12	10	0.59 ± 0.10
10	0.64 ± 0.11	20	0.55 ± 0.09
20	0.34 ± 0.11 **	50	0.62 ± 0.11
50	0.24 ± 0.13 **	80	0.53 ± 0.10
100	0.10 ± 0.05 **	100	0.45 ± 0.08 **
Benzbromarone (µmol/l)			
Control	0.61 ± 0.08		
0.5	0.41 ± 0.10		
2	0.30 ± 0.10 *		
5	0.24 ± 0.08 **		
10	0.19 ± 0.10 **		
50	0.26 ± 0.06 **		

In order to localize the inhibitory effect of β-oxidation more precisely, two enzymes of the β-oxidation cycle were investigated. In the presence of 100µmol/L amiodarone, benzarone, benzbromarone or 2-butylbenzofuran, acyl-CoA dehydrogenase activity was inhibited by 28%, 33%, 34% or 22%, respectively, as compared to control values. For β-ketothiolase, the last enzyme of the β-oxidation cycle, the average decrease in the presence of 100µmol/L benzarone or benzbromarone was 11% or 25%, respectively, whereas amiodarone and 2-butylbenzofuran revealed no inhibitory effect. The discrepancy between inhibition of β-oxidation (determined using intact mitochondria) and individual enzymes of the β-oxidation cycle as well as ketogenesis (both determined using broken mitochondria) may be explained by an inhibition of the activation of palmitate and/or transport across the inner mitochondrial membrane. It is well established that CPT I, an enzyme involved in the import of long-chain fatty acids into the mitochondrial matrix, can be rate-limiting for hepatic fatty acid metabolism (26, 27).

8.4.4. Production of ROS

As a byproduct of the formation of ATP by oxidative phosphorylation, mitochondria produce also ROS (12, 28). Blockade of the electron flow through the electron transport chain stimulates ROS production, particularly in the presence of an uncoupler (29). In contrast, in the presence of an uncoupler only, the electron transport chain works more efficiently and leads to less leakage of electrons and therefore lower levels of ROS are generated (30-32). ROS generation is claimed to play an important role in induction of mitochondrial mediated cell death (33-36). Since amiodarone, benzarone or benzbromarone inhibit the electron transport chain and are uncouplers of oxidative phosphorylation (Table 1), their effect on ROS generation was investigated in HepG2 cells, using 2,7-dichlorofluorescin diacetate as an indicator (37). These investigations showed a concentration-dependent production of ROS in the presence of these substrates, which started to be detectable at concentrations of 0.1nmol/L for benzbromarone, 10nmol/L for benzarone and 1μmol/L for amiodarone (Figure 4). In contrast, 2-butylbenzofuran and benzofuran were not associated with an increase in ROS production. Antimycin (1μmol/L), an inhibitor of the electron transport from cytochrome b to ubiquinone, led to a significant increase in the ROS production, whereas dinitrophenol (100μmol/L), an uncoupler of oxidative phosphorylation, did not augment ROS generation. To ensure the specificity of the assay used, we blocked ROS generation by adding ascorbic acid at a concentration of 250μmol/L (38) to selected incubations (Figure 4).

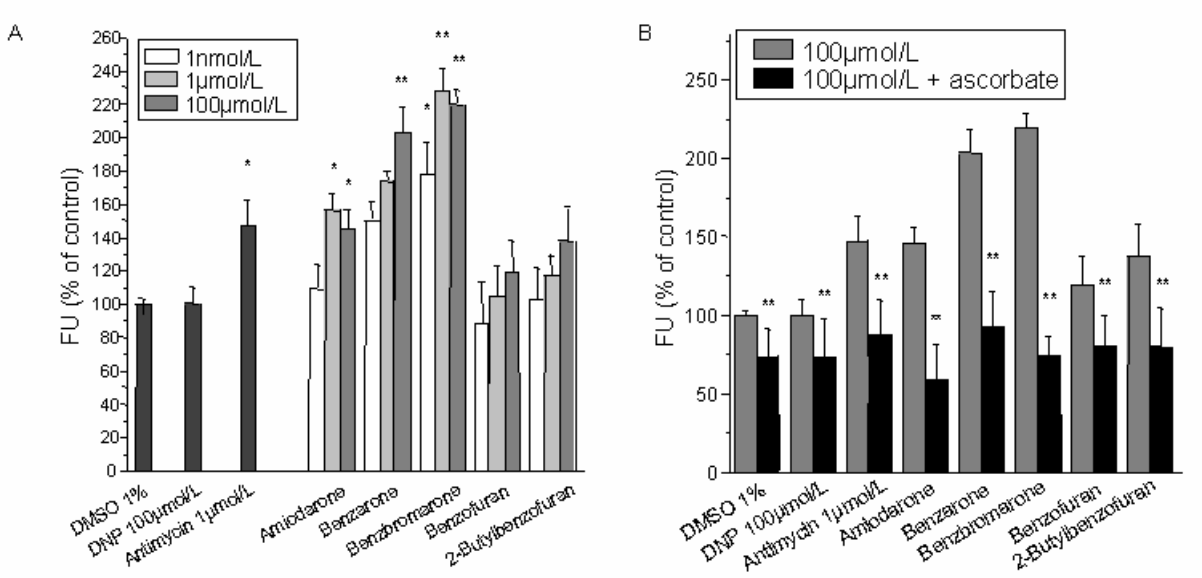

Figure 4: ROS formation by HepG2 cells. Confluent monolayers of HepG2 cells were exposed to different compounds for 1h at 37°C (A), in the presence or absence of ascorbate (250 □mol/L) (B). ROS formation was detected using 2,7-dichlorofluorescin diacetate (indicated as fluorescence units, FU). Mean ± SEM of at least three independent experiments in quadruplicate. Asterisks indicate values significantly different from control (panel A) or from the incubation in the absence of ascorbate (panel B). *P< 0.05 or at **p< 0.01. FU= fluorescence units.

8.4.5. Mitochondrial swelling

Since production of ROS can be associated with opening of the mitochondrial membrane pore (13) mitochondrial swelling was investigated as an indicator for mitochondrial permeability transition

(mpt). As shown in Figure 5, addition of Ca^{2+}-ions (1mmol/L) induced swelling which could be partially inhibited by the addition of cyclosporin A, indicating that swelling was dependent on mpt. A significant increase in mitochondrial size (at least partially inhibitable by cyclosporin A, results not shown) was also detectable for amiodarone, benzbromarone and benzarone at 100μmol/L (Figure 5).

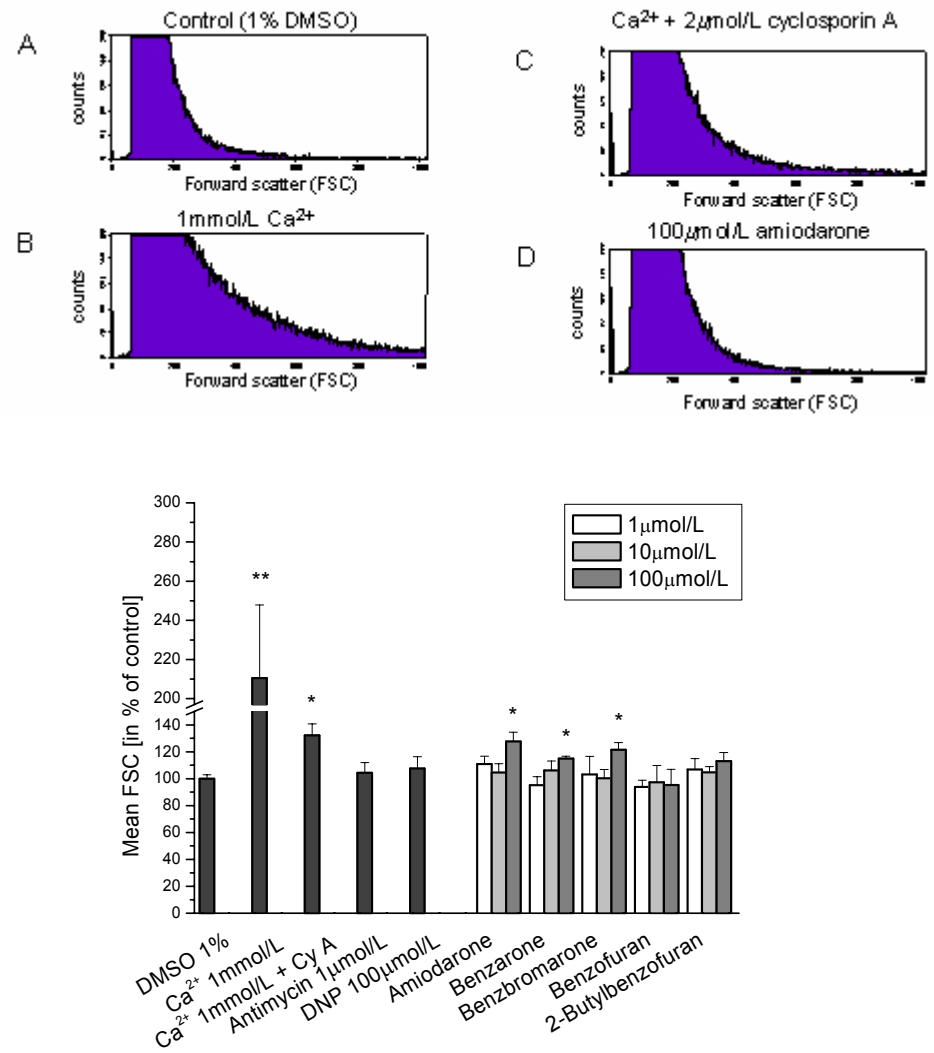

Figure 5: Mitochondria studied by flow cytometry. Left panel: Histograms (forward scatter vs. counts) of flow cytometry analyses of freshly isolated rat liver mitochondria. The forward scatter assesses the mitochondria's size, and "counts" the number of mitochondria of this size. Right panel: Quantification of the mitochondrial volume as the mean forward scatter (FSC). Mitochondrial volume was measured in the absence (A) or presence of Ca^{2+} (1mmol/L) (B), Ca^{2+}/cyclosporin A (2μmol/L) (C) and with test compounds, i.e. amiodarone 100μmol/L (D). Ca^{2+}, a known inducer of mitochondrial swelling, increases mitochondrial volume. Cyclosporin A partially blocks mitochondrial swelling by Ca^{2+}. Amiodarone, benzarone and benzbromarone also induce swelling, but less pronounced than Ca^{2+} (E). Mean ± SEM of at least 3 independent experiments. *P < 0.05 vs. 1% DMSO; ** p < 0.01 vs. 1% DMSO.

8.4.6. Apoptosis and necrosis

Mtp-induced swelling can lead to a disruption of the outer mitochondrial membrane with consecutive release of cytochrome c, which can activate caspases and induce apoptosis (13, 39). As

shown in Figure 6, 100 μmol/L amiodarone, benzarone or benzbromarone were all associated with leakage of cytochrome c into the cytoplasm of HepG2 cells, whereas this was not the case for benzofuran or 2-butylbenzofuran.

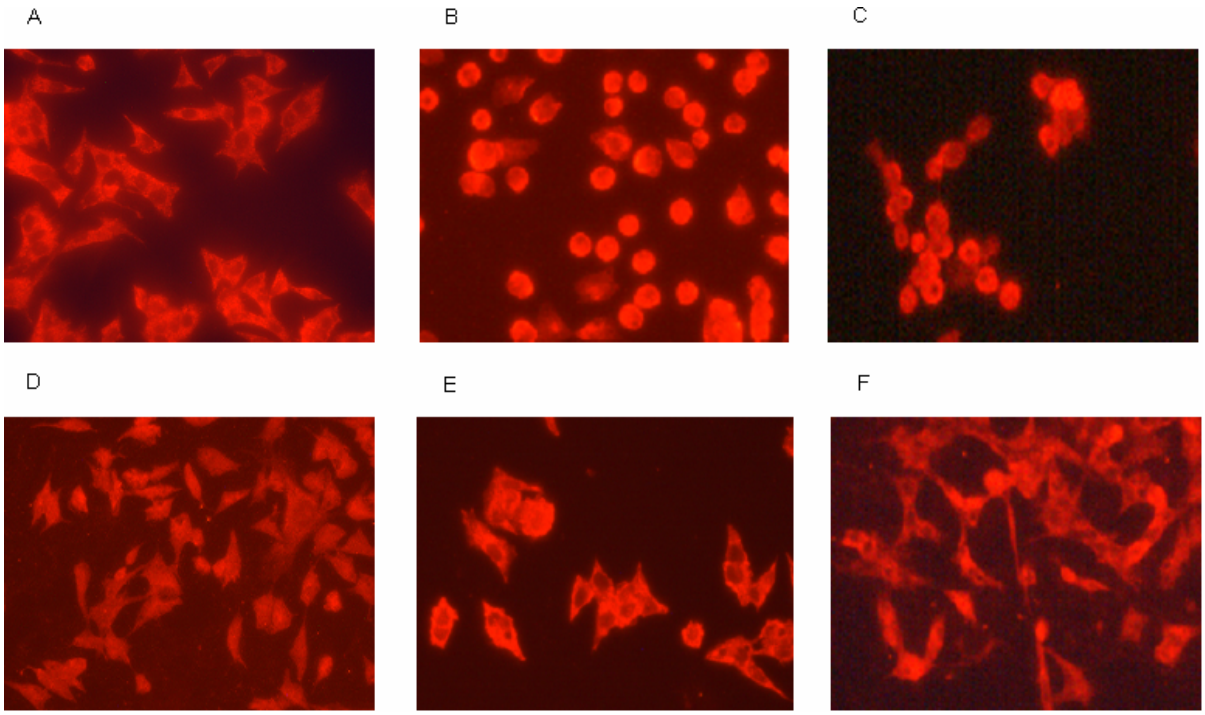

Figure 6: Mitochondrial cytochrome c release caused by treatment of HepG2 cells with test compounds (each 100μmol/L) for 8 h, and detected by immunocytochemistry. In the presence of 1% DMSO (control, panel A), benzofuran (panel B) or 2-butylbenzofuran (panel F) no leakage of cytochrome c into the cytoplasm occurred, as indicated by a diffuse, punctual pattern of immunoreactivity. In these incubations, immunoreactivity is linked to mitochondria (punctual pattern), rendering the nuclei clearly visible. After treatment with amiodarone (panel B), benzbromarone (panel C) or benzarone (panel D), cells may partially detach from the surface and the immunoreactivity is spread over the entire cells. The homogenous, diffuse pattern of immunoreactivity, which covers the nuclei, indicates release of cytochrome c from the mitochondrial intermembrane space followed by cytoplasmic spreading.

Chromatin fragmentation and/or condensation occurring during apoptosis can be visualized by fluorescence microscopy upon staining with dyes intercalating with DNA. As shown in Figure 7, untreated cells showed an apoptosis rate of 3%. Apoptosis was induced by amiodarone, benzarone and by benzbromarone in a concentration-dependent manner (not shown). At a concentration of 100μmol/L, the proportion of apoptotic cells was 10% for amiodarone, 13% for benzarone and 11% for benzbromarone. Fas-ligand, used as a positive control, induced DNA fragmentation in 9% of the cells, whereas 100μmol/L benzofuran or 2-butylbenzofuran showed DNA fragmentation frequencies similar to control incubations.

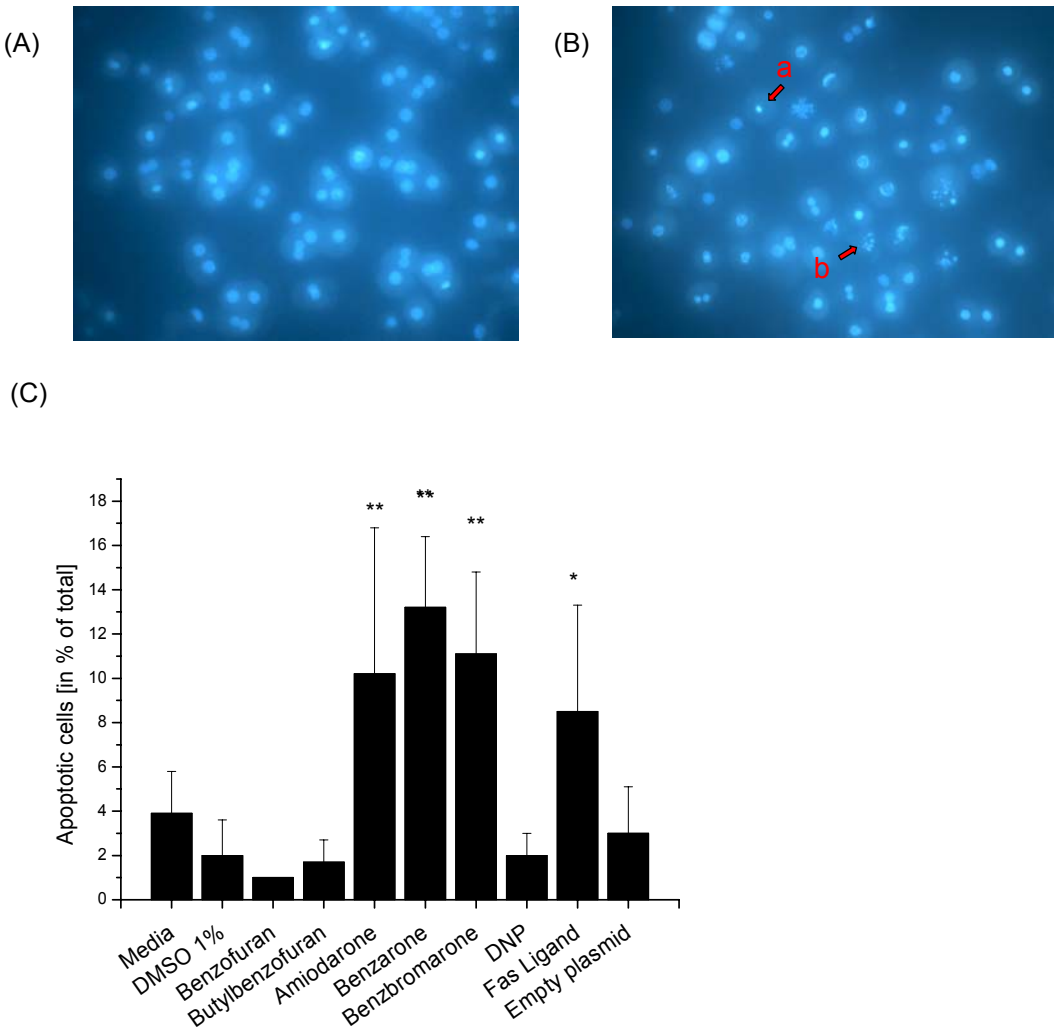

Figure 7: Illustration and quantification of apoptosis. Rat hepatocytes were treated with test compounds at a concentration of 100 μmol/L. After 8h of exposure, the cells were stained with Hoechst 33342 for 15 min and analyzed by fluorescence microscopy. Apoptotic cells are characterized by chromatin condensation (arrow a) and/or chromatin fragmentation (arrow b). (A) untreated cells as a control, (B) benzarone 100μmol/L, (C) percentage of cells with apoptotic nuclei. Mean ± SEM of at least three independent experiments. * $P < 0.05$ vs. 1% DMSO; ** $p < 0.01$ vs. 1% DMSO.

A hallmark of the early stages of apoptosis is the translocation of phosphatidylserine from the inner to the outer leaflet of the plasma membrane. Externalized phosphatidylserine can then be detected using Annexin V, a protein with high affinity for this phospholipid. Cells were co-stained with PPI as a marker of cell membrane permeability, which increases during the later stages of apoptosis and also of necrosis. Since PPI only enters cells with already disintegrated membranes, early apoptotic cells can be distinguished from late apoptotic and necrotic cells. Similar to staining with Hoechst 33342, flow cytometric analysis of the cells revealed progressive decrease of viable, unstained cells with increasing concentrations of amiodarone, benzarone or benzbromarone. At 100μmol/L, only 38% of cells exposed to amiodarone, 53% exposed to benzarone and 11% exposed to benzbromarone were viable (Figure 8). These findings suggest that apart from apoptosis, also necrosis was initiated since the amount of cells undergoing cell death are considerably higher than the cells undergoing chromatin fragmentation and/or condensation.

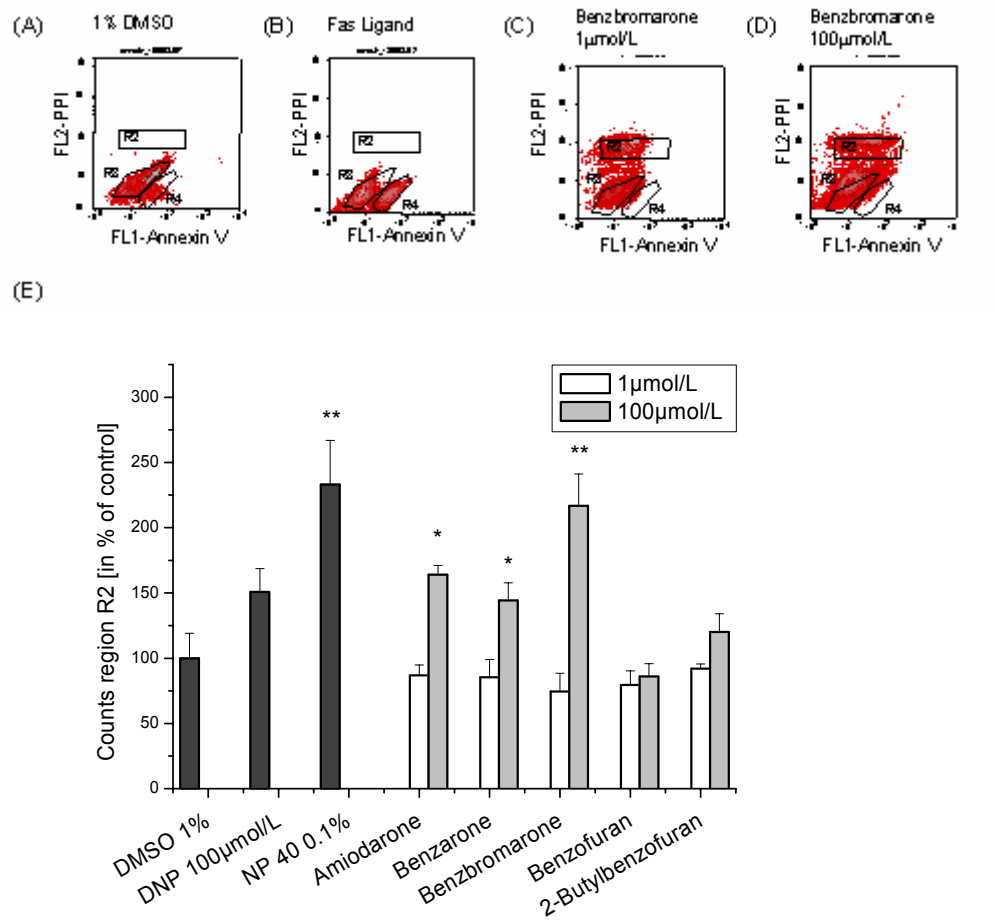

Figure 8: Annexin V binding and PPI uptake by rat hepatocytes. Hepatocytes were incubated for 8h at a concentration of 1 or 100µmol/L of each test compound and subsequently stained with Annexin V and PPI. The samples were analyzed by flow cytometry (see graphs A, B, C and D). Region R3 represents the unstained, thus viable cells. In region R4, the cells are undergoing early apoptosis and are stained only with Annexin V. Region R2 represents the double stained cells undergoing necrosis or later stages of apoptosis. Under control conditions, the vast majority of cells are located in region R3 (A). Fas-ligand is inducing apoptosis (B), whereas benzbromarone is increasing the counts in region R2 in a concentration dependent manner (C: benzbromarone 1µmol/L, D: benzbromarone 100µmol/L). Graph E: percentage of cells undergoing necrosis or late stages of apoptosis relative to control values. NP 40 is a detergent used as a positive control for necrosis. Mean ± SEM of at least three independent experiments. *P<0.05 vs. 1% DMSO, **p<0.01 vs. 1% DMSO.

Since ATP is a prerequisite for apoptosis (40, 41), the cellular ATP content was determined in hepatocytes incubated for 8h with compounds tested. The ATP content of control incubations was 4.0±0.8 µmol/10^6 hepatocytes and remained stable in the presence of 1 or 100µmol/L benzofuran or 2-butylbenzofuran. In the presence of 1µmol/L amiodarone, benzarone or benzbromarone, it was 93±5%, 80±20% or 68±15% of the control incubations, respectively. In the presence of 100µmol/L amiodarone, benzarone or benzbromarone, it dropped to 30±13%, 68±8% or 18±5% of the control incubations, respectively. These results give further support to the notion that apoptosis and necrosis occur under these conditions, in particular in the presence of benzbromarone.

If ROS generation were involved in initiation of cell death, addition of an antioxidant, which was proven to reduce ROS production, should lead to a decrease of cell death. Therefore, the above

mentioned experiments (Figure 4) were repeated in the presence or absence of 250μmol/L ascorbic acid. In the presence of ascorbate, the fraction of cells undergoing chromatin fragmentation and/or condensation was significantly reduced but not completely prevented (Figure 9). Similar results were obtained with the Annexin V PPI staining (data not shown).

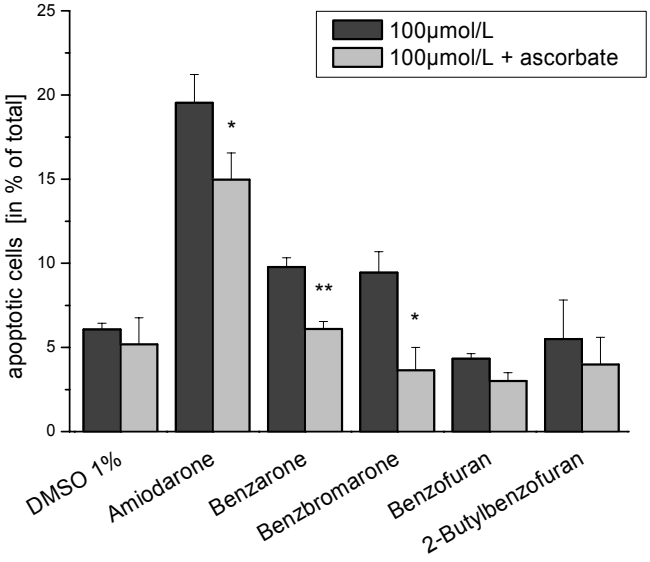

Figure 9: Reduction of apoptosis in the presence of an antioxidant. In the presence of 250μmol/L ascorbate, the fraction of cells undergoing chromatin condensation/fragmentation during incubation with test compounds is diminished. Mean ± SEM of at least three independent experiments. Asterisks indicate values significantly different from the incubations in absence of ascorbate. *P < 0.05 and ** p < 0.01.

8.5. Discussion

Our investigations demonstrate that amiodarone, benzarone and benzbromarone are inhibitors of the mitochondrial respiratory chain and of β-oxidation, and are uncouplers of oxidative phosphorylation. Furthermore they can induce production of ROS and mitochondrial swelling, and lead to apoptosis and necrosis of cells.

The mitochondrial electron transport chain has been recognized as one of the major sources of reactive oxygen species, in particular complex I and complex III (42). Electrons passing across the electron transport chain can escape from this chain and can react with molecular oxygen to form superoxide (O^{2-}). Under normal conditions, superoxide is degraded by intramitochondrial, antioxidative systems such as glutathione and superoxide dismutase (33, 34). In the presence of uncouplers, protons are transported into the mitochondrial matrix bypassing the F_0F_1-ATPase. During uncoupling, the respiratory chain works more efficiently to reestablish the proton gradient, and therefore, ROS production is usually not increased or can even be reduced (30). In the presence of inhibitors of the respiratory chain, generation of ROS is increased, since electrons may escape from the electron transport chain and react with molecular oxygen. Indeed, inhibitors of the electron transport chain, for

instance rotenone or antimycin, have been shown to increase ROS generation in mitochondria (30, 42, 43). In this context, it is interesting to note that amiodarone, benzarone and benzbromarone are both uncouplers and inhibitors of the electron transport chain. Since inhibition of the electron transport chain may generate a higher amount of ROS in the presence of an uncoupler (42), such substances may be particularly toxic for mitochondria.

It is well known that ROS within the mitochondrial matrix can trigger mpt pore opening (13). An increase in mpt is an important route by which mitochondrial toxins can activate cell death in mammalian cells (13, 44). ROS generation and induction of mpt and have been identified as possible common effectors of cell death by apoptotic as well as by necrotic stimuli (45, 46). Pore opening induces release of cytochrome c, which is located on the outer surface of the inner mitochondrial membrane (Figure 6). After release, cytochrome c triggers the subsequent effector steps for apoptosis, in particular caspase activation. ATP is critical for the action cytochrome c, since it is required for Apaf-1 oligomerization, which is followed by caspase activation. Low cellular ATP concentrations, as observed in hepatocytes incubated with 100 μmol/L amiodarone, benzbromarone or benzarone, can therefore switch apoptotic stimuli towards cell necrosis. Depending on the intensity of the oxidative stimuli, and the extent by which generation of ATP is impaired (e.g. by inhibition of the electron transport chain, uncoupling or impairment of β-oxidation) ROS generation can therefore be associated with both, apoptosis and necrosis. Further evidence for the before mentioned hypothesis that ROS generation works as a trigger for cell death induction was provided by demonstrating a reduction of cell death in the presence of ascorbate.

Besides their effects on oxidative phosphorylation and mitochondrial electron transport, amiodarone, benzarone and benzbromarone are efficient inhibitors of mitochondrial β-oxidation. The inhibition of β-oxidation is independent from the inhibition of the electron transport chain, since the corresponding concentrations for 50% inhibition are clearly lower for β-oxidation than for state 3 oxidation. After depletion of glycogen, e.g. during starvation, the liver depends mainly on β-oxidation for production of energy. It is therefore likely that under such circumstances and in the presence of inhibitors of mitochondrial β-oxidation, the cellular ATP content may decrease, possibly leading to necrosis of hepatocytes.

Concerning the structure-toxicity relationship, our investigations demonstrate clearly that the benzofuran structure *per se*, which was assumed to mediate mitochondrial toxicity (5), is not hepatotoxic. Our studies show that the hepatotoxicity of benzofuran is dependent on the presence of sidechains in position 1 and/or 2 of the furan ring. Bromide atoms in the p-hydroxybenzene moiety are not essential for hepatotoxicity associated with these compounds but clearly enhance it.

We conclude that benzarone, benzbromarone as well as amiodarone are toxic to isolated rat liver mitochondria as well as to whole hepatocytes. The benzofuran structure alone is not responsible for the hepatotoxic effects, sidechains at the furan ring are necessary. Hepatic injury associated with the ingestion of these drugs can be explained by mitochondrial damage with subsequent induction of apoptosis and necrosis.

8.6. References

1. Pessayre D, Mansouri A, Haouzi D, Fromenty B. Hepatotoxicity due to mitochondrial dysfunction. Cell Biol Toxicol 1999;15:367-373.

2. Fromenty B, Pessayre D. Inhibition of mitochondrial beta-oxidation as a mechanism of hepatotoxicity. Pharmacol Ther 1995;67:101-154.
3. Mahler H, Pasi A, Kramer JM, Schulte P, Scoging AC, Bar W, Krahenbuhl S. Fulminant liver failure in association with the emetic toxin of Bacillus cereus. N Engl J Med 1997;336:1142-1148.
4. Fromenty B, Fisch C, Labbe G, Degott C, Deschamps D, Berson A, Letteron P, et al. Amiodarone inhibits the mitochondrial beta-oxidation of fatty acids and produces microvesicular steatosis of the liver in mice. J Pharmacol Exp Ther 1990;255:1371-1376.
5. Spaniol M, Bracher R, Ha HR, Follath F, Krahenbuhl S. Toxicity of amiodarone and amiodarone analogues on isolated rat liver mitochondria. J Hepatol 2001;35:628-636.
6. Fromenty B, Fisch C, Berson A, Letteron P, Larrey D, Pessayre D. Dual effect of amiodarone on mitochondrial respiration. Initial protonophoric uncoupling effect followed by inhibition of the respiratory chain at the levels of complex I and complex II. J Pharmacol Exp Ther 1990;255:1377-1384.
7. Ferber H, Bader U, Matzkies F. The action of benzbromarone in relation to age, sex and accompanying diseases. Adv Exp Med Biol 1980;122A:287-294.
8. Hautekeete ML, Henrion J, Naegels S, DeNeve A, Adler M, Deprez C, Devis G, et al. Severe hepatotoxicity related to benzarone: a report of three cases with two fatalities. Liver 1995;15:25-29.
9. Babany G, Larrey D, Pessayre D, Degott C, Rueff B, Benhamou JP. Chronic active hepatitis caused by benzarone. J Hepatol 1987;5:332-335.
10. van der Klauw MM, Houtman PM, Stricker BH, Spoelstra P. Hepatic injury caused by benzbromarone. J Hepatol 1994;20:376-379.
11. Kramer R, Muller MM. Inhibition of enzymes of the internal mitochondrial membrane by benzbromarone. Experientia 1973;29:391-392.
12. Newmeyer DD, Ferguson-Miller S. Mitochondria: releasing power for life and unleashing the machineries of death. Cell 2003;112:481-490.
13. Green DR, Reed JC. Mitochondria and apoptosis. Science 1998;281:1309-1312.
14. Kroemer G, Reed JC. Mitochondrial control of cell death. Nat Med 2000;6:513-519.
15. Hoppel C, DiMarco JP, Tandler B. Riboflavin and rat hepatic cell structure and function. Mitochondrial oxidative metabolism in deficiency states. J Biol Chem 1979;254:4164-4170.
16. Gornall AG, Bardawill GJ, David M. Determination of serum proteins by means of the biuret reaction. Journal of Biological Chemistry 1949;177:751-766.
17. Berry MN. High-yield preparation of morphologically intact isolated parenchymal cells from rat liver. Methods Enzymol 1974;32:625-632.
18. Wan B, Doumen C, Duszynski J, Salama G, LaNoue KF. A method of determining electrical potential gradient across mitochondrial membrane in perfused rat hearts. Am J Physiol 1993;265:H445-452.
19. Chappell JB. The oxidation of citrate, isocitrate and cis-aconitate by isolated mitochondria. Biochem J 1964;90:225-237.
20. Krahenbuhl S, Chang M, Brass EP, Hoppel CL. Decreased activities of ubiquinol:ferricytochrome c oxidoreductase (complex III) and ferrocytochrome c:oxygen oxidoreductase (complex IV) in liver mitochondria from rats with hydroxycobalamin[c-lactam]-induced methylmalonic aciduria. J Biol Chem 1991;266:20998-21003.

21. Eastabrook R. Mitochondrial respiratory control and polarographic measurement of ADP:O ratios. Methods Enzymol 1967;10:41-47.
22. Morse RM, Valenzuela GA, Greenwald TP, Eulie PJ, Wesley RC, McCallum RW. Amiodarone-induced liver toxicity. Ann Intern Med 1988;109:838-840.
23. Chapman MJ, Miller LR, Ontko JA. Localization of the enzymes of ketogenesis in rat liver mitochondria. J Cell Biol 1973;58:284-306.
24. Olsen C. An enzymatic fluorimetric micromethod for the determination of acetoacetate, -hydroxybutyrate, pyruvate and lactate. Clin Chim Acta 1971;33:293-300.
25. Yang NC, Ho WM, Chen YH, Hu ML. A convenient one-step extraction of cellular ATP using boiling water for the luciferin-luciferase assay of ATP. Anal Biochem 2002;306:323-327.
26. Drynan L, Quant PA, Zammit VA. Flux control exerted by mitochondrial outer membrane carnitine palmitoyltransferase over beta-oxidation, ketogenesis and tricarboxylic acid cycle activity in hepatocytes isolated from rats in different metabolic states. Biochem J 1996;317 (Pt 3):791-795.
27. Spurway TD, Sherratt HA, Pogson CI, Agius L. The flux control coefficient of carnitine palmitoyltransferase I on palmitate beta-oxidation in rat hepatocyte cultures. Biochem J 1997;323:119-122.
28. Boveris A, Chance B. The mitochondrial generation of hydrogen peroxide. General properties and effect of hyperbaric oxygen. Biochem J 1973;134:707-716.
29. Wallace DC. Animal models for mitochondrial disease. Methods Mol Biol 2002;197:3-54.
30. Tan S, Sagara Y, Liu Y, Maher P, Schubert D. The regulation of reactive oxygen species production during programmed cell death. J Cell Biol 1998;141:1423-1432.
31. Siraki AG, Pourahmad J, Chan TS, Khan S, O'Brien PJ. Endogenous and endobiotic induced reactive oxygen species formation by isolated hepatocytes. Free Radic Biol Med 2002;32:2-10.
32. Wachsman JT. The beneficial effects of dietary restriction: reduced oxidative damage and enhanced apoptosis. Mutat Res 1996;350:25-34.
33. Troy CM, Shelanski ML. Down-regulation of copper/zinc superoxide dismutase causes apoptotic death in PC12 neuronal cells. Proc Natl Acad Sci U S A 1994;91:6384-6387.
34. Dobmeyer TS, Findhammer S, Dobmeyer JM, Klein SA, Raffel B, Hoelzer D, Helm EB, et al. Ex vivo induction of apoptosis in lymphocytes is mediated by oxidative stress: role for lymphocyte loss in HIV infection. Free Radic Biol Med 1997;22:775-785.
35. Fadeel B, Ahlin A, Henter JI, Orrenius S, Hampton MB. Involvement of caspases in neutrophil apoptosis: regulation by reactive oxygen species. Blood 1998;92:4808-4818.
36. Pace GW, Leaf CD. The role of oxidative stress in HIV disease. Free Radic Biol Med 1995;19:523-528.
37. Rosenkranz AR, Schmaldienst S, Stuhlmeier KM, Chen W, Knapp W, Zlabinger GJ. A microplate assay for the detection of oxidative products using 2',7'-dichlorofluorescin-diacetate. J Immunol Methods 1992;156:39-45.
38. Chepda T, Cadau M, Girin P, Frey J, Chamson A. Monitoring of ascorbate at a constant rate in cell culture: effect on cell growth. In Vitro Cell Dev Biol Anim 2001;37:26-30.
39. Zamzami N, Kroemer G. Apoptosis: Mitochondrial Membrane Permeabilization - The (W)hole Story? Curr Biol 2003;13:R71-73.
40. Nicotera P, Leist M, Ferrando-May E. Intracellular ATP, a switch in the decision between apoptosis and necrosis. Toxicol Lett 1998;102-103:139-142.

41. Lemasters JJ, Qian T, Bradham CA, Brenner DA, Cascio WE, Trost LC, Nishimura Y, et al. Mitochondrial dysfunction in the pathogenesis of necrotic and apoptotic cell death. J Bioenerg Biomembr 1999;31:305-319.
42. Liu Y, Fiskum G, Schubert D. Generation of reactive oxygen species by the mitochondrial electron transport chain. J Neurochem 2002;80:780-787.
43. Young TA, Cunningham CC, Bailey SM. Reactive oxygen species production by the mitochondrial respiratory chain in isolated rat hepatocytes and liver mitochondria: studies using myxothiazol. Arch Biochem Biophys 2002;405:65-72.
44. Crompton M. Mitochondrial intermembrane junctional complexes and their role in cell death. J Physiol 2000;529:11-21.
45. Eguchi Y, Shimizu S, Tsujimoto Y. Intracellular ATP levels determine cell death fate by apoptosis or necrosis. Cancer Res 1997;57:1835-1840.
46. Leist M, Single B, Castoldi AF, Kuhnle S, Nicotera P. Intracellular adenosine triphosphate (ATP) concentration: a switch in the decision between apoptosis and necrosis. J Exp Med 1997;185:1481-1486.

9. Mitochondrial Toxicity of Statins

Priska Kaufmann, Michael Török, Saskia Lüde, Stephan Krähenbühl

Divison of Clinical Pharmacology and Toxicology and Department of Research,
University Hospital Basel, Switzerland

Submission in 2005

9.1. Summary

Background: Treatment with statins is rarely associated with myotoxicity, particularly rhabdomyolysis. Statin-induced rhabdomyolysis is a dose-dependent adverse reaction, but its mechanism could not be clarified entirely. Mitochondrial dysfunction may contribute to statin-induced rhabdomyolysis. Therefore we investigated mitochondrial toxicity of four lipophilic (cerivastatin, fluvastatin, atorvastatin, simvastatin) and one hydrophilic statin (pravastatin).

Methods and results: Lactate dehydrogenase-leakage, mitochondrial membrane potential, uncoupling of oxidative phosphorylation, cytochrome c leakage and apoptosis were measured in L6 rat skeletal muscle cells, whereas oxygen consumption, β-oxidation and mitochondrial swelling was assessed in isolated rat skeletal muscle mitochondria. In cells, lipophilic statins (100µmol/L) were cytotoxic, inducing death in 27-49% of the cells, whereas pravastatin did not show cytotoxicity up to 1mmol/L. Additionally, cerivastatin, fluvastatin, and atorvastatin (100µmol/L) decreased the mitochondrial membrane potential in 35 %, 51%, and 40% of the cells whereas simvastatin caused a minor and pravastatin no effect. In mitochondria, all statins except pravastatin decreased state 3 oxidation and the respiratory control ratio (IC_{50}-values: cerivastatin 57µmol/L, fluvastatin 81µmol/L, simvastatin 78µmol/L, atorvastatin 136µmol/L). Beta-oxidation was decreased by 74-99% in the presence of 100µmol/L cerivastatin, fluvastatin, simvastatin and atorvastatin, but was not affected by pravastatin. Mitochondrial swelling, cytochrome c release, DNA fragmentation and phosphatidylserine exposure was induced by lipophilic statins.

Conclusions: The lipophilic statins are potent toxins for skeletal muscle mitochondria, whereas the hyrdrophilic pravastatin did not reduce cell viability. Rhabdomyolysis in response to statin treatment can be explained by mitochondrial toxicity and subsequent apoptosis induction in myocytes. Underlying mitochondrial diseases may represent an additional risk factor for statin-induced rhabdomyolysis.

9.2. Introduction

Statins (3-hydroxy-3-methyl-glutaryl coenzyme A reductase inhibitors, HMG-Co A reductase inhibitors) reduce cholesterol production by inhibiting the synthesis of mevalonate, a critical intermediary in the cholesterol pathway (see Figure 1 for chemical structures). They are well tolerated by most patients but can produce a variety of muscle-related, dose-dependent complaints, ranging from mild myopathy to frank rhabdomyolysis. The most serious risk for patients treated with statins is rhabdomyolysis, which occurs with a frequency of approximately 1:100’000 patient years (1). The economical importance of this adverse drug effect has been demonstrated recently by the withdrawal of cerivastatin (2, 3).

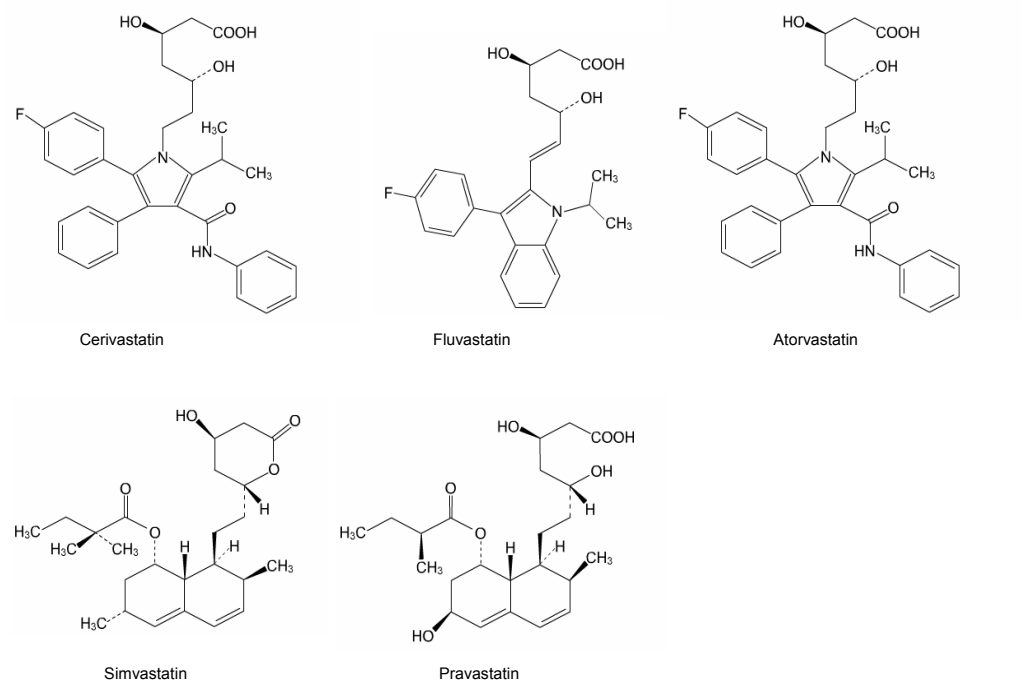

Figure 1: Chemical structures of the investigated statins

The frequency of rhabdomyolysis is low, with a reported incidence of fatal rhabdomyolysis of 0.15 deaths per million prescriptions (3, 4). The fact that the rate of rhabdomyolysis was higher for cerivastatin than for other statins raised the question of whether there are differences in the myotoxic potential of the different statins and whether such differences relate to physiochemical properties of the statins. Statins are either hydrophobic (cerivastatin, fluvastatin, atorvastatin, or simvastatin) or hydrophilic molecules (pravastatin) leading to different tissue bioavailabilities and/or tissue distribution patterns (Table 1) (5, 6), possibly accounting for differences in the toxic potential. Since some statins are metabolized by cytochrome P450 (CYP) isozymes, concomitant treatment with CYP inhibitors has been identified as a risk factor for statin-induced myotoxicity. However, rhabdomyolysis has been reported for all statins, indicating that the physiochemical properties of statins are not the only factors for explaining myotoxicity associated with statins.

Table 1: Physiochemical properties, pharmakokinetics and metabolism of statins studied (1, 7-9)

	Lipo-philicity	Metabolism	Bioavailability [%]	Protein binding [%]	Renal/fecal elimination [%]	Volume of distribution [L]	Hepatic extraction [%]
Cerivastatin	high	Cyp 3A4/2C8	60	99	30 / 70	50	< 40
Fluvastatin	high	Cyp 2C9	6	98	6 / 90	99	> 68
Atorvastatin	high	Cyp 3A4	12	80	2 / 70	381	> 70
Simvastatin	high	Cyp 3A4	5	95	13 / 58	113	~ 80
Pravastatin	low	Conj	18	50	20 / 71	36	44-66

CYP = cytochrome P450; Conj = conjugation

Little is known regarding the mechanism by which statins produce muscle injury. A variety of different hypotheses have been suggested to account for the myotoxic effects. HMG-CoA reductase catalyses the formation of mevalonate from HMG-CoA. Mevalonate is an important precursor not only

for cholesterol but also for ubiquinone, dolichols and isopentyl adenine (10). All these products are involved in various essential cell functions. A deficit in them may therefore adversely affect myocytes, predisposing them to cell death (6, 7). This was confirmed by the finding that the myotoxicity could be abolished by the addition of mevalonate in vitro (10, 11). Ubiquinone is a compound of the mitochondrial electron transport chain, responsible for the transport of electrons between the enzyme complexes. Reduced levels of ubiquinone could be found in patients with mitochondrial myopathies. Reduced synthesis of ubiquinone may result in an impaired function of the electron transport chain (7, 12) and thus decreased ATP synthesis, predisposing cells for necrosis. Moreover, light microscopic changes in muscle biopsy tissue of patients with myopathy associated with either simvastatin or pravastatin, were similar to those observed in patients with mitochondrial myopathy (13, 14). Mitochondrial dysfunction, independently whether it originates from mutations in the mitochondrial genome or is drug-induced, appears to be associated with apoptosis. In skeletal muscle of patients with mitochondrial diseases, cells undergoing apoptosis have been described (15). In addition, mitochondrial permeability transition appears to be a key step in statin-associated cell damage (16).

On the basis of the above considerations, the aim of the present study was to investigate the effect of five different statins on isolated skeletal muscle mitochondria and on myoblasts as well as to assess the role of the mitochondria in statin-induced cell death.

9.3. Materials and Methods

9.3.1. Materials

Fluvastatin was a kind gift from Novartis Pharma AG (Basel, Switzerland), simvastatin from Merck Sharp Dohme Ltd (Rahaway, NJ, USA), cerivastatin from Bayer AG (Zürich, Switzerland) and pravastatin from Bristol-Meyers Squibb (Sankyo, Japan). Atorvastatin was kindly provided by Prof J. Drewe (Clinical Pharmacology & Toxicology, University Hospital Basel). JC-1 was obtained from Alexis Biochemicals (Lausen, Switzerland) and [1-^{14}C]palmitic acid from Amersham Pharmacia Biotech (Dübendorf, Switzerland).

The cell culture media, fetal calf serum and all supplements were from Gibco (Paisley, UK). The 96-well plates were purchased from Becton Dickinson (Franklin Lakes, NJ, USA) and the 8-chamber slides from Nalge Nunc (Rochester, NY, USA). The Vybrant™ Apoptosis Assay Kit #2 was purchased from Molecular probes (Eugene, OR, USA). All other chemicals used were of best quality available and purchased from Sigma–Aldrich (Schnelldorf, Germany).

9.3.2. Animals

Male Sprague Dawley rats (Charles River, Les Onins, France) were used for all experiments. They were fed *ad libitum*, hold on a 12-hour dark and light cycle and weighed before their use. The study protocol has been accepted by the Animal Ethics Committee of the Canton Basel-Stadt (Switzerland).

9.3.3. Cells

The L6 cell line (rat skeletal muscle myoblasts) was obtained from LGC Promochem (Wesel, Germany). The cell line was cultured in Dulbecco's Modified Eagle's Medium (Gibco 61965-026; with

4 mmol/L GlutaMAX®, 4.5 g/L glucose and 3.7g/L sodium bicarbonate) supplemented with 10% heat inactivated fetal calf serum, 1 mmol/L sodium pyruvate and penicillin-streptomycin (100U/mL). Culture conditions were 5 % CO_2 and 95 % air atmosphere at 37°C.

9.3.4. Preparation of simvastatin acid

After dissolution in dimethylsulfoxide (DMSO), simvastatin lactone was hydrolyzed to simvastatin acid by hydrolysis with 0.05 N NaOH solution with stirring at 20°C for 30min. The hydrolysed solution was adjusted to pH 7.4 with 0.2mol/L HCl and stored at -20°C until used (17).

9.3.5. Isolation of rat skeletal muscle mitochondria

At the time of killing the rats weighed (mean 388.7g). The animals were put down with carbon dioxide and euthanized by decapitation. The skeletal muscle (mean 19.0g per rat) was prepared as described elsewhere (18) with minor modifications. After several rinses with isolation medium (100mmol/L KCl, 50mmol/L 3-[N-morpholino]propanesulfonic acid (MOPS), 5mmol/L $MgSO_4$, 0.8mmol/L ethylenediaminetetraacetic acid (EDTA) and 1mmol/L ATP) the skeletal muscle mince was suspended in 10 volumes (wt/vol) of the same medium and treated with the protease Nagarse (5 mg/g mince) for 10min on ice with constant stirring. Mitochondria were isolated by differential centrifugation as described by Chappell et al (19, 20).

The mitochondrial protein content (mitochondrial protein/g muscle) was determined using the biuret method with bovine serum albumin (BSA) as standard (21).

9.3.6. In vitro cytotoxicity assays

Cell injury was assessed by the measurement of release of lactate dehydrogenase (LDH) in the supernatant as compared with LDH of lysed cells (treatment with Triton X-100 0.8%). LDH-leakage was analyzed as described previously (22) and calculated as described by Huang (23). The results were expressed in a dose-dependent manner. Different compound concentrations were added to the culture medium in a 96-well-plate for 24 hours before the supernatants were harvested.

9.3.7. Mitochondrial membrane potential ($\Delta\Psi_m$)

Cells were detached from cell culture flask by adding 10mmol/L EDTA in phosphate buffered saline pH 7.4 (PBS). After filtration, cells were adjusted to a density of 0.5 x 10^6 cells/mL and incubated in complete medium in the dark for 10 min with 4μg/mL JC-1. Flow cytometry was performed using a FACS Calibur flow cytometer (Becton Dickinson, San José, CA, USA). The fluorescence emission wavelength of JC-1 depends on the aggregation of the JC-1 molecules that in turn depends on the $\Delta\Psi_m$ (the greater the $\Delta\Psi_m$, the greater the aggregation to J-complexes). Changes in $\Delta\Psi_m$ were measured by monitoring JC-1 fluorescence. Dinitrophenol (as an uncoupler) and benzbromarone (as a substance that induces depolarization of $\Delta\Psi_m$) were used as positive controls.

9.3.8. Oxygen consumption

Oxygen consumption was monitored polarographically using a 1mL chamber equipped with a Clark-type oxygen electrode (Yellow Springs Instruments, Yellow Springs, OH, USA) at 30°C as described previously (24). The oxygen content of incubation buffer equilibrated with air was assumed to be 223nmol O_2/mL at 30°C (25). The final concentration for L-glutamate was 20mmol/L.

Oxygen consumption by intact mitochondria: The respiratory control ratio (RCR), a marker of the functional integrity of the mitochondria and of the coupling of oxidative phosphorylation was calculated according to Estabrook (26) as the ratio between the rate of oxygen consumption in the presence of a substrate and added adenosine diphosphate (ADP) (state 3) and the rate obtained after complete conversion of ADP to adenosin triphosphate (ATP) (state 4). After depletion of endogenous substrates by the addition of ADP, a substrate was added to the incubation before state 3 respiration was initiated by adding ADP. The test compounds were added to the mitochondrial incubations before the addition of the respective substrate. Control experiments were carried out in the presence of the solvent (DMSO) containing no inhibitor.

Oxygen consumption by L6 muscle cells: 1 x 10^6 cells were treated with oligomycin (final concentration 5µg/mL) in order to inhibit mitochondrial ATPase. After 2 minutes, the test compounds were added to the incubation chamber and the oxygen consumption was determined as a marker for the uncoupling potential of the test compounds. Control experiments were carried out with solvent only.

9.3.9. Activity of NADH-oxidase

The activity of NADH-oxidase was determined at 30°C with the oxygen electrode using freeze-thawed mitochondria as described originally by Blair et al. (27).

9.3.10. In vitro mitochondrial β-oxidation

The β-oxidation of [1-^{14}C] palmitic acid by skeletal muscle mitochondria was assessed by the CO_2 trapping method according Lindstedt et al. (28) with modifications (29). In the incubation vials, which contained 900µl of incubation medium (pH 7.4) (30), a scoop with a folded filter paper was fixed. The filter paper was soaked in 90µl 0.1mol/L KOH in order to trap the volatile $^{14}CO_2$.

After 5min of preincubation at 37°C, the reaction was started by adding 100µL of incubation buffer containing [1-^{14}C]palmitic acid (final concentration 40µmol/L) and bovine serum albumin (final concentration 2.5mg/mL) to the incubation medium. The incubations were carried out in closed vials for 30min at 37°C with slow shaking. Preliminary tests had shown that the reaction was in the linear phase at this time point. The reaction was stopped by adding 200µL of 30% perchloric acid (v/v) and by placing the vials on ice for 5min to precipitate the unchanged isotopically labeled palmitate. Subsequently the vials were left at room temperature for 1.5h to allow complete collection of $^{14}CO_2$. The filters were then added to 5mL of scintillation fluid in a 20mL vial, the contents well mixed, and the radioactivity measured in a β-counter during 5min. The acidified contents of the incubation vials were centrifuged (9500g, 2min) and an aliquot (600µL) of the supernatant was used to determine the formed ^{14}C-labeled acid soluble products (citric acid cycle intermediates such as α-ketoglutarate, succinate, oxalacetate).

9.3.11. Activities of mitochondrial β-oxidation enzymes

All enzyme activities were determined using spectrophotometric assays at 37°C. Freeze-thawed mitochondria were treated 1:1 with 5% cholic acid in order to disrupt the mitochondrial membranes. The solution was then diluted one hundred times with 50mmol/L potassium phosphate buffer (pH 7.4). The concentrations used for atorvastatin, fluvastatin and simvastatin were 50μmol/L and 200μmol/L, for cerivastatin 25μmol/L and of 100μmol/L, and for pravastatin 200μmol/L and of 400μmol/L.

Acyl-CoA Dehydrogenase: The activity was determined according to the method of Hoppel et al (24) using palmitoyl-CoA as a substrate. The incubations contained 50μg mitochondrial protein. The activity was calculated using an extinction coefficient of 21mmol · L^{-1} cm^{-1} for reduced cytochrome c.

Beta-hydroxy acyl-CoA dehydrogenase: Beta-hydroxy-acyl-CoA dehydrogenase activity was determined essentially according to Brdiczka et al. (31)

Beta-ketothiolase: Thiolysis of acetoacetyl-CoA was followed at pH 8.1 and 37°C in a final volume of 0.5mL according to Hoppel et al (24). The slow decrease in extinction due to alkaline hydrolysis was followed for about 30sec (32) before the reaction was started by the addition of 0.25mmol/L CoA. The decrease of absorbance was monitored at 303nm as 3-oxoacyl thioesters have a strong absorption at this wavelength with an apparent extinction coefficient of 12.2 mmol · L^{-1} cm^{-1}.

Enzyme activities are expressed as mU (nanomoles per minute) per mg mitochondrial protein.

9.3.12. Determination of mitochondrial swelling

Mitochondrial permeability transition pore opening in vitro results in mitochondrial swelling. Permeability transition was monitored by measuring the decrease in light scattering at 540nm using a SpectraMAX 250 plate reader (Paul Bucher Analytik und Biotechnologie, Basel, Switzerland). The decrease in light scattering has been shown to closely relate to the percentage of the mitochondrial population undergoing permeability transition (33). Experiments were run within 4 hours following decapitation of the rat. Experiments were initiated by addition of test compounds to a fixed amount of mitochondria in an isotonic swelling buffer pH 7.3, containing 150mmol/L KCl, 20mmol/L MOPS, 10mmol/L Tris(hydroxymethyl)-aminomethan (TRIS), 2mmol/L nitrilotriacetic acid and 2μmol/L calcium ionophore, A23187. Swelling was calculated from the slope between 60 sec and 2000 sec after addition of test compounds.

9.3.13. Cytochrome c immunocytochemistry

For immunocytochemistry cells were grown in an 8 chamber-slide for 24 hours at 37°C and then treated with test compounds, each in a concentration of 100μmol/L, for 24 hours. Afterwards the cells were fixed in 4% paraformaldehyde in PBS for 15min at 37°C and then washed three times with blocking buffer (0.05% saponin, 3% BSA, in PBS). The cells were incubated with 50μL anti-cytochrome c antibody diluted 1:300 (3.33 μL/mL) in blocking buffer and incubated for one hour in a humidified chamber at 37°C. The cells were again washed three times with blocking buffer and incubated for one hour at 37°C in a humidified chamber with 50μL anti-sheep IgG conjugated with Cy3™ diluted 1:200 (5μL/mL) in blocking buffer. The cells were then washed once with blocking buffer

and twice with PBS. To mount each chamber slide, 10-15μL Fluor Save™ reagent was added and the slides were sealed with a clear coverslip. The cells were examined under a fluorescence microscope (Olympus IX 50, Hamburg, Germany) and images were taken.

9.3.14. Determination of apoptosis

Both assays were performed using L6 muscle cells cultured on poly-D-lysine coated (0.1mg/mL, 30min) cell culture dishes.

Hoechst 33342 nuclear staining: A confluent cell layer was treated for 24h with test compounds, then incubated for 30 minutes at room temperature with Hoechst 33342 dye (50μmol/L in PBS) and visualized by fluorescence microscopy (Olympus IX 50, Hamburg, Germany).

Annexin V and propidium iodide (PPI) staining: An *in situ* Apoptosis Detection Kit was used for Annexin V binding and propidium iodide staining (Vybrant™ Apoptosis Assay Kit #2). Cells were treated with the test compounds in a concentration-dependent manner. After a 24h-incubation period, cells were stained with 25μL Annexin V-Alexa Fluor® 488 and 2μL PPI (final concentration: 1.5μg/L). After 15 minutes of incubation at room temperature, samples were analyzed by flow cytometry, using a FACS Calibur flow cytometer (Becton Dickinson, San José, USA).

9.3.15. Statistical analysis

Data are presented as mean ± standard error of the mean (SEM). For statistical comparisons, data of groups were compared by analysis of variances (ANOVA). If ANOVA revealed significant differences, comparisons between the control and the other incubations were performed by Dunnett's post test procedure. T-test (unpaired, two-tailed) was performed, if only two groups were analyzed. The level of significance was $p \leq 0.05$.

9.4. Results

9.4.1. In vitro cytotoxicity assays

The cellular toxicity of the different statins was investigated by treating L6 cells with various concentrations of each compound for 24 hours. The extent of muscle cell LDH leakage, an indicator of cell damage, is shown in figure 2. At 100μmol/L, cerivastatin, fluvastatin, atorvastatin and simvastatin showed significant toxicity. In contrast, pravastatin did not cause any cell damage up to 1mmol/L. In order to gain more insight into the mechanism associated with statin toxicity, we performed the following investigations.

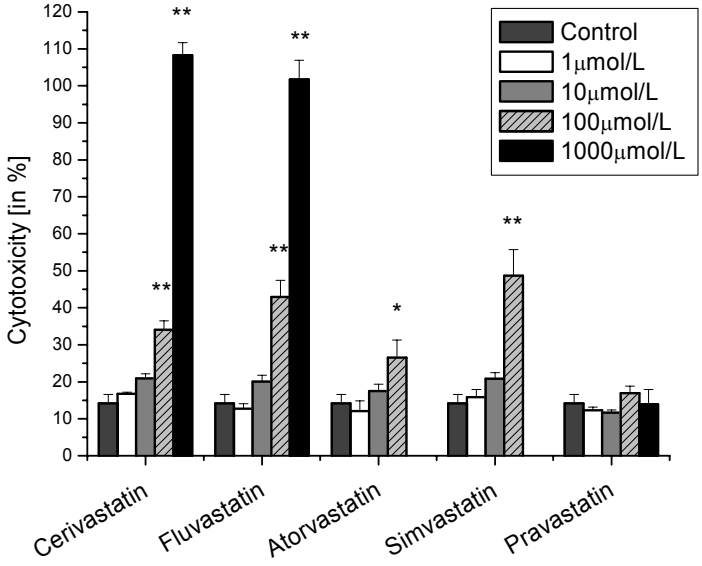

Figure 2: Cytotoxicity of the test compounds was assessed by extracellular LDH in percent of total LDH. Cerivastatin, fluvastatin, atorvastatin and simvastatin caused a concentration-dependent release of LDH from the cytoplasm into the cell culture media. In contrast, the cell membrane remained tight under treatment with pravastatin up to 1mmol/L. Data are given as mean ± SEM of at least three individual experiments. *p<0.05 vs. control, **p<0.01 vs. control.

9.4.2. Mitochondrial membrane potential

In recent years, mitochondrial damage has been recognized as an important mechanism of drug-induced toxicity (34). Moreover, statin induced myopathie has been associated with mitochondrial dysfunction (13, 14). Therefore, we investigated whether mitochondria are involved in the statin-mediated toxicity. In a first step, we measured the mitochondrial membrane potential which can be used as a broad indicator for mitochondrial damage. Furthermore, it has been demonstrated that maintenance of the mitochondrial membrane potential is critical for myocyte survival (35) and also plays a crucial role in the induction of apoptosis (36). Cerivastatin, fluvastatin, atorvastatin and simvastatin led to a concentration dependent loss of the mitochondrial membrane potential (Figure 3). At a concentration of 100µmol/L 35% of the cells showed a dissipated potential with cerivastatin. The corresponding values for fluvastatin, atorvastatin and simvastatin were 51%, 40% and 26%, respectively. In comparison, pravastatin was not toxic up to 1mmol/L.

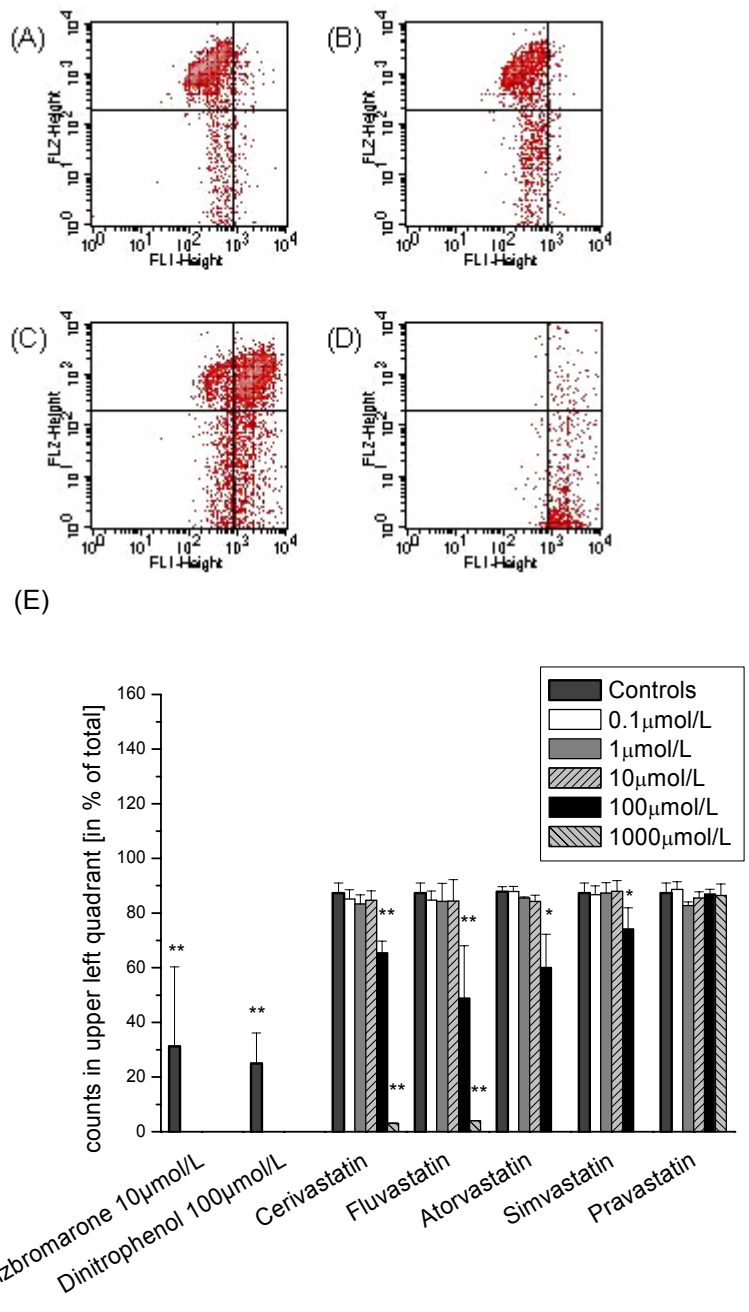

Figure 3: The mitochondrial membrane potential was determined by an ion distribution technique. Cells were labeled with the cationic dye JC-1. Mitochondrial depolarization is indicated by a shift of the fluorescence emission from green to red. Distinct populations of cells with different extents of mitochondrial depolarization were detectable with different treatment. In the upper left quadrant, cells with polarized mitochondria are located (panel A; DMSO 1%), whereas cells with dissipated potential are found in the upper or lower right panel (panel B-D for fluvastatin 10μmol/L, 100μmol/L or 1000μmol/L). The results of the counts in the upper left quadrant are given as rates compared to total counts defined as 100%. Data are given as mean ± SEM of at least three individual experiments. *p<0.05 vs. control, **p<0.01 vs. control.

9.4.3. Oxygen consumption

In order to further specify the mitochondrial dysfunction induced by statins we assessed the toxicity of these substances on oxidative metabolism of isolated rat skeletal muscle mitochondria. In

the presence of L-glutamate as a substrate cerivastatin, fluvastatin, atorvastatin and simvastatin induced a progressive depression of the RCR, which reflects in part the integrity of the inner mitochondrial membrane and the tightness of the coupling of oxidative phosphorylation (37) (see table 2). The corresponding IC_{50} values were: 57µmol/L for cerivastatin, 81µmol/L for fluvastatin , 136µmol/L for atorvastatin and 78µmol/L for simvastatin. For pravastatin, no inhibition was detected up to 400µmol/L and therefore no IC_{50} value was determined.

Table 2: Effects of cerivastatin, fluvastatin, atorvastatin, simvastatin and pravastatin on oxidative metabolism by isolated rat skeletal muscle mitochondria. See method section for experimental details. Mean ± SEM of three experiments using different mitochondrial preparations.

	State 3		State 4		RCR	
Control (no inhibitor)	232.66 ± 20.85		66.16 ± 14.12		3.7 ± 0.77	
Cerivastatin (µmol/L)						
2	255.56 ± 22.61		69.13 ± 9.57		3.96 ± 0.60	
5	239.50 ± 30.70		69.13 ± 5.77		3.48 ± 0.43	
25	288.56 ± 34.99		87.86 ± 10.16		3.37 ± 0.45	
50	273.84 ± 34.99		136.92 ± 15.31	*	1.98 ± 0.04	
100	186.87 ± 19.39		186.87 ± 19.40	**	1.00 ± 0.00	**
Fluvastatin (µmol/L)						
5	240.84 ± 14.57		62.44 ± 7.28		3.90 ± 0.22	
25	224.49 ± 8.28		41.63 ± 21.44		3.52 ± 0.28	
50	266.11 ± 24.34		64.67 ± 6.44		2.27 ± 0.44	
100	191.78 ± 41.20		126.37 ± 28.25		1.73 ± 0.52	
200	31.22 ± 17.42	**	115.96 ± 10.54		1.00 ± 0.00	**
Atorvastatin (µmol/L)						
5	170.97 ± 28.28		49.06 ± 3.41		3.44 ± 0.33	
25	173.20 ± 19.71		56.49 ± 1.49		3.06 ± 0.30	
50	161.30 ± 45.23		45.34 ± 8.76		3.46 ± 0.64	
100	149.41 ± 5.90		71.36 ± 11.00		2.19 ± 0.32	
200	45.34 ± 4.52	**	45.34 ± 4.52		1.00 ± 0.00	**
Simvastatin (µmol/L)						
5	199.96 ± 32.28		56.41 ± 6.48		3.03 ± 0.31	
25	213.34 ± 56.42		74.33 ± 15.52		2.79 ± 0.36	
50	156.84 ± 40.64		86.23 ± 18.09		1.94 ± 0.53	
100	122.65 ± 14.51		80.28 ± 13.38		1.68 ± 0.47	*
200	82.51 ± 9.01	*	82.51 ± 9.01		1.00 ± 0.00	**
Pravastatin (µmol/L)						
50	272.06 ± 24.56		92.17 ± 10.41		3.03 ± 0.43	
100	338.22 ± 40.60		95.00 ± 27.68		2.77 ± 0.51	
200	270.57 ± 35.53		81.77 ± 5.36		3.35 ± 0.52	
300	246.79 ± 41.31		89.94 ± 12.24		2.72 ± 0.09	
400	278.01 ± 73.48		87.71 ± 10.72		3.05 ± 0.49	

*p < 0.05 vs. control; ** p < 0.01 vs. control

While the depression of the RCR by fluvastatin, atorvastatin and simvastatin was mainly due to an inhibition of the state 3 respiration rate, i.e. inhibition of the electron transport chain, for cerivastatin the decrease was mostly because of induction of state 4 oxygen consumption. An induction of state 4

can be due to either uncoupling of oxidative phosphorylation or conversion of ATP to ADP in the mitochondrial matrix. Therefore, oxygen consumption of muscle cells was determined in order to investigate uncoupling directly. Figure 4 shows the influence of the statins on glutamate-supported state 4 respiration of rat skeletal muscle cells in the presence of the phosphorylation inhibitor oligomycin. Under these conditions only cerivastatin showed an induction of state 4, corresponding well with oxygen consumption by isolated mitochondria. Figure 4 convincingly demonstrates that cerivastatin behaved differently among the lipophilic statins, being the only statin acting as an uncoupler of oxidative phosphorylation.

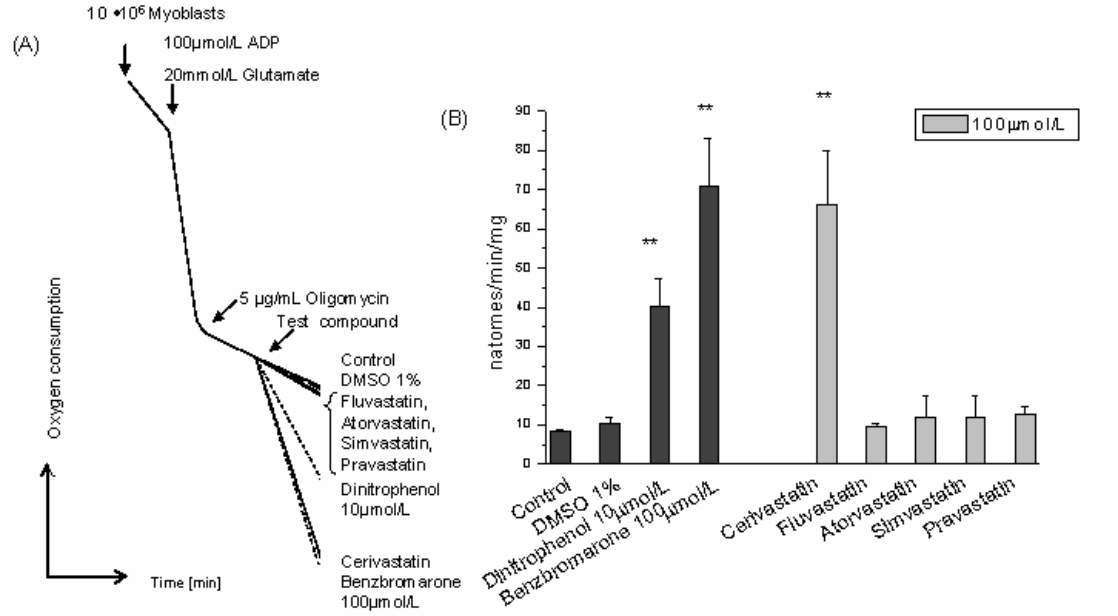

Figure 4: Effects on glutamate-supported oligomycin induced mitochondrial state 4 respiration in rat skeletal myoblasts. In a normal, hence coupled mitochondrion, blocking of F_0F_1-ATPase by oligomycin results in a restricted electron transport and restricted oxygen consumption (state 4). If a test compound works as an uncoupler, oxygen consumption increases, in spite of inhibited phosphorylation (see panel A). Of the tested statins only cerivastatin worked as an uncoupler, whereas fluvastatin, atorvastatin, simvastatin or pravastatin did not increase oxygen consumption. Dinitrophenol and benzbromarone served as positive controls. *p<0.05 vs. control, **p<0.01 vs. control.

9.4.4. Activities of mitochondrial NADH-oxidase

In order to exclude the possibility that the observed lack of toxicity of pravastatin is only due to differences in physiochemical properties of the molecule and in membrane permeability, activity of the mitochondrial NADH oxidase, an enzyme of the electron transport chain, was measured with broken mitochondria. The substrates and test compounds used can therefore interact directly with the complex of the electron transport chain and no membrane barrier has to be overcome. As shown in table 3, pravastatin showed no inhibition up to 1mmol/L, whereas cerivastatin and fluvastatin significantly inhibited NADH oxidase. A tendency was seen for atorvastatin and simvastatin at 100µmol/L. We could show that also in absence of membrane barriers pravastatin didn't affect the electron transport chain.

Table 3: Activity of mitochondrial NADH-oxidase measured in freeze-thawed mitochondrial preparations. Activities are expressed relative to control values Data are given as mean SEM of at least three individual mitochondrial preparations.

	Activity (in %)	
Control (no inhibitor)	100.0 ± 11.5	
Rotenone 10µmol/L	9.8 ± 1.0	**
Antimycin 10µmol/L	6.6 ± 3.3	**
Benzbromarone 100µmol/L	55.4 ± 4.2	**
Cerivastatin (µmol/L)		
0.1	100.3 ± 9.2	
1.0	91.5 ± 3.9	
10.0	88.2 ± 6.7	
100.0	87.9 ± 6.6	
1000.0	51.1 ± 0.8	**
Fluvastatin (µmol/L)		
0.1	89.9 ± 7.0	
1.0	85.7 ± 8.4	
10.0	87.5 ± 4.0	
100.0	85.6 ± 8.8	
1000.0	49.6 ± 3.3	**
Atorvastatin (µmol/L)		
0.1	91.2 ± 11.8	
1.0	82.7 ± 8.1	
10.0	76.6 ± 8.4	
100.0	78.1 ± 4.3	
Simvastatin (µmol/L)		
0.1	84.1 ± 3.6	
1.0	89.2 ± 16.4	
10.0	72.5 ± 9.4	
100.0	71.9 ± 6.0	
Pravastatin (µmol/L)		
0.1	87.2 ± 6.9	
1.0	83.0 ± 8.6	
10.0	90.3 ± 1.5	
100.0	87.1 ± 5.6	
1000.0	78.6 ± 4.2	

*p < 0.05 vs. control; ** p < 0.01 vs. control

9.4.5. Beta-oxidation

Measurement of β-oxidation in skeletal muscle cells reflects both, acid soluble products and formation of CO_2 in the tricarboxylic acid cycle. Formation of CO_2 represents 1 to 30% of the total amount of degradation products of palmitic acid, whereas 60 to 95% are found in the acid soluble fraction (38). Since the activity of the respiratory chain can be rate-limiting for mitochondrial fatty acid metabolism (39), acetoacetate was added to the incubations. Acetoacetate converts nicotinamide adenine dinucleotide (NADH) to NAD^- by the action of β-hydroxybutyrate dehydrogenase (an enzyme of the mitochondrial matrix) and thereby eliminates the indirect impairment of mitochondrial β-oxidation by inhibitors of the electron transport chain (such as fluvastatin, simvastatin and atorvastatin).

Cerivastatin (100μmol/L), fluvastatin, atorvastatin and simvastatin (each 200μmol/L) inhibited mitochondrial β-oxidation between 83 and 97%. Pravastatin revealed to have an inhibitory effect of 50% at 400μmol/L (see table 4). The corresponding IC_{50} for the acid soluble fraction were: 14.4μmol/L for cerivastatin, 9.0μmol/L for fluvastatin, 29.0μmol/L for atorvastatin, 75.3μmol/L for simvastatin and 303.6μmol/L for pravastatin. Since there is no ketogenesis taking place in muscle cells, we could convincingly show, that mitochondrial β-oxidation was impaired.

Table 4: Effects of cerivastatin, fluvastatin, atorvastatin, simvastatin and pravastatin on β-oxidation in isolated rat liver mitochondria.

	Supernatant Activity (µUnits/mg)		CO_2 trapping Activity (µUnits/mg)	
Cerivastatin (µmol/l)				
control	175.9 ± 72.6		32.0 ± 20	
2	118.6 ± 29.0		26.0± 9	
5	80.1 ± 41.7		12.6 ± 4	
25	24.1 ± 17.9		9.0 ± 0.4	
50	19.6 ± 16.1		2.2 ± 1.1	
100	28.2 ± 25.1		0.9 ± 0.4	
Fluvastatin (µmol/l)				
Control	12.7 ± 5.5		15.1 ± 9.9	
5	9.0 ± 3.5		7.6 ± 3.8	
25	0.7 ± 0.7	*	1.2 ± 0.2	
50	0.6 ± 0.3	*	1.0 ± 0.2	
100	0.1 ± 0.01	*	0.9 ± 0.1	
200	0.4 ± 0.3	*	0.8 ± 0.2	
Atorvastatin (µmol/l)				
Control	56.4 ± 30.8		20.6 ± 8.2	
5	62.6 ± 41.8		13.4 ± 10.4	
25	57.6 ± 28.4		16.0 ± 9.0	
50	36.0 ± 25.6		11.1 ± 9.1	
100	5.8 ± 2.3		1.3 ± 0.4	**
200	13.3 ± 7.4		1.0 ± 0.5	**
Simvastatin (µmol/l)				
Control	59.0 ± 20.7		35.5 ± 13.3	
5	68.6 ± 28.8		21.1 ± 8.6	
25	62.1 ± 33.7		22.8 ± 8.8	
50	68.1 ± 50.8		11.3 ± 3.8	
100	4.5 ± 2.4		1.5 ± 0.4	
200	4.5 ± 3.3		1.5 ± 0.5	
Pravastatin (µmol/l)				
Control	170.9 ± 64.7		24.7 ± 10.7	
50	148.2 ± 29.5		30.2 ± 9.7	
100	154.4 ± 39.5		27.2 ± 10.3	
200	116.0 ± 14.9		17.3 ± 6.3	
300	91.5 ± 16.5		15.4 ± 6.0^{3}	
400	76.5 ± 51.2		11.8 ± 7.1^{-3}	

*p < 0.05 vs. control; ** p < 0.01 vs. control.

In order to further localize the inhibitory effect of β-oxidation in more detail, three enzymes of the β-oxidation were investigated: long-chain acyl-CoA dehydrogenase, ketothiolase and β-hydroxy-acyl-CoA dehydrogenase. Acyl-CoA dehydrogenase, which is potentially rate-limiting for β-oxidation (24, 40), was assessed using palmitoyl-CoA as substrate. In the presence of 100µmol/L cerivastatin, or 200µmol/L fluvastatin, atorvastatin or simvastatin, or 400µmol/L pravastatin this enzyme was inhibited by 26.4%, 33.4%*, 27.7%*, 37.1%* or 19.9% respectively, reaching statistical significance for fluvastatin, atorvastatin and simvastatin.

The enzyme β-hydroxy-acyl-CoA dehydrogenase was inhibited by 18.5%*, 21.6%*, 9.8%, 16.3%* or 2.3% in the presence of 100µmol/L cerivastatin, or 200µmol/L fluvastatin, atorvastatin or

simvastatin, or 400μmol/L pravastatin, reaching statistical significance for cerivastatin, fluvastatin and simvastatin. The third enzyme assessed was β-ketothiolase, the last enzyme in the β-oxidation cycle, using acetyl-CoA as a substrate. This enzyme was not significantly inhibited by the statins.

9.4.6. Mitochondrial swelling

As already demonstrated, statins did cause a loss of the mitochondrial membrane potential. This led to the hypothesis that statins, like other drugs, act directly on mitochondria by inducing mitochondrial permeability transition (41), which in turn results in mitochondrial depolarization, cytochrome c release and swelling (42). In this process, the impermeability of the inner mitochondrial membrane is reversed (43), due to the formation of a proteinaceous pore (the mitochondrial permeability transition pore) which consists of several mitochondrial proteins (44). Cerivastatin, fluvastatin, atorvastatin and simvastatin were inducing mitochondrial swelling in a concentration dependent manner, whereas pravastatin did not cause an opening of the mitochondrial permeability transition pore (figure 5).

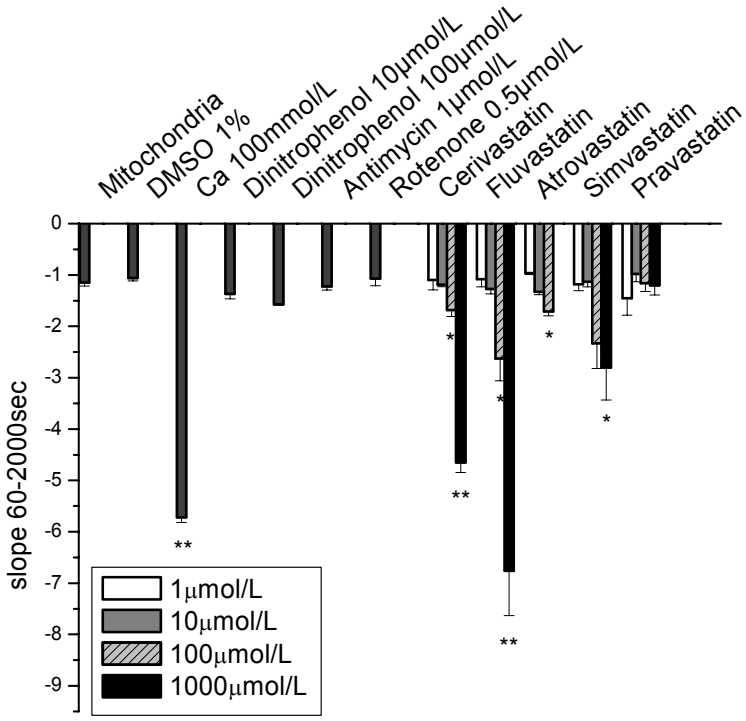

Figure 5: Mitochondrial permeability transition was monitored as a decrease in absorbance at 540nm. Upon pore opening, osmotically driven influx of water into the mitochondrial matrix leads to swelling of mitochondria, which causes a change in light scattering properties of mitochondria. Ca^{2+} was used as positive control. Among the tested statins only pravastatin did not induce mitochondrial permeability transition, whereas cerivastatin, fluvastatin, atorvastatin and simvastatin did cause a concentration-dependent increase in mitochondrial size. * $p < 0.05$ vs. control; ** $p < 0.01$ vs. control.

9.4.7. Cytochrome c release

As a consequence of the mitochondrial permeability transition pore opening, cytochrome c release from the mitochondrial intermembrane space into the cytoplasma should occur, which in turn can trigger the mitochondrial pathway of apoptosis (45-47). To confirm that mitochondria were indeed involved in apoptosis induction, cytochrome c release was determined in L6 cells. As shown in figure 6, only pravastatin did not induce a release of cytochrome c, whereas for cerivastatin, fluvastatin, atorvastatin or simvastatin cytochrome c could be detected in the cytoplasm.

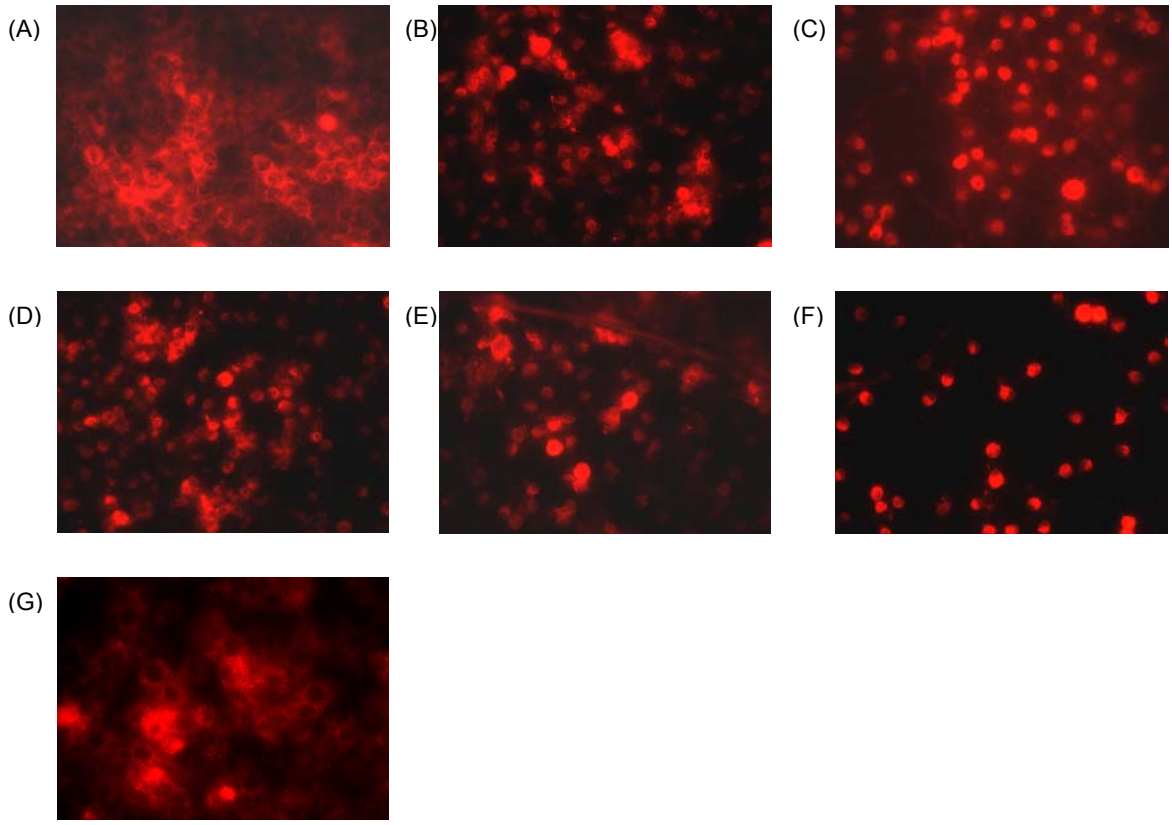

Figure 6: Cytochrome c release caused by test compounds (each 100µmol/L) after 24 hours of exposure detected by immunocytochemistry: With 1% DMSO (panel A) pravastatin (panel G) no leakage into the cytoplasma occurred, as indicated by a punctual pattern of immunoreactivity. The nuclei remained visible. After treatment with benzbromarone (positive control, panel B), cerivastatin (panel C), fluvastatin (panel D), atorvastatin (panel E) or simvastatin (panel F) cytochrome c was released from the mitochondrial intermembrane space and shows a widespread immunoreactivity and covered nuclei, indicating cytoplasmatic localization.

9.4.8. Determination of apoptosis

Released cytochrome c can activate caspases and induce apoptosis (45, 48). DNA fragmentation occurring during apoptosis can be visualized by fluorescence microscopy upon staining with dyes intercalating with DNA. As shown in Figure 7, untreated cells showed an apoptosis rate of

1.1%. At a concentration of 100μmol/L the proportion of apoptotic cells was 10% for cerivastatin, 8% for fluvastatin, 9% for atorvastatin, 8% for simvastatin or 1% for pravastatin.

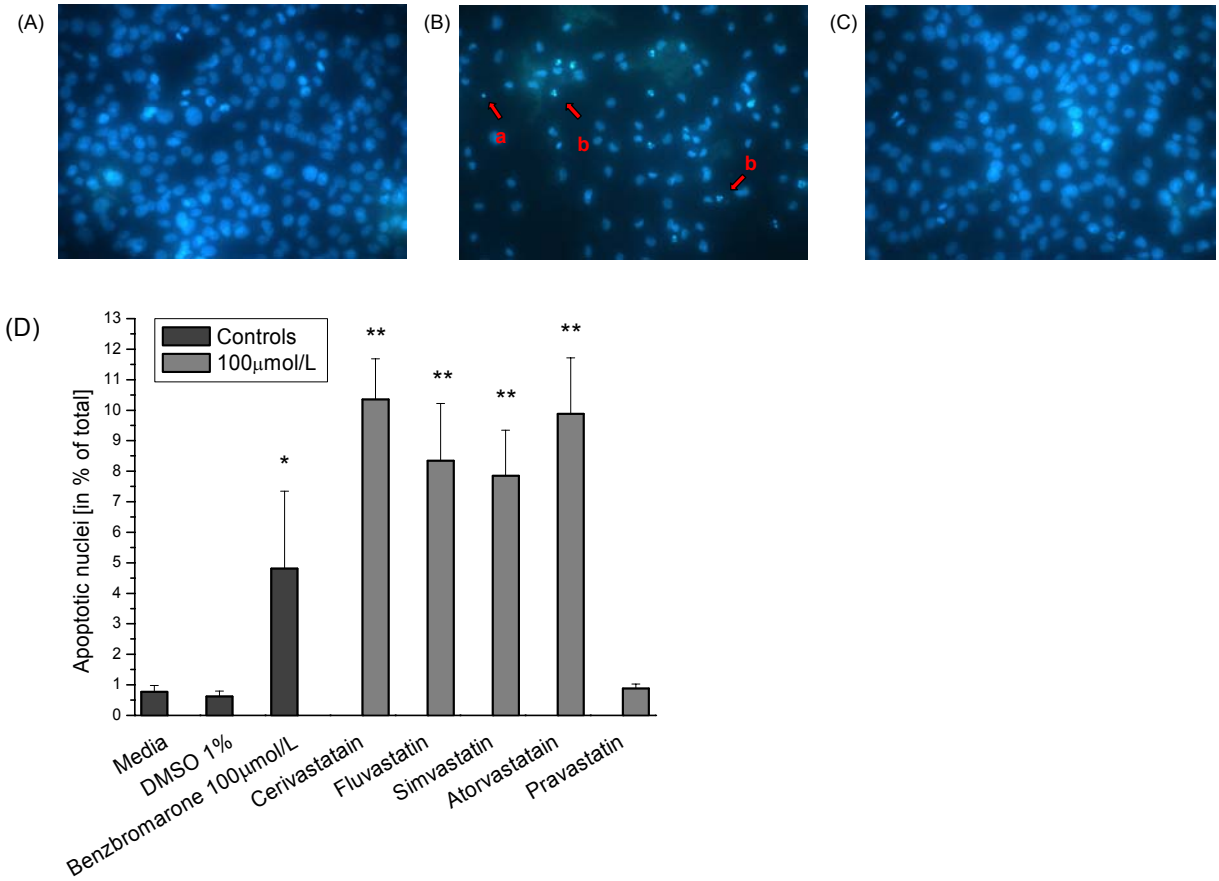

Figure 7: Rat myoblasts were treated with test compounds at a concentration of 100μmol/L for 24 hours and subsequently stained with Hoechst 33342. The cell nuclei were visualized using fluorescence microscopy (panel (A) control, panel (B) atorvastatin, panel (C) pravastatin). Apoptotic cells were characterized by DNA condensation (panel B, arrow a) and DNA fragmentation (panel B, arrow b). Panel (D) summarizes the percentage of cells undergoing apoptosis. Pravastatin was the only statin not inducing apoptosis. * $p < 0.05$ vs. control; ** $p < 0.01$ vs. Control.

Another hallmark of the early stages of apoptosis is the translocation of phosphatidylserine from the inner leaflet to the outer leaflet of the plasma membrane. Externalized phosphatidylserine can be detected using Annexin V, a protein with high affinity for this phospholipid. Cells were co-stained with PPI as a marker of cell membrane permeability, which increases during the later stages of apoptosis and also in necrosis. In necrotic cells, Annexin-V can enter the cells and bind to the phosphatidylserine exposed on the inner leaflet of the cell membrane as well, which might lead to false-positive results if Annexin-V was used as the only staining tool. Since PPI only enters cells with already disintegrated membranes, early apoptotic cells can be distinguished from late apoptotic and necrotic cells. Similar to the stainings with Hoechst 33342, flow cytometric analysis of the cells revealed progressive increase of the annexin V signal, thus early apoptotic cells, with increasing concentrations of cerivastatin, fluvastatin, atorvastatin and simvastatin. At 100μmol/L between 9 and 17% of cells exposed to cerivastatin, fluvastatin, atorvastatin or simvastatin underwent early apoptotic stages. In contrast, only 3% of cells treated with pravastatin were annexin V positive (Figure 8). Fas

ligand, used as a positive control for apoptosis induction induced early apoptosis in 12% of cells. The late apoptotic and necrotic fraction of cells, represented by the population in the upper right quadrant, showed also a concentration-dependent increase. Between 20 and 25% of the cells treated with 100µmol/L of a lipophilic statin were in this stage of cell death (data not shown). If necrosis was a major mode of cell death, the proportion of cells in this field should be considerably higher. These findings suggest that apoptosis is the major mode of cell death.

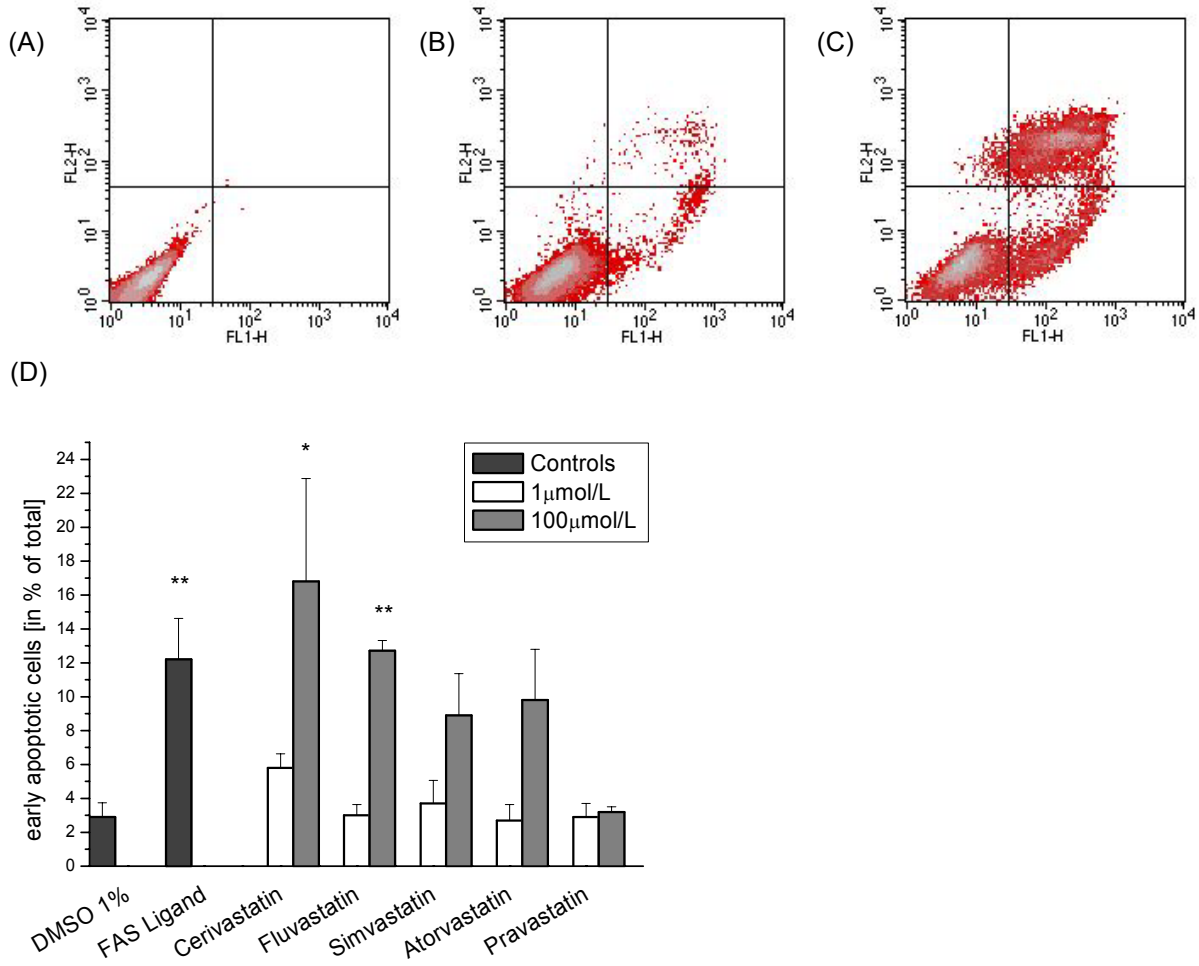

Figure 8: Annexin V binding and PPI uptake by L6 cells. L6 cells were incubated for 24h at concentration of 1 and 100µmol/L of each test compound and subsequently stained with Annexin V and PPI. The samples were analyzed by flow cytometry (see panel A: control, panel B: fluvastatin 1µmol/L, panel C: fluvastatin 100µmol/L).The lower left quadrant represents the unstained, thus viable cells. The cells in the lower right quadrant are undergoing early apoptosis and are stained only with Annexin V. The upper right quadrant represents the double stained cells undergoing necrosis or later stages of apoptosis. Under control conditions, the vast majority of cells were located in the lower left part (panel A), whereas fluvastatin was inducing apoptosis in a concentration dependent manner (panel B: fluvastatin 1µmol/L, panel C fluvastatin 100µmol/L). Panel D: percentage of cells undergoing early stages of apoptosis relative to control values. Fas ligand was used as positive control for apoptosis. Data are given as mean ± SEM of at least three individual experiments. *p<0.05 vs 1% DMSO, **p<0.01 vs 1% DMSO.

9.5. Discussion

In the present study, we could demonstrate that there is an important difference between hydrophobic and hydrophilic statins in their toxic effect on isolated skeletal muscle mitochondria and whole skeletal muscle cells. We showed that the effects of hydrophobic statins on cell viability and mitochondrial function was entirely different from those for a hydrophilic statin. It was previously shown that hydrophilic statins are distributed much more selectively in hepatic cells than hydrophobic ones. Extrahepatically, hydrophilic molecules cannot penetrate the lipid bilayer and thus cannot cause intracellular events, whereas the hepatic cell membrane contains organic anion transporters, which transport hydrophilic statins into the hepatic cytoplasma. In contrast, lipophilic statins can enter hepatic and extrahepatic cells and therefore exert their effect in peripheral tissues, such as skeletal muscle (5, 6). Our findings in skeletal muscle cells are consistent with data in the literature for different cell types, such as endothelial cells (49), hepatocytes (50), cardiac myocytes (51) or vascular smooth muscle cells (52, 53). However, consistent results were obtained with disrupted mitochondria, indicating that the differences in distribution patterns and permeabilities does not entirely account for the differences in toxicity between hydrophilic and lipophilic statins.

It could convincingly be shown that the injury in skeletal muscle induced by lipophilic statins is due to apoptosis. It has been demonstrated that hydrophobic statins cause mitochondrial dysfunction, which resulted in a dissipation of the electronic potential across the inner mitochondrial membrane and mitochondrial permeability transition. The inner mitochondrial membrane potential is generated through the activity of proton pumps of the respiratory chain and is the driving force for ATP generation by the F_1F_0-ATPase, thus essential for cell energy supply. The mitochondrial membrane permeabilization is considered to be a point-of-no-return of apoptotic cell death (48, 54). Mpt culminates in a loss of the barrier function of the outer mitochondrial membrane and the consequent release of apoptosis inducing proteins, such as cytochrome c from the mitochondrial intermembrane space. The induction of the mitochondrial apoptotic pathway in this case might be further enhanced by the fact, that the cell may lack of prenylated (farnesylated or geranylated) small GTP-proteins, such as Rho, Ras or Rac, which promote cell maintenance, cell survival and attenuate apoptosis (3, 49, 55, 56). Apoptosis is a crucial mechanism designed to maintain tissue structure. If inappropriately activated, apoptosis can produce pathological conditions. In the case of statin therapy, apoptosis induction might be responsible of the slowdown for generation of atherosclerotic plaques by inhibiting proliferation of vascular smooth muscle cells, whereas apoptosis in skeletal muscle under statin treatment could produce the observed muscle damage (3). These findings further confirm a hypothesis mentioned in the literature (10), that myotoxicity is, at least in part, a direct consequence of the inhibition of the cholesterol synthesis pathway. So adverse effect and desired effect rely on the same mode of action. Therefore, it will be most difficult to distinguish the myotoxic unwanted effect from the wanted reduction of cholesterol synthesis.

Our findings support the results of Kubato et al (50) in hepatocytes. Compatible with our results the authors showed that lipophilic statins did cause an apoptotic injury in hepatocytes. Pravastatin did neither reduce cell viability nor induce apoptosis. In this case, it is unlikely that the lack of hepatotoxic effect of pravastatin results from the limited access of this compound to cell, since a reduction of cholesterol synthesis could be shown. Maybe a combination of factors rather than a single reason like limited access of pravastatin to the cell interior explains lack of toxicity.

As mentioned before, all hydrophobic statins tested did induce apoptosis in skeletal muscle cells. They all showed a consistent pattern of effects, only varying, albeit to a minor degree, in their toxic potential. For the uncoupling capacity, however, among all the statins measured only cerivastatin showed uncoupling of oxidative phosphorylation. Uncoupling seems not to be related to the inhibitory concentrations of HMG CoA reductase, since atorvastatin and simvastatin show similar IC_{50} values to those of cerivastatin (5). It has recently become evident that the risk of severe myotoxic events with cerivastatin was markedly higher than for other statins (4, 5, 57) and has demonstrated that the safety of stains is not a class effect (58). If mitochondrial uncoupling occurs, protons are transported into the mitochondrial matrix by bypassing the F_1F_0-ATPase. As a consequence, the mitochondrial membrane potential is decreased, cellular ATP can be depleted and in the long run, cytotoxicity can be induced (42). Based on this, it can be assumed, that occurrence of uncoupling for cerivastatin, in addition to the other toxic principles, aggravates the toxicity and eventually translates into an increased in vivo incidence of cerivastatin induced myotoxicity.

Having measured the muscle toxicity of statins *in vitro*, the question arises, to what extent our findings translate into the *in vivo* situation. The data available about plasma concentrations of statins after oral administration is not consistent (1, 8) and one might argue that toxicity of hydrophobic statins *in vitro* occurred at concentrations higher than the plasma concentrations achieved under statin therapy. In this regard, two points should be considered. Firstly, the volume of distribution of lipophilic statins clearly indicates that peripheral tissue binding is extensive (see table 1). Consequently, the mass transport of lipophilic transport into tissue is high, which is in accordance with their high membrane permeability due to the nonpolar nature of the drugs. So it is highly likely that concentrations in skeletal muscle are markedly higher than the concentrations measured in the plasma. Secondly, a concept known for other mitochondrial toxins such as salicylate or valproate (59) might apply for myotoxicity and statins. Inherited metabolic disorders, e.g. defects in mitochondrial functions such as β-oxidation, can be causal in or contribute to toxic processes (60). If a patient treated with statins has an underlying mitochondrial defect and is treated with a statin as a mitochondrial toxin, this patient might be more susceptible to myotoxicity, which may get apparent at lower concentrations. It is interesting to note, that stains not only inhibit β-oxidation, as we could show in our study, but they also undergo β-oxidation themselves on the hydroxyheptanoic acid side chain. Metabolites shortened by two or in case of pravastatin even four carbon units, resulting in pentanoic derivatives or propanoic products, respectively, have been observed in vivo (61-63). Lipophilic statins basically autoinhibit this metabolic pathway, whereas with pravastatin, β-oxidation is not affected. Certainly, this inhibition itself is not the reason for the observed toxicity of hydrophobic statins, however, the question is what happened, if this inhibition coincides with an underlying mitochondrial defect in β-oxidation. It is possible, that in this case, the statin induced inhibition and the inherited defect raise to apparent toxicity.

In conclusion, lipophilic statins reduced cell viability and did impair mitochondrial functions, such as β-oxidation and respiratory chain, which are essential for cell survival. As a consequence, the mitochondrial membrane potential dissipated, the mitochondrial permeability transition pore opened and apoptosis inducing factors were released. Mitochondrial dysfunction and the subsequent release of mitochondrial proteins are tightly linked to the process of programmed cell death, also called apoptosis. Consistently, induction of apoptosis could be convincingly demonstrated, since lipophilic statins did cause DNA fragmentation and an increase in annexin V stained cells. Myotoxicity, in particular rhabdomyolysis in response to lipophilic statin treatment can be explained by mitochondrial

toxicity and the subsequent induction of apoptosis of myocytes. Underlying mitochondrial diseases may represent an additional risk factor for statin-induced rhabdomyolysis.

9.6. References

1. Ballantyne CM, Corsini A, Davidson MH, Holdaas H, Jacobson TA, Leitersdorf E, et al. Risk for myopathy with statin therapy in high-risk patients. Arch Intern Med 2003; 163: 553-564. Order.
2. Thompson CA. Cerivastatin withdrawn from market. Am J Health Syst Pharm 2001; 58: 1685.
3. Thompson PD, Clarkson P, Karas RH. Statin-associated myopathy. Jama 2003; 289: 1681-1690.
4. Ballantyne CM, Corsini A, Davidson MH, Holdaas H, Jacobson TA, Leitersdorf E, et al. Risk for myopathy with statin therapy in high-risk patients. Arch Intern Med 2003; 163: 553-564.
5. Rosenson RS. Current overview of statin-induced myopathy. Am J Med 2004; 116: 408-416.
6. Ichihara K, Satoh K. Disparity between angiographic regression and clinical event rates with hydrophobic statins. Lancet 2002; 359: 2195-2198.
7. Evans M, Rees A. Effects of HMG-CoA reductase inhibitors on skeletal muscle: are all statins the same? Drug Saf 2002; 25: 649-663.
8. Lennernas H. Clinical pharmacokinetics of atorvastatin. Clin Pharmacokinet 2003; 42: 1141-1160.
9. Singhvi SM, Pan HY, Morrison RA, Willard DA. Disposition of pravastatin sodium, a tissue-selective HMG-CoA reductase inhibitor, in healthy subjects. Br J Clin Pharmacol 1990; 29: 239-243.
10. Masters BA, Palmoski MJ, Flint OP, Gregg RE, Wang-Iverson D, Durham SK. In vitro myotoxicity of the 3-hydroxy-3-methylglutaryl coenzyme A reductase inhibitors, pravastatin, lovastatin, and simvastatin, using neonatal rat skeletal myocytes. Toxicol Appl Pharmacol 1995; 131: 163-174.
11. Flint OP, Masters BA, Gregg RE, Durham SK. Inhibition of cholesterol synthesis by squalene synthase inhibitors does not induce myotoxicity in vitro. Toxicol Appl Pharmacol 1997; 145: 91-98.
12. Muscari A, Puddu GM, Puddu P. Lipid-lowering drugs: are adverse effects predictable and reversible? Cardiology 2002; 97: 115-121.
13. Giordano N, Senesi M, Mattii G, Battisti E, Villanova M, Gennari C. Polymyositis associated with simvastatin. Lancet 1997; 349: 1600-1601.
14. Schalke BB, Schmidt B, Toyka K, Hartung HP. Pravastatin-associated inflammatory myopathy. N Engl J Med 1992; 327: 649-650.
15. Umaki Y, Mitsui T, Endo I, Akaike M, Matsumoto T. Apoptosis-related changes in skeletal muscles of patients with mitochondrial diseases. Acta Neuropathol (Berl) 2002; 103: 163-170. Epub 2001 Oct 2031.
16. Kobayashi T, Kuroda S, Tada M, Houkin K, Iwasaki Y, Abe H. Calcium-induced mitochondrial swelling and cytochrome c release in the brain: its biochemical characteristics and implication in ischemic neuronal injury. Brain Res 2003; 960: 62-70.
17. Bogman K, Peyer AK, Torok M, Kusters E, Drewe J. HMG-CoA reductase inhibitors and P-glycoprotein modulation. Br J Pharmacol 2001; 132: 1183-1192.

18. Kerner J, Hoppel CL. Radiochemical malonyl-CoA decarboxylase assay: activity and subcellular distribution in heart and skeletal muscle. Anal Biochem 2002; 306: 283-289.
19. Chappell JB, Perry SV. Biochemical and osmotic properties of skeletal muscle mitochondria. Nature 1954; 173: 1094-1095.
20. Cadenas S, Brand MD. Effects of magnesium and nucleotides on the proton conductance of rat skeletal-muscle mitochondria. Biochem J 2000; 348: 209-213.
21. Gornall AG, Bardawill GJ, David M. Determination of serum proteins by means of the biuret reaction. Journal of Biological Chemistry 1949; 177: 751-766.
22. Vassault A. Lactate dehydrogenase. In: H. U. Bergmeyer, H. U. Bergmeyers. Methods of Enzymatic Analysis. Weinheim: VHC; 1983.p.118-125
23. Huang TH, Lii CK, Chou MY, Kao CT. Lactate dehydrogenase leakage of hepatocytes with AH26 and AH Plus sealer treatments. J Endod 2000; 26: 509-511.
24. Hoppel C, DiMarco JP, Tandler B. Riboflavin and rat hepatic cell structure and function. Mitochondrial oxidative metabolism in deficiency states. J Biol Chem 1979; 254: 4164-4170.
25. Chappell JB. The oxidation of citrate, isocitrate and cis-aconitate by isolated mitochondria. Biochem J 1964; 90: 225-237.
26. Eastabrook R. Mitochondrial respiratory control and polarographic measurement of ADP:O ratios. Methods Enzymol 1967; 10: 41-47.
27. Blair PV, Oda T, Green DE. Studies on the Electron Transfer System. Liv. Isolation of the Unit of Electron Transfer. Biochemistry 1963; 128: 756-764.
28. Lindstedt G, Lindstedt S, Nordin I. Gamma-butyrobetaine hydroxylase in human kidney. Scand J Clin Lab Invest 1982; 42: 477-485.
29. Morse RM, Valenzuela GA, Greenwald TP, Eulie PJ, Wesley RC, McCallum RW. Amiodarone-induced liver toxicity. Ann Intern Med 1988; 109: 838-840.
30. Spaniol M, Bracher R, Ha HR, Follath F, Krahenbuhl S. Toxicity of amiodarone and amiodarone analogues on isolated rat liver mitochondria. J Hepatol 2001; 35: 628-636.
31. Brdiczka D, Pette D, Brunner G, Miller F. Compartmental dispersion of enzymes in rat liver mitochondria. Eur J Biochem 1968; 5: 294-304.
32. Holland P, Senior AE, H.S.A. S. Biochemical effects on the hypoglycaemic compound pent-4-enoic acid and related non-hypoglycaemic fatty acids. Biochemical Journal 1973; 136: 174-184.
33. Haworth RA, Hunter DR. The Ca2+-induced membrane transition in mitochondria. II. Nature of the Ca2+ trigger site. Arch Biochem Biophys 1979; 195: 460-467.
34. Pessayre D, Mansouri A, Haouzi D, Fromenty B. Hepatotoxicity due to mitochondrial dysfunction. Cell Biol Toxicol 1999; 15: 367-373.
35. Jones SP, Teshima Y, Akao M, Marban E. Simvastatin attenuates oxidant-induced mitochondrial dysfunction in cardiac myocytes. Circ Res 2003; 93: 697-699. Epub 2003 Sep 2025.
36. Ding WX, Nam Ong C. Role of oxidative stress and mitochondrial changes in cyanobacteria-induced apoptosis and hepatotoxicity. FEMS Microbiol Lett 2003; 220: 1-7.
37. Rustin P, Chretien D, Bourgeron T, Gerard B, Rotig A, Saudubray JM, et al. Biochemical and molecular investigations in respiratory chain deficiencies. Clin Chim Acta 1994; 228: 35-51.
38. Sherratt HS, Watmough NJ, Johnson MA, Turnbull DM. Methods for study of normal and abnormal skeletal muscle mitochondria. Methods Biochem Anal 1988; 33: 243-335.

39. Latipaa PM, Karki TT, Hiltunen JK, Hassinen IE. Regulation of palmitoylcarnitine oxidation in isolated rat liver mitochondria. Role of the redox state of NAD(H). Biochim Biophys Acta 1986; 875: 293-300.
40. Osmundsen H, Bremer J. A spectrophotometric procedure for rapid and sensitive measurements of beta-oxidation. Demonstration of factors that can be rate-limiting for beta-oxidation. Biochem J 1977; 164: 621-633.
41. Xue L, Borutaite V, Tolkovsky AM. Inhibition of mitochondrial permeability transition and release of cytochrome c by anti-apoptotic nucleoside analogues. Biochem Pharmacol 2002; 64: 441-449.
42. Lemasters JJ, Qian T, Bradham CA, Brenner DA, Cascio WE, Trost LC, et al. Mitochondrial dysfunction in the pathogenesis of necrotic and apoptotic cell death. J Bioenerg Biomembr 1999; 31: 305-319.
43. Oliveira PJ, Coxito PM, Rolo AP, Santos DL, Palmeira CM, Moreno AJ. Inhibitory effect of carvedilol in the high-conductance state of the mitochondrial permeability transition pore. Eur J Pharmacol 2001; 412: 231-237.
44. Zoratti M, Szabo I. The mitochondrial permeability transition. Biochim Biophys Acta 1995; 1241: 139-176.
45. Green DR, Reed JC. Mitochondria and apoptosis. Science 1998; 281: 1309-1312.
46. Kroemer G, Reed JC. Mitochondrial control of cell death. Nat Med 2000; 6: 513-519.
47. Newmeyer DD, Ferguson-Miller S. Mitochondria: releasing power for life and unleashing the machineries of death. Cell 2003; 112: 481-490.
48. Zamzami N, Kroemer G. Apoptosis: Mitochondrial Membrane Permeabilization - The (W)hole Story? Curr Biol 2003; 13: R71-73.
49. Kaneta S, Satoh K, Kano S, Kanda M, Ichihara K. All hydrophobic HMG-CoA reductase inhibitors induce apoptotic death in rat pulmonary vein endothelial cells. Atherosclerosis 2003; 170: 237-243. Order.
50. Kubota T, Fujisaki K, Itoh Y, Yano T, Sendo T, Oishi R. Apoptotic injury in cultured human hepatocytes induced by HMG-CoA reductase inhibitors. Biochem Pharmacol 2004; 67: 2175-2186.
51. Ogata Y, Takahashi M, Takeuchi K, Ueno S, Mano H, Ookawara S, et al. Fluvastatin induces apoptosis in rat neonatal cardiac myocytes: a possible mechanism of statin-attenuated cardiac hypertrophy. J Cardiovasc Pharmacol 2002; 40: 907-915.
52. Guijarro C, Blanco-Colio LM, Ortego M, Alonso C, Ortiz A, Plaza JJ, et al. 3-Hydroxy-3-methylglutaryl coenzyme a reductase and isoprenylation inhibitors induce apoptosis of vascular smooth muscle cells in culture. Circ Res 1998; 83: 490-500.
53. Guijarro C, Blanco-Colio LM, Massy ZA, O'Donnell MP, Kasiske BL, Keane WF, et al. Lipophilic statins induce apoptosis of human vascular smooth muscle cells. Kidney Int Suppl 1999; 71: S88-91.
54. Waterhouse NJ, Ricci JE, Green DR. And all of a sudden it's over: mitochondrial outer-membrane permeabilization in apoptosis. Biochimie 2002; 84: 113-121.
55. Nishida M, Nagao T, Kurose H. Activation of Rac1 increases c-Jun NH(2)-terminal kinase activity and DNA fragmentation in a calcium-dependent manner in rat myoblast cell line H9c2. Biochem Biophys Res Commun 1999; 262: 350-354.

56. Suri S, Monkkonen J, Taskinen M, Pesonen J, Blank MA, Phipps RJ, et al. Nitrogen-containing bisphosphonates induce apoptosis of Caco-2 cells in vitro by inhibiting the mevalonate pathway: a model of bisphosphonate-induced gastrointestinal toxicity. Bone 2001; 29: 336-343.
57. Farmer JA. Learning from the cerivastatin experience. Lancet 2001; 358: 1383-1385.
58. Davidson MH. Controversy surrounding the safety of cerivastatin. Expert Opin Drug Saf 2002; 1: 207-212.
59. Krahenbuhl S, Mang G, Kupferschmidt H, Meier PJ, Krause M. Plasma and hepatic carnitine and coenzyme A pools in a patient with fatal, valproate induced hepatotoxicity. Gut 1995; 37: 140-143.
60. Ulrich RG, Bacon JA, Brass EP, Cramer CT, Petrella DK, Sun EL. Metabolic, idiosyncratic toxicity of drugs: overview of the hepatic toxicity induced by the anxiolytic, panadiplon. Chem Biol Interact 2001; 134: 251-270.
61. Prueksaritanont T, Ma B, Fang X, Subramanian R, Yu J, Lin JH. beta-Oxidation of simvastatin in mouse liver preparations. Drug Metab Dispos 2001; 29: 1251-1255.
62. Boberg M, Angerbauer R, Kanhai WK, Karl W, Kern A, Radtke M, et al. Biotransformation of cerivastatin in mice, rats, and dogs in vivo. Drug Metab Dispos 1998; 26: 640-652.
63. Dain JG, Fu E, Gorski J, Nicoletti J, Scallen TJ. Biotransformation of fluvastatin sodium in humans. Drug Metab Dispos 1993; 21: 567-572.

10. Mechanisms of venoocclusive disease for the combination of cyclophosphamide and roxithromycin

Priska Kaufmann[1,3], Michael Török[1,3], Johannes Beltinger[2], Katrijn Bogman[1,3], Markus Wenk[1,3], Luigi Terracciano[4], Stephan Krähenbühl[1,3]

Divisions of Clinical Pharmacology & Toxicology[1] and of Gastroenterology[2], and Departments of Research[3] and of Pathology[4], University Hospital Basel, Switzerland

Submission in 2005

10.1. Abstract

Background: High doses (≥ 500 mg/m^2) of cyclophosphamide are known to cause venoocclusive disease (VOD). We recently observed a patient treated with immunosuppressive cyclophosphamide doses (100 mg/day) and roxithromycin developing VOD. Since roxithromycin inhibits cytochrome P450 (CYP) 3A4 and P-glycoprotein, the patient may have been exposed to higher cyclophosphamide and/or cyclophosphamide metabolite concentrations.

Methods: The effect of roxithromycin on the metabolism and toxicity of cyclophosphamide was studied using a human endothelial cell line and human hepatic microsomes.

Results: While cyclophosphamide and roxithromycin were individually almost not toxic on endothelial cells, their combination was toxic. While roxithromycin did not favor the generation of toxic metabolites from cyclophosphamide, it led to cyclophosphamide accumulation due to inhibition of both CYP3A4 and CYP2B6. Although roxithromycin inhibited P-glycoprotein, this was not the mechanism for increased cyclophosphamide toxicity, since other P-glycoprotein inhibitors were not toxic. In the presence of roxithromycin, cyclophosphamide induced apoptosis in endothelial cells, most probably by mitochondrial membrane permeability transition and release of cytochrome c.

Conclusions: The combination cyclophosphamide and roxithromycin, but not the individual compounds, is toxic on endothelial cells. Apoptosis is the principle mechanism of the toxicity of this combination, whereas inhibition of P-glycoprotein and formation of toxic metabolites are unlikely.

10.2. Introduction

Cyclophosphamide is an alkylating drug used widely in the treatment of cancer and autoimmune diseases (1, 2). It requires hepatic cytochrome P450 (CYP)-catalyzed transformation to generate alkylating metabolites. The current understanding of the metabolism of cyclophosphamide is presented in Figure 1 (3). Both activation and deactivation of cyclophosphamide are mediated by several CYP isozymes. Roughly, the activation pathway is mainly mediated by CYP 2B6 and to a smaller extent by CYP 3A4, whereas the inactivation is mediated almost exclusively by CYP 3A4.

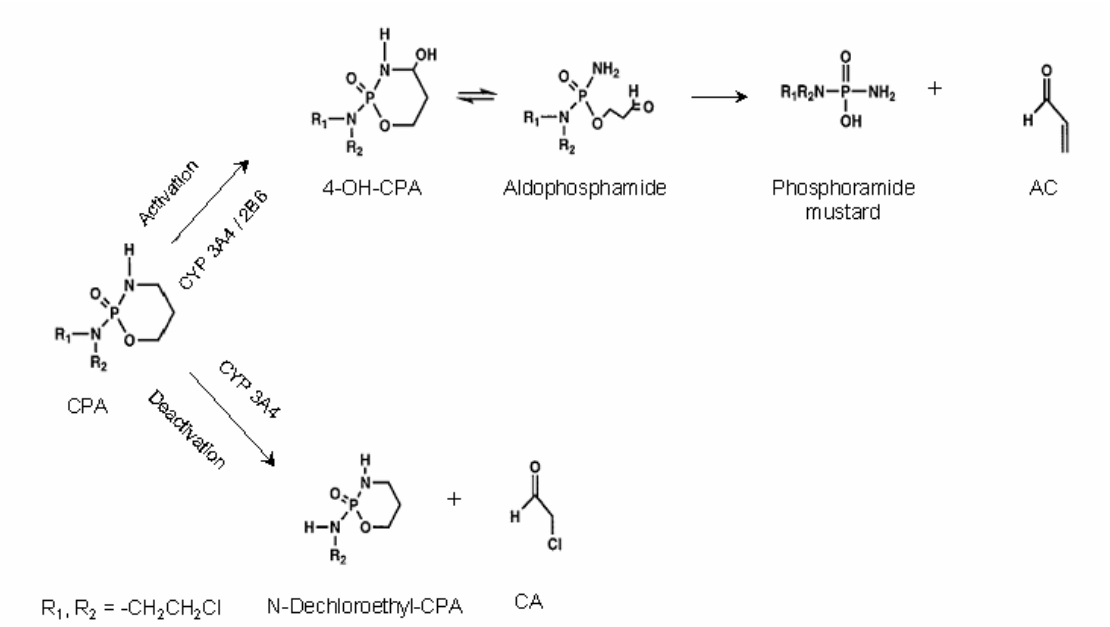

Figure 1: Cytochrome P450 (CYP)-catalyzed metabolism of cyclophosphamide via the 4-hydroxylation (drug activation) and N-chlorodeethylation (drug inactivation) pathways. CPA = cyclophosphamide, AC = acrolein, CA = 2-chloroacetaldehyde.

Hepatic venoocclusive disease (VOD) is characterized by a fibrous obliteration of the central and of small sublobular veins. VOD is a well described complication after bone marrow transplantation, and can be caused by high doses of cyclophosphamide (≥ 500 mg/m^2) (4-6). The incidence of VOD following the cyclophosphamide/bulsufan regimen for preparation to bone marrow transplantation is between 27 and 36% (5, 6). So far, no data have been published about the induction of VOD with low dose cyclophosphamide therapy (1-2 mg/kg) used for the treatment of autoimmune diseases. We have recently observed a patient treated with 100 mg cyclophosphamide and with 300 mg roxithromycin per day who developed VOD (7). Roxithromycin is a semisynthetic macrolide antibiotic with *in vivo* antibacterial activities similar to erythromycin but with a longer duration of action and a higher potency (8). Several macrolide antibiotics and its metabolites, including troleandomycin, erythromycin, clarithromycin and roxithromycin, have been shown to inhibit CYP3A catalytic activities by forming inactive P450-Fe^{2+} metabolite complexes after activation. Inhibition of CYP 3A4 represents the major mechanism of drug-drug interactions between macrolide antibiotics and other drugs (9). To the best of our knowledge, no data is available about the inhibitory effects of macrolide antibiotics on CYP2B6.

The aim of the present study was to investigate the mechanisms by which VOD was caused in the patient treated with cyclophosphamide and roxithromycin as described above. Considering that roxithromycin is an inhibitor of CYP3A4, we speculated that there might be a shift towards CYP2B6-mediated activation of cyclophosphamide. The patient's liver and, in particular, hepatic endothelial cells may therefore have been exposed to higher levels of toxic metabolites than expected from the dose of cyclophosphamide administered. By the use of cultured human umbilical endothelial cells, we could confirm the toxicity of the cyclophosphamide/roxithromycin combination and were able to investigate the underlying mechanisms of cell death.

10.3. Materials and Methods

10.3.1. Materials

All chemicals used were of best quality available and purchased from Merck (Darmstadt, Germany), Fluka or Sigma (Buchs, Switzerland). Fetal calf serum and all culture media were from Gibco (Paisley, UK), 96-well microtiter plates were from Costar (Cambridge, MA), Optiplate™-96 were from Packard (Zürich, Switzerland) and the Lab-Tek chambered coverglass system from Nunc (Napperville, IL, USA).

10.3.2. Cell lines and cell culture conditions

The murine monocytic leukemia cell line P388/MDR was obtained from Dr. C. Geroni (Pharmacia & Upjohn, Centro Ricerche e Sviluppo, Milano, Italy). The cell line was cultured as described previously (10). The human umbilical vein endothelial cell line ECV 304 (11) was cultured in DMEM (Gibco, Paisly, UK) supplemented with 10% heat-inactivated fetal calf serum, 110μg/mL sodium pyruvate, 1mg/mL-glucose, 2μmol/mL L-glutamine, 0.40 μg/mL pyridoxine, 100U/mL penicillin and 100 μg/mL streptomycin. The CCRF-MDR cell line was cultured in RPMI glutamax 1640 (Gibco, Paisly, UK) supplemented with 10% heat-inactivated fetal calf serum, 50μg/mL gentamycin and 1μg/mL vincristine. One day prior to the experiments, cells were switched to vincristine-free medium. Culture conditions for all lines were 5% CO_2/95% air atmosphere at 37°C.

10.3.3. Solutions and incubations

Cyclophosphamide stock solutions were dissolved in phosphate-buffered saline (PBS, pH 7.4), roxithromycin in DMSO. The DMSO concentration did not exceed 1% in any incubation. To all incubations, the same amount of DMSO was added as for the incubations containing roxithromycin.

10.3.4. LDH leakage assay

Cell injury was assessed as the release of lactate dehydrogenase (LDH) into the supernatant and compared to cells lysed with Triton X-100 (final concentration 0.8%). LDH activity was analyzed as described previously (12) and calculated as described by Huang (13).

10.3.5. P-glycoprotein

P-glycoprotein expression: P-glycoprotein (P-gp) was visualized by Western blot analysis using the monoclonal antibody C219 (Alexis, Lausen, Switzerland). The cells were lysed in a buffer, pH 6.8, composed of 5mmol/L EDTA, 20mmol/L Tris HCl, 1% Triton and a protease inhibitor mixture (Roche AG, Basel, Switzerland) using a syringe. Proteins were electrophoresed (1 h, 120V) in the presence of molecular weight standards (Gibco, Paisly, UK) on a 6% polyacrylamide sodium dodecyl sulfate (SDS) gel using a running buffer containing 25mmol/L Tris, 192mmol/L glycine, 0.1% SDS, pH 8.3. Electrophoresed proteins were transferred onto a nitrocellulose filter (Hybond ECL, Apbiotech, Uppsala, Sweden) for 1 h (120mA) using a wet transfer cell (Biorad, Hercules, CA, USA). After the transfer, the membranes were incubated for 2 hours with the primary monoclonal antibody C219

(0.5μg/mL). After repeated washing, a peroxidase conjugated sheep anti-mouse antibody (Amersham Life Science, Little Chalfont, UK) was added for 45min at room temperature. The immunoreactive bands were visualized by enhanced chemiluminescence (ECL, Amersham International, Little Chalfont, UK) according to manufacturer's protocol.

Efflux assay: The impact of several test compounds on P-gp was measured in P-gp-overexpressing P388/MDR cells as described previously (10).

10.3.6. In vitro microsomal assay

Incubations were carried out in open tubes containing 100μL (total volume) of 100mmol/L potassium phosphate buffer (pH 7.4), NADPH 1mmol/L, 3mmol/L $MgCl_2$, 100μg human microsomal protein, and 25mmol/L cyclophosphamide. Reaction mixtures were incubated at 37°C for 15 minutes in a shaking water bath and stopped by the sequential addition of 40μL of ice-cold 5.5% $ZnSO_4$, 40μL of saturated barium hydroxide, and 20μL of 10mmol/L HCl. After spinning at 10'000g for 20min, the supernatant was split into two 80μL aliquots for the determination of 2-chloroacetaldehyde and acrolein, respectively.

10.3.7. Quantification of cyclophosphamide metabolites

Sample preparation: 2-Chloroacetaldehyde was derivatized with adenosine (14). After the derivatization, 1-N^6-ethenadenosine-3',5'-cyclic monophosphate was added as internal standard (final concentration 500μmol/L). Acrolein was derivatized with 3-aminophenol as described elsewhere (14).

Solid phase extraction: Solid phase extraction was performed using disposable reversed-phase macropolymer sorbent columns (OASIS HBL 30mg, Waters Corporation, MA, USA). After preconditioning with 1mL of 5% methanol in water (v:v) followed by 1mL H_2O, samples (400μL) were loaded, washed with 1mL 5% methanol and eluted with 1mL acetonitril for 2-chloroacetaldehyde or 1mL methanol for acrolein, respectively. The eluate was collected in glass tubes and evaporated to dryness at 55°C. The residues were dissolved in 400μL H_2O, vortexed for 1min and centrifuged at 100g for 1 minute.

HPLC analysis: For the determination of 2-chloroacetaldehyde, samples (25μL) were chromatographed on a Luna phenyl-hexyl-column, 150 x 4.60mm (5μm particles, Phenomenex, CA, USA). Samples were eluted isocratically with 7.5% methanol in potassium phosphate buffer (50mM, pH 3.5) with a flow rate of 0.8ml/min. The fluorescent product 1-N^6-ethenadenosine was eluted at 12min, the internal standard at 22min. Detection was achieved using an excitation wavelength of 270nm and an emission wavelength of 411nm. Analysis of acrolein was performed on a C_{18} reversed-phase column, 150 x 4.6mm (5μm particles, LUNA, Phenomenex) as described elsewhere (14).

10.3.8. Determination of apoptosis

Assays were performed with confluent adherent endothelial cells grown on poly-D-lysine coated (0.1mg/ml, 30min) glass slides. Cells were incubated with cyclophosphamide and roxithromycin individually and in combination as described in the Result section. Cells were treated for 24h with different concentrations of test compounds, incubated for 30 minutes at room temperature in

Hoechst 33342 dye (50μmol/L in PBS) and visualized by fluorescence microscopy (Olympus IX 50, Hamburg, Germany).

10.3.9. Cytochrome c immunocytochemistry

Cells were grown in an 8 chamber-slide (coated with poly-D-lysine) for 20 hours at 37°C and then treated with the test compounds for 24 hours. Afterwards, cytochrome c was visualized using an anti-cytochrome c antibody and an anti-sheep IgG antibody-conjugated Cy3™ (Jackson Laboratories, West Grove, PA, USA) according to the manufacturer's protocol.

10.3.10. Mitochondrial membrane potential

Cells were detached from cell culture flask by adding 10mmol/L EDTA in PBS. After filtration, cells were adjusted to a density of 0.5 x 10^6 cells/ml and incubated for 10 min in the dark in complete medium containing 4μg/mL JC-1 (Molecular Probes, Eugene, Oregon, USA). Flow cytometry was performed by FACS analysis (Calibur, Becton and Dickinson, San José, CA, USA). Changes in $\Delta\Psi_m$ were measured by monitoring JC-1 fluorescence at 590nm. Benzbromarone, a substance that induces depolarization of the mitochondrial membrane potential, was used as a positive control.

10.3.11. Statistical analysis

Data are presented as mean ± SEM. Comparison within groups were performed by one-way ANOVA (analysis of variance). If the ANOVA revealed a statistical significance, Dunnett's procedure was performed as a secondary test. $P < 0.05$ was considered to be statistically significant.

10.4. Results

10.4.1. In vitro cytotoxicity

Cellular toxicity of cyclophosphamide and roxithromycin was investigated by treating human umbilical vein endothelial cells with various concentrations of test compounds for 24 hours. As shown in Figure 2, the incubation with the individual substances cyclophosphamide or roxithromycin did not reveal any toxicity up to 500μmol/L. A significant toxicity was observed only in incubations containing both cyclophosphamide (variable concentrations) and roxithromycin (constant at 500μmol/L) at concentrations above 50μmol/L of cyclophosphamide. In comparison, erythromycin (500μmol/L), another macrolide antibiotic used as a control, was neither toxic individually nor in combination with cyclophosphamide.

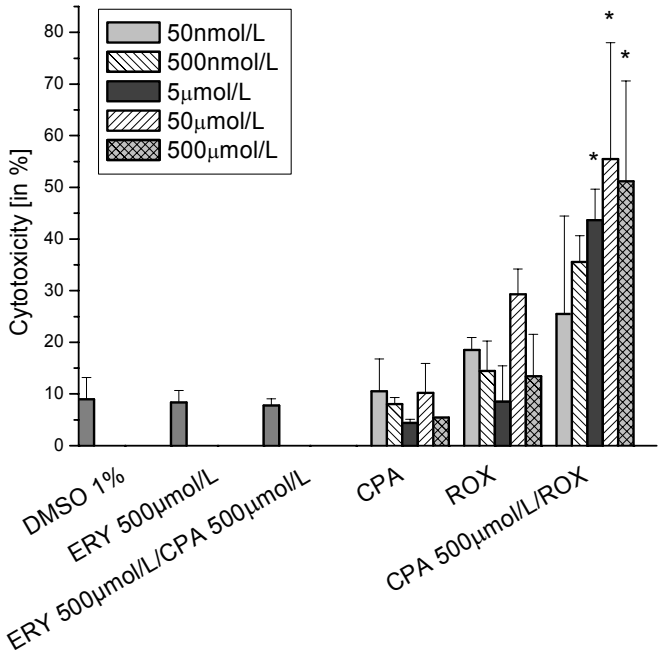

Figure 2: Cytotoxicity of the test compounds on the human endothelial cell line ECV 304 as assessed by LDH leakage. Units are the percentage from total LDH activity (activity after cytolysis with 0.8% Triton X-100). Data are given as mean ± SEM of at least three individual experiments. ERY = erythromycin, CPA = cyclophosphamide, ROX = roxithromycin. *P<0.05 vs. control, **p<0.01 vs. control.

Cyclophosphamide is a substrate of several CYPs, and it is known that roxithromycin and its metabolites are inhibitors of CYP 3A4. Additionally, it is important to note that the CYP system, especially the isoform CYP3A, has overlapping substrate specificity with P-gp (15, 16). Following these considerations, we decided to study the effect of roxithromycin on P-gp and on CYP-associated metabolism of cyclophosphamide, since interactions of roxithromycin with these proteins could explain, at least in part, the augmented cytotoxicity of cyclophosphamide.

10.4.2. P-glycoprotein

The expression of P-gp in endothelial cells was demonstrated by Western blotting. As shown in Figure 3, ECV 304 cells show immunoreactivity in the molecular weight range of 150kDa, the molecular weight of P-gp. A similar band was observed in P-gp-expressing CCRF-MDR cells, which served as a positive control.

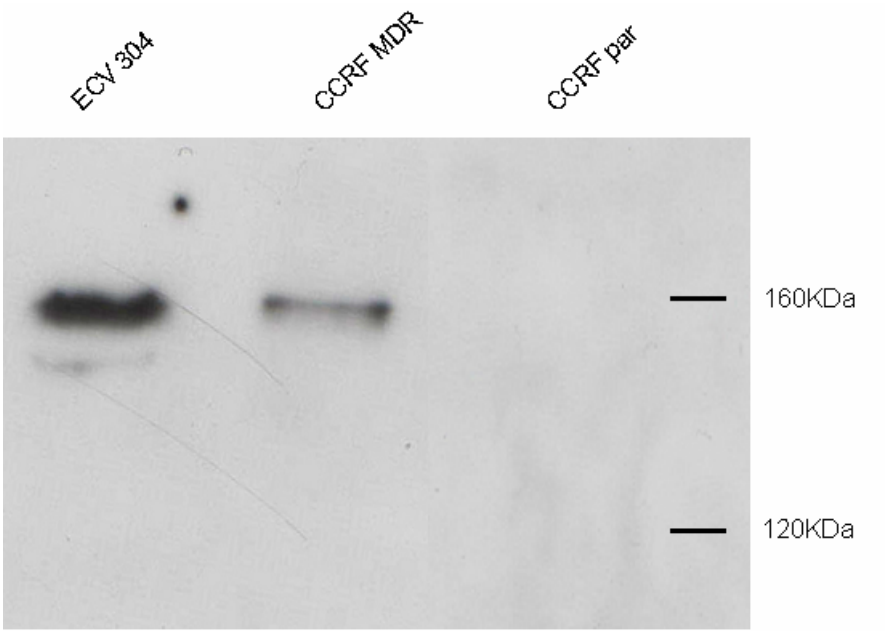

Figure 3: Western blot analysis of P-glycoprotein expression in ECV 304 cells. CCRF-par and CCRF-MDR cells are human T-lymphoblastoid cell lines from which lysates were used as negative or positive control, respectively. P-glycoprotein was detected by the monoclonal antibody C219. Immunoreactive protein was detected in the molecular weight range of 150kD with lysates from CCRF-MDR and ECV 304 cells, but not from CCRF-par cells, which are devoid of P-glycoprotein.

To investigate the test substances for their P-gp-modulating properties, we measured rhodamine 123 (R123) efflux in a P-gp overexpressing cell line using a microtiter-based fluorimetric assay. The R123-assay revealed that roxithromycin inhibited P-gp with an IC_{50} of 194μmol/L (Figure 4). In contrast, neither cyclophosphamide nor the two metabolites acrolein or 2-chloroacetaldehyde showed an inhibitory effect on P-gp (data not shown). Despite cyclophosphamide did not inhibit P-gp, it could still be a substrate of this transport protein, since P-gp has a very broad substrate specificity. In that case, inhibition of P-gp with roxithromycin should increase the intracellular cyclophosphamide concentration and cellular toxicity. However, an increase in the toxicity of cyclophosphamide could not be demonstrated by co-incubation with the P-gp inhibitors erythromycin (Figure 2) or verapamil (data not shown).

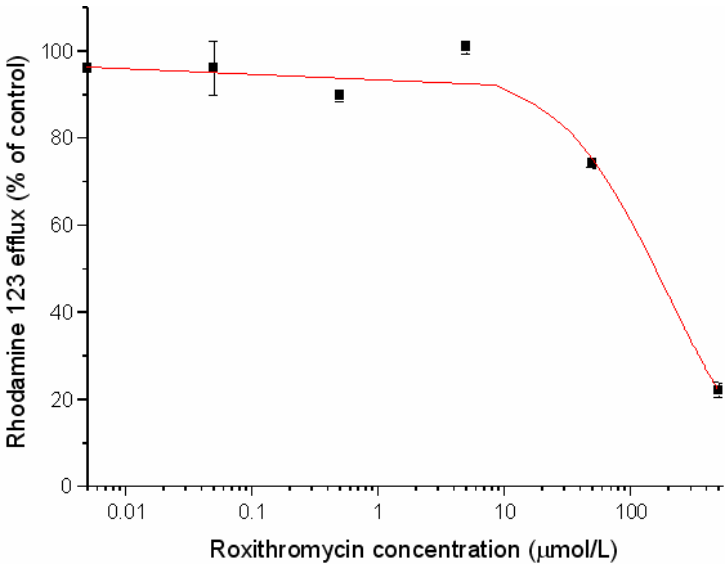

Figure 4: P-glycoprotein (P-gp) inhibition by roxithromycin as assessed by a microtiter plate based fluorimetric assay. P388/MDR cells were preloaded with the P-gp substrate rhodamine 123. Rhodamine 123 efflux was monitored in the presence of increasing concentrations of roxithromycin. The experiments reveal an inhibition of rhodamine 123 efflux (indicating inhibition of P-gp) with increasing roxithromycin concentrations (IC_{50} 194μmol/L). Data are expressed as a percentage of the rhodamine 123 efflux in absence of inhibitor. Values represent means ± SEM for at least n=3 determinations.

10.4.3. In vitro microsomal metabolism

Incubations were performed in the presence or absence of roxithromycin at various concentrations. As a reference for CYP3A4 inhibition, ketoconazole was used. The CYP3A4 specificity of ketoconazole is concentration-dependent. At concentrations >2μmol/L CYP isozymes other than CYP3A4 are also inhibited (17). The ketoconazole concentrations used in the experiments therefore covered CYP3A4 specific (0.5μmol/L) as well as unspecific concentrations (5 and 50μmol/L).

Analysis of the 2-chloroacetaldehyde and acrolein pathways of cyclophosphamide revealed that the rate of metabolite production was linear between 0 and 20 minutes. The CYP3A4-mediated 2-chloroacetaldehyde pathway was inhibited by roxithromycin with an IC_{50} of 24μmol/L, whereas ketoconazole inhibited this pathway with an IC_{50} of 0.09μmol/L (see Table 1). The CYP2B6-mediated acrolein pathway was inhibited by roxithromycin with an IC_{50} of 107μmol/L whereas the corresponding IC_{50} for ketoconazole was 50μmol/L. As shown in Table 1, the ratio of the IC_{50} for CYP2B6 and CYP3A4 is much higher for ketoconazole than roxithromycin, showing a higher selectivity for CYP3A4 for ketoconazole. In agreement with this observation, at 0.5μmol/L ketoconazole, an increase in product formation by the acrolein pathway could be observed, suggesting a shift from the CYP3A4-driven 2-chloroacetaldehyde to the more CYP2B6-driven acrolein pathway (Figure 5). This phenomenon was not observed with roxithromycin, since the inhibition of CYP3A4 by roxithromycin is much less specific as compared to ketoconazole (Table 1 and Figure 5). The results of the *in vitro* experiments therefore indicate that selective inhibition of CYP3A4 indeed increases cyclophosphamide metabolism by CYP2B6, but that roxithromycin inhibits both pathways simultaneously.

Table 1: IC_{50} values for both metabolic pathways of cyclophosphamide (see Figure 1) in the presence of roxithromycin or ketoconazole as inhibitors. The assay conditions are described in the Method section. Mean ± SEM of at least 3 experiments.

	Roxithromycin (μmol/L)	**Ketoconazole (μmol/L)**
CA-pathway (CYP3A4)	24.2 ± 10.4	0.1 ± 0.06
AC-pathway (CYP2B6)	107 ± 32	13.1 ± 6.4
CYP2B6/CYP3A4	4.42	131

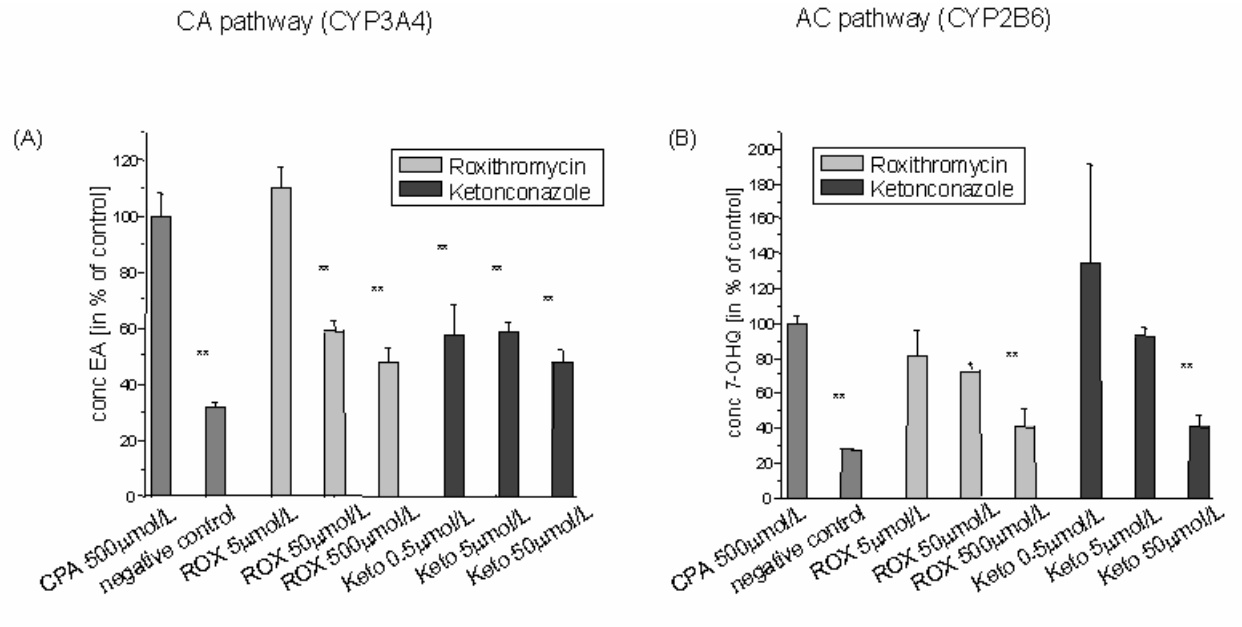

Figure 5: Effect of roxithromycin and ketoconazole on cyclophosphamide metabolism by human liver microsomes. N-chlorodeethylation (CA pathway, panel A) and 4-hydroxylation (AC pathway, panel B) were determined as described in Materials and Methods at a cyclophosphamide concentration of 25mmol/L. As a negative control, microsomes were incubated in the absence of NADPH. As shown in panel A, ketoconazole inhibits the CYP3A4-mediated CA pathway in all concentrations tested (IC_{50} 0.1μmol/L). Roxithromycin is an equally effective inhibitor from 50μmol/L upwards with an IC_{50} of 24μmol/L. As shown in panel B, ketoconazole is a far less potent inhibitor of the CYP2B6-mediated AC pathway, inhibiting acrolein formation with an IC_{50} of 13μmol/L. At the lowest concentration of ketoconazole (0.5μmol/L), the formation of AC appears to be increased as compared to control values (not reaching statistical significance). Roxithromycin inhibits this pathway with an IC_{50} of 102μmol/L, which is only slightly higher than for the CA pathway. CPA = cyclophosphamide, Keto = ketoconazole, ROX = roxithromycin. *P < 0.05 vs. CPA 500μmol/L, ** p < 0.01 vs. CPA 500μmol/L. Data are given as mean ± SEM of at least three individual experiments.

10.4.4. Mechanism of cell death

Since increased toxicity of cyclophosphamide in the presence of roxithromycin could not be explained by inhibition of P-gp or CYP3A4 by roxithromycin, we decided to investigate the mechanism of cell death in more detail, first looking for markers of apoptosis. As illustrated in Figure 6, staining with Hoechst 33342 revealed many endothelial cells with fragmented or condensed nuclei when incubated with cyclophosphamide and roxithromycin. In contrast, cells incubated with the individual compounds did not show such changes. Cell counts revealed that 27% of the cells incubated with 500μM cyclophosphamide and roxithromycin underwent apoptosis, while this was the case for only 0.7% of the cells in the presence of 500μmol/L cyclophosphamide or 0% in the presence of 500μmol/L roxithromycin. These findings are consistent with those obtained for LDH leakage, and demonstrate that the combination of roxithromycin and cyclophosphamide induces apoptosis of endothelial cells.

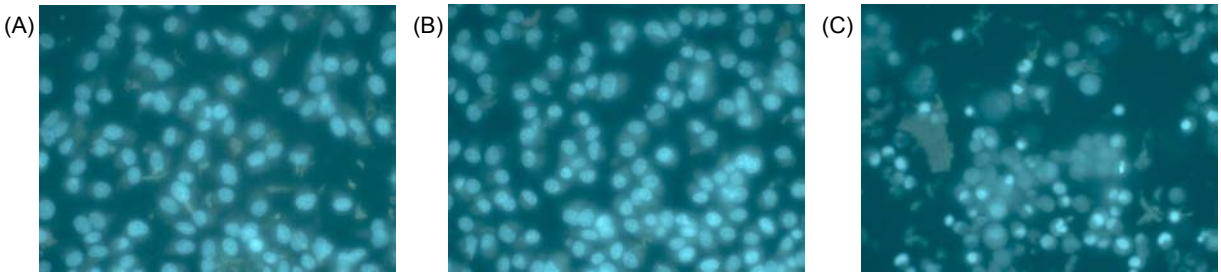

(E)

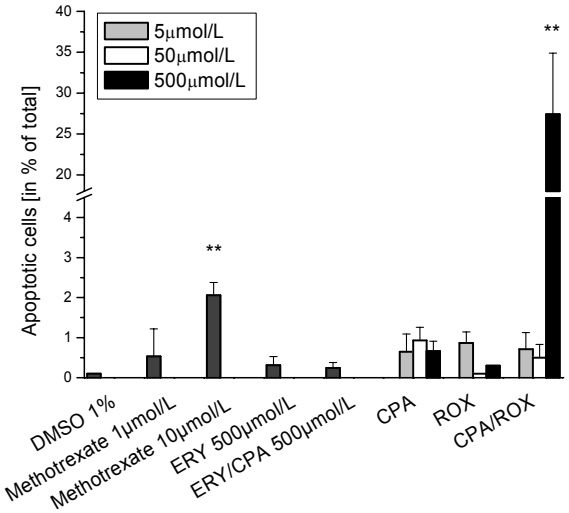

Figure 6: Induction of apoptosis by cyclophosphamide and roxithromycin. ECV 304 cells were treated with test compounds at the concentrations indicated in the Figure. After 20h of exposure, the cells were stained with Hoechst 33342 for 15min and analyzed using fluorescence microscopy. Apoptotic cells were characterized by DNA condensation. (A) cyclophosphamide, (B) roxithromycin, (C) cyclophosphamide + roxithromycin, (D) percentage of cells with DNA condensation relative to the total amount of cells. Methotrexate was used as a positive control. ERY = erythromycin, CPA = cyclophosphamide, ROX = roxithromycin. * $P < 0.05$ vs. DMSO 1%; ** $p < 0.01$ vs. DMSO 1%. Data are given as mean ± SEM of at least three individual experiments.

10.4.5. Mechanism of apoptosis

Since mitochondrial damage has been recognized as an important mechanism of drug-induced toxicity (18), we investigated whether mitochondria are involved in the cyclophosphamide/roxithromycin-mediated toxicity. If mitochondrial pathways of apoptosis induction were initiated, a release of cytochrome c from the mitochondrial intermembrane space into the cytoplasm should occur (19-21). As shown in Figure 7, only the combination cyclophosphamide/roxithromycin, but not the individual substances, lead to a release of cytochrome c from the mitochondrial intermembrane space into the cytoplasm, suggesting a mitochondrial contribution to apoptosis.

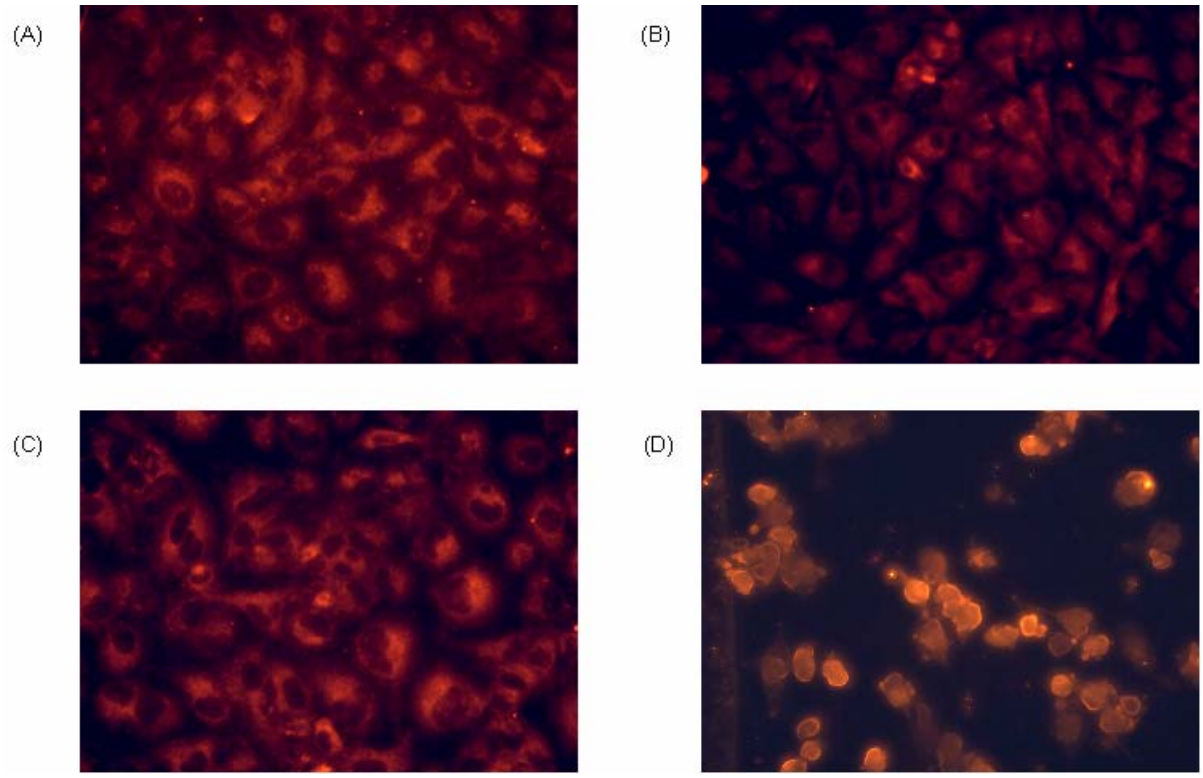

Figure 7: Mitochondrial leakage of cytochrome c in endothelial cells treated for 20 hours with test compounds. In the presence of 1% DMSO (panel A), 500μmol/L cyclophosphamide (panel B) or 500μmol/L roxithromycin (panel C), cytochrome c stays within mitochondria (granular pattern all over the cells with the nuclei clearly visible) and no leakage into cytoplasm occurs. After treatment with the combination of 500μmol/L cyclophosphamide and roxithromycin (panel D), cytochrome c is leaking out of the mitochondrial intermembrane space into the cytoplasm. Cytochrome c immunoreactivity is now spread diffusely over the cells, covering the nuclei (30).

To answer the question whether mitochondria are damaged in the presence of cyclophosphamide and roxithromycin, we next studied the potential across the inner mitochondrial membrane. Functional alterations of mitochondria are usually manifested by the changes in this potential, which can therefore be used as an indicator for mitochondrial damage (22). As shown in Figure 8, cyclophosphamide or roxithromycin did not affect the mitochondrial membrane potential up to a concentration of 500μmol/L. The combination of cyclophosphamide and roxithromycin, however, was associated with a partial loss of the mitochondrial membrane potential (Figure 8). At 250μmol/L

roxithromycin and 500μmol/L cyclophosphamide, the potential of approximately 20% of the mitochondria was dissipated.

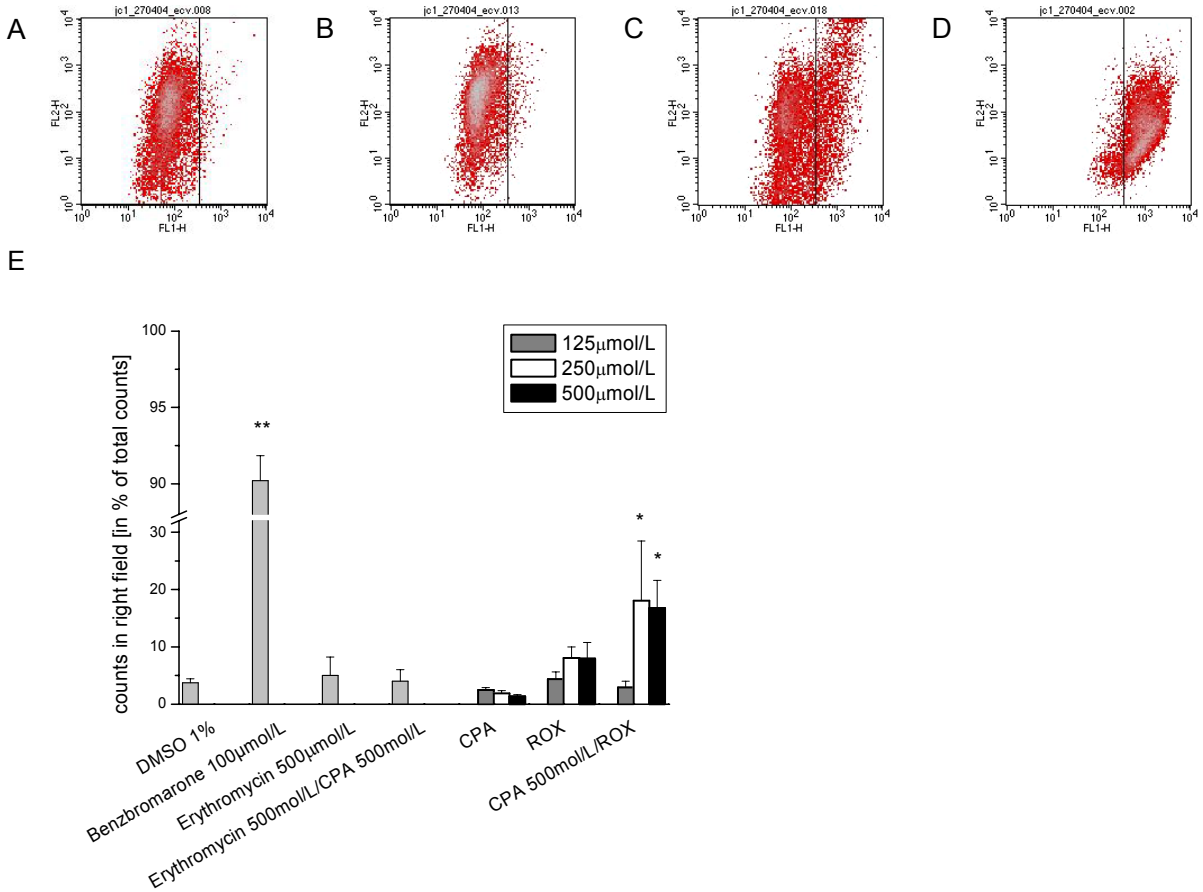

Figure 8: Effect of cyclophosphamide and roxithromycin on the mitochondrial membrane potential. The mitochondrial membrane potential was determined by an ion distribution technique. Endothelial cells were loaded with the cationic dye JC-1 that is taken up by mitochondria according to the mitochondrial membrane potential, changing the fluorescence emission from red to green. Cells with polarized mitochondria are located in the left field (green fluorescence), whereas cells with dissipated potential are found in the right field (red fluorescence). Panel A: cyclophosphamide 500μmol/L, B: roxithromycin 500μmol/L, C: cyclophosphamide and roxithromycin (each 500μmol/L), D: benzbromarone 100μmol/L (used as a positive control), E: Results given as the percentage of cells in the right field from total cells tested. Results are expressed as mean ± SEM of at least three individual experiments. CPA = cyclophosphamide, ROX= roxithromycin. *P < 0.05 vs. control, **p < 0.01 vs. control.

10.5. Discussion

Clinical experience from patients with bone marrow transplantation shows that VOD can occur after treatment with high doses of cyclophosphamide. So far, there is no publication about induction of VOD with low dose cyclophosphamide as used in patients with autoimmune diseases. Since the patient described by us (7) was also treated with roxithromycin, a known inhibitor of CYP 3A4 and P-gp, it was assumed that the presence of roxithromycin aggravated cyclophosphamide toxicity. Due to the vascular origin of VOD (4), we decided to study first the toxicity of cyclophosphamide and roxithromycin using a human endothelial cell line. Our investigations showed that neither

cyclophosphamide, nor roxithromycin, induced significant cell death up to a concentration of 500μmol/L. Cell damage occurred only, when cyclophosphamide was combined with roxithromycin.

Since roxithromycin inhibits P-gp, which is expressed in endothelial cells, inhibition of P-gp could be a reason for increased toxicity of cyclophosphamide in the presence of roxithromycin. However, other P-gp inhibitors, e.g. erythromycin and verapamil, did not increase the toxicity of cyclophosphamide on endothelial cells, showing that inhibition of the export of cyclophosphamide or toxic metabolites from endothelial cells could not explain increased toxicity of cyclophosphamide in the presence of roxithromycin. Other mechanisms had therefore to account for the toxicification of cyclophosphamide by roxithromycin.

Cyclophosphamide is a prodrug requiring hepatic activation. Roxithromycin and its metabolites are known inhibitors of CYP3A4 (9), an enzyme involved in the cyclophosphamide inactivation pathway (Figure 1). The activation pathway is primarily driven by CYP2B6, generating the active compounds as well as known toxic metabolites (3). We therefore hypothesized that the increase in cyclophosphamide toxicity in combination with roxithromycin could be due to shifting of cyclophosphamide metabolism from inactivation by CYP3A4 to toxification by CYP2B6. In our experiments, we could confirm this concept by using ketoconazole, which is a more specific inhibitor of CYP3A4 than roxithromycin (Table 1). In comparison, in the presence of roxithromycin, both pathways of cyclophosphamide metabolism were inhibited at all concentrations tested. These results suggest that also under in vivo conditions, both CYP3A4 and CYP2B6 are inhibited simultaneously in the presence of roxithromycin. By this mechanism, roxithromycin may have increased the exposure of the patient's liver to cyclophosphamide, but at the same time decreased the pharmacological activity of the drug and also the exposure to toxic metabolites. The inhibition of CYP isozymes by roxithromycin could therefore not explain increased vascular toxicity of cyclophosphamide in the presence of roxithromycin.

Apart from the influence of roxithromycin on cyclophosphamide metabolism, another aspect concerning roxithromycin may be taken into consideration. CYP2B6 is one of the less well characterized CPY isozymes, probably because it was initially thought to be expressed only at low levels (23). Recently, a number of structurally diverse, but frequently used drugs have been recognized as CYP2B6 substrates, among them bupropion, ifosphamide, nicotine, lidocaine, verapamil, artemisinin and propofol. Since we could show that roxithromycin inhibits CYP2B6, drug-drug interactions between roxithromycin and drugs metabolized by CYP2B6 have to be expected.

By investigating the mechanism of cell death induced by the combination of cyclophosphamide and roxithromycin, we could show that this drug combination was causing apoptosis in endothelial cells at concentrations where the individual drugs were not toxic. The observed decrease of the mitochondrial membrane potential in the presence of cyclophosphamide and roxithromycin suggests that mitochondria are involved in the induction of apoptosis. In support of this hypothesis, we could demonstrate leakage of cytochrome c into the cytoplasm of endothelial cells undergoing apoptosis. These findings suggest mitochondrial membrane permeability transition with rupture of the outer mitochondrial membrane and leakage of cytochrome c as an initial mechanism of induction of apoptosis (19-21). However, our data do not allow to exclude that the cellular pathway of apoptosis was also initiated, possibly affecting the mitochondria at a later stage in the cascade. This would be in agreement with published data suggesting that cyclophosphamide is an inducer of CD 95-mediated apoptosis in T lymphocytes (24-28) and melanocytes (25, 27). However, similar to our observation in endothelial cells, in mouse embrionic and in tumor cells, induction of the mitochondrial pathway of

apoptosis has been observed (26, 28). In this context, it is interesting to note that low concentrations of cyclophosphamide (7.5 μmol/L) can induce apoptosis in primary lung endothelial cells. According to these investigations, cancer and/or perivascular cells express thrombospondin-1 in the presence of cyclophosphamide, whose activation may mediate apoptosis of endothelial cells (29). While these studies show that cyclophosphamide can be toxic on endothelial cells under certain circumstances, they do not explain our observation that induction of apoptosis was most effective in the presence of the combination cyclophosphamide and roxithromycin.

In conclusion, we could show that cyclophosphamide is toxic in combination with 500μmol/L roxithromycin from 50μmol/L cyclophosphamide upwards. Roxithromycin causes an overall inhibition of hepatocyte cyclophosphamide metabolism and inhibition of P-gp, leading to an accumulation of cyclophosphamide in hepatocytes and possibly also endothelial cells. Apoptosis is the principle mechanism of toxicity of cyclophosphamide in endothelial cells, most probably associated with activation of the mitochondrial pathway of initiation of apoptosis.

Acknowledgements

The study was supported by a grant of the Swiss National Science Foundation to SK (3100-59812-03/1).

10.6. References

1. Brodsky RA. High-dose cyclophosphamide for aplastic anemia and autoimmunity. Curr Opin Oncol 2002; 14: 143-146.
2. Bohnenstengel F, Hofmann U, Eichelbaum M, Kroemer HK. Characterization of the cytochrome P450 involved in side-chain oxidation of cyclophosphamide in humans. Eur J Clin Pharmacol 1996; 51: 297-301.
3. Busse D, Busch FW, Bohnenstengel F, Eichelbaum M, Fischer P, Opalinska J, et al. Dose escalation of cyclophosphamide in patients with breast cancer: consequences for pharmacokinetics and metabolism. J Clin Oncol 1997; 15: 1885-1896.
4. Ortega JA, Donaldson SS, Ivy SP, Pappo A, Maurer HM. Venoocclusive disease of the liver after chemotherapy with vincristine, actinomycin D, and cyclophosphamide for the treatment of rhabdomyosarcoma. A report of the Intergroup Rhabdomyosarcoma Study Group. Childrens Cancer Group, the Pediatric Oncology Group, and the Pediatric Intergroup Statistical Center. Cancer 1997; 79: 2435-2439.
5. Ozkaynak MF, Weinberg K, Kohn D, Sender L, Parkman R, Lenarsky C. Hepatic veno-occlusive disease post-bone marrow transplantation in children conditioned with busulfan and cyclophosphamide: incidence, risk factors, and clinical outcome. Bone Marrow Transplant 1991; 7: 467-474.
6. Styler MJ, Crilley P, Biggs J, Moul J, Copelan E, Topolsky D, et al. Hepatic dysfunction following busulfan and cyclophosphamide myeloablation: a retrospective, multicenter analysis. Bone Marrow Transplant 1996; 18: 171-176.
7. Beltinger J. Veno-occlusive disease associated with immunosuppressive cyclophosphamide and roxithromycin. Journal of Hepatology 2004; submitted:

8. Yamazaki H, Inoue K, Chiba K, Ozawa N, Kawai T, Suzuki Y, et al. Comparative studies on the catalytic roles of cytochrome P450 2C9 and its Cys- and Leu-variants in the oxidation of warfarin, flurbiprofen, and diclofenac by human liver microsomes. Biochem Pharmacol 1998; 56: 243-251.
9. Yamazaki H, Urano T, Hiroki S, Shimada T. Effects of erythromycin and roxithromycin on oxidation of testosterone and nifedipine catalyzed by CYP3A4 in human liver microsomes. J Toxicol Sci 1996; 21: 215-226.
10. Bogman K, Peyer AK, Torok M, Kusters E, Drewe J. HMG-CoA reductase inhibitors and P-glycoprotein modulation. Br J Pharmacol 2001; 132: 1183-1192.
11. Takahashi K, Sawasaki Y, Hata J, Mukai K, Goto T. Spontaneous transformation and immortalization of human endothelial cells. In Vitro Cell Dev Biol 1990; 26: 265-274.
12. Vassault A. Lactate dehydrogenase. In: H. U. Bergmeyer, H. U. Bergmeyers. Methods of Enzymatic Analysis. Weinheim: VHC; 1983.p.118-125
13. Huang TH, Lii CK, Chou MY, Kao CT. Lactate dehydrogenase leakage of hepatocytes with AH26 and AH Plus sealer treatments. J Endod 2000; 26: 509-511.
14. Huang Z, Waxman DJ. High-performance liquid chromatographic-fluorescent method to determine chloroacetaldehyde, a neurotoxic metabolite of the anticancer drug ifosfamide, in plasma and in liver microsomal incubations. Anal Biochem 1999; 273: 117-125.
15. Wacher VJ, Wu CY, Benet LZ. Overlapping substrate specificities and tissue distribution of cytochrome P450 3A and P-glycoprotein: implications for drug delivery and activity in cancer chemotherapy. Mol Carcinog 1995; 13: 129-134.
16. Kim RB, Wandel C, Leake B, Cvetkovic M, Fromm MF, Dempsey PJ, et al. Interrelationship between substrates and inhibitors of human CYP3A and P-glycoprotein. Pharm Res 1999; 16: 408-414.
17. Rodrigues AD. Use of in vitro human metabolism studies in drug development. An industrial perspective. Biochem Pharmacol 1994; 48: 2147-2156.
18. Pessayre D, Mansouri A, Haouzi D, Fromenty B. Hepatotoxicity due to mitochondrial dysfunction. Cell Biol Toxicol 1999; 15: 367-373.
19. Green DR, Reed JC. Mitochondria and apoptosis. Science 1998; 281: 1309-1312.
20. Kroemer G, Reed JC. Mitochondrial control of cell death. Nat Med 2000; 6: 513-519.
21. Newmeyer DD, Ferguson-Miller S. Mitochondria: releasing power for life and unleashing the machineries of death. Cell 2003; 112: 481-490.
22. Ding WX, Nam Ong C. Role of oxidative stress and mitochondrial changes in cyanobacteria-induced apoptosis and hepatotoxicity. FEMS Microbiol Lett 2003; 220: 1-7.
23. Lang T, Klein K, Fischer J, Nussler AK, Neuhaus P, Hofmann U, et al. Extensive genetic polymorphism in the human CYP2B6 gene with impact on expression and function in human liver. Pharmacogenetics 2001; 11: 399-415.
24. Beranek JT. Apoptosis contributes to cyclophosphamide-induced cardiomyopathy. Bone Marrow Transplant 2002; 29: 91.
25. Strauss G, Osen W, Debatin KM. Induction of apoptosis and modulation of activation and effector function in T cells by immunosuppressive drugs. Clin Exp Immunol 2002; 128: 255-266.
26. Schwartz PS, Waxman DJ. Cyclophosphamide induces caspase 9-dependent apoptosis in 9L tumor cells. Mol Pharmacol 2001; 60: 1268-1279.

27. Sharov AA, Li GZ, Palkina TN, Sharova TY, Gilchrest BA, Botchkarev VA. Fas and c-kit are involved in the control of hair follicle melanocyte apoptosis and migration in chemotherapy-induced hair loss. J Invest Dermatol 2003; 120: 27-35.
28. Little SA, Mirkes PE. Teratogen-induced activation of caspase-9 and the mitochondrial apoptotic pathway in early postimplantation mouse embryos. Toxicol Appl Pharmacol 2002; 181: 142-151.
29. Hamano Y, Sugimoto H, Soubasakos MA, Kieran M, Olsen BR, Lawler J, et al. Thrombospondin-1 associated with tumor microenvironment contributes to low-dose cyclophosphamide-mediated endothelial cell apoptosis and tumor growth suppression. Cancer Res 2004; 64: 1570-1574.
30. Goldstein JC, Waterhouse NJ, Juin P, Evan GI, Green DR. The coordinate release of cytochrome c during apoptosis is rapid, complete and kinetically invariant. Nat Cell Biol 2000; 2: 156-162.

11. Discussion

11.1. Conclusions and Outlook

This thesis at large has been covering several aspects of toxicity and toxicology. We were dealing with hepatic toxicity, skeletal muscle toxicity, hepatic blood vessel damage, drug interactions, animal models, in vitro analysis, investigating single compounds or analyzing classes of drugs. Independently of the definite protocol of each individual study, all our investigations served one mutual purpose of deciphering some secrets of toxicology.

The studies put together in this thesis represent an example of how clinical findings related to drug therapy can be followed by laboratory investigations in order to help to understand what was happening and why something was happening. Ideally, the conclusions from laboratory work go back from bench to either bedside or pharmaceutical industry. For instance, we could show in our study about hepatic toxicity of benzarone and benzbromarone, that structures containing a benzofuran structure coupled to a p-hydroxybenzolring are prone to induce mitochondrial dysfunction. So development of hypothetical new chemical entities with structural features mentioned before should be carried on cautiously and carefully with regard to mitochondrial toxicity and its consequences. Moreover, these data can be of interest in order to develop chemically modified derivatives for amiodarone with reduced risk of liver damage but still unimpaired antiarrhythmic activity. Hopefully, lab investigations are of use for the clinicians in terms of putting basic science into practice. Basic science can provide knowledge on mode of actions along with mechanisms of adverse drug reactions or drug interactions to clinicians, which can be of use in order to either prevent complications related to drug therapy or optimize therapy models.

Although all the projects had an accurately defined focus, however, conclusions of general interest and use could be drawn from them. In our studies, we could show that mitochondria are prominent targets for xenobiotics, in a direct or indirect manner. In the first study the administered compound hit mitochondria only indirectly, in contrast to the succeeding two projects. THP was used in order to mimic and induce a disease pattern known from the clinics. THP did cause a change in the biochemical and molecular environment of a cell, which then was responsible for mitochondrial dysfunction and liver steatosis. The study was not explicitly designed to find out the mechanisms leading to mitochondrial dysfunction in the first place. Most importantly, the study could help to clarify the mechanism leading to liver steatosis. Since liver steatosis, microvesicular steatosis in particular, is a well known problem of many drugs; exploration of its mechanism is of broad toxicological and pharmacological interest. The second and the third study pointed into the same direction. Both studies tried to elucidate in vitro the mechanisms of known ADRs. They were triggered by clinical findings. Even though also the fourth study was starting with clinical findings, this project was dealing with another aspect of toxicology, with drug-drug interactions. It could be clearly demonstrated that even a nontoxic drug may turns into toxic agent by the mere combination with another nontoxic drug and then can have dangerous consequences. The precise mechanism of the drug drug interaction studied remained to be clarified entirely but also in this case, mitochondrial involvement could be confirmed.

Taking together data from the literature and our studies, one can say that there are several ways to die but it seems that there is no way to bypass mitochondria in process of cell death. Mitochondria are the point of converge for extrinsic and intrinsic apoptotic pathways. They can either induce or route signals. These organelles seem to sit at the crossroad between life and death, exerting

the task of an organellar gatekeeper of cell death. Impairment of these vital organelles is a crucial event in a cascade, which may ends up with cell death and subsequent tissue damage. It is this very central role in cell survival, which explains the essential need of further investigations in this field. It is of pivotal importance to develop and improve screening assays in order to assess a drug's potential to affect mitochondrial function.

However, up to now drugs continue to be pulled from the market with disturbing regularity because of late discovery of toxicity. In many cases hepatic toxicity is responsible for withdrawal (benzbromarone, kava-kava, troglitazone) or, less frequently, withdrawal is due to toxicity in other tissues, such as skeletal muscle (cerivastatin). Of course, toxicity of a compound is not only determined by the nature or dose of the compound itself but also by other factors such as other drugs administered at the same time, an individual's gene expression profile, antioxidant status and capacity of regenerations. Many factors take influence on the vulnerability of a specific patient. It turned out that also in the question of susceptibility of a patient to ADR, mitochondria play a significant role. It is possible that a patient with preexisting mitochondrial diseases (e.g. due to mitochondrial cytopathies or drug induced mitochondrial dysfunction) may be at risk for ADR after treatment with a mitochondrial toxin. This hypothesis is supported by recent reports in the literature. A patient with decreased activity of enzyme complexes of the respiratory chain developed liver failure during treatment with valproate. Valproate is a well known toxin for liver mitochondria (1). Moreover a case report was published about a physician and his son, developing liver failure after ingestion of rewarmed pasta, which was contaminated with bacillus cereus. Cereulide, the toxin of this bacterium, was shown to be a mitochondrial toxin. While the father was recovering fully, the son died from liver failure. It is of interest to note, that in contrast to the father the son was treated with 1g of aspirin, a mitochondrial toxin. It is possible that the son had an additional inhibitory effect on mitochondria, which in combination with cereulide had devastating consequences (2). These findings have important clinical implications. Before treatment with a drug, known to cause mitochondrial dysfunction, at least a careful family and personal history should be obtained, accurate clinical investigations should be performed and the therapy plan screened for mitochondrial toxins. Patients with findings compatible with mitochondrial disorders (e.g. drug-induced or inherited) should be either excluded from treatment with mitochondrial toxins or assessed very profoundly. Since nowadays it is not yet possible to assess mitochondrial function with standard laboratory tests, many cases of mitochondrial toxicity undoubtedly go undetected. This gap should be addressed in future investigations. Efforts are required in order to detect mitochondrial function and thus improve drug safety related to mitochondria.

So far, we could demonstrate in our studies that mitochondria and their dysfunction could be responsible for the induction of tissue damage after treatment with drugs. Mitochondria are also associated with diseases. Up to now, several genetic mutations concerning mitochondria are known to cause diseases. Moreover, recent results put mitochondria and mitochondrial dysfunction back in the centre of neurodegenerative diseases as well. Studies in human postmortem material and in animals indicate consistently that decrements in mitochondrial complex I are linked to pathogenesis of Parkinson's disease (PD). 1-Methyl-4-phenyl-1,2,3,6-treadhydropyridine (MPTP) for instance inhibits complex I and mimics most features of PD. MPTP selectivity to dopamine neurons is due to its active metabolite 1-methyl-4-phenylpyridinium (MPP^+), which is then concentrated in dopamine neurons via the dopamine transporter, where it kills neurons through inhibition of complex I. Dysfunction of complex I leads to increased oxidative stress, ROS generation, reduction of ATP formation and finally to cell damage and subsequent cell death (2, 3). Also for Alzheimer's disease (AD) the stage is now

set: mitochondrial abnormalities lie at the heart of AD pathogenesis, whereas the fundamental pathological changes of the disease are coordinated responses to control oxidative damage. But which factor is responsible for the mitochondrial abnormalities remains to be clarified. Current evidence points to changes in the balance of redox transition metals, especially iron and copper. However, the key aspect of AD is selective neuronal death. Recent findings show, that damaged neurons revealed an oxidative stress response. So far, however, there has not been a mechanism linking damage to death (5). Also in this field, further studies will be conducted in the forthcoming years.

Einstein once said, “Everything should be made as simple as possible, but not simpler”. Research is constantly evolving and it is to expect that in a few years time, knowledge in this field will be expanded dramatically, possibly leading to new conclusions. Whether the conclusions of today will be compatible with those in a few years time remains questionable. Most likely it will turn out that our today’s hypothesis were not considering all aspects and thus simplifying things. Already today, there are firm hints in the literature indicating that there is way more lying beneath than we know today and that it won’t take long for these news to come up. This is of course true for many aspects of life but also in particular with regard to some aspects touched on in this thesis. Firstly, there seems to be more to life and death than mitochondria. Recent publications (6, 7) revealed and highlighted the endoplasmic recticulum (ER) as a key upstream signaling organelle for the regulation of apoptosis. Despite emerging evidence that the ER is an important location for the regulation of apoptosis, the mechanisms have yet to be discovered. One relevant candidate may be the control of the ER Ca^{2+} levels. It seems that members of the Bcl-2 protein family, which are known to play an important either pro- or antiapoptotic role within mitochondria are also involved in the ER-related apoptotic processes. The ER can act upstream of mitochondria in the initiation of apoptosis and it is hypothesized that they can act even independently of mitochondria (6). Clearly, the results so far are interesting and suggest that many possibilities remain to be explored. Secondly, the complexity of the multiple, intertwining pathways in cell death induction necessitated simplification, provided by the distinction in two clearly separated modes of cell death. Although apoptosis and necrosis have long been viewed as opposed antinomy, recent data led to the assumption that both forms of cell death constitute two extremes of a continuum with uncountable presentations (8), which, are, although difficult, to be investigated and differentiated in detail in the future. A third research field which is highly competitive is the mitochondrial permeability transition. The mechanism responsible for membrane permeabilization remains controversial, even though it is clear that many proteins can inhibit, prevent or affect the process by local effects on mitochondrial membranes. So far and in general, two classes of mechanisms have been described. In the first class of mechanism a pore opens in the inner membrane, allowing water and molecules up to ~ 1.5 kDa to pass through. This model postulates a role of the adenine nucleotide transporter in the inner membrane and the voltage- dependent anion channel in the outer membrane. Even though there are many publications on this model, it is still hypothetical. Newer data postulate that the inner membrane does not necessarily need to be permeabilized. The outer membrane permeabilization appears to be mediated by members of the Bcl-2 family of apoptosis-regulating proteins acting directly on the outer mitochondrial membrane. It appears that there is more than one way of mitochondrial membrane permeabilization (9). Considering the importance of cell death signaling, much impetus for further research projects in this area is around.

In conclusion: although many things are still unknown and currently under investigation, evidence tightly confirmed that MPT is the central coordinating event of apoptosis as well as necrosis. Various damage pathways and proapoptotic signal transduction cascades converge at the level of MPT, in line with the fact that MPT can be induced by numerous effects. Once MPT has been triggered, a series of common pathways of cell death are initiated, each of which lethal. To sum up, based on today's knowledge, MPT has at least two major consequences: (1) a bioenergetic and redox catastrophe disrupting cellular metabolism and (2) liberation of protease and endonuclease activators from mitochondria. Depending on which of these processes wins the race, either primary necrosis or apoptosis ensues.

11.2. References

1. Krahenbuhl S, Brandner S, Kleinle S, Liechti S, Straumann D. Mitochondrial diseases represent a risk factor for valproate-induced fulminant liver failure. Liver 2000; 20: 346-348.
2. Mahler H, Pasi A, Kramer JM, Schulte P, Scoging AC, Bar W, et al. Fulminant liver failure in association with the emetic toxin of Bacillus cereus. N Engl J Med 1997; 336: 1142-1148.
3. Dawson TM, Dawson VL. Molecular pathways of neurodegeneration in Parkinson's disease. Science 2003; 302: 819-822.
4. Love R. Mitochondria back in the spotlight in Parkinson's disease. Lancet Neurol 2004; 3: 326.
5. Cash AD, Perry G, Ogawa O, Raina AK, Zhu X, Smith MA. Is Alzheimer's disease a mitochondrial disorder? Neuroscientist 2002; 8: 489-496.
6. Annis MG, Yethon JA, Leber B, Andrews DW. There is more to life and death than mitochondria: Bcl-2 proteins at the endoplasmic reticulum. Biochim Biophys Acta 2004; 1644: 115-123.
7. Szabadkai G, Rizzuto R. Participation of endoplasmic reticulum and mitochondrial calcium handling in apoptosis: more than just neighborhood? FEBS Lett 2004; 567: 111-115.
8. Kroemer G, Dallaporta B, Resche-Rigon M. The mitochondrial death/life regulator in apoptosis and necrosis. Annu Rev Physiol 1998; 60: 619-642.
9. Green DR, Kroemer G. The pathophysiology of mitochondrial cell death. Science 2004; 305: 626-629.

12. Cirrculum Vitae

Personal Details

Name and address	Priska M. Kaufmann Häsingerstrasse 44 CH-4055 Basel Tel +41 61 321 37 74 Email: priska.kaufmann@unibas.ch
Date of birth	17. October 1974
Place of birth	Rheinfelden/AG
Citizenship	Wikon /LU
Nationality	Swiss
Marital status	single

Education

2001-current: PhD thesis (Phil Nat Sci)
Division of Clinical Pharmacology and Toxicology & Department of Research, University Hospital Basel

Project titles:

- *Mechanisms of liver steatosis in rats with systemic carnitine deficiency due to treatment with trimethylhydraziniumpropionate*
- *Hepatic toxicity of benzarone and benzbromarone*
- *Mitochondrial toxicity of statins*
- *Venoocclusive disease in a patient treated with cyclophosphamide and roxithromycin treatment: investigating the underlying mechanism*
- *Fibroblasts from patients with mitochondrial defects as a model for investigating drug idiosyncrasy*
- *Contractile function & metabolic characterization of rodent skeletal muscle in presence & absence of carnitine deficiency*

Other:

- *Drug development & discovery seminars*
- *Lectures attended in analytical chemistry, molecular mechanisms of toxicity, clinical pharmacology, epidemiology*
- *Personal Animal License holder (LTK modul 1)*
- *Microscopy course: two week course, University Basel*

Advisor: Prof. Dr. Dr. Stephan Krähenbühl

1999	Master of Pharmacy, University Basel
1994-1999	Study of Pharmacy, University Basel
1993	Matura Typus E, Gymnasium Kriegacker, Muttenz/BL
1990-1993	High school, Gymnasium Muttenz/BL

Employment History

1997-2004	Pharmacist at Hard Apotheke, Birsfelden/BL
2001	Chief Pharmacist in St. Moritz/GR
1996-1997	Practical year in “Hard Apotheke” Birsfelden/BL

Expertise

Laboratory: Cell Biology

- Tissue culture
- Cytotoxicity assays
- Apoptosis assays

- Immunocytochemistry

Molecular Biology
- RNA isolation
- Rt PCR

Protein Analysis
- Quantitative assays
- Enzyme kinetics
- Western blot analysis

Metabolic Functions
- β-oxidation
- Mitochondrial oxygen consumption
- Uncoupling of oxidative phosphorylation
- ROS generation
- Mitochondrial swelling
- Mitochondrial membrane potential
- Microsomal incubations

Analytics
- UV spectroscopy
- Fluorescence spectroscopy
- Light and fluorescence microscopy
- HPLC
- Flow cytometry

Personal Management
- Training and supervising of students and other staff
- Assisting in undergraduate practical classes
- KLIPS: assisting at the drug information center in order to answer a patient specific or drug safety question in general. Answers are usually given in writing.

General Administration
- Maintenance and ordering of Lab supplies
- Proficient computer skills (Power point, Excel, Word, Prism, internet navigation, literature retrieval etc)

13. Publication Record

Abstracts

Kaufmann P, Török M, Hänni A, Gasser R, Krähenbühl S. Mechanisms of benzarone and benzbromarone induced hepatic toxicity. *J Hepatol 2004;40(Supplement 1):27.*

Kaufmann P, Török M, Lüde S, Krähenbühl S. Statin induced mitochondrial toxicity. *Kardiovaskuläre Medizin 2004;7:35.*

Kaufmann P, Török M, Lüde S, Krähenbühl S. Mitochondrial toxicity of statins. *Schweiz Med forum 2004;4(Supplement 17):28.*

Kaufmann P, Beltinger J, Bogman K, Török M, Krähenbühl S. Drug-drug interaction of roxithromycin and cyclophosphamide. *Schweiz Med forum 2003;4(Supplement 18)*

Kaufmann P, Hänni A, Gasser R, Török M, Krähenbühl S. Heptic toxicity of benzarone and benzbromarone. In Tulunay F, Orme M, editors. Collaboration: Towards Drug Development and Rational Drug Therapy. Berlin, Heidelberg, New York: Springer 2003: 114

Kaufmann P, Hänni A, Gasser R, Török M, Krähenbühl S. Veno-occulsive disease (VOD) in a patient treated with cyclophosphamide (CPA) and roxithromycin (ROX). In Tulunay F, Orme M, editors. Collaboration: Towards Drug Development and Rational Drug Therapy. Berlin, Heidelberg, New York: Springer 2003: 114

Spaniol M, Kaufmann P, Beier K, Wüthrich J, Scharnagel H, März W, Krähenbühl S. Mechanisms of liver statosis in rats with systemic carnitine deficiency due to treatment with trimethylhydraziniumproprionate. *J Hepatol 2002;36(Supplement 1):23.*

Papers

Kaufmann P, Török M, Lüde S, Krähenbühl S.
Mitochondrial toxicity of statins
Submission in 2005

Kaufmann P, Beltinger J, Bogman K, Wenk M, Török M, Krähenbühl S.
Mechanisms of venoocclusive disease for the combination of cyclophosphamide and roxithromycin
Submission in 2005

J. Beltinger, P. Kaufmann, M. Michot, L. Terracciano, S. Krähenbühl
Veno-occlusive disease associated with immunosuppressive cyclophosphamide and roxithromycin
Submission 2005

Saladin C, Kaufmann P, Poddar M, Wallimann C, Schaffner W, Simmen U.
Metabolism of Valerian and St. John's wort extracts *in vitro*: relevance for pharmacological activity and *in vivo* prediction
Planta Medica 2005; in press

Kaufmann P, Török M, Hänni A, Roberts P, Gasser R, Krähenbühl S.
Mechanisms of benzarone and benzbromarone induced hepatic toxicity
Hepatology 2005;41:925-35.

Porta F, Weikert C, Takala J, Kaufmann P, Krähenbühl S, Jakob SM.
In vitro dopamine and dobutamine effect on endotoxin-incubated muscle mitochondria
Am J Respir Crit Care Med 2004; submitted

Roberts P, Kaufmann P, Urwyler A, Krähenbühl S.
Contractile function & metabolic characterization of rodent skeletal muscle in the presence & absence of carnitine deficiency
J Physiol 2004, submitted

Zaugg C, Spaniol M, Kaufmann P, Bellahcene M, Barbosa V, Tolnay M, Buser P, Krähenbühl S.
Myocardial function and energy metabolism in carnitine-deficient rats
Cell Mol Life Sci 2003;60:767-75.

Spaniol M, Kaufmann P, Beier K, Wuthrich J, Török M, Scharnagl H, Marz W, Krähenbühl S.
Mechanisms of liver steatosis in rats with systemic carnitine deficiency due to treatment with trimethylhydraziniumpropionate
J Lipid Res 2003;44:144-53.

14. Appendix: Supporting Literature

14.1. Myocardial function and energy metabolism in carnitine deficient rats

C. E. Zaugg[a],*, M. Spaniol[b], P. Kaufmann[b], M. Bellahcene[a],V. Barbosa[a, c], M. Tolnay[d], P. T. Buser[c] and S. Krähenbühl[b]

[a]Department of Research, [b]Division of Clinical Pharmacology & Toxicology, [c]Division of Cardiology, [d]Institute of Pathology, University Hospital, Basel, Switzerland

Cell Mol Life Sci 2003;60:767-75.

14.1.1. Summary

Carnitine is essential for mitochondrial metabolism of long-chain fatty acids and thus for myocardial energy production. Accordingly, carnitine deficiency can be associated with cardiomyopathy. To better understand this disease, we determined myocardial function and energy metabolism in a rat model of carnitine deficiency. Carnitine deficiency was induced by a 3- or 6-week diet containing N-trimethyl-hydrazine-3-propionate, reducing cardiac and plasma carnitine by 70–85%. Myocardial function was investigated in isolated isovolumic heart preparations. Carnitine-deficient hearts showed left ventricular systolic dysfunction, reduced contractile reserve, and a blunted frequency-force relationship independently of the substrate used (glucose or palmitate). After glycogen depletion, palmitate could not sustain myocardial function. Histology and activities of carnitine palmitoyl transferase, citrate synthase, and cytochrome c oxidase were unaltered. Thus, as little as 3–6 weeks of systemic carnitine deficiency can lead to abnormalities in myocardial function. These abnormalities are masked by endogenous glycogen and are not accompanied by structural alterations of the myocardium or by altered activities of important mitochondrial enzymes.

14.1.2. Introduction

Carnitine is essential for mitochondrial transport and metabolism of long-chain fatty acids and, thus, for myocardial energy metabolism. Specifically, because the inner mitochondrial membrane is impermeable to long-chain fatty acyl-CoAs, carnitine is required to transport these substrates across this membrane [1]. Furthermore, carnitine is important for carbohydrate metabolism by stimulating glucose oxidation via reversing the inhibition of pyruvate dehydrogenase [2, 3]. Moreover, carnitine shifts the ratio of acyl-CoA to CoA-SH in the direction of CoASH and is involved in trapping acyl residues from peroxisomes and mitochondria [1, 4, 5].

As a consequence of these important functions, deficiency of carnitine manifests mainly as a dysfunction of skeletal muscles and myocardium, where fatty acids constitute an essential energy substrate [4]. Due to decreased metabolism of fatty acids, carnitine deficiency results in accumulation of lipids within skeletal muscle, myocardium, and liver. Ultrastructurally, myofibrils are disrupted and aggregates of mitochondria and lipid deposits accumulate within the skeletal muscle and myocardium [6]. For these reasons, carnitine deficiency can cause hypertrophic or dilated cardiomyopathy in children [7], which is associated with a mortality of over 50% [8]. Moreover, myocardial carnitine levels are reduced in the hearts of patients with dilated cardiomyopathy, but the significance of this observation is currently not known [7].

The results of clinical and animal studies suggest that a short period (2 weeks) of moderate carnitine deficiency (50% reduction) does not have a major effect on cardiac contractile function [9]. However, after longer periods (>20 weeks) of carnitine deficiency, alterations occur in the heart that may result in impaired contractile performance, particularly at high workloads [9]. At this point, however, the precise mechanisms responsible for this cardiac depression are uncertain. To better understand the pathophysiology of carnitine deficiency, some of us have recently developed and characterized a rat model of carnitine deficiency [10]. In this model, rats developed systemic carnitine deficiency after 3 weeks on a diet containing Ntrimethyl- hydrazine-3-propionate (THP; also known as mildronate or MET-88) [11] which inhibits carnitine biosynthesis and increases renal carnitine excretion [10].

In the present study, we sought to investigate in this model whether as little as 3 or 6 weeks of *severe* systemic carnitine deficiency can lead to abnormalities of myocardial function. Additionally, we sought to investigate whether this carnitine deficiency would lead to structural alterations of the myocardium or to altered activities of important mitochondrial enzymes involved in fatty acid and energy metabolism including carnitine palmitoyl transferase, citrate synthase, and cytochrome c oxidase. For this purpose, we studied isolated isovolumically contracting hearts of control and THP-treated rats. Perfusing glucose (carnitine independent) or palmitate (carnitine dependent) as substrate, we measured various hemodynamic variables including left ventricular (LV) pressure, indices of contractility and relaxation, as well as coronary flow. Additionally, we measured both the contractile reserve (assessed as postextrasystolic potentiation) and the frequency- force relationship (staircase), as these myocardial characteristics are often altered in cardiomyopathy. Finally, as myocardial glycogen may compensate for an insufficient energy supply during perfusion with palmitate in

carnitine-deficient hearts, we depleted glycogen in some hearts using substrate-free perfusion before LV pressure analysis.

14.1.3. Materials and methods

14.1.3.1. Animals and induction of carnitine deficiency

Male Sprague-Dawley rats (Süddeutsche Versuchstierfarm, Tuttlingen, Germany and RCC, Füllinsdorf, Switzerland) weighing 290–490 g were used in this study. The animal use protocol was approved by the veterinary department of Basel (Switzerland) and was in line with the 'Ethical Principles and Guidelines for Scientific Experiments on Animals' of the Swiss Academy of Medical Sciences. Carnitine deficiency was induced as previously described [10] using vegetarian food poor in carnitine (Kliba Futter 2435, Basel, Switzerland) and THP (20 mg/100 g per day) for 3 or 6 weeks (n = 6 rats each). Control rats were kept for the same periods of time with vegetarian rat chow ad libitum (n =7 and 6 rats, respectively). All rats weighed approximately 200 g at the beginning of the diet/THP treatment and received tap water ad libitum throughout the study.

14.1.3.2. Perfused heart model

After anesthesia (50 mg/kg sodium pentobarbital intraperitoneally; Nembutal; Abbott Laboratories, Chicago, Ill.), rat hearts were excised rapidly and perfused according to a modified Langendorff method as previously described [12]. All hearts were perfused at a perfusion pressure of 110 cm H2O at 36 °C with a filtered (pore size 0.65 µm) nonrecirculating modified Krebs-Henseleit solution containing 117.0 mM NaCl, 4.3 mM KCl, 1.5 mM CaCl2, 1.2 mM Mg Cl2, 25.0 mM NaHCO3, 1% albumin, and 11.0 mM glucose or 0.4 mM Na palmitate as substrate. The perfusate was saturated with a gas mixture of 95% O2 and 5% CO2. Ventricular pacing was carried out using a pair of platinum wire electrodes connected to PowerLab/8e using Chart and Scope software (ADInstruments, Castle Hill, Australia) on a G3 Macintosh computer (Ingeno, Basel, Switzerland). The pacing electrodes were implanted superficially in the right ventricular free wall. To record a bipolar epicardial electrocardiogram (ECG), a pair of electrodes was placed on the right atrial appendage and the right ventricular base.

14.1.3.3. Experimental protocol

These experiments were designed to investigate the physiological contractile and energetic state of the hearts with a normal myocardial glycogen content. Therefore, rats were studied in the fed state, one control and one THPtreated rat per day in randomized order. Twenty minutes after isolation and perfusion of the hearts, stable baseline values of LV pressure and coronary flow were recorded with one of the substrates at a pacing rate of 200 beats per minute (bpm). The sequence of the substrates (glucose or palmitate) was randomized to eliminate confounding effects of varying perfusion time or glycogen content. To determine the LV contractile reserve, all hearts underwent the postextrasystolic potentiation protocol (see below). Subsequently, to determine the frequency-force relationship, we studied the effects of increasing the heart rate on LV pressure in the staircase protocol (see below). Then, the substrate was switched and after 20 min, of perfusion with the new substrate, baseline recordings and the two protocols (staircase and postextrasystolic potentiation) were repeated. At the end of the experiments, hearts were immediately cut transversely. The base was stored in 10% formalin for histological analysis and the apex was frozen in liquid nitrogen for measurement of cardiac carnitine concentrations, mitochondrial enzymes (carnitine palmitoyl transferase, citrate synthase, and cytochrome c oxidase), and of the high-energy phosphates, adenosine triphosphate (ATP) and phosphocreatine. In the fed state, endogenous myocardial glycogen may compensate for insufficient energy supply during perfusion with palmitate in carnitine-deficient hearts. This may mask contractile differences between control and carnitine- deficient animals. Therefore, we depleted glycogen in some hearts using substrate-free perfusion (n = 4 hearts per group) as described previously [13]. Pilot experiments showed that 60 min of substrate-free perfusion was sufficient to deplete the glycogen stores in rat harts (see fig. 1).

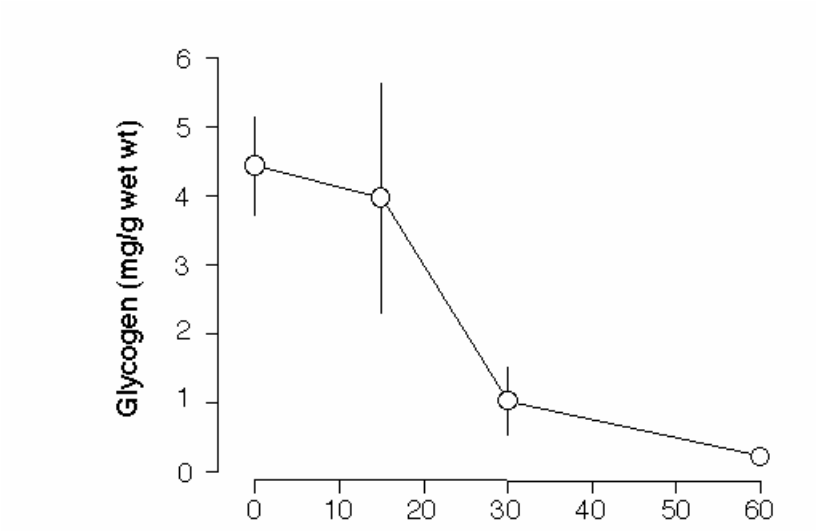

Figure 1. Effect of substrate-free perfusion (0, 15, 30, or 60 min) on the glycogen concentration in the left ventricle of isolated hearts from control rats. Values are mean ± SD; n = 6, 5, 6, or 7 hearts, respectively.

Glycogen was isolated and analyzed by a spectrophotometric method described previously [14]. After 60 min of substrate-free perfusion, LV-developed pressure began to decrease. Subsequently, the hearts were first perfused with Na palmitate and then with glucose (to prevent restoring of glycogen). In these hearts, we analyzed LV pressure but could not perform further protocols due to the continuing deterioration of LV pressure particularly during palmitate perfusion of hearts from carnitine-deficient rats. For baseline recordings as well as during the protocols for staircase and postextrasystolic potentiation, simultaneous measurements of LV pressure, coronary flow, and the ECG were performed on PowerLab/8e at a sampling rate of 1000 Hz. Further dependent variables included peak positive first-order time derivative of the LV pressure decline (dP/dtmax) as an index of contractility as well as two relaxation indices *t* and *b* (computed off-line using the differential or curve fit extensions of Chart).

14.1.3.4. Measurment of carnitine concentration in the heart and the plasma

Carnitine content in the heart and plasma (collected after sternotomy) was determined using a radioenzymatic method as described previously [15]. Heart and plasma samples were prepared for analysis in 3% perchloric acid (v : v). The perchloric acid-soluble fraction was assayed directly for free carnitine, and after alkaline hydrolysis for total acid-soluble carnitine (representing the sum of free carnitine and short-chain acylcarnitine). The short-chain acylcarnitine content (acyl group chain length less than ten carbons) was obtained by subtraction (total acid-soluble minus free carnitine content). Long-chain acylcarnitine contents (acyl group chain length ten or more carbons) were determined in the perchloric acid pellets. Total carnitine content refers to the sum of long-chain acylcarnitine content and total acid-soluble carnitine content.

14.1.3.5. Measurements of LV pressure and coronary flow

A 60-*m*l thin latex balloon (size 4; Hugo Sachs Elektronik-Harvard Apparatus, March-Hugstetten, Germany) was inserted into the left ventricle through the left atrium. LV pressure was measured by a plastic tube located inside the balloon, sutured at the proximal end of the balloon, and connected to an Isotec pressure transducer (Hugo Sachs Elektronik-Harvard Apparatus) that was at the same height as the heart. The volume of the saline-filled balloon was adjusted using a microsyringe to establish a constant physiological end-diastolic pressure in the range of 5–10 mm Hg [12]. Thus, the left ventricle contracted isovolumically throughout the experiment. LV developed pressure was defined as the difference between systolic and diastolic values of LV pressure. Coronary flow was measured within the aortic canula using an in-line flowprobe (Transonic 2N) connected to a transit time flowmeter (Transonic TTFM-SA type 700; Hugo Sachs Elektronik- Harvard Apparatus).

14.1.3.6. Analysis of LV relaxation

LV relaxation was analyzed on LV pressure recordings using two different relaxation indices. These indices were based on mono- and double-exponential function curve fitting to digital LV pressure data at baseline and a consistent heart rate of 200 bpm. The first index was the widely used time constant *t*of monoexponential LV pressure decline according to equation 1:

P(t) = (P0 – P•) e– t–*t*+ P• (Eq. 1)

where P(t) denotes LV pressure as a function of time t, P0 is LV pressure at minimal dP/dt (inflection point), and P•relates to lower asymptotic LV pressure [16]. However, *τ* considers only the final LV pressure decline, and contains no information about the initial decline before the inflection point of LV pressure. Therefore, a second relaxation index was applied using parameter *b* of an asymmetric double-exponential function according to equation 2:

P(t)= *g*0 – *g*e– *a*· e– *b*· t (Eq. 2)

where P(t) denotes LV pressure as a function of time t, and *g*0 and *g*relate to upper asymptote and amplitude of LV pressure. Parameter *a*relates to the phasic delay of decline onset, whereas *b*principally relates to the rate of the entire LV pressure decline [17].

14.1.3.7. Measurement of contractile reserve and interval-force relationship

To determine the contractile reserve, three different postextrasystolic potentiation protocols were introduced using PowerLab 8/e and Scope software. Specifically, after eight regular beats at 250-ms intervals (240 bpm), one premature beat was introduced at different intervals (75, 130, and 145 ms) followed by a pause (215, 335, and 265 ms, respectively). The intervals of the premature beats and the pauses were chosen to maximize postextrasystolic potentiation of the following beat [12]. The contractile reserve was estimated as the difference of LV developed pressure between the potentiated beats and the previous regular beat (averaged from three to five repetitions of each of the three potentiation protocols). Because of perturbing effects of arrhythmias on LV pressure, only arrhythmia-free sequences were used for this analysis. To determine the interval-force relationship, we assessed the effects of increasing heart rates on LV developed pressure. For this purpose, the heart rate was increased stepwise over a physiological range in a preprogrammed staircase pacing protocol at 240, 300, 360, 420, and 480 bpm generated by PowerLab 8/e using the stimulator function of Chart. Each step lasted for 6 s allowing LV pressure to reach a new steady state. Again, only arrhythmia-free sequences were used for this analysis. It should be noted that, in contrast to human hearts, rat hearts demonstrate a negative staircase at physiological heart rates [18].

14.1.3.8. Histological analysis

Histological examination of the hearts (carnitine-deficient diet for 3 or 6 weeks and controls, n = 6 rats each) was performed on 10% formalin-fixed and paraffin-embedded tissue as well as on fresh frozen tissue. Paraffin-embedded tissue sections were stained with hematoxylin-eosin (H&E) and elastica van Gieson while frozen sections where stained with H&E, periodic acid-Schiff (with and without diastase treatment), and modified Gomori trichrome. The histochemical analyses included myofibrillar ATPase (preincubated at pH 4.3 and pH 4.6), nicotinamide adenine dinucleotide-tetrazolium reductase (NADH-TR), succinate dehydrogenase (SDH) and cytochrome oxidase. Oil red O was used as a stain for neutral lipids.

14.1.4. Measurement of carnitine palmitoyl transferase, citrate synthase, and cytochrome c oxidase

Activities of the mitochondrial enzymes carnitine palmitoyl transferase, citrate synthase, and cytochrome c oxidase were determined using routine methods [19-21]. Briefly, carnitine palmitoyl transferase activity was measured after incubation of the heart tissue homogenate with palmitoyl CoA

and radioactively labeled carnitine to produce labeled palmitoylcarnitine. Palmitoylcarnitine was extracted with butanol and counted in a Packard 1900 TR *b*-counter (Canberra, Groningen, The Netherlands) [20]. Citrate synthase activity was measured spectrophotometrically at 412 nm using 5,5′-dithio-bis-2-nitrobenzoic acid reacting with CoA-SH that is produced in the reaction from acetyl-CoA and oxaloacetate to citrate [19]. Finally, cytochrome c oxidase activity was measured spectrophotometrically at 550 nm after oxygen-induced oxidation of ferrocytochrome c (produced freshly reducing ferricytochrome c with dithionite) [20]. The net activity was obtained by subtracting the rate obtained in the presence from the rate in the absence of the specific inhibitor sodium azide [20].

14.1.4.1. Measurement of ATP, phosphocreatine, and lactate

Concentrations of ATP and phosphocreatine in frozen heart samples were measured spectrophotometrically at 340 nm using enzymatic assays as described previously (Sigma-Aldrich Diagnostics ATP assay, no. 366 and custom-made assay, respectively) [22, 23]. The plasma lactate concentrations were determined fluorimetrically as described by Olsen [24].

14.1.4.2. Data evaluation and statistical analysis

LV pressure values, dP/dtmax, and the relaxation indices τ and β were averaged from five cardiac cycles digitally recorded at a heart rate of 200 bpm. To eliminate confounding effects of varying LV developed pressure on the contractility index, dP/dtmax was normalized for LV-developed pressure. Furthermore, to compare frequency-force relationships among groups, the sums of the rate-pressure products were computed over the entire heart rate range for each experiment (240–480 bpm). Moreover, out of 57 hearts, 3 were excluded from analysis due to unstable perfusion conditions (1 from the 3-week control group and 2 before glycogen depletion).

All results are expressed as mean ± SD except for carnitine data that were not normally distributed and were therefore expressed as median with interquartile range (25th–75th percentile). Comparisons of normally distributed interval variables among groups (carnitine-deficient vs control rats and 3-week vs 6-week treatment) were performed by one-way ANOVA followed by Bonferroni's test for selected multiple comparisons. Comparisons of carnitine data among groups (carnitine-deficient vs control rats and 3-week vs 6-week treatment) were performed by corresponding nonparametric tests (Kruskal-Wallis test) followed by Dunn's test for selected multiple comparisons. Comparisons of variables within groups (glucose vs palmitate) were performed by repeated-measures ANOVA followed by Bonferroni's test for selected multiple comparisons.

Statistical computations were done using Prism software (version 3.0a; GraphPad, San Diego, Calif.). For all statistical analyses, the null hypothesis was rejected at the 95% level, considering a two-tailed $p < 0.05$ significant. In an approximation of sample size determination for this study, six rats in each group had 90% power to detect differences of 20% in most variables assuming a SD of 10% and a 0.05 two-sided significance level [25].

14.1.5. Results

14.1.5.1. Carnitine concentrations in heart and plasma

After both 3 and 6 weeks of diet and THP treatment, carnitine concentrations in the heart and plasma were significantly reduced (table 1). Specifically, hearts and plasma of THP-treated rats had 15–30% of the total carnitine concentrations of control rats. Furthermore, all THPtreated rats showed signs of systemic carnitine deficiency including steatosis and enlargement of the liver. Despite these signs, THP-treated rats had similar body and heart weights in comparison to control rats (table 1). Additionally, after 6 weeks of diet and THP treatment, total carnitine concentrations in the heart and plasma were not significantly lower than after 3 weeks. However, after 6 weeks, control rats had higher total carnitine concentrations than after 3 weeks. The plasma lactate concentration was 2.4±0.5 mmol/l in control rats, and 2.1±0.5 or 1.7±0.1 mmol/l in rats treated with THP for 3 or 6 weeks (each group $n = 6$, $p<0.05$ for rats treated with THP for 6 weeks vs control rats).

Table 1. Characterization of the animals and carnitine concentrations in the heart and plasma.

	3 weeks		6 weeks	
	control	THP-treated	control	THP-treated
Body weight (g)	334 ± 16	319 ± 28	418 ± 46 **	414 ± 46 **
Heart wet weight (g)	1.16 ± 0.11	1.20 ± 0.08	1.17 ± 0.07	1.23 ± 0.18
Heart				
Free carnitine (nmol/mg muscle)	0.53 (0.46–0.61)	0.19 (0.19–0.45)	0.30 (0.22–0.34)	0.09 (0.06–0.11)
SCA carnitine (nmol/mg muscle)	0.44 (0.28–0.52)	0.00 (0.00–0.01)*	0.43 (0.42–0.73)	0.09 (0.08–0.11)*
LCA carnitine (nmol/mg muscle)	0.04 (0.03–0.05)	0.01 (0.01–0.02)*	0.04 (0.03–0.06)	0.01 (0.01–0.01)*
Total carnitine (nmol/mg muscle)	1.05 (1.01–1.07)	0.24 (0.21–0.48)*	0.78 (0.66–1.17)	0.21 (0.17–0.22)*
Plasma				
Free carnitine (µmol/l)	40.7 (30.7–43.3)	10.0 (9.4–10.8)*	67.4 (64.3–71.5)	8.1 (7.0–8.7)*
SCA carnitine (µmol/l)	6.2 (5.3–7.3)	1.9 (1.1–2.5)	14.1 (6.1–36.8)	3.2 (1.6–3.8)*
LCA carnitine (µmol/l)	7.3 (6.0–9.9)	2.0 (1.8–2.1)*	10.4 (6.0–10.7)	1.8 (1.7–2.0)*
Total carnitine (µmol/l)	53.4 (41.7–58.4)	13.9 (12.6–14.9)*	89.0 (84.6–93.0)**	12.8 (12.5–13.4)*

Values are mean ± SD (weights) or median with interquartile range (carnitine) after 3 or 6 weeks diet and treatment with THP (n = 6 hearts per group). SCA, short-chain acylcarnitine; LCA, long-chain acylcarnitine: * $p < 0.05$ vs control at corresponding age; ** $p < 0.05$ vs corresponding group after 3 weeks.

14.1.5.2. Hemodynamics, contractility, and relaxation

After 3 weeks of diet and THP treatment, no significant differences could be detected among the groups regarding LV pressure, dP/dtmax, or the relaxation indices τ and β (table 2). Specifically, hearts of carnitine-deficient rats did not differ from hearts of control rats in any hemodynamic variable independently of the substrate used (11 mM glucose or 0.4 mM Na palmitate).

However, after 6 weeks, hearts of carnitine-deficient rats showed significantly lower LV systolic pressure than control hearts during both glucose and palmitate perfusion (table 2). Consequently, hearts of carnitine-deficient rats also showed lower LV developed pressure than hearts of control rats (as LV end-diastolic pressure was set at a physiological range of 5–10 mm Hg). However, hearts of carnitine-deficient rats showed a similar dP/ dtmax as control hearts indicating unaltered contractility. Similarly, hearts of carnitine-deficient rats showed similar relaxation indices τ and β as control hearts. Finally, hearts of carnitine-deficient rats had a similar coronary flow as control hearts independently of the substrate throughout all experiments (overall mean 16.3 ml/min).

Table 2. Effect of carnitine deficiency on LV pressure, contractility, and relaxation indices in isolated rat hearts.

	3 weeks				6 weeks			
	glucose		palmitate		glucose		palmitate	
	control	carnitine-deficient	control	carnitine-deficient	control	carnitine-deficient	control	carnitine-deficient
LVSP (mm Hg)	75 ± 6	70 ± 10	74 ± 4	70 ± 13	84 ± 14	65 ± 6*	83 ± 12	66 ± 11*
LVEDP (mm Hg)	10 ± 2	8 ± 2	8 ± 3	8 ± 3	9 ± 4	8 ± 2*	10 ± 3	10 ± 3
LVDP (mm Hg)	65 ± 5	62 ± 9	65 ± 5	61 ± 12	75 ± 15	57 ± 6*	73 ± 15	55 ± 11*
dP/dt_{max} (mm Hg/s)	1151 ± 161	1159 ± 99	1157 ± 161	1167 ± 117	1123 ± 131	1136 ± 124	1139 ± 66	1144 ± 126
τ (ms)	52 ± 9	50 ± 8	45 ± 9	50 ± 15	50 ± 6	57 ± 13	49 ± 14	59 ± 19
β	24 ± 4	25 ± 4	27 ± 5	25 ± 6	22 ± 6	23 ± 4	25 ± 6	24 ± 6

Values are mean ± SD after 3 or 6 weeks diet and treatment with THP (n = 6 hearts per group) recorded at 200 bpm. LVSP, LV systolic pressure; LVEDP, LV end-diastolic pressure; LVDP, LV developed pressure; dP/dt_{max} was normalized for LVDP. * $p < 0.05$ vs control during corresponding substrate perfusion.

14.1.5.3. Contractile reserve and frequency-force relationship

After 3 and 6 weeks of carnitine deficiency, the contractile reserve was significantly reduced independently of the substrate used (fig. 2). Specifically, hearts of carnitinedeficient rats showed a reduced postextrasystolic potentiation of LV developed pressure relative to control hearts. This

reduction was similar after 3 and 6 weeks of carnitine deficiency and was not affected by the choice of substrate.

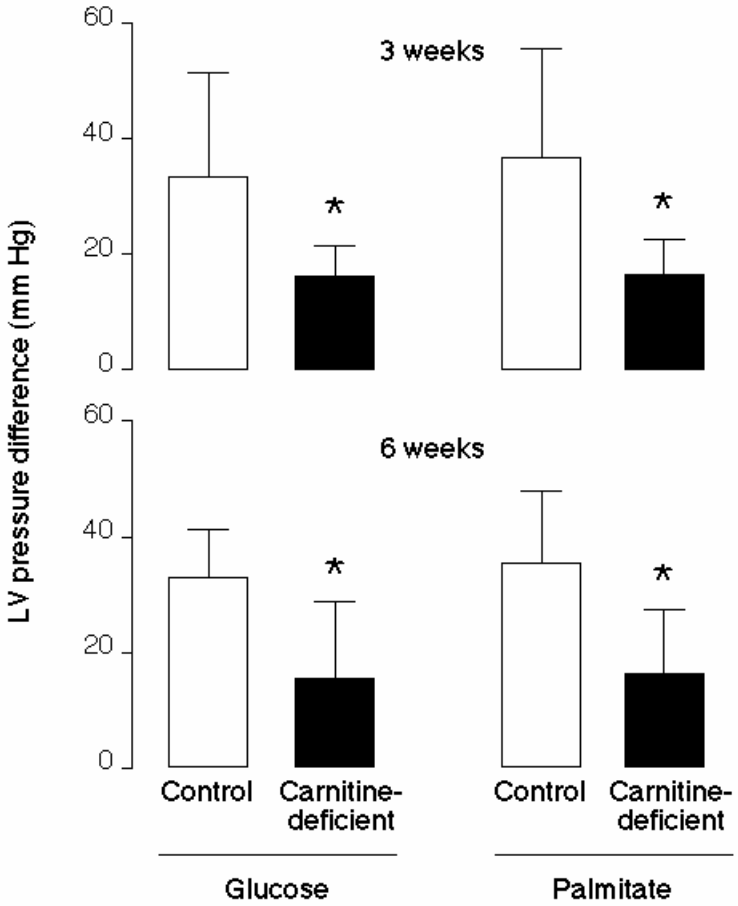

Figure 2. Contractile reserve of isolated hearts from control rats and carnitine-deficient rats during glucose or palmitate perfusion after 3 and 6 weeks diet and THP treatment. The contractile reserve was assessed as the difference of LV developed pressure between postextrasystolic potentiated beats and preceding regular beats. Values are mean ± SD; n = 6 hearts per group. * $p < 0.05$ vs control at corresponding age and perfusion condition.

Similar to the contractile reserve, the frequency-force relationship was blunted in hearts of carnitine-deficient rats independently of the substrate used (fig. 3). After 3 weeks of carnitine deficiency, the frequency-force relationship was already slightly altered at high heart rates during palmitate perfusion. However, the rate-pressure product over the entire heart rate range was not significantly different. Nevertheless, after 6 weeks, hearts of carnitinedeficient rats developed significantly less LV pressure than control hearts over the entire heart rate range. This difference was largely due to differences in LV systolic pressure between carnitine-deficient and control rats. LVdiastolic pressure, in contrast, did not differ among the groups.

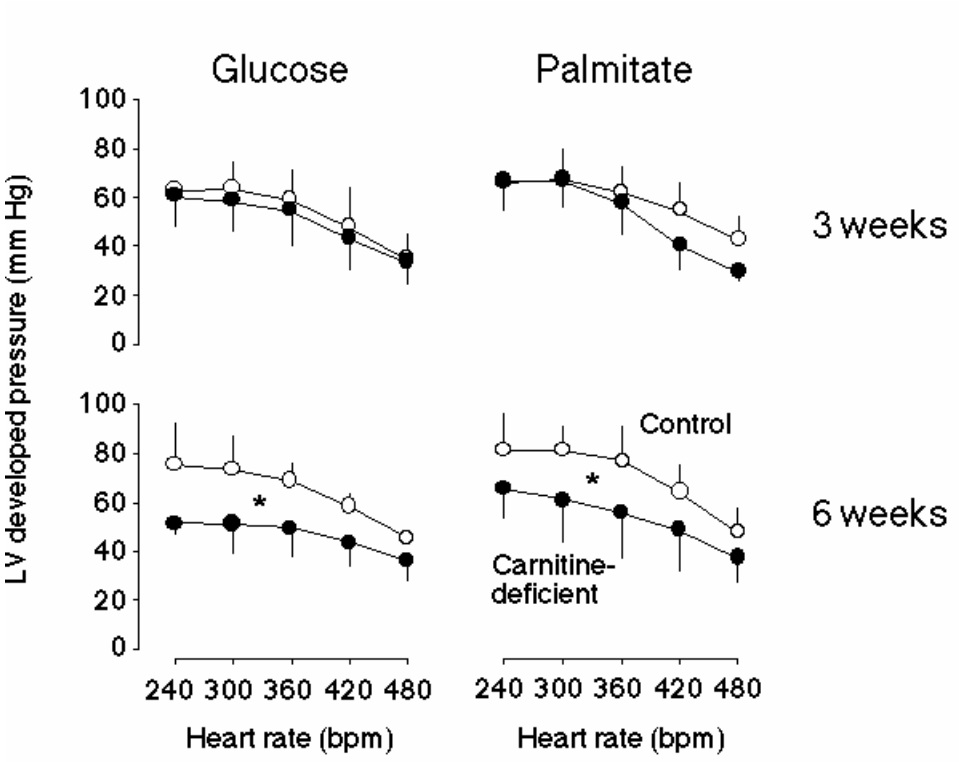

Figure 3. Frequency-force relationship of isolated hearts from control rats and carnitine-deficient rats during glucose or palmitate perfusion after 3 and 6 weeks diet and THP treatment. The frequency- force relationship was assessed as effect of increasing heart rate from 240 to 480 bpm on LV developed pressure. Values are mean ± SD; n = 6 hearts per group. * $p < 0.05$ vs control evaluated as rate-pressure product over the entire heart rate range.

14.1.5.4. Histological findings

Histological examination revealed no structural changes of the myocardium in carnitine-deficient rats. Specifically, we found no vacuolation of muscle fibers and oil red O staining revealed no excess of lipid storage in our rats. In addition, we found no disruption of muscle fibers, and glycogen storage was normal in both carnitine-deficient and control rats. Finally, we found no fibers with excess mitochondria using Gomori trichrome stain, NADH-TR, SDH, or cytochrome oxidase reaction. Thus, histologically and histochemically, the myocardium of carnitine-deficient rats did not differ from that of control rats.

14.1.5.5. Mitochondrial enzymes, ATP and phosphocreatine

After 3 and 6 weeks of carnitine deficiency, the activities of all three mitochondrial enzymes measured were not significantly different from controls (table 3). Specifically, hearts of carnitine-deficient rats showed similar activities of carnitine palmitoyl transferase, citrate synthase, and cytochrome c oxidase as control hearts, excluding a significant proliferation of mitochondria in hearts of carnitine-deficient rats.

Table 3. Mitochondrial enzymes.

	3 weeks		6 weeks	
	control	carnitine-deficient	control	carnitine-deficient
Carnitine palmitoyl transferase (mU/mg heart tissue)	1.7 ± 0.4	1.9 ± 0.2	2.3 ± 0.1	2.1 ± 0.4
Citrate synthase (U/mg heart tissue)	104 ± 32	85 ± 12	99 ± 32	103 ± 32
Cytochrome c oxydase (U/mg heart tissue)	5.9 ± 1.6	8.0 ± 3.9	6.9 ± 2.2	6.0 ± 1.6

Values are mean ± SD after 3 or 6 weeks diet and treatment with THP (n = 5–6 hearts per group).

Concentrations of ATP and phosphocreatine did not significantly differ among hearts of carnitine-deficient rats and control rats after 3 or 6 weeks diet at the end the experimental protocol (data not shown).

14.1.5.6. Effect of glycogen depletion

Pilot studies using hearts of control rats had shown that after 60 min of substrate-free perfusion, glycogen was almost completely depleted (fig. 1) and LV pressure started to decrease. The effect of glycogen depletion on myocardial function was subsequently investigated using hearts of carnitine-deficient and control rats (n = 4 hearts for both groups). When LV pressure began to decrease (usually after 60 min of substrate-free perfusion), these hearts were perfused with Na palmitate and subsequently with glucose. Compared to values obtained using hearts with normal glycogen stores (see table 2), glycogendepleted hearts of control rats produced normal LV systolic and diastolic pressures during perfusion with both substrates (fig. 4). In comparison, glycogen-depleted hearts of carnitine-deficient rats produced LV systolic pressures which were approximately 10% lower compared to control rats, irrespective of the substrate used. This decrease did not reach statistical significance, however, due to high variations in control rats. Diastolic pressure was significantly higher in hearts from carnitine-deficient rats perfused with palmitate. Importantly, upon subsequent perfusion with glucose, diastolic pressure decreased to values similar to those of control rats. It is noteworthy that arrhythmias were frequent findings in glycogen-depleted hearts, in particular in hearts from carnitine-deficient rats perfused with palmitate.

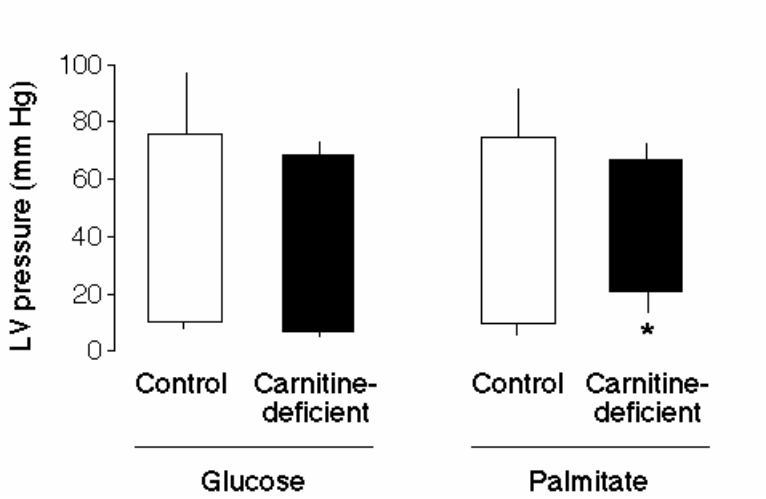

Figure 4. Effect of glycogen depletion on LV systolic and diastolic pressure (upper and lower bar end, respectively) of isolated hearts from control and carnitine-deficient rats during glucose or palmitate perfusion after 6 weeks diet and THP treatment. Values are mean ± SD; n = 3 hearts per group. * $p < 0.05$ vs control at corresponding perfusion condition.

14.1.6. Discussion

In the present study in a rat model of carnitine deficiency, we demonstrated that as little as 3–6 weeks of severe systemic carnitine deficiency can lead to abnormalities in myocardial function including systolic dysfunction, reduced contractile reserve, and a blunted frequency-force relationship. These abnormalities may be masked by endogenous glycogen and are not accompanied by structural alterations of the myocardium or by altered activities of important mitochondrial enzymes involved in fatty acid and energy metabolism.

Specifically, we found that both 3 and 6 weeks of vegetarian food poor in carnitine plus THP treatment (20 mg/100 g per day) led to severe systemic carnitine deficiency in rats (table 1). After 3 weeks of carnitine deficiency, we found a significant reduction in the contractile reserve assessed as postextrasystolic potentiation of isolated isovolumically contracting heart preparations using glucose or palmitate as substrate (fig. 2). After 6 weeks of carnitine deficiency, we found further abnormalities in myocardial function including LV systolic dysfunction (table 2), reduced contractile reserve, and a blunted frequency- force relationship (fig. 3).

At a mechanistic level, our findings suggest that as long as myocardial workloads are low, ATP production may still be sufficient in carnitine-deficient hearts. Accordingly, ATP and phosphocreatine concentrations as well as relaxation indices were similar in carnitine-deficient and control hearts. However, at high workloads, such as during high heart rates, functional abnormalities occurred, suggesting that carnitine deficiency-induced alterations in substrate metabolism result in transiently inadequate ATP production as proposed previously [26]. Furthermore, reduced postextrasystolic potentiation after 3 and 6 weeks of carnitine deficiency in our experiments suggests that altered intracellular calcium handling is an early step in the development of functional abnormalities. Specifically, severe carnitine deficiency may reduce the amount of activator calcium and/or interfere with sarcoplasmic reticular calcium uptake and/or transport [12, 27]. In our histological analysis, we found no disruptions of myofibers that could have explained abnormal myocardial function (in particular systolic dysfunction) in carnitine-deficient rats. Systolic dysfunction might arise from accumulating long-chain acyl-CoAs due to impaired activity of carnitine palmitoyltransferase I (CPT I) in the presence of low intracellular carnitine levels, as demonstrated in the liver of rats treated with THP [28]. Long-chain acyl-CoAs can damage biological membranes and impair the function of membrane-associated enzymes and/or transport proteins such as the adenine nucleotide translocase which is critical for mitochondrial energy metabolism [29]. This mechanism explains why in non-glycogen-depleted hearts cardiac dysfunction was observed under both conditions, perfusion with glucose or with palmitate.

The Km for M-CPT I, the predominating CPT I isoform in adult rats [30], is in the range of 500 μmol/l for carnitine [31]. Since the cardiac concentrations of free carnitine in carnitine-deficient rats were 190 μmol/kg at 3 and 90 μmol/kg at 6 weeks of THP treatment, an energy deficit with an associated impaired cardiac function was expected in hearts perfused with palmitate. However, endogenous myocardial glycogen stores may have at least partially compensated for an insufficient energy supply during perfusion with palmitate in carnitine-deficient hearts. Our histological examination did not reveal differences in my- ocardial glycogen content between carnitine-deficient and control hearts. Since this examination was not quantitative and did not control for glycogen formation during perfusion, we repeated our studies with hearts after depletion of cardiac glycogen by substrate-free perfusion for 60 min. After depletion of glycogen, LV diastolic pressure was higher during palmitate perfusion in carnitine-deficient hearts as compared to glucose perfusion, possibly due to insufficient energy supply to maintain a normal diastolic intracellular calcium concentration. Based on this finding, we propose that in severe disorders of fatty acid metabolism such as systemic carnitine deficiency, the myocardial energy supply can depend on endogenous glycogen stores. This is particularly the case in the absence of suitable substrates such as glucose, short-chain fatty acids, ketone bodies, or amino acids, and also during periods of increased energy consumption, for example, during high heart rates. If such periods are prolonged, myocardial glycogen stores may be depleted and glycogenolysis may be insufficient to meet the metabolic needs of the carnitine-deficient myocardium.

In patients suffering from mitochondrial diseases, proliferation of mitochondria in the affected organ (e. g., skeletal muscle and/or heart) is a frequent finding [32, 33]. In contrast, in our carnitine-deficient rats, the observed alterations of myocardial function were not accompanied by increased

activities of mitochondrial enzymes or histological abnormalities, excluding mitochondrial proliferation. However, after a longer duration of severe systemic carnitine deficiency, mitochondrial proliferation may occur. Interestingly, juvenile visceral steatosis mice, an animal model of inherited severe systemic carnitine deficiency, develop cardiac hypertrophy and mitochondrial proliferation [34]. Importantly, the present study provides the first description of carnitine deficiency-induced abnormalities of myocardial function in rats after as little as 3–6 weeks of systemic carnitine deficiency. In previous studies, 20 weeks of carnitine deficiency (induced by sodium pivalate in drinking water) was considered the minimal duration to induce functional abnormalities in rats [26]. This difference may be due to the lower degree of carnitine deficiency in previous studies (50–60% reduction) than in the present study (70–85% reduction). As carnitine concentrations did not differ between the third to the sixth week in our experiments, one may reasonably speculate that both the severity and duration of carnitine deficiency determine the development of functional abnormalities and ultimately cardiomyopathy.

In conclusion, our study in rats shows that as little as 3–6 weeks of severe systemic carnitine deficiency can lead to abnormalities in myocardial function including systolic dysfunction, reduced contractile reserve, and a blunted frequency-force relationship. These abnormalities are partially masked by endogenous glycogen and are not accompanied by structural alterations of the myocardium or altered activities of important mitochondrial enzymes involved in fatty acid and energy metabolism. The functional abnormalities in carnitine-deficient hearts may represent early signs of a metabolic cardiomyopathy.

Acknowledgements. The studies were financially supported by grants from the Swiss National Science Foundation
(31-59812.99 and 3200-068259), the Swiss Heart Foundation, and the Swiss Foundation of Muscle Research to S.K.C.E.Z. was supported by an academic career development grant of the University of Basel, Switzerland.

14.1.7. References

1. Bremer J. (1983) Carnitine--metabolism and functions. Physiol Rev. 63: 1420-80.
2. Broderick T. L., Quinney H. A. and Lopaschuk G. D. (1992) Carnitine stimulation of glucose oxidation in the fatty acid perfused isolated working rat heart. J Biol Chem. 267: 3758-63.
3. Bremer J. (1969) Pyruvate dehydrogenase, substrate specificity and product inhibition. Eur J Biochem. 8: 535-40.
4. Lango R., Smolenski R. T., Narkiewicz M., Suchorzewska J. and Lysiak-Szydlowska W. (2001) Influence of L-carnitine and its derivatives on myocardial metabolism and function in ischemic heart disease and during cardiopulmonary bypass. Cardiovasc Res. 51: 21-9.
5. Brass E. P. and Hoppel C. L. (1980) Relationship between acid-soluble carnitine and coenzyme A pools in vivo. Biochem J. 190: 495-504.
6. Gilbert E. F. (1985) Carnitine deficiency. Pathology. 17: 161-71.
7. Wynne J. and Braunwald E. (1997) The cardiomyopathies and myocarditides. In: Heart Disease: A textbook of Cardiovascular Medicine, 5th edn, pp. 1404-1463, Braunwald E. (ed.), Saunders, Philadelphia
8. Winter S., Jue K., Prochazka J., Francis P., Hamilton W., Linn L. and Helton E. (1995) The role of L-carnitine in pediatric cardiomyopathy. J Child Neurol. 10: S45-51.
9. Paulson D. J. (1998) Carnitine deficiency-induced cardiomyopathy. Mol Cell Biochem. 180: 33-41.
10. Spaniol M., Brooks H., Auer L., Zimmermann A., Solioz M., Stieger B. and Krahenbuhl S. (2001) Development and characterization of an animal model of carnitine deficiency. Eur J Biochem. 268: 1876-87.
11. Simkhovich B. Z., Shutenko Z. V., Meirena D. V., Khagi K. B., Mezapuke R. J., Molodchina T. N., Kalvins I. J. and Lukevics E. (1988) 3-(2,2,2-Trimethylhydrazinium)propionate (THP)--a novel gamma-butyrobetaine hydroxylase inhibitor with cardioprotective properties. Biochem Pharmacol. 37: 195-202.
12. Zaugg C. E., Kojima S., Wu S. T., Wikman-Coffelt J., Parmley W. W. and Buser P. T. (1995) Intracellular calcium transients underlying interval-force relationship in whole rat hearts: effects of calcium antagonists. Cardiovasc Res. 30: 212-21.

13. Soares P. R., de Albuquerque C. P., Chacko V. P., Gerstenblith G. and Weiss R. G. (1997) Role of preischemic glycogen depletion in the improvement of postischemic metabolic and contractile recovery of ischemia-preconditioned rat hearts. Circulation. 96: 975-83.
14. Barbosa V., Sievers R. E., Zaugg C. E. and Wolfe C. L. (1996) Preconditioning ischemia time determines the degree of glycogen depletion and infarct size reduction in rat hearts. Am Heart J. 131: 224-30.
15. Brass E. P. and Hoppel C. L. (1978) Carnitine metabolism in the fasting rat. J Biol Chem. 253: 2688-93.
16. Gilbert J. C. and Glantz S. A. (1989) Determinants of left ventricular filling and of the diastolic pressure-volume relation. Circ Res. 64: 827-52.
17. Tamiya K., Beppu T. and Ishihara K. (1995) Double-exponential curve fitting of isometric relaxation: a new measure for myocardial lusitropism. Am J Physiol. 269: H393-406.
18. Field M. L., Azzawi A., Unitt J. F., Seymour A. M., Henderson C. and Radda G. K. (1996) Intracellular [Ca2+] staircase in the isovolumic pressure--frequency relationship of Langendorff-perfused rat heart. J Mol Cell Cardiol. 28: 65-77.
19. Srere P. A. (1969) Citrate Synthase. Methods Enzymol. 13: 3-11.
20. Krahenbuhl S., Chang M., Brass E. P. and Hoppel C. L. (1991) Decreased activities of ubiquinol:ferricytochrome c oxidoreductase (complex III) and ferrocytochrome c:oxygen oxidoreductase (complex IV) in liver mitochondria from rats with hydroxycobalamin[c-lactam]-induced methylmalonic aciduria. J Biol Chem. 266: 20998-1003.
21. Bremer J. (1981) The effect of fasting on the activity of liver carnitine palmitoyltransferase and its inhibition by malonyl-CoA. Biochim Biophys Acta. 665: 628-31.
22. Adams H. (1963) Adenosin-5'-triphosphate, determination with phosphoglycerate kinase, In: Methods of Enzymatic Analysis, pp. 539-543, Bergmayer H.U. (ed.) Academic Press, New York
23. Willer B., Stucki G., Hoppeler H., Bruhlmann P. and Krahenbuhl S. (2000) Effects of creatine supplementation on muscle weakness in patients with rheumatoid arthritis. Rheumatology (Oxford). 39: 293-8.
24. Olsen C. (1971) An enzymatic fluorimetric micromethod for the determination of acetoacetate, -hydroxybutyrate, pyruvate and lactate. Clin Chim Acta. 33: 293-300.
25. Dawson.Saunders B. and Trapp R. G. (1990) Basic and Clinical Biostatistics, Appleton & Lange, San Mateo, California
26. Paulson D. J. (1998) Secondary L-carnitine deficiency-induced cardiomyopathy. Cardiologia. 42 (Suppl 2): 677-683
27. Wood E. H., Heppner R. L. and Weidmann S. (1969) Inotropic effects of electric currents. I. Positive and negative effects of constant electric currents or current pulses applied during cardiac action potentials. II. Hypotheses: calcium movements, excitation-contraction coupling and inotropic effects. Circ Res. 24: 409-45.
28. Spaniol M., Kaufmann P., Beier K., Wuthrich J., Torok M., Scharnagl H., Marz W. and Krahenbuhl S. (2003) Mechanisms of liver steatosis in rats with systemic carnitine deficiency due to treatment with trimethylhydraziniumpropionate. J Lipid Res. 44: 144-53.
29. Faergeman N. J. and Knudsen J. (1997) Role of long-chain fatty acyl-CoA esters in the regulation of metabolism and in cell signalling. Biochem J. 323: 1-12.
30. Brown N. F., Weis B. C., Husti J. E., Foster D. W. and McGarry J. D. (1995) Mitochondrial carnitine palmitoyltransferase I isoform switching in the developing rat heart. J Biol Chem. 270: 8952-7.
31. McGarry J. D. and Brown N. F. (1997) The mitochondrial carnitine palmitoyltransferase system. From concept to molecular analysis. Eur J Biochem. 244: 1-14.
32. Haller R. G., Lewis S. F., Estabrook R. W., DiMauro S., Servidei S. and Foster D. W. (1989) Exercise intolerance, lactic acidosis, and abnormal cardiopulmonary regulation in exercise associated with adult skeletal muscle cytochrome c oxidase deficiency. J Clin Invest. 84: 155-61.
33. Hoppel C. L., Kerr D. S., Dahms B. and Roessmann U. (1987) Deficiency of the reduced nicotinamide adenine dinucleotide dehydrogenase component of complex I of mitochondrial electron transport. Fatal infantile lactic acidosis and hypermetabolism with skeletal-cardiac myopathy and encephalopathy. J Clin Invest. 80: 71-7.

34. Horiuchi M., Yoshida H., Kobayashi K., Kuriwaki K., Yoshimine K., Tomomura M., Koizumi T., Nikaido H., Hayakawa J., Kuwajima M. and et al. (1993) Cardiac hypertrophy in juvenile visceral steatosis (jvs) mice with systemic carnitine deficiency. FEBS Lett. 326: 267-71.

14.2. Contractile function and metabolic characterisation of rodent skeletal muscle in the presence and absence of carnitine deficiency

Paul A. Roberts, Priska Kaufmann, Albert Urwyler*
& Stephan Krähenbühl

Institute of Clinical Pharmacology & Toxicology, Department of Research & *Department of Anaesthesia, University Hospital Basel, CH-4031, Switzerland,

J Physiol 2004, submitted

14.2.1. Summary

The consequences of carnitine depletion upon the metabolic and contractile characteristics of otherwise healthy skeletal muscle remains largely unexplored. The present study wishes to investigate the integration of fat & carbohydrate metabolism and contractile function in predominantly slow- (soleus) and fast-twitch (extensor digitorum longus) rodent skeletal muscles following treatment with N-trimethyl-hydrazine-3-propionate (THP); a competitive inhibitor of both renal carnitine reuptake and the final enzyme within carnitine biosynthesis. Male Sprague Dawley rats were fed a standard rat chow in the absence (CON; n=8) and presence of THP (22.2±0.2 mg THP·100g^{-1} body mass day^{-1}; n=8) for 3 weeks. Following treatment, rats were fasted for 24h prior to the tendon-to-tendon excision of their soleus and EDL muscles for biochemical characterisation at rest and following 5min of contraction *in vitro*. THP treatment reduced the total-carnitine pool to the same extent in both soleus and EDL muscles from CON (~80%; P<0.01). Carnitine depletion was associated with atrophy (-30%; P<0.05) and a reduced magnitude of pyruvate dehydrogenase complex (PDC) activation during contraction (-63%; P<0.05) in soleus muscle whilst contractile function, total-coenzyme-A and water content remained unaltered from CON. In EDL muscle, carnitine depletion was associated with impaired peak tension development (-48%, P<0.05), ATP homeostasis (-40%, P<0.05), reduced free-coenzyme-A availability (-25%, P<0.05) and increased glycogen hydrolysis (55%, P<0.05) during contraction, whilst PDC activation, muscle weight and water content remained unaltered from CON. In conclusion, whilst the biochemical and functional properties of soleus muscle fibres is largely normal, it appears that carnitine-deficiency results in a selective loss of slow-twitch fibres. Conversely, despite the preservation of EDL mass, the biochemical and functional properties of this predominantly fast-twitch muscle were impaired, with an increased reliance upon energy production from non-oxygen dependent routes when compared to CON. Based on this evidence, the muscle myopathy often associated with carnitine deficiency is most likely attributable to impaired mitochondrial energy production in fast-twitch muscle fibres.

14.2.2. Introduction

Carnitine is a naturally occurring compound that is found in all mammalian tissues, which marks the 100th anniversary of its original discovery in skeletal muscle extracts this year (Gulewitsch & Krimberg, 1905). L-Carnitine, the biologically effective isomer of carnitine, plays a key role within several cellular energy producing pathways (Bremer, 1983). By way of example, carnitine is essential towards the transport of long-chain fatty acids across the inner-mitochondrial membrane towards their oxidative fate inside the mitochondrial matrix (Fritz, 1955), is important towards the removal of potentially toxic acyl-CoAs from the mitochondria by forming acylcarnitines (Brass & Hoppel, 1980; Bieber *et al.* 1982), serves as a temporal acetyl group buffer in the oxidation of carbohydrates during periods of augmented pathway flux (Childress *et al.* 1966; Roberts *et al.* 2002) and is an osmoprotectant (Hofmeister, 1888); thus can impact upon cell volume and osmotic stress responses (Peluso *et al*. 2000). There is also expanding evidence indicating that L-carnitine has more complex functions within the cell, towards the regulation of gene expression (Giovenali *et al*. 1994, Horiuchi *et al*. 1999) and the blockage of apoptosis at multiple levels (Andrieu-Abadie *et al*. 1999, Mutomba *et al*. 2000, Vescovo *et al*. 2002).

In humans, a typical 70 kg healthy omnivore male contains ~21 grams of carnitine, in both free and acetylated forms (Brass, 1995), with ~95% of the carnitine pool located in skeletal muscle and heart, where ~90% of this cellular reserve exists outside of the mitochondria. There is limited synthesis of carnitine within the body, with ~30% of the daily requirement being met by *de novo* production in the kidneys (*humans*; Rebouche & Engel, 1980) or liver (*rats*; Rebouche, 1982) and to a lesser extent brain and testes from the amino acid precursors of L-methionine and L-lysine (Fig. 1A). The remaining 70% of the requirement is received in our diet from the consumption of carnitine-rich foods; such as red & white meats, fish and to a lesser extent dairy produce and vegetables (Mitchell, 1978). The dietary absorption of carnitine, which occurs in the small intestine, and cellular uptake, which often occurs against a concentration gradient, is facilitated by a high-affinity (sodium-dependent) active transport system termed organic cation transporter new two (OCTN2; Sekine *et al.* 1998, Tamai *et al*. 1998). The final component of carnitine homeostasis is the slow net-turnover and excretion of carnitine in the urine (5μmol/kg/day; Lombard *et al*. 1989), which is aided by the marked efficiency (90-95%) of

the kidney to reabsorb carnitine from the urine, due to the high activity of the OCTN2 transporter in proximal tubules (Wu *et al*. 1999; Fig. 1B)

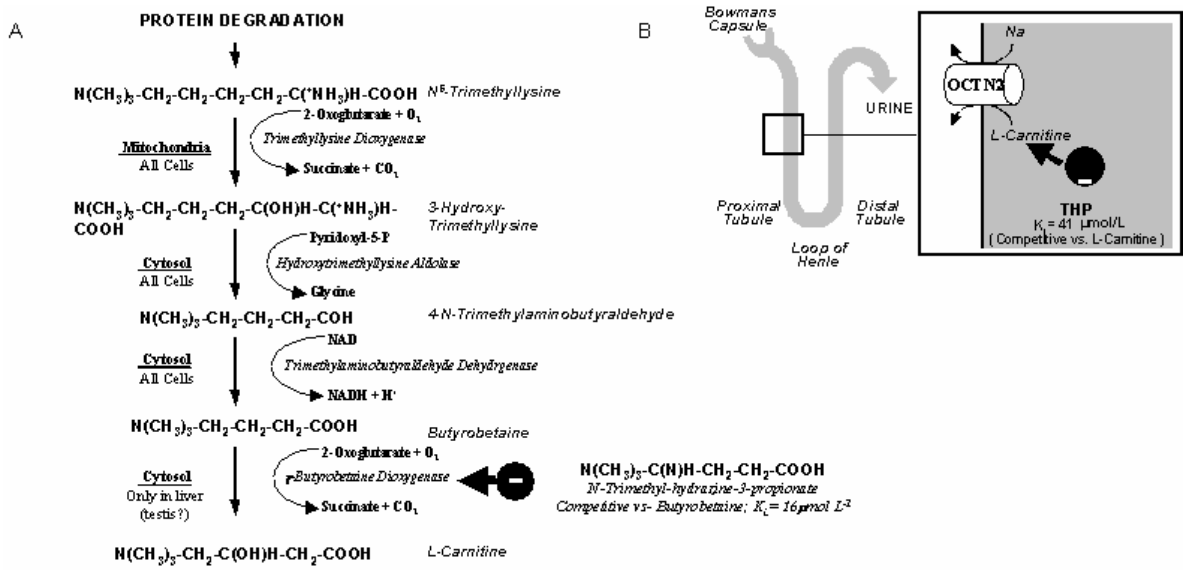

Figure 1:N-trimethyl–hydrazine-3-propionate (THP) induced alterations in rodent carnitine biosynthesis (A) & nephron carnitine reabsorption in the kidney (B) upon whole-body carnitine homeostasis. *Abbreviations*; Organic Cation Transporter New Two (OCTN2).

Fundamental to our understanding of the role of carnitine within the body is the ability to manipulate the size of the cellular carnitine pool and to investigate the consequences of such upon cellular, tissue and whole-body function, at rest and in response to external stresses; such as muscular contraction. This desire is complicated by the fact that it is difficult to markedly elevate carnitine reserves (especially within muscle) through prolonged carnitine supplementation in healthy (omnivore) individuals (for review see Karlic & Lohninger, 2004). This makes investigating the consequences of carnitine depletion (hypocarnitinemia) within clinical patients and animal models of disorders in carnitine uptake and homeostasis often the only research-avenue open.

The first case of carnitine deficiency was reported by Engel & Angelini in human skeletal muscle in 1973 (Engel & Angelini, 1973). Since this discovery, hypocarnitinemia has been shown to occur via several inborn defects or deficiencies in the cellular uptake and handling of carnitine, frequently termed systemic or primary carnitine deficiencies, with mutations in the genes encoding the OCTN2 transporter often causative (Brooks & Krähenbühl, 2001). A multitude of secondary, indirectly-induced, carnitine deficiencies have also been reported in response to several disease states (AIDS, Reye's syndrome, endocrine disorders), during clinical treatments (renal dialysis, valproic acid, zidovudine, quinidine) and as a consequence of pregnancy and carnitine malnourishment (Lombard *et al*. 1989). The side effects associated with these secondary carnitine deficiencies can often be overcome with oral or intravenous L-carnitine supplementation.

Advancements in our understanding of carnitine deficiencies have been made with the discovery of juvenile visceral steatosis (JVS) mice (Koizumi *et al*. 1988), which have a point mutation defect in the gene encoding OCTN2, and thereby display a greatly impaired reuptake of carnitine by the kidney resulting in net carnitine loss (Kuwajima *et al*. 1991, Horiuchi *et al*. 1994). Given the locus of their carnitine abnormality, the likelihood of compensatory changes within intermediary metabolism during neonatal development and the chronic nature of this deficiency (even when dietary carnitine is provided; Kuwajima *et al*. 1999) the JVS mouse is not an ideal model to compare towards humans, especially those who develop secondary carnitine deficiencies. Clearly, this need would best be served by an animal model whereby a systemic carnitine deficiency could be induced acutely in otherwise healthy tissue.

Recent work by our group has developed a rodent model of systemic carnitine deficiency, which can be induced in response to acute feeding with the carnitine and butyrobetaine analogue N-trimethyl-hydrazine-3-propionate, in otherwise healthy Sprague Dawley rats (Spaniol *et al* 2001). N-trimethyl-hydrazine-3-propionate (THP); also known as mildronate (Eremeev *et al*. 1984) or MET-88 (Simkhovich *et al*. 1988) within the literature, effectively leaches carnitine from the body by

competitively inhibiting the final, γ-butyrobetaine hydroxylase reaction within carnitine biosynthesis, with respect to its natural substrate butyrobetaine (Fig. 1A; Heinonen & Takala, 1994, Tsoko *et al*. 1995, Spaniol *et al*. 2001) and by competing against carnitine for OCTN2 mediated re-absorption by the kidney (Fig. 1B; Spaniol *et al*. 2001). Three weeks of THP treatment has been shown to reduce the tissue carnitine content of heart, liver, plasma and skeletal muscle (quadriceps femoris) by 72-83%, to cause liver steatosis, peroxisomal proliferation, impaired palmitate metabolism and result in abnormalities in lipid storage and myocardial function (Spaniol *et al*. 2001, Spaniol *et al*. 2003, Zaugg *et al*. 2003). To date, the characterisation of this novel model of carnitine-deficiency has focussed predominantly upon THP's effect upon liver and kidney (main sites of production), plasma and heart carnitine stores, whereby its role within skeletal muscle, the major storage site (consumer) of carnitine within the body, has received relatively little attention thus far (Spaniol *et al*. 2001).

The present study wishes to address this point, by examining the consequences of THP pre-treatment upon the composition of coenzyme-A and carnitine pools, tissue water content and the integration of fat and carbohydrate metabolism at rest and in response to contraction in rodent skeletal muscle. To further our understanding, we examined the above in two functionally / biochemically distinct muscle groups, namely; soleus (84% slow-twitch fibres; Ariano *et al*. 1973) & extensor digitorum longus (EDL; 98% fast-twitch fibres; Armstrong & Phelps, 1984), where the role of the carnitine pool varies from predominantly facilitating fat translocation to preserving the free coenzyme-A content for sustained carbohydrate oxidation.

14.2.3. Methods

14.2.3.1. Animal handling

All *in vivo* procedures were performed in full accordance with the 'Ethical Principles and Guidelines for Scientific Experiments on Animals' of the Swiss Academy of Medical Sciences and following Cantonal approval from the Veterinary Department of Basel, Switzerland. Sixteen male Sprague Dawley rats, weighing ~200g, were obtained from the Süddeutsche Versuchstierfarm (Tuttlingen, Germany) and were acclimatised to the laboratory one week prior to the start of the study. The animals were housed in a temperature (20-22^{o}C) and light (12h light – 12h dark cycle) controlled animal facility.

14.2.3.2. Treatment groups

Following a week of habituation, animals were randomly assigned to one of two treatments groups and received either a standard powdered rat chow (Kliba Futter 3433, Basel, Switzerland) in the absence (CON; n=8) or presence of 20mg THP 100g^{-1} body mass day^{-1} for 21 days (THP, n=8) with water provided *ad libitum* throughout the study. The THP was commercially prepared by ReseaChem GmbH (Burgdorf, Switzerland), and the amount of THP to be added to the animal's individual chow feed each day was based upon the previous day's food consumption for each animal; which typically did not vary from ~35g of chow per day. Notwithstanding, food consumption, actual THP dosing and changes in body weight were examined daily (Fig. 2). Based upon the findings of our previous study, rats were fed a standard rat chow (carnitine content 16.9 nmol g^{-1}; Kliba Futter, Basel, Switzerland), as the effect of carnitine-deficient food upon carnitine homeostasis is minor in the rat (Spaniol *et al*. 2001). This can be expected based upon the mechanisms by which THP induces systemic carnitine deficiency; i.e. via inhibition of carnitine biosynthesis (Fig. 1A) and by inhibiting carnitine reabsorption by the kidney (Fig. 1B).

14.2.3.3. Anaesthesia & muscle excision

To investigate the consequences of muscular carnitine depletion upon contractile function, in isolation of the systemic (central) THP-induced carnitine deficiencies, muscle groups (soleus and EDL) were excised and stimulated to contract *ex vivo* under physiological conditions.

Following 21 days of CON or THP treatment, animals were starved for 24 h, in an attempt to stress intermediary metabolism towards the oxidation of lipid reserves, prior to the induction of anaesthesia with 160 mg kg^{-1} i.p. ketamine (Ketalar, Park-Davis, Zurich, Switzerland). Once adequate

anaesthesia was established, the animal's soleus and EDL muscles were quickly and carefully isolated (total time <5 mins), tendon-to-tendon, from both the left and right hind-limbs. Immediately following their excision, one soleus and one EDL muscle were snap-frozen in liquid nitrogen for future biochemical analysis of basal metabolite values in response to treatment. The distal and proximal tendons of the remaining soleus and EDL muscles were tied with braided nylon (non-absorbable) suture (Surgilon, grade 3-0) prior to their removal from the animal and were immediately placed in continually gassed (95% oxygen – 5% carbon dioxide) Krebs buffer (135mM NaCl, 5mM KCl, 1mM $Na_2H_2PO_4$, 15mM $NaHCO_3$, 11mM glucose, 1mM $MgSO_4$, 2.5mM $CaCl_2$; pH 7.4; 25^oC). In an attempt to maintain the *in vivo* appearance, fibre alignment and 3D architecture of the muscles, the Krebs incubated soleus and EDL muscles were loaded with ~1.2g upon the distal tendon whilst in Krebs suspension prior to the assessment of their *in vitro* contractile properties. Following the excision of the two soleus and two EDL muscles, the animal was killed by decapitation whilst still under anaesthesia.

14.2.3.4. Contractile function of isolated muscles

Muscles were mounted within the electrical stimulatory apparatus following their excision from the animal (<10min). The contractile properties of the isolated muscles were individually assessed, with the EDL muscle always the first to be studied followed by the soleus muscle. No differences in tissue handling existed between the CON and THP groups. Muscles were vertically mounted in the water-tight chamber of the electrical stimulatory apparatus (manufactured in-house), by the anchoring of the distal tendon to a fixed hook at the base of the bath and the attachment of the proximal tendon, by thread, to the isometric force transducer (Grass FT03, Quincy, Medfield, MA, USA). The force transducer, was mounted upon the micropositioner and was calibrated over the range of 0.25-1.00g prior to each electrical stimulation protocol. Following muscle connection, the chamber of the apparatus was filled with Krebs buffer and continually gassed with a mixture of 96% O_2 and 5% CO_2 and maintained at 37.5^oC (Julabo 5B, JD Instruments, Houston, TX, USA) for the duration of the muscle stimulation protocol. Optimal muscle length (length producing maximal twitch tension) was determined by varying the muscle length in increments of 1mm with the micropositioner and by performing a single 'twitch' stimulus. Once optimal muscle length was determined, all subsequent measurements were made at this setting and the muscle was allowed to equilibrate for 5 min prior to the commencement of the contractile, electrical stimulation protocol. Muscular contraction was electrically induced through the bathing (Krebs) solution by two platinum-plate electrodes located at the proximal and distal origins of the muscle. Muscles were stimulated for 5 mins (1 s train interval, 333 ms train duration, 25 ms pulse interval, 1 ms pulse duration, 130 V), in accordance with the work of Brass *et al*. (1993). Contractile function was recorded using a 1-channel chart recorder (LKB Bromma 2210, Bromma, Sweden). Following the assessment of the EDL muscle, the stimulatory protocol was repeated for the soleus muscle. Immediately following the contraction protocol (<1 s), muscles were snap frozen in liquid nitrogen for subsequent biochemical determinations.

14.2.3.5. Muscle sample handling & analysis

All muscle samples, basal and post-contraction, were divided into two equal portions under liquid nitrogen. Subsequently, one portion was freeze-dried, dissected free from visible blood and connective tissue and powdered. Freeze-drying and powdering of muscle samples not only ensures a more homogenous muscle sample but allows the correct determination of metabolite contents independent of fluctuations in tissue water content. Total muscle water content of samples was determined by weighing the samples before and after freeze-drying. Freeze-dryed samples were then extracted in 0.5 M perchloric acid containing 1 mmol EDTA, with the resulting supernatant neutralised with 2.2 M $KHCO_3$ and used for the spectrophotometric determination of ATP, phosphocreatine (PCr), creatine and muscle lactate (Harris *et al.* 1974). The extract was also used for the radio-isotopic determination of free-carnitine, acetylcarnitine, total-CoASH and acetyl-CoA (Cederblad *et al*. 1990). Finally, the extract was analysed fluorometrically for the determination of the tricarboxylic acid cycle intermediate citrate (Moellering & Gruber, 1966, Passoneau & Lowry, 1993). Freeze-dried muscle powder was also used for the spectrophotometric determination of muscle glycogen (Harris *et al.* 1974). The remaining portion of frozen, wet muscle was used to assess the activation status of the pyruvate dehydrogenase complex (Constantin-Teodosiu *et al*. 1991).

14.2.3.6. Calculations & statistics

All data are reported as means ± S.E.M. Comparisons between treatments were carried out using two-way analysis of variance (ANOVA) with repeated-measures. When a significant F-value was obtained ($P<0.05$) an LSD post-hoc test was used to locate any differences (SPSS Base 12.0).

14.2.4. Results

14.2.4.1. Animal Data

No differences in body mass existed between treatment groups during the 21 days of powdered chow feeding in the presence and absence of THP; with each group linearly gaining ~90g during the course of the study (Fig. 2). Daily food consumption was no different between treatment groups during the 21 days of CON and THP treatment (CON = 38.7 ± 0.2 vs. THP = 38.3 ± 0.3 g per day, Fig. 2); equating to a THP dosage of 22.2 ± 0.2 mg THP $100g^{-1}$ body mass per day.

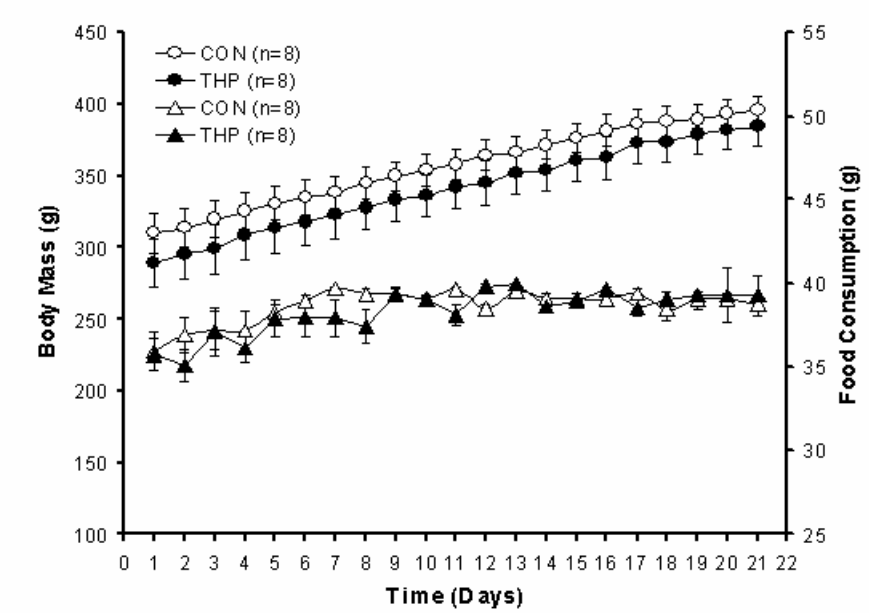

Figure 2: Daily alterations in rodent body mass (g; circles) and food consumption (g; triangles) during 21 days of powdered-chow feeding in the absence (CON, open symbols, n=8) and presence of N-trimethyl–hydrazine-3-propionate treatment (THP, closed symbols, n=8). Results are expressed as means ± S.E.M. * Different from corresponding CON value ($P<0.05$).

14.2.4.2. Muscle mass & water content

No differences in muscle water content existed between CON and THP groups following 21 weeks of treatment in either the EDL (CON = 76.9 ± 0.3 vs. THP = 76.5 ± 0.2 % water) or soleus muscles (CON = 75.4 ± 0.2 vs. THP = 75.3 ± 0.1 % water), with water accounting for ~75% of the wet mass within each muscle.

The absolute muscle weight of tendon-to-tendon excised soleus muscle was reduced by 30 % in THP pre-treated animals when compared to CON (CON = 186.7 ± 18.9 vs. THP = 132.1 ± 14.7 mg wet muscle, $P<0.05$). This muscle atrophy was maintained when soleus weight was expressed relative to the animals body weight (CON = 0.47 ± 0.05 vs. THP = 0.34 ± 0.03 mg wet muscle g^{-1} body mass, $P<0.05$). No reduction in absolute weight (CON = 140.7 ± 3.7 vs. THP = 124.4 ± 15.3 mg wet muscle) or muscle weight relative to body weight (CON = 0.35 ± 0.01 vs. THP = 0.32 ± 0.03 mg wet muscle g^{-1} body mass) was observed from CON following THP pre-treatment in EDL muscle.

14.2.4.3. Composition of muscular carnitine pool

Pre-treatment of rodent skeletal muscle with THP markedly reduced muscular acetylcarnitine concentration by ~75% from that observed in CON in both soleus and EDL muscles, whilst at rest and following 5 min of electrically-induced contraction ($P<0.01$, Fig. 3A). No differences in acetylcarnitine content existed between EDL and soleus muscle in both the CON and THP pre-treated animals at rest and in response to contraction (Fig. 3A). No increase in acetylcarnitine concentration from basal values was observed in response to contraction in both CON and THP pre-treated EDL and soleus muscles (Fig. 3A).

Pre-treatment of rodent skeletal muscle with THP markedly reduced muscular free-carnitine concentration by ~85% from that observed in CON in both EDL and soleus muscles whilst at rest and following contraction ($P<0.01$, Fig. 3B), with no differences in free-carnitine existing from their respective basal values in response to contraction (Fig. 3B). No reduction in free-carnitine concentration from basal was observed in response to contraction in both CON and THP pre-treated EDL and soleus muscles (Fig. 3B).

In accordance with the changes in acetylcarnitine and free-carnitine, muscular total-carnitine was reduced by 75-82 % in EDL and soleus muscle at rest and following contraction in THP vs. CON pre-treated muscle ($P<0.01$, Fig. 3C).

Despite the marked reductions in both muscular acetylcarnitine and free-carnitine content in response to THP feeding, the acetylcarnitine to free-carnitine ratio was increased by ~95% in EDL muscle ($P<0.05$, Fig. 3D) and by ~125% in soleus muscle ($P<0.01$, Fig. 3D) following THP treatment when compared to CON at rest and also following isometric contraction in EDL muscle ($P<0.05$, Fig. 3D) and soleus muscle ($P<0.01$, Fig. 3D). No differences in the acetylcarnitine to free-carnitine ratio were observed between muscle groups at rest or following contraction in the CON group (Fig. 3D). However, the acetylcarnitine to free-carnitine ratio was higher in the soleus vs. EDL muscle at rest following THP treatment ($P<0.05$, Fig. 3D).

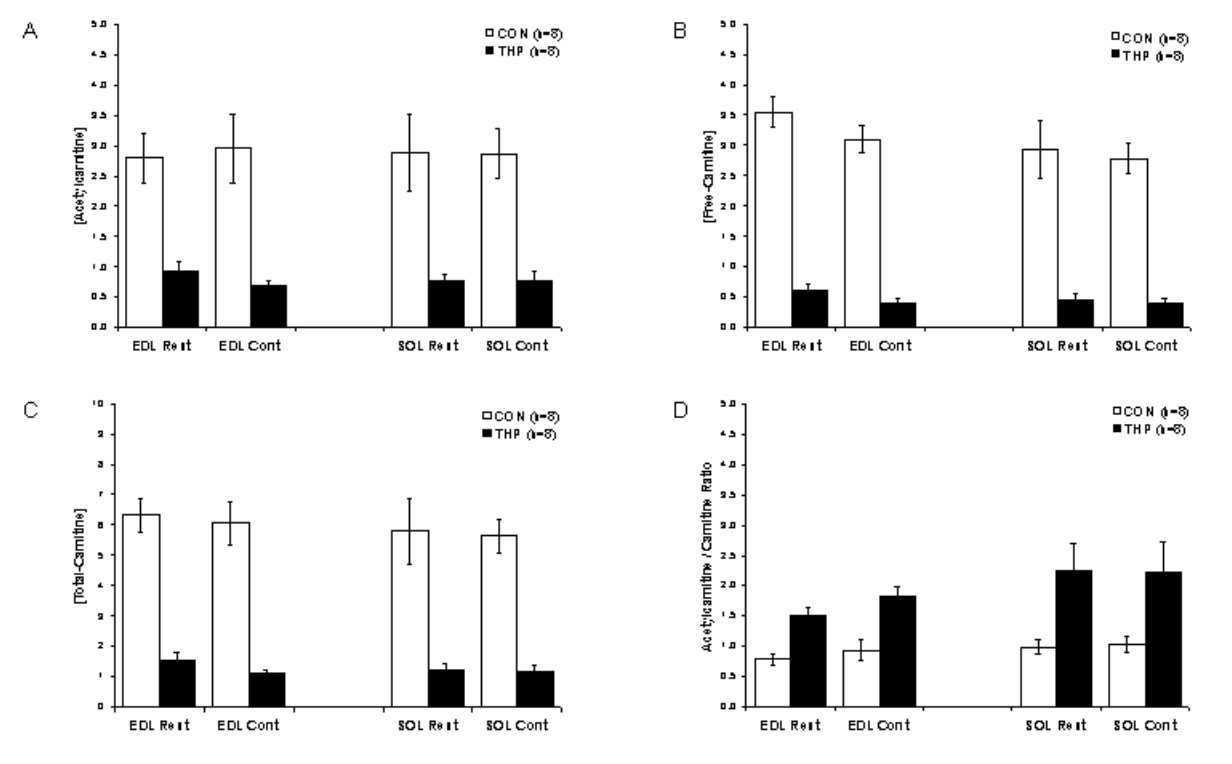

Figure 3: Acetylcarnitine (A), free-carnitine (B) & total-carnitine (C) concentrations & the acetylcarnitine to free-carnitine ratio (D) in rodent extensor digitorum longus (EDL) and soleus (SOL) muscles at rest and following 5 min of electrically induced contraction (Cont) in control (CON) and N-trimethyl –hydrazine-3-propionate (THP) pre-treated muscles. Results are expressed as means ± S.E.M. with units of mmol kg^{-1} dry muscle * Different from CON ($P<0.05$); † different from corresponding EDL muscle within the same treatment group ($P<0.05$).

14.2.4.4. Composition of muscular coenzyme-A pool

No differences in muscular acetyl-CoA concentration existed between CON and THP treatment groups at rest or in response to contraction in either EDL or soleus muscles (Fig. 4A). No alteration in muscle acetyl-CoA content from rest was observed in either EDL or soleus muscle following 5 min of electrical stimulation (Fig. 4A). However, the concentration of acetyl-CoA was significantly higher in CON and THP pre-treated EDL muscle when compared to the corresponding soleus muscle ($P<0.01$, Fig. 4A).

No differences in muscular free-CoASH concentration existed between control and THP treatment groups at rest and following contraction in soleus muscle (Fig. 4B). However, THP pre-treatment markedly reduced free-CoASH content in EDL muscle from CON at rest and following contraction ($P<0.01$, Fig. 4B). No alteration in muscle free-CoASH content from rest was observed in either EDL or soleus muscle in response to the 5 min of electrical stimulation (Fig. 4B).

In accordance with the alterations in tissue acetyl-CoA and free-CoASH concentrations, THP pre-treatment markedly reduced EDL total-CoASH content from CON at rest and following contraction ($P<0.05$, Fig. 4C). However, muscle total-CoASH content was unaltered from CON at rest and following contraction in soleus muscle following THP treatment (Fig. 4C). No alteration in muscle total-CoASH content from rest was observed in either EDL or soleus muscle in response to the 5 min of electrical stimulation (Fig. 4C).

No differences in the acetyl-CoA to free-CoASH ratio was observed following THP treatment when compared to CON at rest and also following isometric contraction in soleus muscle (Fig. 4D). However, the acetyl-CoA to free-CoASH ratio was markedly elevated following THP treatment when compared to CON at rest and also following isometric contraction in EDL muscle ($P<0.05$, Fig. 4D). Electrical stimulation markedly elevated the acetyl-CoA to free-CoASH ratio from its basal value in THP pre-treated EDL muscle ($P<0.05$, Fig. 4D). The ratio of acetyl-CoA to free-CoASH was higher in

CON and THP treated EDL muscle when compared to their corresponding soleus muscle (P<0.01, Fig. 4D).

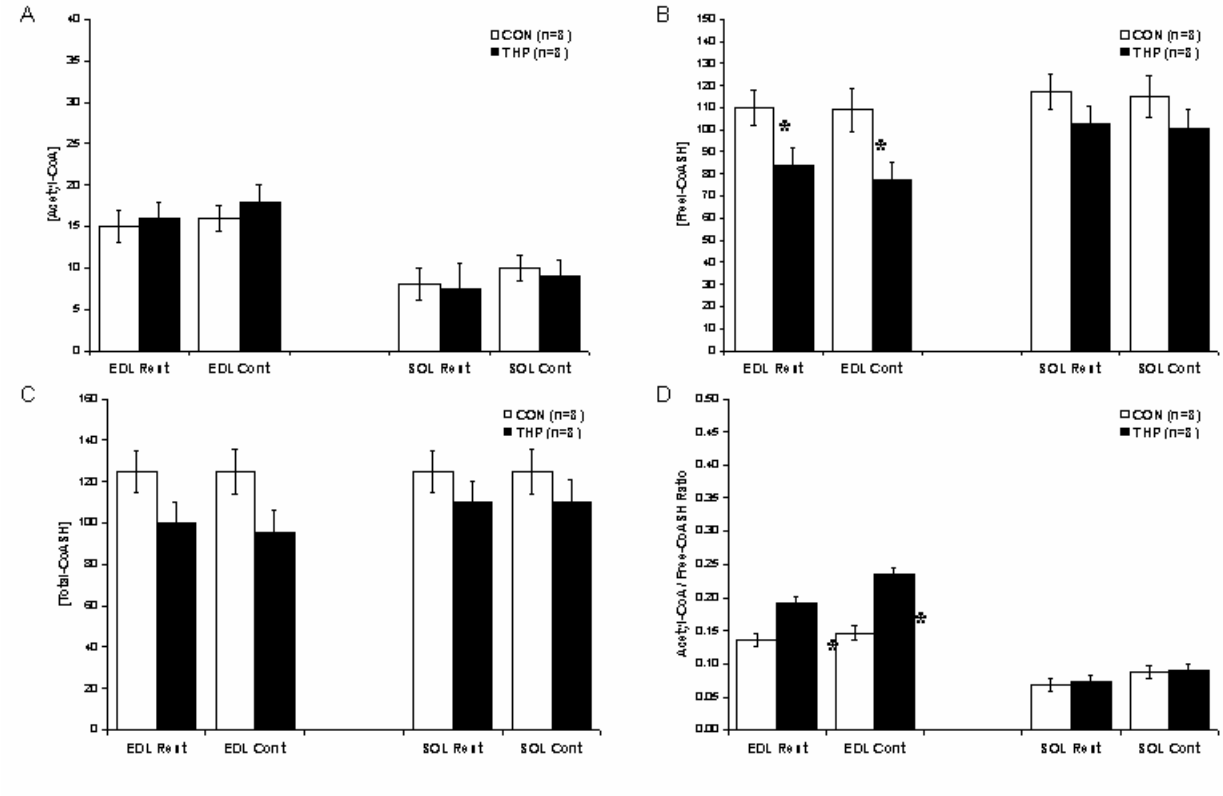

Figure 4: Acetyl-CoA (A), free-CoASH (B) & total-CoASH (C) concentrations & the acetyl-CoA to free-CoASH ratio (D) in rodent extensor digitorum longus (EDL) and soleus (SOL) muscles at rest and following 5 min of electrically induced contraction (Cont) in control (CON) and N-trimethyl–hydrazine-3-propionate (THP) pre-treated muscles. Results are expressed as means ± S.E.M. with units of μmol kg^{-1} dry muscle * Different from CON (P<0.05).

14.2.4.5. Muscle metabolites at rest & during contraction (ex vivo)

No differences in ATP concentrations existed between groups at rest or following contraction in either EDL or soleus muscle (Table 1). The concentration of ATP was maintained at basal levels following contraction in CON treated EDL and CON and THP pre-treated soleus muscle groups (Table 1). However, after 5 min of contraction ATP concentration in the THP pre-treated EDL muscle was significantly lower than its basal value (P<0.05, Table 1).

No differences in PCr concentration existed between groups at rest or following contraction in either EDL or soleus muscle (Table 1). Following 5 min of electrically-induced contraction, PCr concentrations were significantly lower than rest in both CON and THP pre-treated EDL and soleus (P<0.05, Table 1).

Similarly, no differences in creatine concentration existed between groups at rest or following contraction in either EDL or soleus muscle (Table 1). No alteration in cellular creatine content was observed from basal following contraction in any treatment group or specific muscle. (Table 1).

In accordance with the alterations in tissue PCr and creatine content, muscle total creatine (the sum of creatine + phosphocreatine) was no different between CON and THP treatment groups at rest and following contraction in either EDL or soleus muscle (Table 1). Paradoxically, there was a significant reduction in total-creatine concentration in CON and THP pre-treated soleus muscle in response to contraction when compared to their resting (basal) value (P<0.05, Table 1).

Resting muscle glycogen concentration was no different between treatment groups at rest in EDL and soleus muscles and following contraction with the sole exception of THP pre-treated soleus muscle, where the rate of glycogenolysis was doubled from that observed in CON (P<0.05, Table 1). Muscle glycogen content was maintained at its basal value in response to 5 min of muscular

contraction with the sole exception of THP pre-treated soleus muscle, where the glycogen content was halved (P<0.05, Table 1).

Resting muscle lactate concentration was no different between treatment groups at rest in EDL and soleus muscles and in response to contraction (Table 1). Muscle lactate content was maintained at its basal value in response to 5 min of muscular contraction with the sole exception of CON pre-treated EDL muscle, where lactate was significantly elevated. (P<0.05, Table 1).

Resting muscle citrate concentration was unaltered at rest in soleus muscle, yet was higher than the CON group at rest following THP pre-treatment in EDL skeletal muscle (P<0.05; Table 1).

Table 1: Muscle metabolite concentrations in rodent extensor digitorum longus (EDL) and soleus (SOL) muscles at rest and following 5 min of electrically-induced contraction (Cont) in control (CON) and N-trimethyl–hydrazine-3-propionate (THP) pre-treated muscles

		EDL (Rest)	EDL (Cont)	SOL (Rest)	SOL (Cont)
[ATP]	**CON**	29.0 ± 3.8	21.8 ± 3.6	24.8 ± 4.2	21.7 ± 1.9
	THP	31.5 ± 4.2	18.7 ± 4.0†	25.1 ± 2.8	21.3 ± 1.6
[PCr]	**CON**	33.3 ± 5.5	11.6 ± 2.5†	19.3 ± 5.1	4.2 ± 3.3†
	THP	39.5 ± 9.0	9.0 ± 1.9†	16.7 ± 3.7	5.6 ± 0.8†
[Creatine]	**CON**	151 ± 6	157 ± 10	142 ± 7	131 ± 4
	THP	144 ± 11	157 ± 11	139 ± 5	129 ± 5
[Total-Creatine]	**CON**	184 ± 6	169 ± 10	161 ± 9	135 ± 6†
	THP	183 ± 7	166 ± 10	155 ± 4	134 ± 5†
[Lactate]	**CON**	41 ± 7	63 ± 6†	46 ± 9	50 ± 5
	THP	49 ± 15	70 ± 7	46 ± 10	48 ± 3
[Glycogen]	**CON**	47 ± 5	50 ± 4	51 ± 6	50 ± 5
	THP	46 ± 10	22 ± 8*†	39 ± 10	44 ± 8
[Citrate]	**CON**	0.25 ± 0.04	n/a	0.29 ± 0.07	n/a
	THP	0.52 ± 0.06*	n/a	0.35 ± 0.06	n/a

*All values are expressed as means ± S.E.M. ATP, PCr, creatine, total-creatine, lactate and citrate are expressed as mmol kg^{-1} dry muscle, (each n = 8). Glycogen expressed as mmol glycosyl units kg^{-1} dry muscle. * Different from CON (P<0.05); † different from rest within the same group (P<0.05).*

14.2.4.6. Pyruvate dehydrogenase complex activation

No differences in PDC activation status existed between CON and THP treatment groups at rest or in response to electrical stimulation in either the soleus or EDL muscle groups (Fig. 5). PDC activation increased from basal following 5 min of contraction in THP and CON pre-treated EDL muscles and in CON treated soleus muscle (P<0.05, Fig. 5), however, no contraction-induced increase in PDC activation was observed in THP pre-treated soleus muscle (Fig. 5). Indeed, the magnitude of PDC activation, from basal to the cessation of contraction, was reduced by 63% in THP treated soleus muscle when compared to the corresponding CON value (CON 0-5 min = 0.72 ± 0.20 vs. THP 0-5 min = 0.26 ± 0.15 mmol acetyl-CoA min^{-1} kg^{-1} wet muscle @ 37^{O}C; P<0.05). No difference in the magnitude of PDC activation in response to contraction was observed between treatment groups in the EDL muscles (Fig. 5).

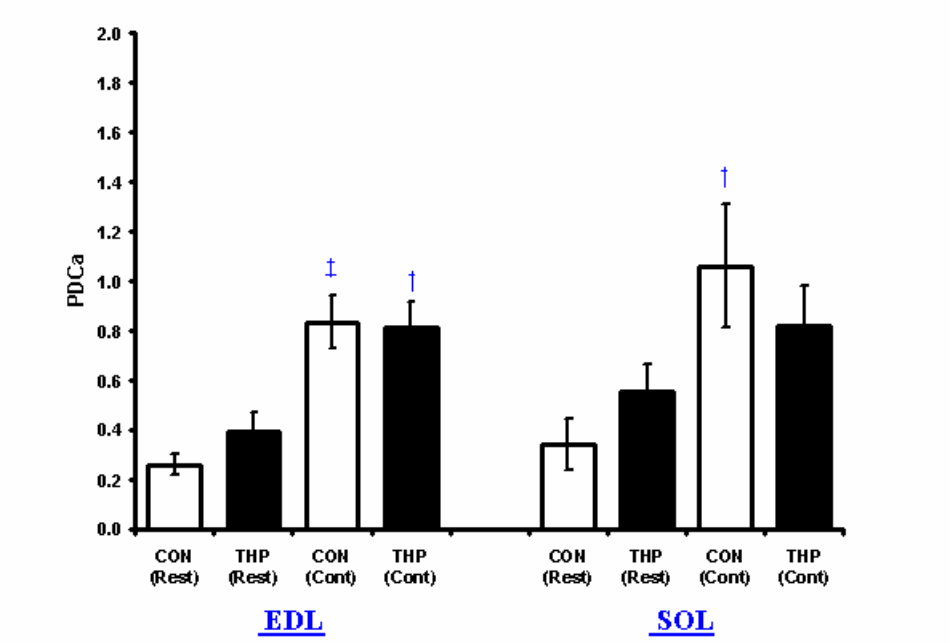

Figure 5: Pyruvate Dehydrogenase Complex activation (PDCa) in rodent extensor digitorum longus (EDL) and soleus (SOL) muscles at rest and following 5 min of electrically induced contraction (Cont) in control (CON) and N-trimethyl–hydrazine-3-propionate (THP) pre-treated muscles. Results are expressed as means ± S.E.M. with units of mmol acetyl-CoA min^{-1} kg^{-1} wet muscle @ $37^{O}C$ * Different from CON ($P<0.05$); † different from rest within the same group ($P<0.05$).

14.2.4.7. Muscular contractile properties

No differences in resting tension existed between CON and THP treatment groups in either EDL (CON = 736 ± 108 vs. THP = 723 ± 98 g tension $100g^{-1}$ wet muscle) or soleus muscles (CON = 824 ± 98 vs. THP = 830 ± 100 g tension $100g^{-1}$ wet muscle).

Peak isometric tension was reduced by 48% in the EDL muscle following THP pre-treatment when compared to CON and remained significantly lower throughout contraction ($P<0.01$, Fig. 6A). Despite this difference in peak tension, no difference in the rate of fatigue development existed between treatment groups, which fell from peak tension by 29% and 39% in the CON and THP groups respectively following 5 min of contraction (Fig. 6A).

No difference in soleus peak isometric tension development existed between CON and THP pre-treated muscles (Fig. 6B). Similarly, no difference in the rate of fatigue development existed between treatment groups, which fell from peak tension by 33% and 38% in the CON and THP groups respectively following 5 min of contraction (Fig. 6B).

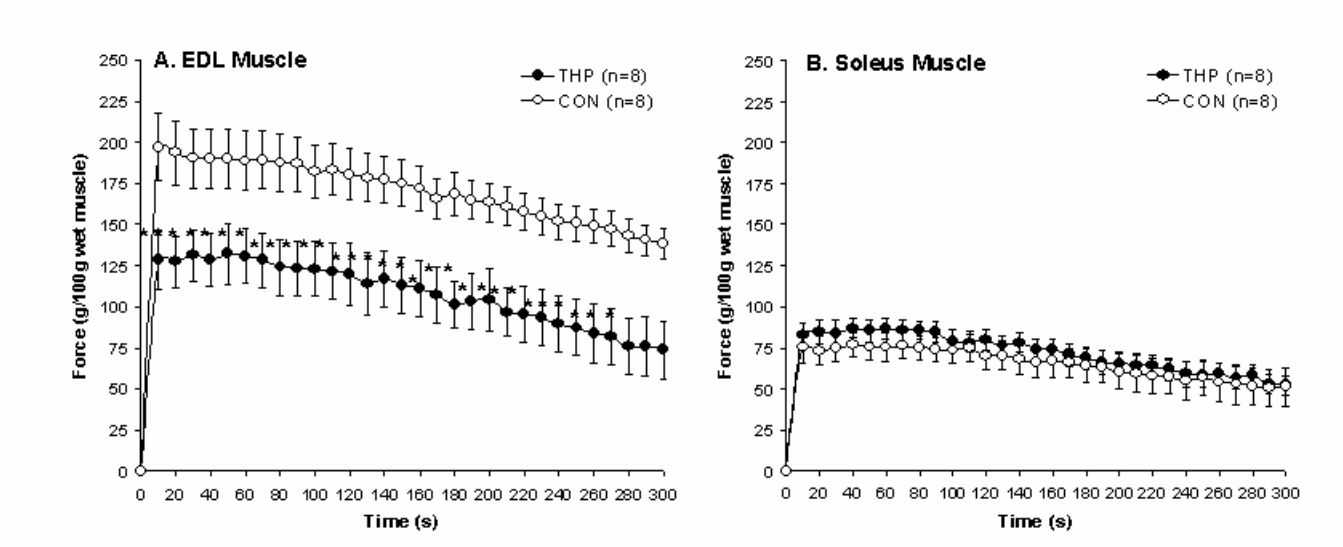

Figure 6: Isometric tension production & fatigue development in tendon-to-tendon excised rodent extensor digitorum longus (EDL; A) & soleus muscles (B) during 5 min of electrically induced contraction in the presence (CON) and absence of 3 weeks of N-trimethyl–hydrazine-3-propionate (THP) treatment. Results are expressed as means ± S.E.M. with units of g of tension per 100g of wet muscle @ 37^{O}C. * Different from CON (P<0.05).

14.2.5. Discussion

This is the first study to examine the consequences of carnitine depletion upon the metabolic and contractile characteristics of predominantly slow- and fast-twitch skeletal muscles from otherwise healthy rats. Twenty-one days of THP treatment, a competitive inhibitor of carnitine biosynthesis and re-uptake by the kidney, reduced the total-carnitine pool to the same extent in both soleus and EDL muscles from that measured in control animals (~80%; P<0.01) and to a level comparable to that reported in JVS mice (Higashi *et al.* 2001) and in human sufferers of carnitine-deficiencies (Shapira *et al*. 1993). The THP-induced leaching of carnitine was associated with a marked atrophy (-30%; P<0.05) and a reduced magnitude of pyruvate dehydrogenase complex (PDC) activation during subsequent contraction (-63%; P<0.05) in soleus muscle whilst contractile function, total-coenzyme A and water content remained unaltered from control treated soleus muscle. In contrast, carnitine depletion was associated with impaired peak tension development (-48%, P<0.05), ATP homeostasis (-40%, P<0.05), a reduction in free-coenzyme A availability (-25%, P<0.05) and increased glycogen hydrolysis (55%, P<0.05) during contraction in EDL muscle whilst PDC activation, muscle weight and water content remained unaltered from control treated muscle.

14.2.5.1. Contractile function

At present very little is known in the literature regarding carnitine's effect upon the contractile properties of skeletal muscle; especially with regard to peak tension development and towards the maintenance of contractile function. Work by Brass *et al*. (1993) examining the contractile properties of soleus and EDL muscle strips *in vitro* documented an improved maintenance of contractile function throughout 5 mins of electrical stimulation when soleus was incubated in a media rich in carnitine, when compared to control muscles (Brass *et al*. 1993). However, no carnitine-mediated improvements in contractile function were observed from control in EDL muscle. Based on these findings, carnitine depletion could be expected to increase the fatigue index of the musculature (soleus in particular) by virtue of the reduced ability to transport lipids across the mitochondrial membrane and buffer excess acetyl-CoA generated through carbohydrate oxidation. However, peak tension and the decline in contractile function during 5 min of electrical stimulation of soleus muscle in vitro was unaffected by 21 days of THP pre-treatment when compared to CON in the present study (Fig. 6B). The absence of any THP-induced impairment in function could be due to the intensity and duration of stimulation. Given that no elevation in acetylcarnitine content was observed in THP & CON soleus from rest in response

to contraction, it appears that acetyl-CoA delivery through the carbohydrate oxidising pathways closely matched the demands of the TCA cycle for this oxidative substrate. Therefore, carnitine's ability to buffer excess acetyl-CoA was not sufficiently tested using the current intensity of contraction, which was likely too low (<65% maximal oxygen uptake; Roberts *et al.* 2002*)* to test the functional role of the carnitine pool in this regard. Furthermore, given the slow onset of lipid derived energy production upon the initiation of contraction, it is likely that the duration of stimulation was too brief to view differences in ATP generation via this route and its effect upon contractile function. Interestingly, peak isometric tension production was reduced in EDL muscle in response to THP pre-treatment, although the maintenance of peak tension was identical to that observed in the CON treatment (Fig. 6A). As discussed later in this discussion, this was most likely due to the reduced availability of free-CoASH to stimulate oxidative ATP synthesis and due to a reduced total-CoASH content in response to THP pre-treatment.

14.2.5.2. Integration of fat & carbohydrate metabolism

Based upon their findings in alloxan diabetic rats, Philip Randle and co-workers first described a mechanism for the integration and regulation of carbohydrate and lipid metabolism; which they termed the glucose-fatty acid cycle (GFC; Randle et al. 1963; Randle, 1986). Central to the operation of this cycle is the activation status of the pyruvate dehydrogenase complex (PDC), which catalyses the irreversible reaction that commits the glycolytic product pyruvate to its oxidative fate inside the mitochondrion and hence controls the overall rate of carbohydrate oxidation (Randle, 1986). When the availability and utilisation of fat is increased a restriction upon the oxidation of the limited intramuscular stores of carbohydrates is put in place. Rising acetyl / acyl-CoA to free-CoASH and NADH to NAD^+ ratios, resulting from the β-oxidation of lipid reserves, feeds back to inhibit the transformation of the PDC to its active (dephosphorylated) form, leading to the accumulation of the tricarboxylic acid cycle intermediate citrate; a known inhibitor of the glycolytic flux controlling enzyme phosphofructokinase (Cooper *et al.* 1975, Hansford & Cohen, 1978, Hansford *et al.* 1990). Decreased flux through phosphofructokinase leads to an upstream accumulation of glucose-6-phosphate in the glycolytic pathway, which in turn inhibits hexokinase activity restricting further glucose uptake by the cell and thereby glycogen hydrolysis. Essential to the operation of this metabolic cycle is that the reverse should also be possible. Therefore, a THP-induced reduction in carnitine and thereby, lipid derived acetyl-CoA generation, should shift intermediary metabolism towards the more favourable oxidation of carbohydrates (i.e. greatest amount of ATP per unit of oxygen).

THP pre-treatment markedly reduced carnitine content in the soleus muscle (Fig. 3A-C) and achieved this independent of any alteration in composition of the coenzyme A pool at rest (Fig. 4A-D). In accordance with the operation of the GFC, the similar acetyl-CoA to free-CoASH ratio resulted in no alteration in PDC activation (Fig. 5), the concentration of citrate and glycogen content from CON muscle at rest (Table 1). Therefore, it would appear that carnitine deficiency did not impinge upon the integration of fat and carbohydrate metabolism in the predominantly slow-twitch soleus muscle. Despite these similarities, there was a marked reduction in the magnitude of PDC activation in response to contraction in THP pre-treated soleus muscle when compared to CON (Fig. 5). Although activation is a pre-requisite for an increase in flux through the PDC, flux is further controlled by the availability of various reaction substrates and products as well as numerous co-factors (Wieland, 1983).

Similarly to soleus muscle, THP pre-treatment reduced the carnitine content in EDL muscle (Fig. 3A-D). However, in contrast to soleus, the acetyl-CoA to free-CoASH ratio was increased (Fig. 4D) and the concentration of free-CoASH, a key substrate for the PDC reaction, was lowered when compared to CON muscle (Fig. 4C). Despite these differences in free-CoASH availability in EDL muscle, no difference in PDC activation existed between groups at rest, yet the concentration of citrate was elevated in THP muscle when compared to CON (Table 1). This finding indicates that despite a similar degree of PDC activation, acetyl-CoA delivery via this enzyme complex (i.e. flux) was reduced in THP vs. CON muscle. This is most likely due to the availability of free-CoASH being limited in THP treated EDL muscle, thus reducing PDC flux (Fig. 4B). The selective decline in free-CoASH concentration in EDL vs. soleus muscle following 21 days of THP is a surprising observation that warrants further investigation. This is most likely attributable to an increased acetyl-CoA to free-CoASH ratio (Fig. 4D) in response to the decline in tissue carnitine content and a concomitant reduced ability of carnitine acyltransferase to buffer excess acetyl groups to maintain free-CoASH for sustained

PDC flux. An additional complication of an elevated acetyl-CoA to free-CoASH ratio is its effect upon pantothenate kinase, the master regulator of coenzyme A biosynthesis in mammalian cells (Robishaw & Neely, 1985). Evidence is emerging that acetyl-CoA and free-CoASH differentially regulate pantothenate kinase; with acetyl-CoA potently inhibiting activity, leading to a reduction in total-CoASH content (Fig. 4C), with free-CoASH stimulating coenzyme A biosynthesis (Rock *et al*. 2000). In conclusion, the integration of fat and carbohydrate metabolism is largely unaffected by THP pre-treatment in soleus muscle, however, this integration is lost in EDL muscle due to inhibitory pressures upon both fat and carbohydrate oxidation and coenzyme A synthesis.

Based upon the resting and post-contraction concentrations of ATP, PCr and muscle lactate (Table 1), and using the calculation of Spriet *et al*. (1987), we estimated the contribution of oxygen-independent ATP resynthesis towards the energy demands of contraction in THP vs. CON pre-treated soleus and EDL muscle (Oxygen-independent ATP provision = [Δ PCr + (1.5 x Δ lactate) + (2 x Δ ATP)]). No difference in oxygen-independent ATP resynthesis was observed between treatment groups in soleus muscle (CON = 27.8 $\pm$ 4.1 vs. THP = 22.2 $\pm$ 3.9 mmol ATP min^{-1} kg^{-1} dry muscle). Given that no difference in peak tension and the maintenance of contractile output existed between THP and CON groups in soleus muscle (i.e. similar ATP demand for contraction; Fig. 6B), it appears that the THP-induced carnitine deficiency did not affect oxidative metabolism within this muscle group, using the present stimulatory parameters. In contrast, there was a marked elevation in oxygen-independent ATP production in EDL muscle following THP pre-treatment when compared to CON (CON = 68.7 $\pm$ 5.2 vs. THP = 87.6 $\pm$ 6.0 mmol ATP min^{-1} kg^{-1} dry muscle, $P<0.05$). This increase is surprising, as peak tension development, area under the tension curve and therefore the ATP demand for contraction was markedly reduced in EDL muscle in response to THP treatment (Fig. 6A), implying that carnitine-deficiency interferes with oxidative (mitochondrial) ATP production in EDL muscle. This must be accountable to a THP-induced decline in flux through carbohydrate metabolism, most likely due to the reduced availability of free-coenzyme A for PDC flux (Fig. 4B).

14.2.5.3. Atrophy of the soleus muscle

Muscle atrophy refers to the wasting or loss of muscular tissue that occurs as a result of disuse or, in rare occasions, as a consequence of damage to the nerves that supply the muscle or from a disease of the muscle itself (Kandarian & Stevenson, 2002). In the present study, we observed a 30% reduction in the mass of the soleus muscle in response to THP treatment that was not observed in the corresponding EDL muscle. As the soleus muscle is predominantly composed of 84% slow-twitch fibres (Ariano et al. 1973) compared to the largely fast-twitch EDL muscle (Armstrong & Phelps, 1984), this finding would imply a selective type I fibre loss in response to carnitine-depletion. Given that THP treatment results in no alteration in rodent overnight activity (P. Kauffmann, unpublished observation), it would appear that the atrophy reported herein was not the result of disuse but resulted from an abnormality within the muscle itself. It is noteworthy that a type I atrophy has been reported in an 18 year old female with a secondary carnitine deficiency (Fukusako *et al*. 1995).

Programmed cell death, better termed apoptosis, is one of the major determinants of skeletal muscle atrophy (Dalla-Libera *et al*. 1999, Vescovo *et al*. 2000) and *in vitro* studies have demonstrated that L-carnitine can inhibit apoptosis at several levels and thus protect against cell death (Di Marzio, *et al*. 1997, Mutomba *et al*. 2000, Vescovo *et al*. 2002). By way of example, L-carnitine can interfere with Fas-ligand mediated apoptotic signalling, thereby reducing acid sphingomyelinase activity and the ability of ceremide to stimulate the pro-apoptotic Bax / Bad complexes (Di Marzio *et al*. 1997, Moretti *et al*. 1998). L-carnitine can inhibit caspases 3, 7 & 8 and the opening of the mitochondrial membrane permeability transition pore; which normally leads to apoptosis (Pastorino *et al*. 1993, Mutomba *et al*. 2000,). Finally, L-carnitine, through interaction with carnitine palmitoyltransferase 1 (CPT1), can stimulate the activity of the anti-apoptotic BCL2 / BCLX complex and dampen down pro-apoptotic signals (Pugazhenthi *et al*. 1999). Clearly hypocarnitinemia is likely to promote rather than suppress apoptosis. Further studies are required to understand the selective nature of apoptosis in type I vs. type II muscle fibres; which could be attributable to the higher mitochondrial content in the former and reduced carnitine-CPT1 interactions following THP treatment leading to reduced anti-apoptopic signalling (Pugazhenthi *et al*. 1999). It is worth noting that 24 weeks of L-carnitine administration has been shown to have a selective trophic effect upon type I muscle fibres in man (Giovenali *et al*. 1994).

Taken together, the findings of the present manuscript and of Giovenali *et al*. (1994) support a role for L-carnitine supplementation towards the reduction of aged-related muscle atrophy in man.

Recent evidence has shown that THP pre-treatment not only inhibits liver carnitine biosynthesis and reabsorption by the kidney but also leads to a increase in gamma-butyrobetaine concentration in the rat (Dambrova *et al*. 2002, Dambrova *et al*. 2004); which is logical given that THP competes against butyrobetaine as a substrate for the final reaction within carnitine biosynthesis (Fig. 1A). One consequence of butyrobetaine elevation is a transient increase in nitric oxide content in rat tissues (Dzintare *et al*. 2002), which akin to repeated exposure to an ischaemic / hypoxic environment, could lead to muscular adaptation *in vivo* (Dambrova *et al*. 2002). Another interesting finding is that the methylester of butyrobetaine, a major breakdown product of butyrobeatine, possesses dose-dependent acetylcholine like effects through muscarinic receptor binding (Dzintare *et al*. 2002). It is unknown if THP pre-treatment elevated gamma-butyrobetaine in the present study and whether the consequences of carnitine depletion reported herein are directly related to the leaching of carnitine *per se* or result from increased muscarinic receptor or nitric oxide synthase activity.

In conclusion, we have presented novel data demonstrating that a THP-induced carnitine-deficiency, in otherwise healthy skeletal muscle, results in a selective loss of soleus (type I) muscle fibres, whilst the biochemical and functional properties of the soleus muscle remained largely normal. Conversely, despite the preservation of EDL muscle mass, the biochemical and functional properties of this predominantly type II fibred muscle were impaired, with an increased reliance upon energy production from non-oxygen dependent routes when compared to control muscle. Based on this evidence, the muscle myopathy often associated with carnitine deficiency is most likely attributable to impaired mitochondrial energy production in type II muscle fibres.

14.2.6. References

ANDRIEU-ABADIE N, JAFFREZOU JP, HATEM S, LAURENT G, LEVADE T, MERCAIDER JJ. L-carnitine prevents doxorubicin-induced apoptosis of cardiac myocytes: role of inhibition of ceramide generation. *FASEB J* 13: 1501-1510.1999.

ARIANO, M. A., ARMSTRONG, R. B. & EDGERTON, V. R. (1973) Hindlimb muscle fiber populations of five mammals. *Journal of Histochemistry and Cytochemistry* 21, 51-55.

ARMSTRONG, R. B. & PHELPS, R. O. (1984) Muscle fiber type composition of the rat hindlimb. *American Journal of Anatomy* 171, 259-272.

BRASS, E. P. & HOPPEL, C. L. (1980). Relationship between acid-soluble carnitine and coenzyme A pools in vivo. *Biochemical Journal* 190, 495-504.

BRASS, E. P. (1995). Pharmacokinetic considerations for the therapeutic use of carnitine in hemodialysis patients. *Clinical Therapeutics* 17, 176-185.

BRASS, E. P., SCARROW, A. M., RUFF, L. J., MASTERSON, K. A. & VAN LUNTEREN, E. (1993). Carnitine delays rat skeletal muscle fatigue in vitro. *American Journal of Physiology* 75, 1595-1600.

BREMER, J. (1983). Carnitine – metabolism and functions. *Physiological Reviews* 63, 1421-1466.

BROOKS, H. & KRÄHENBÜHL, S. (2001) Identification and tissue distribution of two differentially spliced variants of the rat carnitine transporter OCTN2. *FEBS* 508, 175-180.

CONSTANTIN-TEODOSIU, D., CARLIN, J. I., CEDERBLAD, G. HARRIS, R. C. & HULTMAN, E. (1991). Acetyl group accumulation and pyruvate dehydrogenase activity in human muscle during incremental exercise. *Acta Physiologica Scandinavica* 143, 367-372.

COOPER, R. H., RANDLE, P. J. & DENTON, R. M. (1975). Stimulation of phosphorylation and inactivation of pyruvate dehydrogenase by physiological inhibitors of the pyruvate dehydrogenase reaction. *Nature* 257, 808-809.

DAMBROVA, M., LIEPINSH, E. & KALVINSH, I. (2002) Mildronate: cardioprotective action through carnitine-lowering effect. *Trends in Cardiovascular Medicine* 12, 275-279.

DAMBROVA, M., CHLOPICKI, S., LIEPINSH, E., KIRJANOVA, O., GORSHKOVA, O., KOZLOVSKI, V. I., UHLEN, S., LIEPINA, I., PETROVSKA, R. & KALVINSH, I. (2004) The methylester of γ-butyrobetaine, but not γ-butyrobetaine itself, induces muscarinic receptor-dependent vasodilatation. *Archives of Pharmacology* 369, 533-539.

DI MARZIO, L., ALESSE, E. & RONCAIOLI, P. (1997) Influence of L-carnitine on CD95 cross-lining-induced apoptosis and ceramide generation in human cell lines: correlation with its effects on purified acidic and neutral sphingomyelinases in vitro. *Proc. Assoc. Am. Phys.* 109, 154-163.

ENGEL, A. G. & ANGELINI, C. (1973) Carnitine deficiency of human muscle with associated lipid storage myopathy: a new syndrome. *Science* 179, 899-902.

EREMEEV, A., KALVINSH, I. & SEMENIKHINA, V. (1984). 3-(2,2,2-Tri-methylhydrazinium) propionate and method for the preparation and use thereof. *US patent 4481218.*

FRITZ, I. (1955). The effects of muscle extracts on the oxidation of palmitic acid by liver slices and homogenates. *Acta Physiologica Scandinavia* 34, 367-385.

FUKUSAKO, T., NEGORO, K., TSUDA, N., KATO, M. & MORIMATSU, M. (1995) A case of secondary carnitine deficiency due to anorexia nervosa and severe liver damage. *Rinsho Shinkeigaku* 35, 34-37.

GIOVENALI, P., FENOCCHIO, D., MONTANARI, G., CANCELLOTTI, C., D'IDDIO, S., BUONCRISTIANI, U., PELAGAGGIA, M. & RIBACCHI, R. (1994). Selective trophic effect of L-carnitine in type I and IIa skeletal muscle fibers. *Kidney International* 46, 1616-1619.

GULEWITSCH, W. K. R. & KRIMBERG, R. (1905). Zur Kenntnis der Extraktionsstoffe der Muskeln. 2. Mitteilung über das Carnitin. *Hoppe-Seyler's Z Physiol Chem*. 45, 326–330.

HANSFORD, R. G. & COHEN, L. (1978). Relative importance of pyruvate dehydrogenase interconversion and feed-back inhibition in the effect of fatty acids on pyruvate oxidation by rat heart mitochondria. *Archives of Biochemistry and Biophysics* 191, 65-81.

HANSFORD, R., HOGUE, G., PROKOPCZUK, B., WASILEWSKA, A. & LEWARTOWSKI, B. (1990). Activation of pyruvate dehydrogenase by electrical stimulation and low Na+ perfusion of guinea pig heart. *Biochemica Biophysica Acta*. 1018, 282-286.

HARRIS, R. C., HULTMAN, E. & NORDESJÖ, L. O. (1974). Glycogen, glycolytic intermediates and high energy phosphates determined in biopsy samples of musculus femoris of man at rest. Methods in variance values. *Scandinavian Journal of Clinical and Laboratory Investigation* 33, 109-120.

HEINONEN, O. J. & TAKALA, J. (1994) Moderate carnitine depletion and long-chain fatty acid oxidation, exercise capacity, and nitrogen balance in the rat. *Paediatric Research* 36, 288-292.

HIGASHI, Y., YOKOGAWA, K., TAKEUCHI, N., TAMAI, I., NOMURA, M., HASHIMOTO, N., HAYAKAWA, J.- I, MIYAMOTO, K.- I. & TSUJI, A. (2001). Effect of γ-butyrobetaine on fatty liver in juvenile visceral steatosis mice. *Journal of Pharmacology & Physiology* 53, 527-533.

HORIUCHI, M., KOBAYASHI, K., YAMAGUCHI, S., SHIMIZU, N., KOIZUMI, T., NIKAIDO, H., HAYAKAWA, J., KUWAJIMA, M. & SAHEKI, T. (1994). Primary defect of juvenile visceral steatosis (jvs) mouse with systemic carnitine deficiency is probably in renal carnitine transport system. *Biochem Biophys Acta* 1226, 25-30.

KANDARIAN, S. C. & STEVENSON, E. J. (2002) Molecular events in skeletal muscle during disuse atrophy. *Exercise & Sport Sciences Review.* 30, 111-116.

KOIZUMI, T., NIKAIDO, H., HAYAKAWA, J., NONOMURA, A. & YONEDA T (1988). Infantile disease with microvesicular fatty infiltration of viscera spontaneously occurring in the C3H-H-2(0) strain of mouse with similarities to Reye's syndrome. *Lab. Anim.* 22, 83-87.

KUWAJIMA, M., HORIUCHI, M., HARASHIMA, H., LU, K., HAYASHI, M., SEI, M., OZAKI, K., KUDO, T., KAMIDO, H., ONO, A., SAHEKI, T. & SHIMA K (1999). Cardiomegaly in the juvenile visceral steatosis (JVS) mouse is reduced with acute elevation of heart short-chain acyl-carnitine level after L-carnitine injection. *FEBS Letters* 443, 261-266.

KUWAJIMA, M., KONO, N., HORIUCHI, M., IMAMURA, Y., ONO, A., INUI, Y., KAWATA, S., KOIZUMI, T., HAYAKAWA, J., SAHEKI, T. & TARUI, S. (1991) Animal model of systemic carnitine deficiency: analysis in C3H-H-2 degrees strain of mouse associated with juvenile visceral steatosis. *Biochem Biophys Res Commun* 173, 1090-1094.

LIBERA, L. D., ZENNARO, R., SANDRI, M., AMBROSIO, G. B. & VESCOVO,G. (1999) Apoptosis and atrophy in rat slow skeletal muscles in chronic heart failure. *American Journal of Physiology* 277, C982-C986.

LOMBARD, K. A., OLSEN, A. L., NELSON, S. E. & REBOUCHE, C. J. (1989) Carnitine status of lactoovegetarians and strict vegetarian adults and children. *American Journal of Clinical Nutrition* 50, 301-306.

MITCHELL, M. E. (1978) Carnitine metabolism in human subjects. I. Normal metabolism. *American Journal of Clinical Nutrition* 31, 293-306.

MOELLERING, H. & GRUBER, G. (1966) Determination of citrate with citrate lyase. *Analytical Biochemistry* 17, 369-376.

MORETTI, S., ALESSE, E., DI MARZIO, L., ZAZZERONI, F., RUGGERI, B., MARCELLINI, S., FAMULARO, G., STEINBERG, S. M., BOSCHINI, A., CIFONE, M. G. & DE SIMONE, C. (1998) Effect of L-carnitine on

human immunodeficiency virus-1 infection-associated apoptosis: a pilot study. *Blood* 242, 3817-3824.

MUTOMBA, M. C., YUAN, H., KONYAVKO, M., ADACHI, S., YOKOYAMA, C. B., ESSER, V., MCGARRY, J. D., BABIOR, B. M. & GOTTLIEB, R. A. (2000). Regulation of the activity of caspases by L-carnitine and palmitoylcarnitine. *FEBS Letters* 478, 19-25.

PASSONEAU, J. V. & LOWRY, O. H. (1993) Enzymatic Analysis: a Practical Guide. Humana Press, Totowa, NJ, USA.

PASTORINO, J. G., SNYDER, J. W., SERRONI, A., HOEK, J. B. & FARBER, J. L. (1993) Cyclosporin and carnitine prevent the anoxic death of cultured hepatocytes by inhibiting the mitochondrial permeability transition. *The Journal of Biological Chemistry* 268, 13791-13798.

PELUSO, G., BARBARISI, A., SAVICA, V., REDA, E., NICOLAI, R., BENATTI, P. & CALVANI, M. (2000). Carnitine: an osmolyte that plays a metabolic role. *Journal of Cellular Biochemistry* 80, 1-10.

PUGAZHENTHI, S., MILLER, E., SABLE, C., YOUNG, P., HEIDENREICH, K. A., BOXER, L. M. & REUSCH, J. E. (1999) Insulin-like growth factor-I induces bcl-2 promoter through the transcription factor cAMP-response element-binding protein. *The Journal of Biological Chemistry* 274, 27529-27535.

RANDLE, P. J. (1986). Fuel selection in animals. *Biochemical Society Transactions* 14, 799-806.

RANDLE, P. J., GARLAND, P. B., HALES, C. N. & NEWSHOLME, E. A. (1963). The glucose fatty acid cycle; its role in insulin sensitivity and the metabolic disturbances of diabetes mellitus. *Lancet* 1, 785-789.

REBOUCHE, C. J. & ENGEL, A. G. (1980). Tissue distribution of carnitine biosynthetic enzymes in man. *Biochem Biophys Acta* 630, 22-29.

REBOUCHE, C. J. (1982) Sites and regulation of carnitine biosynthesis in mammals. *Fed. Proc.* 41, 2848-2852.

ROBERTS, P. A., LOXHAM, S. J. G., POUCHER, S. M., CONSTANTIN-TEODOSIU, D. & GREENHAFF, P. L. (2002). The acetyl group deficit at the onset of contraction in ischaemic canine skeletal muscle. *Journal of Physiology* 544, 591-602.

ROBISHAW, J. D. & NEELEY, J. R. (1985). Coenzyme A metabolism. *American Journal of Physiology* 248, E1-E9.

ROCK, C. O., CALDER, R. B., KARIM, M. A. & JACKOWSKI, S. (2000). Pantothenate kinase regulation of the intracellular concentration of coenzyme A. *The Journal of Biological Chemistry* 275, 1377-1383.

SEKINE, T., KUSUHARA, H., UTSUNOMIYA-TATE, N., TSUDA, M., SUGIYAMA, Y., KANAI, Y. & ENDOU, H. (1998) Molecular cloning and characterisation of high-affinity carnitine transport from rat intestine. *Biochemical & Biophysical Research Communications* 251, 586-591.

SHAPIRA, Y., GLICK, B., HAREL, S., VATTIN, J. J. & GUTMAN, A. (1993) Infantile idiopathic myopathic carnitine deficiency: treatment with L-carnitine. *Paediatric Neurology* 9, 35-38.

SIMKHOVICH, B. Z., SHUTENKO, Z. V., MEIRENA, D. V., KHAGI, K. B., MEZAPUKE, R. J., MOLODCHINA, T. N., KALVINS, I. J. & LUKEVICS, E. (1988). 3-(2,2,2-trimethylhydrazinium) propionate (THP): a novel gamma-butyrobetaine hydroxylase inhibitor with cardio-protective properties. *Biochem Pharmacol* 37, 195-202.

SPANIOL, M., BROOKS, H., AUER, L., ZIMMERMANN, A., SOLIOZ, M., STIEGER, B. & KRÄHENBÜHL, S. (2001). Development and characterisation of an animal model of carnitine deficiency. *European Journal of Biochemistry* 268, 1876-1887.

SPANIOL, M., KAUFMANN, P., BEIER, K., WÜTHRICH, J., TÖRÖK, M., SCHARNAGL, H., MÄRZ, W. & KRÄHENBÜHL, S. (2003). Mechanisms of liver steatosis in rats with systemic carnitine deficiency due to treatment with trimethylhydraziniumpropionate. *Journal of Lipid Research* 44, 144-153.

SPRIET, L. L., SÖDERLUND, K., BERGSTRÖM, M. & HULTMAN, E. (1987). Anaerobic energy release in skeletal muscle during electrical stimulation in man. *Journal of Applied Physiology* 62, 611-615.

TAMAI, I., OHASHI, R., NEZU, J., YABUUCHI, H., OKU, A., SHIMANE, M., SAI, Y. & TSUJI, A. (1998) Molecular and functional identification of sodium ion-dependent, high affinity human carnitine transporter OCTN2. *The Journal of Biological Chemistry* 273, 20378-20382.

TSOKO, M., BEAUSEIGNEUR, F., GRESTI, J., NIOT, I., DEMARQUOY, J., BOICHET, J., BEZARD, J., ROCHETTE, L. & CLOUET, P. (1995) Enhancement of activities relative to fatty acid oxidation in the liver of rats depleted of L-carnitine by D-carnitine and a gamma-butyrobetaine inhibitor. *Biochem. Pharmacol.* 49, 1403-1410.

VESCOVO, G., RAVARA, B., GOBBO, V. M, ANGELINI, A., DELLA BARBERA, M., DONA, M., PELUSO, G., CALVANI, M., MOSCONI, L. & DALLA LIBERA, L. (2002). L-carnitine: a potential treatment for blocking apoptosis and preventing skeletal muscle myopathy in heart failure. *American Journal of Physiology* 283, C802-C810.

VESCOVO, G., VOLTERRANI, M., ZENNARO, R., SANDRI, M., CECONI, C., LORUSSO, R., FERRARI, R., AMBROSIO, G. B., DALLA LIBERA, L. (2000) Apoptosis in the skeletal muscle of patients with heart failure: investigation of clinical and biochemical changes. *Heart* 84, 431-437.

WIELAND, O. H. (1983). The mammalian pyruvate dehydrogenase complex: structure and regulation. *Rev Physiol Biochem Pharmacol* 96, 124-170.

WU, X., HUANG, W., PRASAD, P. D., SETH, P., RAJAN, D. P., LEIBACH, F. H., CHEN, J., CONWAY, S. J. & GANAPATHY, V. (1999) Functional characteristics and tissue distribution pattern of organic cation transporter 2 (OCTN2), an organic cation / carnitine transporter. *Journal of Pharmacological & Experimental Therapeutics* 290, 1482-1492.

ZAUGG, C. E., SPANIOL, M., KAUFMANN, P., BELLAHCENE, M., BARBOSA, V., TOLNAY, M., BUSER, P. T. & KRÄHENBÜHL, S. (2003) Myocardial function and energy metabolism in carnitine-deficient rats. *Cellular & Molecular Life Sciences* 60, 767-775.

Acknowledgements

We wish to express our appreciation to Lonza Group, Basel, Switzerland; especially towards Miss Ulla Held & Dr Paula Gaynor, for supporting this research. The authors would also like to thank Dr Michael Török for his kind assistance whilst commencing the animal studies.

14.3. Veno-occlusive disease associated with immuosuppressive cylophosphamide and roxithromycin

J. Beltinger[1], P. Kaufmann[2,3], M. Michot[4], L. Terracciano[5], S. Krähenbühl[2]

Divisions of Gastroenterology[1], Clinical Pharmacology & Toxicology[2] and Medical Intensive Care Unit[4], and Departments of Research[3] and of Pathology[5], University Hospital, Basel, Switzerland

J Hepatol 2004, submitted

14.3.1. Summary

Cyclophosphamide is a well known cause of hepatic veno-occlusive disease when used at high doses (>500 mg/m2) for bone marrow eradication before transplantation. At immunosuppressive doses (≤2 mg/kg) this adverse effect has so far not been reported.

We observed a patient with autoimmune haemolytic anemia who developed hepatic veno-occlusive disease while being treated with immunosuppressive cyclophosphamide in combination with roxithromycin. After stopping all drugs, the patient recovered within 2 weeks.

Since roxithromycin inhibits cytochrome P450 3A4, which is involved cyclophosphamide metabolism, a drug-drug interaction could have been responsible. In addition, roxithromycin is an inhibitor of the drug transporter P-glycoprotein, possibly leading to accumulation of cyclophosphamide in endothelial cells. Since cyclophosphamide has been described to induce apoptosis, roxithromycin could have rendered endothelial cells more vulnerable for apoptosis.

14.3.2. Introduction

Cyclophosphamide can cause hepatic veno-occlusive disease in patients treated with high doses (≥500 mg/m^2) for bone marrow eradication before transplantation (1). In contrast, at immunosuppressive doses (1-2 mg/kg), this adverse reaction has not been described. We describe a patient with autoimmune hemolytic anemia, who developed veno-occlusive disease while being treated with immunosuppressive doses of cyclophosphamide combined with roxithromycin.

14.3.3. Case report

This 66 years-old lady had a history of diabetes mellitus type 2, arterial hypertension and pulmonary embolism, and was treated with insulin, enalapril and oral anticoagulation with phenprocoumon for more than two years. Two years before the actual presentation, she had been diagnosed for idiopathic autoimmune hemolytic anemia. She was treated successfully with prednisone, until she developed another hemolytic episode after one year. After splenectomy, she recovered rapidly and could again be treated successfully with 20 mg prednisone per day. One year later (two months before the actual illness), she presented with cholestasis, and endoscopic retrograde pancreatico-cholangiography (ERCP) revealed sludge in the extrahepatic bile duct. After papillotomy, she recovered completely within the following 2 weeks. Two months later, she developed fever and cough and consulted a general practitioner. Despite negative chest radiographs, he started a treatment with oral roxithromycin (2 x 300 mg per day). Two days later, she got jaundiced without having symptoms or signs of cholestasis. The local hematologist interpreted this episode as a flair-up of autoimmune hemolytic anemia. Prednisone was stopped and oral cyclophosphamide (100 mg per day) was started, while roxythromycin was continued. Four days later, jaundice was progressive and she complained of breathlessness and pain in the right upper quadrant of the abdomen, leading to admission to the University Hospital of Basel.

On admission, she was deeply jaundiced, had a normal blood pressure and a heart rate of 100 per minute. Lungs and heart were clear and the abdomen was soft with normal bowel sounds, but the right upper quadrant was painful upon palpation. Clinically, there was no ascites and there were no edema. Her hemoglobin level was 41 g/L and the leukocyte count slightly elevated due to the presence of erythroblasts. The serum bilirubin concentration was 198 μmol/L, ASAT 2253 U/L (normal range 11 - 37 U/L), ALAT 847 U/L (16 - 37 U/L), GGT 120 U/L (8 – 49 U/L) and alkaline phosphatase 168 U/L (31 – 108 U/L). Her factor V concentration was 78% of normal (70 – 120%). Viral serologies (HAV, HBV, HCV, EBV, CMV, herpes simplex) and auto-antibodies (anti-nuclear, anti-smooth muscle, anti-microsomal) were negative. Upper gastrointestinal endoscopy did not show intestinal bleeding and an ultrasound of the liver did not reveal any signs of extrahepatic cholestasis but showed impaired portal blood flow and some ascites around the liver. The diagnosis of an acute hemolytic crisis was confirmed. The administration of roxithromycin, enalapril and phenprocoumon was stopped and a treatment with 100 mg prednisone per day was started in addition to cyclophosphamide. After the transfusion of packed erythrocytes, her hemoglobin level remained stable at 90 g/L. In order to clarify the reason for the hepatopathy, a transjugular liver biopsy was performed the next day. As shown in the Figure, the histology revealed veno-occlusive disease with some necrosis of hepatocytes in the

centroacinar region, explaining elevated transaminases. After stopping cyclophosphamide, the patient started to recover. When she left the hospital 11 days after entry, transaminases and bilirubin levels were only slightly elevated, and ultrasound and Doppler examinations of the liver were normal. Three weeks later, all liver values had completely normalized and the patient was well.

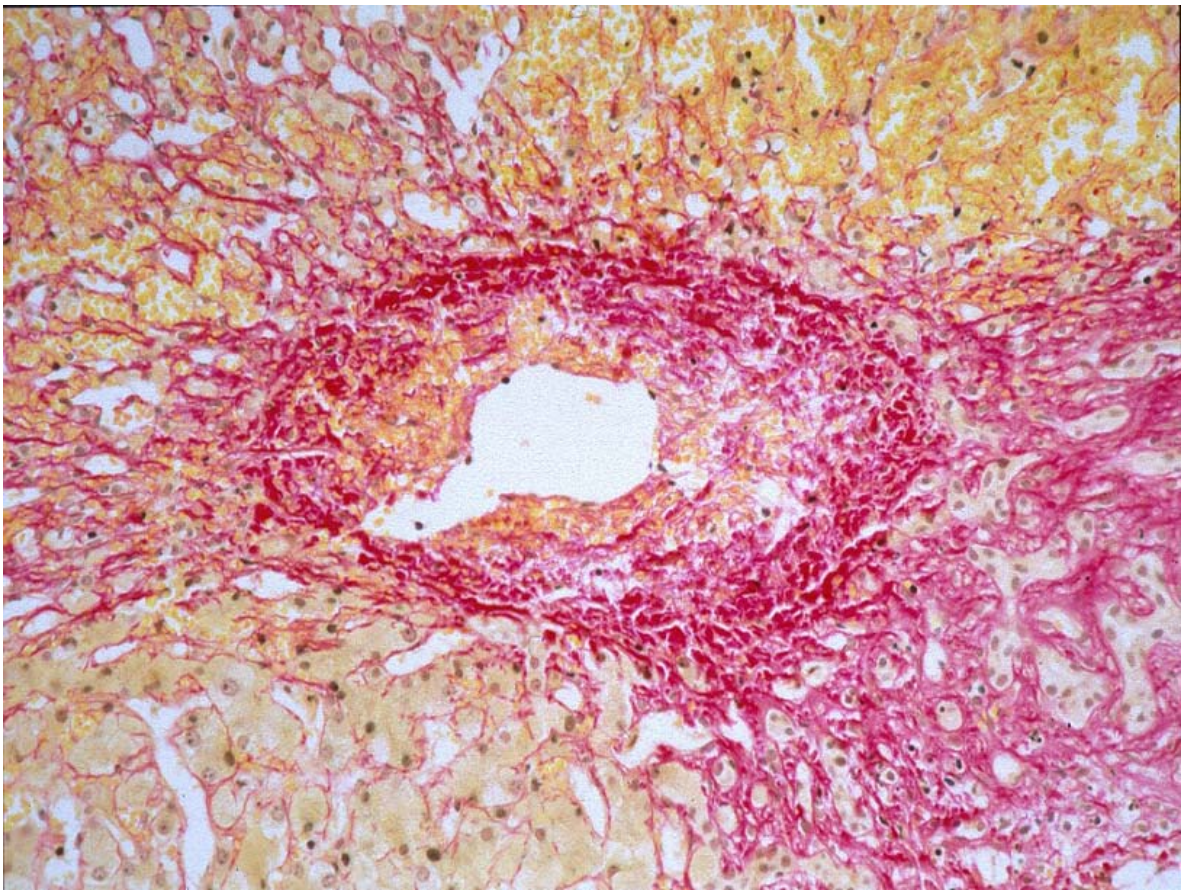

Figure: The central vein in the center of the figure (arrow) shows proliferation of the intima. In the centroacinar region, liver sinusoids are dilated and contain deposits of fibrin. There is necrosis of hepatocytes in the centroacinar region.

14.3.4. Discussion

While high doses of cyclophosphamide, in particular in combination with busulfan for bone marrow eradication, are well known to be associated with hepatic veno-occlusive disease (1), this has so far not been described for immunosuppressive doses of cyclophosphamide. For the other drugs the patient was treated with (enalapril, prednisone, roxithromycin, phenprocoumon and insulin), hepatic veno-occlusive disease has not been described so far. Cyclophosphamide is therefore the most likely offender of veno-occlusive disease in this patient, although it was used at an immunosuppressive dosage. The toxicity of cyclophosphamide may have been enhanced by another drug, most probably by roxithromycin. Roxithromycin is a macrolide antibiotic and is an inhibitor of cytochrome P450 (CYP)3A4 (2), which is partially responsible for the metabolism of cyclophosphamide. By CYP3A4, cyclophosphamide can be N-dealkylated and thereby degraded to N-dechloroethyl- cyclophosphamide and chloroacetaldehyde (3). On the other hand, CYP3A4 and CYP2B6 catalyze the oxidation of cyclophosphamide to phosphoramine mustard and acrolein, which are the active metabolites, but are also toxic (4). Selective inhibition of CYP3A4 may therefore be associated with increased formation of phosphoramine mustard and acrolein in hepatocytes, possibly leading to damage also in the adjacent endothelial cells.

Since inhibitors of CYP3A4 are usually also inhibitors of P-glycoprotein, a transporter of many substances including antineoplastic drugs (5), inhibition of P-glycoprotein might also be involved in the

toxicity of cyclophosphamide observed in our patient. P-glycoprotein is expressed in the canalicular membrane of hepatocytes (5) and may also be expressed in endothelial cells. Inhibition of P-glycoprotein may therefore be associated with decreased biliary excretion of toxic metabolites of cyclophosphamide and/or with trapping of cyclophosphamide and toxic metabolites in endothelial cells.

Finally, the toxicity of cyclophosphamide in the presence of roxithromycin may be unrelated to its inhibitory action on CYP3A4/P-glycoprotein and may involve so far unknown properties of roxithromycin, which are specific for this drug or may be shared by other macrolide antibiotics. Since cyclophosphamide can induce apoptosis, it is possible that roxithromycin sensitized endothelial cells to apoptotic effects of cyclophosphamide.

The differentiation between these mechanisms is clinically relevant, since macrolides and other CYP3A4-inhibitors are drugs used widely. In the accompanying paper, we have therefore investigated the proposed mechanisms in vitro (6). We could show that the combination of cyclophosphamide with roxithromycin induces apoptosis of endothelial cells via a mitochondrial mechanism. This mechanism is specific for roxithromycin, other macrolides or CPP3A4/P-glycoprotein inhibitors did not increase cytotoxicity of cyclophosphamide.

14.3.5. References

1. Gupta V, Lazarus HM, Keating A. Myeloablative conditioning regimens for AML allografts: 30 years later. Bone Marrow Transplant. 2003;32:969-78.

2. Yamazaki H, Shimada T. Comparative studies of in vitro inhibition of cytochrome P450 3A4-dependent testosterone 6beta-hydroxylation by roxithromycin and its metabolites, troleandomycin, and erythromycin. Drug Metab Dispos. 1998;26:1053-7.

3. Bohnenstengel F, Hofmann U, Eichelbaum M, Kroemer HK. Characterization of the cytochrome P450 involved in side-chain oxidation of cyclophosphamide in humans. Eur J Clin Pharmacol. 1996;51:297-301.

4. Blomgren H, Hallstrom M. Possible role of acrolein in 4-hydroperoxycyclophosphamide-induced cell damage in vitro. Methods Find Exp Clin Pharmacol. 1991;13:11-4.

5. Kimura Y, Matsuo M, Takahashi K, Saeki T, Kioka N, Amachi T, Ueda K. ATP hydrolysis-dependent multidrug efflux transporter: MDR1/P-glycoprotein. Curr Drug Metab. 2004;5:1-10.

6. Kaufmann P, Török M, Bletinger J, Bogman K, Wenk M, Terraciano L, Krähenbühl S. Mechanisms of veno-occlusive disease for the combination of cyclophosphamide and roxithromycin. J Hepatol;submitted.